

Electronic Thesis and Dissertation Repository

12-5-2022 3:30 PM

Biogeochemical Prospecting for Gold using Robust Multivariate Statistical Analysis

Zohreh Ghorbani, *The University of Western Ontario*

Supervisor: Banerjee, Neil R., *The University of Western Ontario*

Co-Supervisor: Van Loon, Lisa, L, *The University of Western Ontario*

A thesis submitted in partial fulfillment of the requirements for the Doctor of Philosophy degree in Geology

© Zohreh Ghorbani 2022

Follow this and additional works at: <https://ir.lib.uwo.ca/etd>

Recommended Citation

Ghorbani, Zohreh, "Biogeochemical Prospecting for Gold using Robust Multivariate Statistical Analysis" (2022). *Electronic Thesis and Dissertation Repository*. 9021.

<https://ir.lib.uwo.ca/etd/9021>

This Dissertation/Thesis is brought to you for free and open access by Scholarship@Western. It has been accepted for inclusion in Electronic Thesis and Dissertation Repository by an authorized administrator of Scholarship@Western. For more information, please contact wlsadmin@uwo.ca.

Abstract

The application of biogeochemical techniques in mineral exploration is to use the chemistry of plants to identify the presence and characterizations of concealed mineralization. Gold prospecting using biogeochemical techniques is found to be a viable geochemical tool in the early stages of exploration. This study aims to use a systematic two-phase statistical approach, including process discovery and process validation, to evaluate the multi-element biogeochemical dataset and identify the geochemical process controlling elemental occurrence and distribution in plant samples. To achieve these objectives, three biogeochemical surveys were conducted over the early and advanced gold targets located at two economically promising Archean greenstone-hosted orogenic gold deposits: including the Monument Bay Gold Project (MBGP) and Yellowknife City Gold Project (YCGP). The MBGP is a highly prospective gold deposit located in the northeastern part of Manitoba. The YCGP is a region of intense exploration and drilling near the extensions of the gold-bearing shear zones that host the historic Giant and Con Mines, located close to the city of Yellowknife, Northwest Territories.

Exploratory data analysis (EDA), including univariate and multivariate statistical analysis, was used to interpret biogeochemical data and identify the plant-substrate relationship and, subsequently, zones of gold enrichment. The results of EDA indicated that black spruce can successfully accumulate anomalous values of Au and its pathfinder elements, including As, Ag, Bi, Se, Sb, and Tl. Therefore, it is the preferred plant species for biogeochemical exploration in Canadian boreal forests. In addition, the Inverse distance weighted (IDW) interpolation method demonstrated strong associations between Au and its pathfinder elements. It is revealed that zones of Au enrichments are associated with different sets of pathfinder elements based on the bedrock composition and mineralization style. Arsenic, Se, Tl, and Sb signatures accompanied Au in both MBGP and YCGP. According to the principal component analysis (PCA), the geochemical/mineralization and physiological factors control elemental distribution in black spruce. The results of this study attest to the robustness of multivariate statistical analysis in detecting zones of Au enrichment using biogeochemical exploration methods.

Keywords

Biogeochemical exploration, Robust statistical analysis, Multivariate data analysis, Gold prospecting, Monument Bay Gold Project (MBGP), Yellowknife City Gold Project (YCGP)

Summary for Lay Audience

Biogeochemical techniques in mineral exploration use plants' chemistry to identify the buried mineralization presence. This method is a viable geochemical tool in the early stages of exploration. This study aims to use a statistical approach to evaluate the multi-element biogeochemical dataset and identify the geochemical process controlling elemental occurrence and distribution in plant samples. Three biogeochemical surveys were conducted at the two gold (Au) deposits, including the Monument Bay Gold Project (MBGP) and Yellowknife City Gold Project (YCGP), to achieve these objectives. The MBGP is a highly prospective Au deposit located in the northeastern part of Manitoba. The YCGP contains high-grade Au targets located close to the city of Yellowknife, Northwest Territories.

Exploratory data analysis (EDA), including univariate and multivariate statistical analysis, was used to interpret biogeochemical data and identify the plant-substrate relationship and, subsequently, zones of Au enrichment. The results of EDA indicated that black spruce samples can successfully accumulate high values of Au and its indicator elements, including arsenic (As), silver (Ag), bismuth (Bi), selenium (Se), antimony (Sb), and Thallium (Tl). Therefore, it is the preferred plant species for biogeochemical exploration in Canadian boreal forests. According to the EDA, the geochemical/mineralization and physiological factors control elemental distribution in black spruce. The results of this study attest to the robustness of multivariate statistical analysis in detecting zones of Au enrichment using biogeochemical exploration.

Co-Authorship Statement

Paper 1: located in Chapter 3

Title: Application of multivariate data analysis to biogeochemical exploration at the Twin Lakes Deposit, Monument Bay Gold Project, Manitoba, Canada.

Authors:

Author 1 and Candidate: Zohreh Ghorbani

Author 2: Fatemeh Gholizadeh

Author 3: Juliana Casali

Author 4: Chunyi Hao

Author 5: Hannah E. Cavallin

Author 6: Lisa L. Van Loon

Author 7: Neil R. Banerjee

Author contributions:

Author 1: Conceived the ideas of this study, conducted the research, Performed statistical analysis and interpretation, Wrote the manuscript, and corresponding author (70%).

Author 2: Provided revisions to the statistical analysis part of the manuscript.

Author 3: Provided revisions to the regional geology part of the manuscript.

Author 4: Provided revisions to the regional geology part of the manuscript.

Author 5: Provided access to research components such as data and revisions to the manuscript's scientific content.

Author 6: Supervised the research, provided revisions to the scientific content of the manuscript and provided stylistic and grammatical revisions to the manuscript.

Author 7: Supervised the research, provided revisions to the scientific content of the manuscript, Provided stylistic and grammatical revisions to the manuscript, Provided access to research components such as data and software, and provided the funding.

Publication status: Published, Ghorbani, Zohreh, et al. "Application of multivariate data analysis to biogeochemical exploration at the Twin Lakes Deposit, Monument Bay Gold Project, Manitoba, Canada." *Chemical Geology* 593 (2022): 120739.

Paper 2: located in Chapter 4

Title: Biogeochemical prospecting for gold at the Yellowknife City Gold Project, Northwest Territories, Canada: Part 1-Species optimization.

Authors:

Author 1 and Candidate: Zohreh Ghorbani

Author 2: Alan Sexton

Author 3: Lisa L. Van Loon

Author 4: Neil R. Banerjee

Author contributions:

Author 1: Conceived the ideas of this study, conducted the research, Performed statistical analysis and interpretation, Wrote the manuscript, and corresponding author (85%).

Author 2: Provided access to research components such as data and revisions to the manuscript's scientific content.

Author 3: Supervised the research, provided revisions to the scientific content of the manuscript and provided stylistic and grammatical revisions to the manuscript.

Author 4: Supervised the research, provided revisions to the scientific content of the manuscript, Provided stylistic and grammatical revisions to the manuscript, Provided access to research components such as data and software, and provided the funding.

Publication status: Published, Ghorbani, Zohreh, et al. "Biogeochemical prospecting for gold at the Yellowknife City Gold Project, Northwest Territories, Canada: Part 1-Species optimization." *Applied Geochemistry* 145 (2022): 105423.

Paper 3: located in Chapter 5

Title: Biogeochemical prospecting for gold at the Yellowknife City Gold Project, Northwest Territories, Canada: Part 2-Robust statistical analysis.

Authors:

Author 1, candidate, and corresponding author: Zohreh Ghorbani

Author 2: Alan Sexton

Author 3: Lisa L. Van Loon

Author 4: Neil R. Banerjee

Author contributions:

Author 1: Conceived the ideas of this study, conducted the research, Performed statistical analysis and interpretation, Wrote the manuscript, and corresponding author (85%).

Author 2: Provided access to research components such as data and revisions to the manuscript's scientific content.

Author 3: Supervised the research, provided revisions to the scientific content of the manuscript and provided stylistic and grammatical revisions to the manuscript.

Author 4: Supervised the research, provided revisions to the scientific content of the manuscript, Provided stylistic and grammatical revisions to the manuscript, Provided access to research components such as data and software, and provided the funding.

Publication status: Accepted (under publication process)

Dedication

This thesis is dedicated to my dearest, Reza, for his endless love, support and encouragement over the past ten years. Also, it is dedicated to my parents, Niaz and Fatemeh, for their faith in me and for all sacrifices they have made for me to have a better life. Last but not least, it is dedicated to my beloved friend, Juliana, who taught me the meaning of true friendship and loved me for who I am.

Acknowledgments

I would like to express my heartfelt gratitude to my advisors, Professor Neil R. Banerjee and Lisa L Van Loon, for their endless guidance and support, without which I would never be able to have my dissertation completed. I would consider myself to be exceptionally privileged to have been their student. I benefited enormously from their excellence as researchers and teachers. I am very appreciative to them for being very patient, for all the time they spent conducting experiments and discussing different topics of this thesis, and for going through several versions of this dissertation. I hope to continue researching with them and keep in touch with them for the rest of my academic life.

For the study conducted at the Monument Bay Gold Project, I would like to thank Colin Dunn for sharing his expertise and valuable discussions/data about black spruce as an exploration medium. I also thank Richard Mann, Duncan Mackay, Rob Penczak, and the Yamana Gold Monument Bay Team for conducting the survey, providing data, and valuable discussions. For the study conducted at the Yellowknife City Gold Project, I thank Aaron Doan, Duncan Studd, and the entire Yellowknife City Gold Project team for conducting the survey, providing data, and for valuable discussions. Western University, Yamana Gold Inc., Gold Terra Resources Corp., and the Natural Sciences and Engineering Research Council (NSERC) provided funding for these projects. The results of these studies were published in *Chemical Geology* (chapter 3) and *Applied Geochemistry* (chapter 4). Chapter 5 is under the publication process. Also, I acknowledge these results are not published commercially.

Finally, I would like to thank my Ph.D. examination committee, Colin Dunn, Brian Branfireun, Nigel Blamey, and Dave Good, for sharing their expertise and valuable discussions.

Table of Contents

Abstract	ii
Keywords	ii
Summary for Lay Audience	iii
Co-Authorship Statement.....	iv
Dedication	vii
Acknowledgments.....	viii
Table of Contents	ix
List of Tables	xiii
List of Figures	xiv
Chapter 1	1
1 Introduction and Literature Review	1
1.1 Biogeochemical exploration	1
1.1.1 History of Biogeochemical Exploration	1
1.1.2 Plant Physiology and Biogeochemistry	3
1.1.3 Biogeochemical Survey in Canadian Boreal Forests.....	7
1.1.4 Biogeochemical Prospecting for Gold.....	10
1.2 Exploratory Data Analysis (EDA)	14
1.2.1 Multivariate Data Analysis	20
1.3 Research Objectives and Outcomes.....	25
Chapter 2.....	28
2 Geological Setting.....	28
2.1 Archean Greenstone Hosted Orogenic Gold Deposits.....	28
2.2 The Superior Province	31
2.3 The Slave Province	36

2.4	Geology of Case Studies	39
2.4.1	The Monument Bay Gold Project (MBGP)	39
2.4.2	Yellowknife Greenstone Belt (YGB).....	44
2.4.3	Yellowknife City Gold Project (YCGP).....	47
Chapter 3.....		52
3	Application of Multivariate Data Analysis to Biogeochemical Exploration at the Twin Lakes Deposit, Monument Bay Gold Project, Manitoba, Canada	52
	Abstract	52
3.1	Introduction.....	53
3.2	Regional Geology:	55
3.1	Methodology	58
3.1.1	Sample Collection and Preparation.....	58
3.1.2	Analytical Analysis.....	58
3.1.3	Processing Biogeochemical Data.....	59
3.1.4	Principal Component Analysis (PCA).....	60
3.1	Results and Discussion	63
3.1.1	Summary of Statistics	63
3.1.2	Biogeochemical Distribution of Elements in Black Spruce:	64
3.1.3	Element Associations:.....	65
3.1.4	Robust RQ-Principal Component Analysis (PCA).....	73
3.2	Conclusions.....	76
Chapter 4.....		78
4	Biogeochemical Prospecting for Gold at the Yellowknife City Gold Project, Northwest Territories, Canada: Part 1 - Species Optimization.....	78
	Abstract	78
4.1	Introduction.....	79
4.2	Regional Geology of the YCGP	81

4.3	Methodology	83
4.3.1	2015 Biogeochemical Survey	83
4.3.2	Data Preparation and Assessment	86
4.3.3	Data Precision	87
4.4	Results and Discussion	88
4.4.1	Summary of Statistics	88
4.4.2	Robust RQ-Mode Principal Component Analysis (PCA)	92
4.4.3	K-Means Clustering Analysis	94
4.5	Conclusion	96
Chapter 5		98
5	Biogeochemical Prospecting for Gold at the Yellowknife City Gold Project, Northwest Territories, Canada: Part 2, Robust Statistical Analysis	98
Abstract		98
5.1	Introduction	99
5.2	General Geological Setting:	101
5.3	Methodology	105
5.3.1	Reconnaissance Biogeochemical Survey	105
5.3.2	Data Preparation and Assessment	105
5.3.3	Data Precision	107
5.4	Results and Discussion	108
5.4.1	Summary of Statistics	108
5.4.2	Principal Component Analysis	114
5.4.3	Robust Inverse Distance Weighted (IDW) Interpolation	117
5.4.4	Northbelt Au prospecting:	118
5.4.5	Eastbelt Au prospecting:	122
5.5	Conclusion	123

Chapter 6.....	125
6 Summary	125
6.1 Future Work	131
References.....	133
Appendix A.....	166
Appendix B	197
Appendix C	232
Curriculum Vitae	268

List of Tables

Table 1. Essential elements for plants. Elements in bold are trace elements in plants (modified after Dunn, 2007b).	4
Table 2. Descriptive statistics of Min, Max, mean (average value), median (background value), and mean $\pm 2\sigma$ (background range) values in the black spruce bark, needles and twigs (DL: detection limits, σ : standard deviation, ppm: part per million, ppb: part per billion, pct: percent, σ : standard deviation).....	61
Table 3: Calculation of data precision results using the average coefficient of variation ($CV_{avg}(\%)$) indicate a marginal range for Cd, Tl, Se, Au, and S in 2015 biogeochemical data.	87
Table 4: Descriptive statistics of Min, Max, mean and median values of element concentrations for 625 vegetation samples collected at the YCGP. The number of collected samples for each plant species is shown in brackets. Also, the average concentration of elements in different vegetation types, including alder, black spruce, juniper, and Labrador tea, are provided. The Median or 50 th percentile is considered the background level.....	90
Table 5. Precision of data using the average coefficient of variation ($CV_{avg}\%$) indicate a marginal range for Se in the 2017 biogeochemical data. Other elements are within an acceptable to a good range of precision.	108
Table 6. Descriptive statistics of minimum, maximum, mean, median, and the background level of elements concentration in 2788 black spruce needle samples collected at six different targets, including Duck Lake and former Ptarmigan and Tom Mines at the Eastbelt and Ryan Lake, Sam Otto, Walsh Lake and Homer Lake targets at the Northbelt are provided. Ppb: part per billion, ppm: part per million, pct: percent, BG: background.....	110
Table 7. The comparison between early and advanced Au targets at the YCGP. According to the results of IDW interpolation, Au is accompanied by different sets of pathfinder elements with respect to the underlying lithology/mineralogy. * Contiguous anomalous Au values are detected at Duck Lake target, Ptarmigan Mine, and Ryan Lake target.	118

List of Figures

Figure 1. Plant's responses to deficiency and toxicity of micronutrients (essential trace elements) and non-essential trace elements (modified after Kabata-Pendias, 2001)..... 5

Figure 2. the antagonistic and synergistic behaviour of chemical elements in plants and adjacent to roots (modified after Kabata-Pendias, 2001)..... 7

Figure 3. The comparison between U concentration in ashed black spruce twigs and needles collected along an 8 km traverse near the Athabasca U deposit, Saskatchewan, Canada (Dunn and Cameron, 1983). The uranium concentration of twigs is higher than that of needles due to the barrier mechanism established by needles (modified after Dunn, 2007b)..... 8

Figure 4. Examples of common distribution of data using histograms (modified after AMGEN- Histograms)..... 16

Figure 5. The comparison between raw (up) and CLR transformed (down) data for Ca and Cd values in needle samples at the YCGP. 17

Figure 6. (A) a schematic box plot showing the summary data, (B) box plots showing the skewness of data (modified after Skewed Distribution - Z TABLE) 18

Figure 7. (A) Box plot of sulphur (S) data showing the summary of S data in needles samples collected at the YCGP vs CLR-transformed S data. (B) change in orders of S data abundances in vegetation in raw data and CLR transformed data..... 18

Figure 8. Probability plots of As and CLR-transformed As show data distribution before and after normalization. 19

Figure 9. Examples of different patterns to describe the correlation between two variables in scatter plots (modified after math boot camps)..... 20

Figure 10. Schematic of a new feature space (Principal components) created by eigenvalues and eigenvectors. The eigenvectors show the direction of the new PC, and the eigenvalues define the magnitude (modified after Firman, 2019)..... 22

Figure 11. The dimension reduction method creates new feature space. PC1 is responsible for the variance of variables A and B (modified after Firman, 2019).	23
Figure 12. A schematic of the score and loading plot. Scores are the transformed data value for each sample. Loadings are vectors that define the correlation between scores and PC (Dragon 6 User’s Manual).	23
Figure 13. A simple schematic and formula showing the function of the inverse distance weighted (IDW) interpolation method (modified after Wikipedia).	25
Figure 14. The conceptual representation of the critical factors controlling the formation of orogenic gold deposits. The succession of the process from bottom to top (fluid, ligand, gold, active fault system and efficient mechanism) and in time is required; otherwise, the mineralization system aborts (modified after Cox, 2016).	28
Figure 15. The Canadian Shield (left) and the seven geological provinces within it, including Nain, Grenville, Southern, Superior, Churchill, Slave and Bear provinces (modified after the Canadian Encyclopedia).	31
Figure 16. The Superior Craton is comprised of major subprovinces and domains, including NSS: Northern Superior Superterrane; OSD Oxford-Stull Terrane; NCT: North Caribou Terrane; ERT: English River Domain; WRT: Winnipeg River Domain; WWT: Western Wabigoon Terrane; EWT: Eastern Wabigoon Terrane; MT: Marmion Terrane; QT: Quetico Terrane; WT: Wawa Terrane; MRVT: Minnesota River Valley Terrane; KU: Kapuskasing Uplift; AT: Abitibi Terrane; PT: Pontiac Terrane; OcS: Opatoca Subprovince; AC: Ashuanipi Complex; OnS: Opinaca Subprovince; LG: La Grande Subprovince; BS: Bienville Subprovince; I: Inukjuak Domain; II Tikkerutuk Domain; IV: Lake Minto Domain; V: Goudalie Domain; VI Utsalik Domain; VII: Douglas Harbour Domain. Gold deposits of the Superior Province are shown in yellow circles (modified after Percival, 2007).	32
Figure 17. Before Northern Superior Orogeny (2.72 Ga), the Superior Craton was fragments of microcontinent separated by the E-W trending conduit-like ocean (modified after Percival et al., 2007).	33

Figure 18. During the Uchain Orogeny, the NNS moves southward to NCT and limits OSD, initiating the formation of Superior Craton (modified after Percival et al., 2007).	34
Figure 19. During Central Superior Orogeny, the WRT at the south subducted northward onto the NCT (modified after Percival et al., 2007).	35
Figure 20. The WAT moved northward to collide with the composite Superior Craton during the Shebandowanian Orogeny (Percival et al., 2012).....	35
Figure 21. The MRTV moved northward to collide with the pre-mature craton during the final orogeny event, the Minnesotan Orogeny (modified after Cook et al., 2006).....	36
Figure 22. Lithological map of the Slave Province, Modified after Henderson (1985) (Henderson, 1985).....	37
Figure 23. (a) The tectonostratigraphic terranes in the Slave Province, including Anton, Sleepy Dragon, Contwoyto, and Hackett River volcanic terranes proposed by Kusky (1989), (b) Modified terrane map proposed by Helmstaedt and Pehrsson (2012) (H. H. Helmstaedt, Pehrsson, Percival, Cook, and Clowes, 2012). BB: Bathurst Block, CSST: Central Slave superterrane, CT: Contwoyto Terrane, HRT: Hackett River Terrane) (modified after Padgham, 1985).	38
Figure 24. The location of MBGP in the Oxford-Stull Domain within the NW of the Archean Superior Province (modified after the Yamana technical report, nonpublished).	40
Figure 25. Regional Geology in the Oxford-Stull Domain (modified after Yamana technical report, nonpublished).	41
Figure 26. The regional geology map of Monument Bay Property and Stull Lake Property indicates the major structures and claim outlines. The red stars show the geographical distribution of six distinct zones at the MBGP (modified after Casali, 2020).....	43
Figure 27. (A) The geological map of the Slave Province, modified after Hauggard et al. (2017). (B) The stratigraphic column of the Yellowknife Subgroup, host to the YGB (modified after Botor, 2018).	45

Figure 28. Regional geology of the YGB, Modified after NWT Helmstaedt and Hounsell Compilation map (modified after Armitage, 2021).	46
Figure 29. the Yellowknife City Gold Project (YCGP) advanced targets and new gold prospects within the Northbelt, including Sam Otto, Homer Lake, Ryan Lake, and Walsh lake targets, and within the Eastbelt, including the vicinity of the former Tom and Ptarmigan mines and Duck Lake target (modified after Botor, 2018).	50
Figure 30. (A) Regional geology of the Monument Bay Project, northeastern Manitoba. Modified by the authors from Yamana Gold Inc. (unpublished), 2020). (B) Location of black spruce sampling sites within the Twin Lakes Gold Deposit.	57
Figure 31. Comparison of the logarithmic mean values of selected elements in ashed bark (blue), needles (green), and twigs (red) collected at the Twin Lakes Deposit.	65
Figure 32. Scatter plot matrix of gold and nutrient elements for needles (green), twigs (red), and bark (blue). Scatter plot matrix demonstrates a strong bivariate relationship between Au and micronutrients metals, including Cu, Fe, Ni, Mo and Zn, indicating a plant-substrate relationship. While slightly negative to no meaningful correlation can be seen between Au and B, Ba, Ca, K, Mg, Mn and P due to differences in their chemistry and accumulation organ.	68
Figure 33. The IDW interpolation method exhibits the spatial distribution of gold pathfinder elements over and peripheral to the conceptual pit shell at the Twin Lakes Deposit. The conceptual pit shell is outlined in black. The red dotted line represents the Twin Lakes Shear Zone (TLSZ). The comparison of element profiles along six transects indicates a significant association between Au and As, Se, Bi, and Tl and a relative association with Sb, Cd and Pb. Small black dots indicate Au concentrations below the 80th percentile (<3 ppb). Medium circles represent values between the 81st to 97th percentile (3 to 10 ppb). Large circles represent values over the 98th percentile (11 to 303 ppb), respectively.	71
Figure 34. According to the robust RQ mode-PCA, two components control the distribution pattern of elements in black spruce samples. The geological/ mineralization/Fe factor represents the black spruce-substrate relationship, including elements that reflect bedrock composition, whereas the physiological factor contains a set of nutrition elements. Gold and	

its pathfinder elements, including As, Se, Tl, Bi, Pb and Cd, are a subset of geological/mineralization/Fe, representing the association of bedrock with concealed mineralization. Also, a small angle between sets of nutrients or sets of metals demonstrates their strong correlation. The proximity of needles (green dots) to Mn, Cu, Mg, P, B, K and Zn indicates the high concentration of nutrients in needles, while Ca with structural function is close to bark samples (Blue dots)..... 74

Figure 35: Regional geology of the Yellowknife City Gold Project (YCGP) and the location of samples collected at the 2015 biogeochemical survey (Ghorbani et al., 2022a)..... 85

Figure 36: The comparison of the average concentration of Au (ppb) in ash in foliage by different vegetation species collected over the Barney and Crestaurum Shears. 91

Figure 37: The concentration of Au in alder, juniper, black spruce, and Labrador tea foliage samples collected over the Crestaurum and Barney Shear. Anomalous Au values up to 147 ppb (in ash) were identified in all vegetation types located over the southern portion of the Crestaurum shear. Black spruce needles show a significant Au enrichment compared to other vegetation..... 92

Figure 38: Graphical representation of the robust RQ-mode principal component analysis (PCA) and K-means clustering applied to the 2015 biogeochemical sample. The PCA results indicate that the mineralization/geological factor (PC1) and physiological factor (PC2) are the contributing factors controlling the distribution of elements in plant samples collected at YCGP. PC3 includes only Mo, which is positively loaded in PC2. Based on the K-means clustering, samples are grouped into three clusters shown by square, circle, and triangle shapes, demonstrating the plant-substrate relationship with respect to the lithology/mineralogy beneath. 93

Figure 39. (Right) the Yellowknife City Gold Project (YCGP) advanced and new Au targets within the Northbelt, including Sam Otto, Homer Lake, Ryan Lake, and Walsh lake targets, and within the Estbelt, including the vicinity of the former Ptarmigan and Tom mines and Duck Lake target (Armitage, 2021). (Left) Regional geology of the YCG and the location of needle samples collected at the 2017 biogeochemical survey. From north to south: Yellow dots (Homer Lake target), Orange dots (Walsh Lake target), Red dots (Ryan Lake target),

Green dots (Sam Otto target), Purple dots (Ptarmigan and Tom), and Blue dots (Duck Lake target). 104

Figure 40. Average concentration of elements, normalized to the background level, in black spruce needle collected from the early and advanced Au targets, including Ptarmigan and Tom mines (purple), Duck Lake target (blue), Homer Lake target (Yellow), Ryan Lake target (red), Sam Otto target (green), and Walsh Lake target (orange). Gold shows enrichment in all targets. 114

Figure 41. According to the robust RQmode-PCA, PC1 and PC2 control the distribution pattern of elements in black spruce samples. PC1 indicates geochemical/mineralization and physiological factors contribute to elemental variation in black spruce needle samples. Strong associations of Au with As, Sb, Pb, Mo, and Fe clearly illustrate the plant-substrate relationship. PC2 emphasizes the influence of the geochemical/ mineralization factor. Also, it provides valuable information about the associated pathfinders for Au, including As, Sb, Pb, Tl, Ag, and Bi. Needle samples collected in early and advanced targets are presented in different colours: Duck lake target in blue, Homer lake target in yellow, Ptarmigan and Tom in purple, Ryan Lake target in red, Sam Otto target in green, and Walsh Lake target in orange. Gold values are displayed as circles of different sizes. Larger circles represent higher Au values. Samples with higher Au values are primarily associated with needle samples collected from the Ryan Lake target and Ptarmigan and Tom mines and are proximal to the geochemical/mineralogical factor. 115

Figure 42. Loading of PC 1 to 4 illustrates each PC's elemental correlation. PC1 to 4 accounts for 84.5% of the total variance. PC 1 and 2 are the main components representing the contributing factors controlling the distribution of elements in black spruce needles. The majority of elements in PC3 and PC4 have an absolute loading below 0.4; therefore, they were excluded from the interpretations. 117

Figure 43. Robust center log-ratio (CLR) transformed inverse distance weighted (IDW) interpolation maps of Au pathfinder elements in Northbelt (upper) and Eastbelt (lower). Anomalous Au concentrations above 98 percentiles are shown with bigger circles. Contiguous high Au values are associated with shear zones within mafic/ultramafic host lithologies, including North Giant Extension (NGX) and shear 17, 18, and 20. High

concentrations of As, Sb, Pb, and Cu, and to a lesser extent, Ag and Bi, are observed in these areas. Also, zones of Au enrichment are observed proximal to late felsic bodies intruded into mafic volcanics (Ryan Lake target) and sedimentary rocks (Duck Lake target). Gold in these zones is accompanied by high values of Ag, As, Se, Hg, and Tl. Elevated values of Au also can be seen along the faulted contacts between the felsic-intermediate metavolcanics and sulphide metasediments (Walsh Lake and Sam Otto target), where strong correlations between Au and Bi, Se, Hg, and Zn are identified. High concentrations of Ag, Bi, Tl, Cu, and Zn at the Homer Lake target are seen. The Ptarmigan area is enriched in all pathfinder elements of Au except Zn. 121

Chapter 1

1 Introduction and Literature Review

The mining industry contributes significantly to the Canadian economy. Although the 2022 statistics indicated an appraisal cost of \$1.1B in mining and mineral exploration, the success rates of grassroots exploration are declining (Canada, 2022). Any cost-effective and efficient tool can have a dramatic effect on exploration success. This research aims to assess the potential and robustness of biogeochemical techniques as effective alternatives or supplements to other surficial sampling techniques in the early stages of exploration. Biogeochemical exploration involves the use of chemical analysis of plants to understand the presence and characterizations of concealed mineralization, geological structure, and geochemistry of bedrock, soil, sediments, and water (Dunn, 2007b). This method is beneficial since the extensive root systems of plants can uptake metals from the substrate and integrate the geochemical signature of the concealed outcrop. However, the interpretation of biogeochemical data is more complicated due to the physiological interaction of plants with the environment. Also, the compositional nature of biogeochemical data requires fundamental error-checking as well as a systematic approach for practical interpretations. Therefore, this study applies robust statistical analysis to identify the plant-substrate relationship and discover elemental signatures related to the mineral occurrence.

1.1 Biogeochemical exploration

1.1.1 History of Biogeochemical Exploration

The use of plants to identify zones of metal enrichments dates back to the late 19th century when analytical instruments were adequate to identify element concentrations in trace values (Dunn, 2007b). Before that, geobotanical observations were used to delineate mineralization. Geobotany is a visual method that relies on recognizing specific plant species to discriminate geological differences in the subsurface (Dunn, 2007b). The first use of geobotanical exploration dates back to 10 BC when the architect Vitruvius found a specific plant community limited to swampy environments (Dunn, 2007b; Odhiambo, 2016). Agricola (1556)

observed the physiogeochemical effects of metal on plant growth (Odhiambo, 2016). Barba (1637) reported the use of vegetation to identify mineralization zones (Cannon et al., 1979).

The scarce use of biogeochemistry in mineral exploration dates back to 1898 in the Omai gold mine, where high concentrations of Au (0.3 to 3 ppm) were found in ashed plant samples (Lungwitz, 1900). The first biogeochemistry book was published by Tkalich (1938), who found an arsenopyrite mine by tracking the Fe content in overlying plants (Dunn, 2007b; Ginzburg, 2013). Simultaneously, Brundin (1939) used biogeochemical data to trace V and W (Brundin, 1939; Dunn, 2007b). In 1940, Prof. Warren from the University of British Columbia and his fellow started biogeochemical studies in mineral exploration from the base. His studies took over 50 years, and valuable biogeochemical data were gathered over areas that are now developed as mines. Prof Warren is known as the ‘father of biogeochemistry’ in North America (Dunn, 2007b). He believed that the biogeochemical technique can be a viable geochemical tool when used correctly (Dunn, 2007b; Girling et al., 1979; Warren and Delavault, 1950; Warren et al., 1968). At the same time, Harbaugh (1950) published soil and vegetation chemical analysis results that triggered the discovery of uranium (U) deposits in the USA. Following that, a broad biogeochemical survey was started by the U.S. Geological Survey (USGS) to find zones of U enrichments using the chemistry of plants (Cannon, 1960; Shacklette, 1965). Concurrently in Russia, Kovalevsky (1950) conducted numerous biogeochemical studies from his base, resulting in a wealth of literature, data, and figures (Dunn, 2007b). In 1960, Prof. Brooks in New Zealand commenced over 40 years of biogeochemical and geobotanical studies (Brooks, 1972). Several new species around the world were discovered thanks to his outstanding work. In the mid-1970s, the advances in technology and, following that, analytical instruments such as instrumental neutron activation analysis (INAA) led to advances in biogeochemical exploration (Dunn, 2007b). In the 1980s, interest in biogeochemical methods was raised in North America.

Comprehensive information about the chemistry and physiology of plants was provided by a polish chemist, Kabata-Pendias (Kabata-Pendias, 2001; Kabata-Pendias and Pendias, 1992). She shared over 20 years of experience in the field of biogeochemistry and soil science in her book titled “trace elements in soil and plants (Kabata-Pendias and Pendias, 1992). Finally, in 2007,. Dunn published a comprehensive handbook for particularly geologists about biogeochemistry in mineral exploration (Dunn, 2007b). This book covers over 30 years of his

worldwide experience in biogeochemical exploration and involves tens of thousands of samples and millions of analytical determinations (Dunn, 2007b). Indeed, he has made notable contributions to biogeochemistry during the second half of the 20th century.

1.1.2 Plant Physiology and Biogeochemistry

Over a long time, plants evolved physically and chemically to adapt to the environment they overlie. Also, they developed particular requirements to accumulate elements essential for their metabolism. Kabata-Pendias (2001) believed the selection of certain elements by plants depends on the geochemistry of the environment they overlie (Kabata-Pendias, 2001). According to the botanical thesaurus, there are two groups of elements: essential (nutritional) and non-essential elements (Dunn, 2007b). Essential elements, including C, H, O, N, Na, Mg, P, S, Cl, K, Ca, Mn, Fe, Cu, Zn, and Se, are necessary for plant metabolism. They can further be divided into two groups: macronutrients (e.g., O, H, N, K, Ca, Mg, P, and S) that are needed in high amounts, and micronutrients or essential trace elements (e.g., Cl, Fe, B, Mn, Zn, Cu, Mo, W, and Ni). Some elements, such as Mo and W, can play a surrogate 'essential' role in some cases (Table 1). The requirement of Mo and W is due to their presence in active sites of metalloenzymes that perform the critical transformation for the metabolism of macronutrients such as N, S, and C (Sigel and Sigel, 2002).

Table 1. Essential elements for plants. Elements in bold are trace elements in plants (modified after Dunn, 2007b).

Essential to all plants	Essential to several plants	Essential to many species in one class	Essential to a few species
Hydrogen(H)	Silicon (Si)	Boron (B)	Lithium (Li)
Carbon (C)	Vanadium (V)	Fluorine (F)	Aluminium(Al)
Nitrogen (N)	Cobalt (Co)	Chromium (Cr)	Nickel (Ni)
Oxygen (O)	Molybdenum(Mo)	Bromine (Br)	Strontium (Sr)
Sodium (Na)	Iodine (I)		Barium (Ba)
Magnesium(Mg)			
Phosphorus(P)			
Sulfur(S)			
Chlorine (Cl)			
Potassium (K)			
Calcium (Ca)			
Manganese (Mn)			
Iron (Fe)			
Copper (Cu)			
Zinc (Zn)			
Selenium (Se)			

Micronutrition elements are only required in trace amounts, and their high values can have detrimental effects on plants (Figure 1). Non-essential elements also have very trace quantities in plant samples. Examples of non-essential elements are Au, Ag, and U (Dunn, 2007b). Although the concentrations of non-essential and macronutrient elements in plants are low, they are positively associated with the abundance of these elements in the underlying substrate (Kabata-Pendias, 2001).

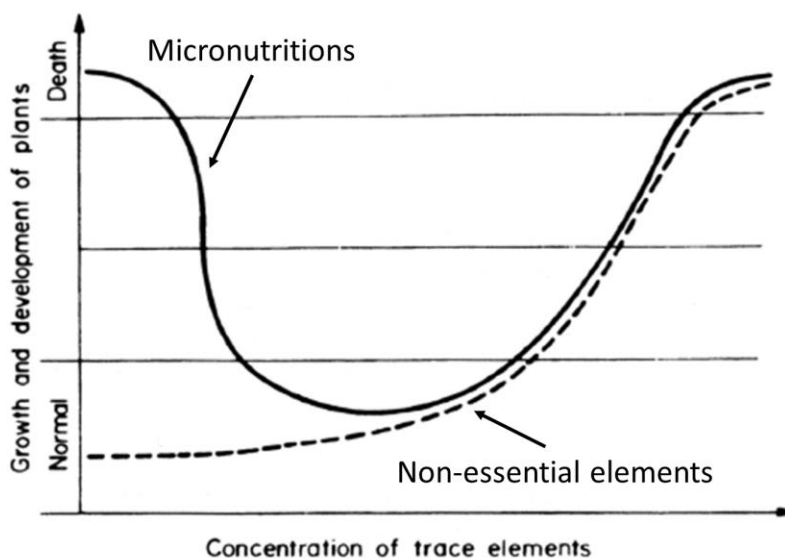


Figure 1. Plant's responses to deficiency and toxicity of micronutrients (essential trace elements) and non-essential trace elements (modified after Kabata-Pendias, 2001).

The role of each element in plants depends on processes such as absorption and translocation, enzymatic processes, concentrations and speciation, depletion and enrichment, and ion competition and interaction. The absorption of trace elements from the substrate to the plant is governed by many factors: climate condition, water chemistry, Eh and pH of the soil, organic and clay content, and the abundance of trace elements (Kabata-Pendias, 2001). Roots play an essential role in the mobilization and absorption of elements. The roots of plants evolved to form a physiological reaction or barrier mechanism to utilize control over uptake to rejection of particular elements (Kabata-Pendias, 2001). The concept of barrier mechanism to element uptake by plants was introduced by Kovalevsky (Kovalevsky, 1974). This concept states that the level of resistance in plant species and even plant tissues varies. Plants can be divided into two groups: barrier and non-barrier plants. The barrier plants establish a mechanism to avoid the accumulation of certain elements that are toxic/non-essential for them. Also, they are able to accumulate surplus concentrations of certain elements in tissues that are not metabolically active such as outer bark (Dunn, 2007b). On the other hand, the non-barrier plants are ideal candidates for biogeochemical exploration since they can uptake an element of interest in a constant plant-to-substrate ratio regardless of the amount of that element in the substrate. Some non-barrier plant species can accumulate high values of non-essential elements. These species were named

hyperaccumulators by Brooke et al. (1977). They usually contain low biomass as they have to consume more energy to adapt to a high level of trace elements in their tissue (Kabata-Pendias, 2001).

The interaction between elements in plants is not well understood, as many factors control the distribution of elements in plants. According to Kabata-Pendias (2001), there are two types of element interactions in plants: antagonistic and synergistic (Kabata-Pendias, 2001). In antagonistic interaction, one or a group of elements prevents the absorption of other elements. While in synergistic interaction, the absorption of some elements is enhanced due to the presence of some other elements. Studies indicate that macronutrients such as Ca, Mg and P have antagonistic interaction with trace elements such as As, Pb, Cd, and Ni (Benz, 2017; Dunn, 2007b; Kabata-Pendias and Pendias, 1992; Mengell, 1987). However, they may also show antagonistic-synergistic behaviour, depending on the plant species (Kabata-Pendias, 2001) (Figure 2). Sometimes, deficiency of an essential trace element can be compensated by the absorption of other micronutrients. This behaviour was reported between Mn and Cu, and Fe and Cu-Zn-Mn (Rengel et al., 1998).

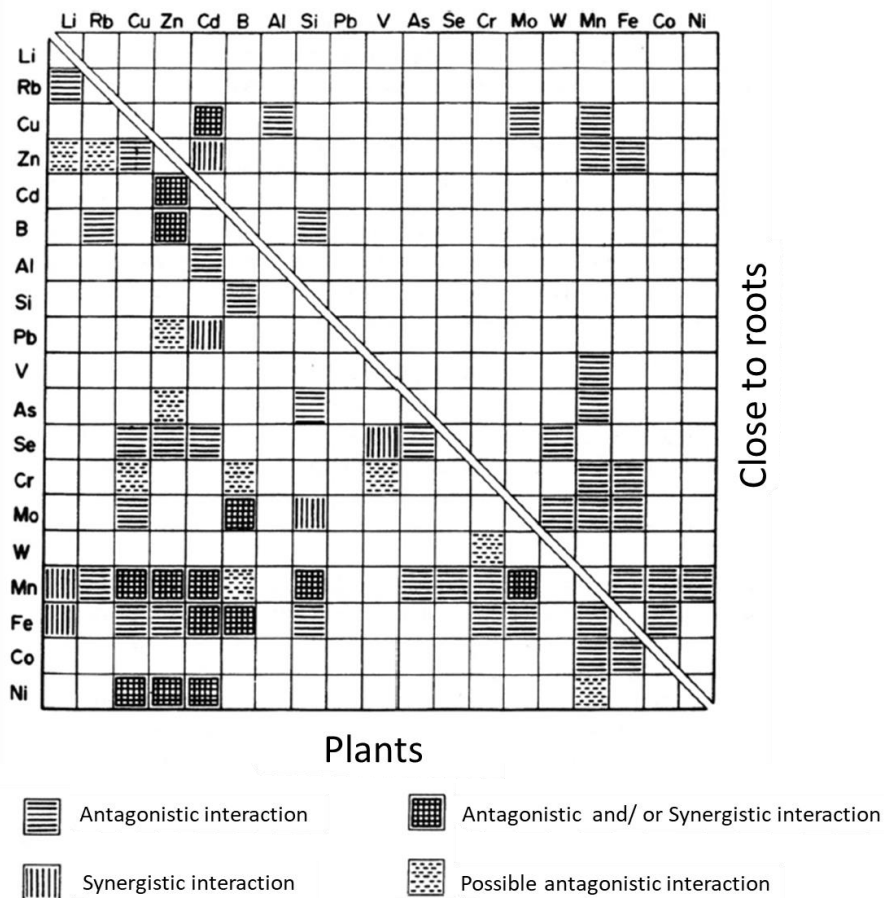


Figure 2. the antagonistic and synergistic behaviour of chemical elements in plants and adjacent to roots (modified after Kabata-Pendias, 2001).

1.1.3 Biogeochemical Survey in Canadian Boreal Forests

The ideal plant species for biogeochemical exploration are plants that are widespread in the study area. Also, plant samples should be selected from the non-barrier plants that are able to accumulate elements of interest above background concentrations from the same substrates. As discussed before, the barrier mechanism can even be established between organs of one plant species. For example, detailed studies by Dunn (1981, 1982, 1983) reported high values of U in black spruce twigs collected over U deposits in the Athabasca Basin, Saskatchewan. In contrast, the attached needles contain low U values as they established a barrier mechanism to prevent U translocation from twigs to needle (Dunn, 1982, 1983; Dunn and Cameron, 1983; Dunn, 1981; Dunn, 2007b) (Figure 3). Another study by Cohen et al. (1987) indicated the same concentration of Au in balsam fir needle and twigs samples collected at Hemlo in Ontario (Cohen et al., 1987).

Therefore, multiple sample media should be collected within an orientation survey and analyzed to have a preliminary insight into the concentration of the element in plants and identify the best sample medium.

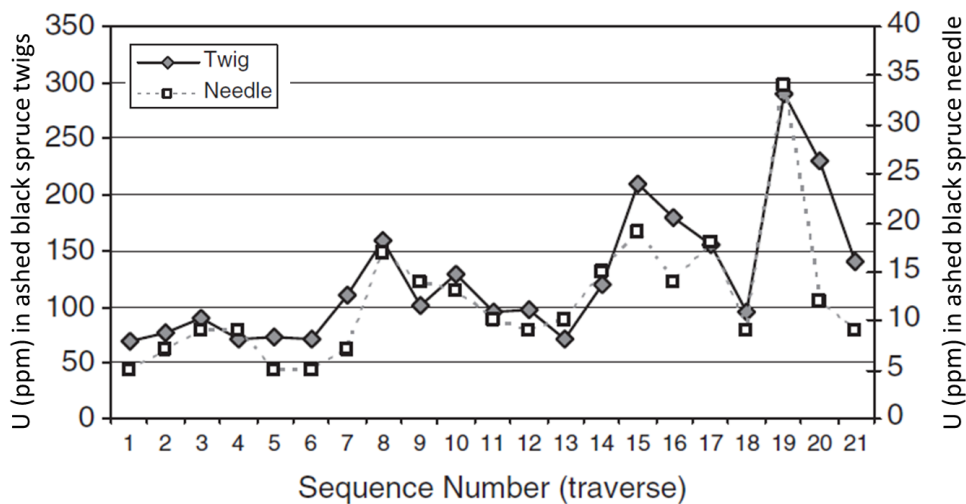


Figure 3. The comparison between U concentration in ashed black spruce twigs and needles collected along an 8 km traverse near the Athabasca U deposit, Saskatchewan, Canada (Dunn and Cameron, 1983). The uranium concentration of twigs is higher than that of needles due to the barrier mechanism established by needles (modified after Dunn, 2007b).

The selection of plant tissue in biogeochemical surveys requires a compromise between the preferred and optimal sample medium (Dunn, 2007b). It is essential to consider the propensity of target elements to accumulate in a particular tissue. For example, Hg tends to accumulate in leaves, while higher values of U and Au were found in twigs and barks. However, the selected sample medium should also be readily available to collect. For instance, where the collection of treetop branches is impractical, bark samples can be taken.

Plant growth and seasonal change can significantly influence the elemental composition of plant tissues. Thus, it is suggested to conduct a biogeochemical survey within a period of 2-3 weeks in spring or 4-6 weeks in summer (Dunn, 1985; Stednick et al., 1987). Biogeochemical surveys in winter can be conducted over a more extended period as plants' metabolism is slower and more stable.

North of the 50th parallel, much of the land surface is covered by boreal forests with a few common plant species (Natural Resources Canada, 2005). Conifers from the Pine family, such as black spruce (*Picea mariana*), tamarack or larch (*Larix laricina*), jack pine (*Pinus banksiana*), juniper (*Juniperus*), and balsam fir (*Abies balsamea*), are the most common species in the Canadian boreal forest. In contrast, broad-leaved deciduous trees such as aspen (*Populus tremuloides*) and white birch (*Betula papyrifera*) and shrubs such as Labrador tea (*Ledum groenlandicum*), willow (*Salix*), and alder (*Alnus crispa*) are less widespread (Archibold, 2012; Dunn, 2007b). Black spruce is the most dominant tree species in the Canadian boreal forest. Many studies have proved the ability of black spruce to accumulate high concentrations of metals such as Au (Dunn, 2001; Dunn et al., 1992; Dunn et al., 1995; Dunn and Heberlein, 2020; Ghorbani et al., 2022). Sample media that can be collected from black spruce include bark, twigs, foliage, trunk wood, treetops, and cones.

Bark samples are easy to collect and process. Studies also reported high concentrations of Au and its associated pathfinders in the bark (Dunn, 2001; Dunn et al., 1992; Dunn and Angélica, 2000; Ghorbani et al., 2022), which makes it an ideal candidate for biogeochemical exploration compared to other tissue types. Bark samples should be collected from around the tree's circumference at chest height to be consistent and practical. Also, it is critical to scrape the outer part of the bark as the majority of metals concentrate in the outer bark (Dunn, 2007b). The comparison between the elemental composition of the outer and inner bark of spruce samples collected over gold mineralization in central Nova Scotia revealed high concentrations of Au, As, Sb, Cr, and Fe in outer bark samples (Dunn, 2007b).

The chemistry of twigs changes as it grows. A study by Dunn and Ray (1995) over the Ladner Creek Au deposit in BC indicated a significant difference in the elemental composition of twig samples according to the years of growth. This study reported the concentrations of Au and As in young twigs are 1590 ppb and 82 ppm in ash, while these values decreased to 530 ppb and 22 ppm in old twigs due to the concentration of heavy and toxic metals to the tip of new growth twigs. Generally, the practical size for twig samples in boreal forests is 25-30 cm in length and 3-5 mm in diameter, representing ten years of growth.

In general, foliage can accumulate lower concentrations of metals than other tissues as they are metabolically active organs and establish a barrier mechanism to avoid translocating heavy metals. Also, the chemistry of leaf samples is more prone to be influenced by seasonal change. Therefore, although the foliage is easier to collect and prepare, it is important to consider the type of foliage and whether they need to be ashed.

Trunk wood is generally not an optimal tissue for biogeochemical exploration due to its low ability to concentrate elements of exploration significance. Treetops and cones also can be used for biogeochemical exploration. It has been reported that elements can translocate to the top of trees and reflect the presence of buried mineralization. Collecting treetops may require hovering in a helicopter over the crown and collecting the uppermost lateral branches. Generally, 30-50 cm of the 2-3 uppermost lateral branches is comprised of 30% needle, 25% twigs, and 45% cones (dry basis) (Dunn, 2007b). Although cones can show a strong anomaly to background ratio due to low ash yield content, they are metabolically active organs and mainly enriched in essential elements (Dunn, 2007b).

The preparation of biogeochemical samples includes washing, milling, ashing, and digesting. Contamination is the primary source of error in biogeochemical surveys. Therefore samples may require to be washed in running water to remove the dust. Biogeochemical samples also need to be milled to a fine size below 1 mm. The ashing process with a temperature of 475 °C is suggested for elements such as Au and As that generally have concentrations below the detection limit in dry samples. Finally, digestion using aqua-regia is required for multi-element analysis.

1.1.4 Biogeochemical Prospecting for Gold

Gold (Au): Evaluating gold concentrations in plants in the attempt to find mineralization areas dates back to 1900 (Lungwitz, 1900). Gold has no essential role in plant growth; therefore, any high gold values likely reflect the presence of concealed mineralization (Dunn, 2007b; Kitayev and Zhukova, 1980). Gold cannot be absorbed in its native state. However, Au can be soluble when it forms complex ions with CN^- , S, and N. This process converts Au(0) to Au(I) and Au (III), which can be absorbed by plants (Kabata-Pendias, 2001; Sheoran et al., 2013). Piccinin et al. (2007) reported higher concentrations in roots than in shoots (Piccinin et al.,

2007). The background concentration of Au in vegetation is below one ppb (dry weight) (Markert, 1994). However, Au hyperaccumulators such as Horsetail can concentrate up to 500 ppb to Au (ash weight) (Cannon et al., 1968). Shacklette et al. (1985) reported that mean Au content in plants collected over mineralized areas varies between 0.5 ppb to 150 ppb. According to Dunn (2007a), the average concentration of Au in the Canadian boreal forest is 5-10 ppb (ash weight) (Dunn, 2007a, 2007b). The distribution pattern of Au should be substantiated by its pathfinder elements to avoid reporting unreal anomalies. Gold pathfinder elements or indicators refer to elements, mostly non-ore (Rose and Hawkes, 1979), that are in association with gold and can be used to delineate zones of gold enrichment. Arsenic, Bi, Cd, Pb, Sb, and Tl have been reported by many researchers as prospective pathfinder elements of gold (Dunn, 2007b; Kovalevsky, 1995; Kovalevsky and Kovalevskaya, 1989).

Antimony (Sb): Antimony is a common element in orogenic gold deposits (R. J. Goldfarb and Groves, 2015) that can be considered a pathfinder of gold (Dunn, 2007b). Antimony has chalcophile properties and shows close geochemical characteristics to As and Bi (Kabata-Pendias, 2001). Antimony can be easily absorbed by plants in soluble forms, although it is a non-essential element for plants. Mean Sb values in plant samples collected over mineralized areas range from 7-50 ppm dry weight (Shacklette et al., 1978). It is expected that 20-30% of Sb may have volatilized during the ashing process by controlled ignition at 475 °C (Dunn, 2007b). Strong associations between Au, As, and Sb in plant samples were reported in studies over zones of Au enrichments (Almasi et al., 2015; Dunn, 2007b; Ghorbani et al., 2022; Viladevall et al., 1978).

Arsenic (As): Arsenic is a non-essential element for plant metabolism (Khalid et al., 2017), and it is usually less than one ppm dry weight (Adriano, 2001). The absorption and translocation of As from soil to plants were described by Thoresby and Thornton (1979). This study observed that old leaves and roots accumulate higher values of As than other tissues. Another study by Tlustos et al. (1998) reported that As absorption by plants depends on the As chemical form, and the accumulation of organic As in needles is higher than inorganic As (arsenate and arsenite). Another study by Chandrakar et al. (2017) indicated that the rate of organic As uptake by plants is slower than inorganic As uptake. However, the pace of organic As translocations from root to shoot is higher (Raab et al. 2005).

Arsenate (As^{5+}) is the predominant form of As in aerobic soils (Zhao et al., 2009). Studies have reported that arsenate can replace phosphate (P^{5+}) using the Pi (inorganic phosphate) channel and cross the root cells (Abbas et al., 2018; Ghosh et al., 2015). On the other hand, arsenite (As^{3+}) is the main form of As in reduced environments such as flooded soils (Li et al., 2018). Arsenite can be transported through plant cells via silicon transporters due to similar chemical characteristics of Si and arsenite (Bakhat et al., 2017)

Arsenic is an incompatible element, and its concentration in felsic rock is more than in mafic rock (Kabata-Pendias, 2001). It is a well-known pathfinder element for the geochemical prospecting of metals as it is associated with many ore deposits (Dunn, 2007b; Kabata-Pendias, 2001). The concentration of As in substrates can likely be reflected in plant samples. Therefore, whether the sample medium is rock, soil, water, or vegetation, As can be of great value as a pathfinder element for metals such as Au (Dunn, 2007b). Among conifers, Douglas Fir can accumulate a significant amount of As in its tissue (Warren et al., 1968). Studies also show high As concentrations in black spruce (Dunn et al., 1995; Ghorbani et al., 2022).

Bismuth (Bi): Bismuth is a rare element in the earth's crust (Babula et al., 2009). It is also a non-essential element for plant metabolic function. The process of Bi absorption and translocation in plants is still unknown. A study by De La Espina et al. (1993) suggested that it may interact with nuclear proteins and then enter plant cells. Similar to As and Sb, Bi has chalcophile properties and is associated with elements such as Ag, Co, Pb, and Zn (Kabata-Pendias, 2001). Bismuth is one of the indicators for many types of mineralization, but its concentration in vegetation is commonly lower than the detection limit of many analytical techniques (Dunn, 2007b). Therefore, high values of Bi need to be inspected closely to determine their significance.

Cadmium (Cd): Cadmium is a non-essential element for the metabolic process of plants (Kabata-Pendias, 2001). However, it can be absorbed by the root system due to its geochemical affinity with Zn (Smeyers-Verbeke et al., 1978). Kabata-Pendias (2001) and Clemens (2006) also reported that Ca, Fe, Mn, Mg, Cu, and Ni can be replaced by Cd. Some of these elements, such as Fe and Ca, have antagonistic interaction with Cd and reduce its absorption by plant roots and, therefore, its translocation to shoots (Gallego et al., 2012). Cadmium in plants is likely to be

captured by the cell wall components and accumulated and stabilized in the bark (Ghorbani et al., 2022). According to Ismael et al. (2019), Cd concentration in plant roots is significantly higher than its shoot. It might be due to the barrier mechanism of the plant preventing circulating toxic elements.

Birch and willow are found to have a high concentration of Cd, which can be related to its ubiquitous geochemical affinity for Zn (Kabata-Pendias, 2001). Therefore, It is suggested that Cd concentrations can be used to identify zones of Zn enrichment (Dunn, 2007b). Studies by Dunn et al. (2005 and 2007a) over the Cariboo zone in central British Columbia indicated a positive relationship between Cd and Au in spruce needles. Cadmium cannot always be considered a promising pathfinder element for gold mineralization. Nevertheless, its spatial relationship to elevated Au zones is sometimes of value in providing a focus for exploration efforts (Dunn, 2007b).

Lead (Pb): Like other gold pathfinders, Pb is not an essential element for plant metabolism. However, it can mimic the biogeochemical and physiological behaviour of Ca and replace it metabolically. Lead is more commonly accumulated in the cell walls as it follows Ca. Positive correlations between Pb in the substrate and overlying plants have been reported, which is helpful for biogeochemical prospecting (Kovalevskiy, 1979; Warren, 1978). As explained before, macronutrients have antagonistic interaction with trace elements. Zinc, P and S reduce Pb absorption and translocations by plants cell (Sharma and Dubey, 2005). In contrast, Cd and Pb have synergistic interactions (Kabata-Pendias, 2001). The outer bark of conifers is reported to accumulate the highest Pb values (Dunn, 2007b).

Thallium (Tl): The concentration of Tl in plants positively correlates with its values in soil (Kabata-Pendias, 2001). Thallium can be enriched in polymetallic deposits along with As and Sb (Warren et al., 1964). Geochemically, It can disperse during the oxidation of sulphides due to its high mobility, making it available to plant roots (Dunn, 2007b). Thallium can be an important biogeochemical prospecting tool for Au (Warren and Horsky, 1986; Dunn, 2007b). Shacklette et al. (1978) reported higher concentrations of Tl in ashed pine needles than in stems.

1.2 Exploratory Data Analysis (EDA)

Geochemical surveys can be conducted using any geochemical media, such as drilled cores, surface rock, soil, water, lake sediment, plant, and airborne particles. A large geochemical dataset, including more than 30 elements (depending on the analytical package), can be extracted after sample collection. Geochemical data are compositional and subjected to basic error-checking before being passed as a suitable dataset for analysis. The major problem in geochemical data includes censored values, non-normal distribution, and the constant-sum problem. Censored data are values that could not be detected due to either a low concentration of elements of interest or low sensitivity of the analytical techniques (Sanford et al., 1993). Censored values are missing data with partial information about their range that is generally reported below the detection limit (DL) (Grunsky, 2010). The censored data can influence the interpretation of geochemical data. Therefore, they must be either eliminated or replaced by a substitution value. A study by Carranza (2011) on stream sediment data with censored values indicated that the multi-element anomaly maps excluding censored data are not better than those including censored data. One approach is to use the measured value (censored value) reported by the lab. This method avoids misusing low-quality data. However, it results in the loss of valuable information (Keith, 1994). Another method is to replace values with $\frac{1}{2}$ or $\frac{3}{4}$ of DL for values below DL and $\frac{4}{3}$ of DL for values above DL (Sanford et al., 1993). It is suggested to use this method when 10 to 20% of data are censored. Otherwise, the accuracy of data and reliability of interpretations would be sacrificed (Sanford et al., 1993). Another method suggested by Pawlowsky-Glahn and Egozcue (2002) is to replace missing or censored values with a geometric mean of all available data (Hron et al., 2010). However, this method can not be applied to the multivariate data structure. Chung (1993) and Grunsky (2020) suggested using the maximum likelihood estimation developed by Cohen (1960) to impute censored values when a large number of data are below DL (Chung, 1993; Cohen, 1961; Grunsky and de Caritat, 2020). This method uses the normal distribution to reproduce mean and skewness and is reported to provide more consistent results than simple arbitrary substitution (Cohen, 1961; Cohen, 1976; Sanford et al., 1993).

The compositional data is expressed as part of some whole such as (part per billion) ppb, (part per million) ppm, or weight percentage (wt.%). It means that the sum of the elemental

composition in geochemical data is constant. Therefore, as some values increase, other values are forced to decrease in order to maintain the sum constant. Also, compositional data are only distributed in real positive space numbers, resulting in incorrect assessments of correlations (Grunsky, 2010). The constant sum or data closure problem is the most important limitation related to compositional data that may lead to bias in correlations between two variables (Filzmoser et al., 2009a, 2009b; Rollinson, 1992; Thió-Henestrosa and Martín-Fernández, 2005). This issue can be addressed using logarithms of ratios developed by Aitchison (1986) (Aitchison, 1982; Buccianti and Grunsky, 2014; Filzmoser et al., 2009a). Log-ratio transformations open the closed number system and normalize compositional data by projecting them into positive and negative real number space. It is important to apply the transformation carefully to prevent masking the presence of multiple populations and outliers (Link and Koch, 1975). There are several types of log transformations, including log-ratio, natural (ln) log-ratio, centred log-ratio (CLR), isometric log-ratio (ILR), and additive log-ratio (ALR) transformations (Aitchison, 1982; Carranza, 2011; Egozcuewt al., 2003), of which CLR transformation was reported to provide a better insight into elemental associations than other types of transformations (Carranza, 2011; Filzmoser et al., 2009b; Reimann et al., 2011). CLR transformation is calculated using

$$\text{clr}(x) = \left[\log \frac{x_1}{g(x)} \cdots \log \frac{x_D}{g(x)} \right],$$

where $g(x)$ is an geometric mean of (x) (Aitchison, 1986).

The maximum amount of information from data can be obtained using exploratory data analysis (EDA) techniques such as univariate and multivariate data analysis. Exploratory data analysis is a preliminary approach to identifying trends and structures in geochemical data. In this method, the individual distribution of data can be evaluated using numerical and graphical methods. The EDA includes (1) a summary of statistics (e.g., min, max, mean, median, and skewness) and (2) visualization methods such as box plots, histograms, scatter plot matrices, probability plots, clustering, and principal component analysis (PCA) (Grunsky, 2010).

Univariate Data Analysis

Univariate data analysis is the most straightforward data analysis in which each variable is measured separately. There are two types of univariate data: categorical and numerical.

Categorical data are non-numerical observations that can be categorized, such as gender, sample medium, or elements. Numerical data are numerical observations, such as the age or concentration of elements in a sample. The popular graphical methods for describing univariate data are histograms, box plots, probability plots, and scatter plots.

Histograms: The distribution of data can be visualized using histograms. Simply the distribution of data can be divided into normal (symmetrical) and non-normal (right or left-skewed) distributions. Also, it can be unimodal or multimodal. Figure 4 illustrates the common shape of datasets using histograms.

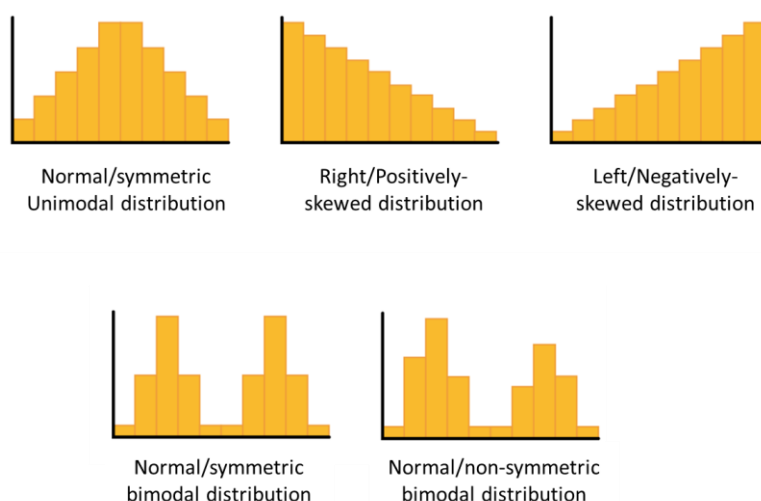


Figure 4. Examples of common distribution of data using histograms (modified after AMGEN- Histograms).

The numerical data in the histogram are grouped into bins or intervals with equal widths. Each bin includes a bar whose height corresponds to the number of data points in each bin. Generally, ten bins suffice for data interpretations. However, to be more accurate, Sturge's rule can be performed, in which the number of bins equals $\text{Log}_2^x + 1$, where x is the number of samples (Scott, 2009).

Figure 5 compares the histogram of raw data (upper) and CLR transformed data (lower) for Ca and Cd. In raw data, the histogram of Ca is left-skewed while Cd is right-skewed,

indicating they are not normally distributed. Their distribution becomes closer to a normal distribution (symmetric) following CLR transformation. Also, the distribution of Ca data appears bimodal, which was hidden in the raw data. The bimodal distribution can be a result of two populations in the dataset.

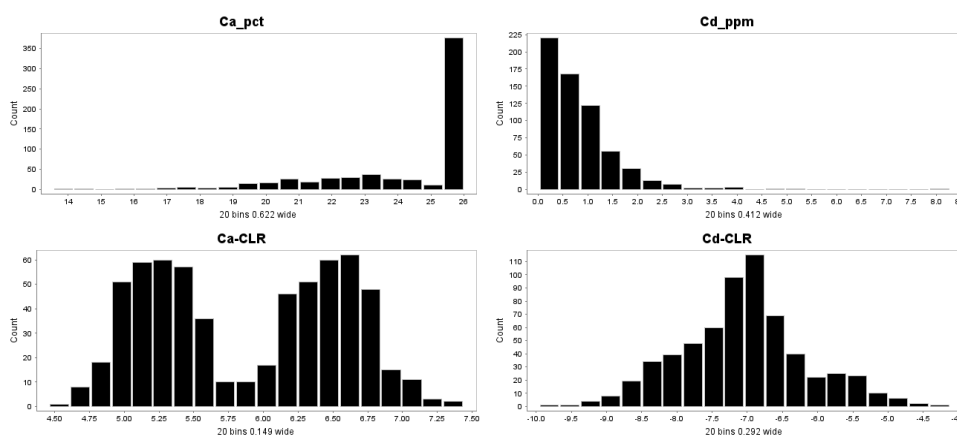


Figure 5. The comparison between raw (upper) and CLR transformed (lower) data for Ca and Cd values in needle samples at the YCGP.

Box Plots: Generally, a box plot is comprised of a box and two whiskers that show the data summary, including minimum, first quartile, median, third quartile, and maximum. Box plots use the quartiles to provide a fast visual estimation of the locality, dispersion, and skewness of numerical data (DuToit et al., 2012). In box plots, outliers can be identified as individual points plotted beyond the box plot's whiskers (Tukey's definition) (Tukey, 1977) (Figure 6). A is a box plot schematic in which the first or lower quartile shows the 25th percentile (Q1), and the third or upper quartile shows the 75th percentile (Q3) of data. The location of the median line (50th percentile-Q2) and the lengths of the whiskers on each side of the box show the symmetry of data distribution. In a symmetric box plot, the lengths of whiskers are the same and equal to the 1.5 interquartile range (IQR). While in the skewed box plot (Figure 6**Error! Reference source not found.**), the median is closer to the Q1 (right-skewed) or the Q3 (left-skewed). Figure 7A is an example of a box plot summarizing the concentration and distribution of S in needle samples collected at the YCGP. The figure shows that the mean and median have different values, data are right-skewed, and contain extreme outliers. Following CLR-transformation, extreme outlier disappeared, mean and median overlapped, and data distribution

turned into a symmetric distribution. Figure 7B shows how orders of abundances of S in vegetation change before and after CLR transformation.

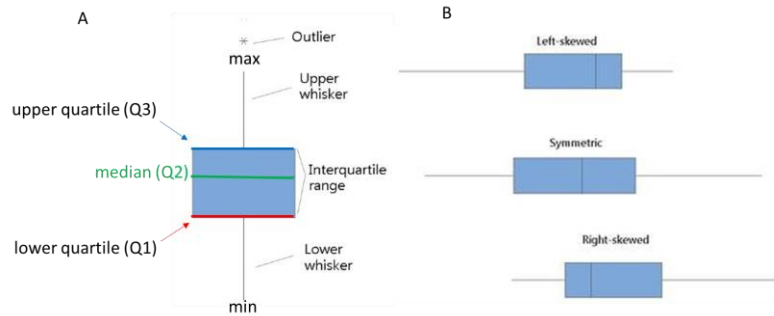


Figure 6. (A) a schematic box plot showing the summary data, (B) box plots showing the skewness of data (modified after Skewed Distribution - Z TABLE)

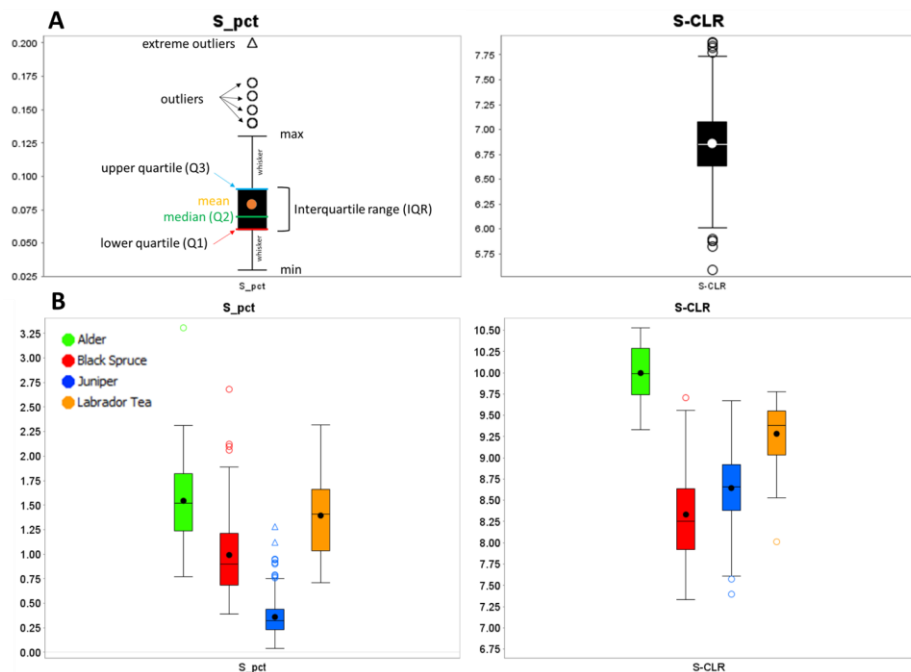


Figure 7. (A) Box plot of sulphur (S) data showing the summary of S data in needles samples collected at the YCGP vs CLR-transformed S data. (B) change in orders of S data abundances in vegetation in raw data and CLR transformed data.

Probability plot: A probability plot is a technique to visualize data distribution and identify outliers and skewness (Sinclair, 1974). In this method, data points are plotted against a

theoretical distribution (z-score), forming a straight line if data is normally distributed. Any deviation from the straight line may show a right- or left-skewed distribution. Figure 8 shows the probability plots of As and CLR-As. Arsenic data points do not follow a straight line, showing that they are not normally distributed and require log transformation.

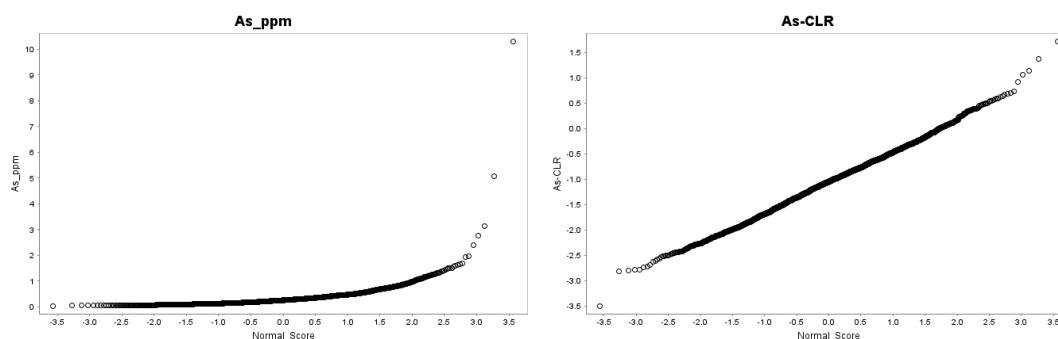


Figure 8. Probability plots of As and CLR-transformed As show data distribution before and after normalization.

Scatter Plots: A scatter plot is a mathematical graph showing the relationship between two quantitative variables in a two-dimensional system. A scatter plot consists of an independent variable (IV) and a dependent variable (DV). The IV is the controlled variable and is generally graphed on the x-axis. While DV, which is graphed on the y-axis, is influenced by the IV. The correlation between two variables can be described using form, direction, and strength. The form of a scatter plot can be linear or non-linear. The correlation between two variables can have a positive or negative direction and sometimes without any direction showing no correlation. Finally, variables can show strong, moderate, or weak correlations. Figure 9 shows examples of different patterns in a scatterplot.

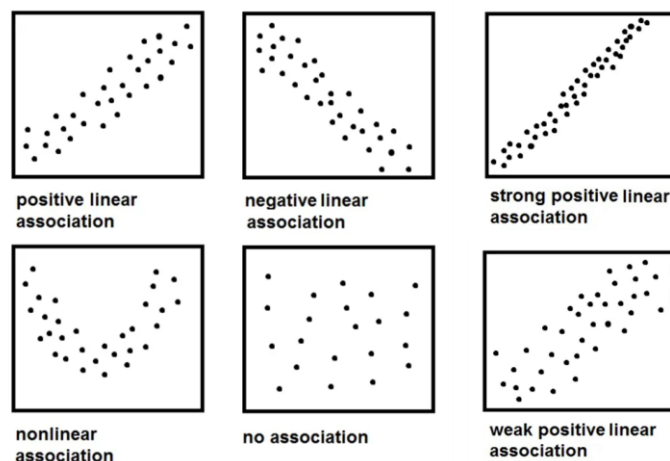


Figure 9. Examples of different patterns to describe the correlation between two variables in scatter plots (modified after math boot camps)

1.2.1 Multivariate Data Analysis

Multivariate analysis is a statistical method that analyzes data using more than one variable. These techniques study the inter-relationship of multiple variables with dependent, independent or both input variables. The multivariate data analysis technique is particularly useful when there is a large dataset with a high degree of correlation between the variables, indicating that there is superfluous information. This type of statistical analysis is also known as a dimension reduction method that reduces the number of variables for data modelling and generates a subset of variables based on the correlations between the original variables. Principal component analysis (PCA) and inverse distance weighted (IDW) interpolation methods are well-known examples of multivariate data analysis.

1.2.1.1 Principal Component Analysis

PCA was first mentioned by Fisher and Mackenzie (1923) as a more suitable analysis for data modelling and then developed by Hotelling (1933) to its current stage. Biplot PCA was presented by Gabriel (1971) as a useful tool for data analysis that allows the visual evaluation of the structure of large data matrices. Following that, RQ-mode PCA was introduced by Zhou et al. (1983) R-mode explains the correlation between variables. This method focuses on the interrelationship between variables, while Q-mode represents the correlation between samples (Chen, 2015; Neff, 1994). This method plots the observations (samples) and variables

(elements) on the same diagram, presenting the principal component scores of the observations and the variables at the same scale. In Earth sciences, a comprehensive introduction to PCA was provided by Davis (1986) and Mellinger (1987), who established the standards and systematic approaches for geological data analysis (Davis and Sampson, 1986; Grunsky, 2010; Wold et al., 1987). Also, in a distinguished book by Brook et al. (1995), a summary of the application of statistical analysis to biogeochemical data was explained.

Generally, PCA is an image processing and data analysis method that reduces the number of correlated variables and forms a subset of linearly uncorrelated variables called the principal component or PC (Hotelling, 1933). The formed PCs, which are derived from correlations or covariance matrix of data, describe the data distribution. The fundamentals for describing and evaluating PCA results are the pairs of eigenvectors-eigenvalues and scores-loadings (Jolliffe and Cadima, 2016). A dataset matrix is described by its eigenvectors and eigenvalues, explaining the total variance of the dataset. The magnitude of each eigenvector is determined by its corresponding eigenvalue. PC vectors are the eigenvectors with the highest eigenvalues that define the directions of the new feature space, explaining the maximum data variability (Figures 10 and 11). According to the Kaiser criterion, eigenvalues greater than one account for the main PCs (Kaiser, 1960).

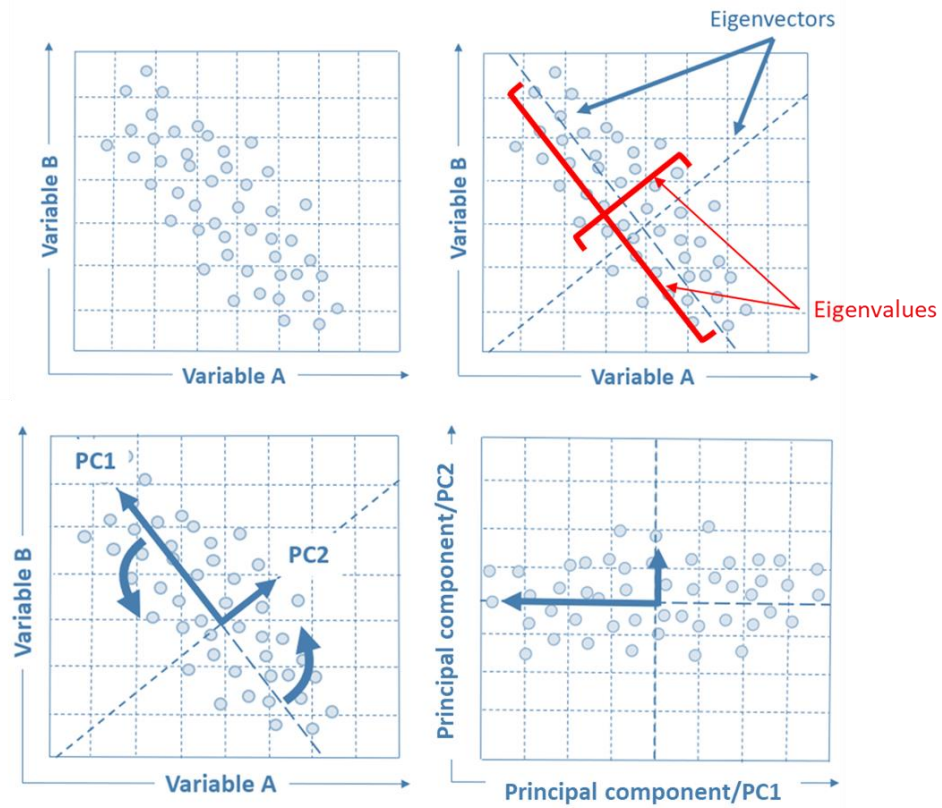


Figure 10. Schematic of a new feature space (Principal components) created by eigenvalues and eigenvectors. The eigenvectors show the direction of the new PC, and the eigenvalues define the magnitude (modified after Firman, 2019).

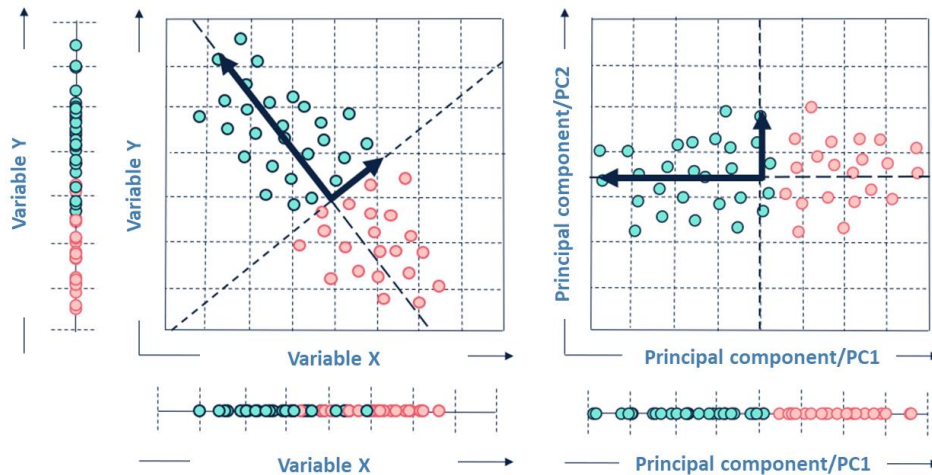


Figure 11. The dimension reduction method creates new feature space. PC1 is responsible for the variance of variables A and B (modified after Firman, 2019).

Scores are the transformed variable values for each sample point, whereas loadings are the weights by which each original standardized variable is multiplied to create the score (Figure 12) (Benz, 2017). Positive loadings mean the positive correlation between a variable and a PC.

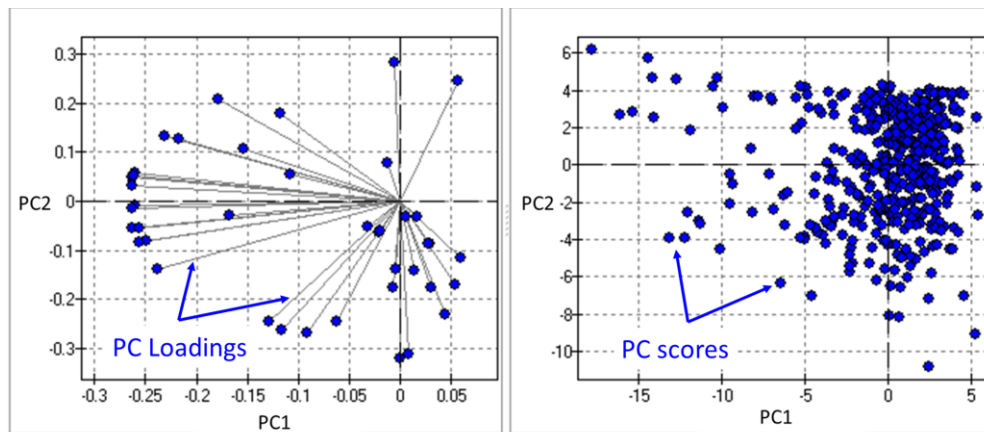


Figure 12. A schematic of the score and loading plot. Scores are the transformed data value for each sample. Loadings are vectors that define the correlation between scores and PC (Dragon 6 User's Manual).

PCA is a well-known method in the evaluation of multi-element associations and interrelationships related to geological processes (Chen, 2015). In PCA, each PC gives a piece of

information about the possible geological/geochemical process controlling the distribution of elements. It can be partial melting, crystal fractionation, alteration/mineralization, metal associations and enrichments, weathering processes, etc. There are several studies on the application of PCA to geochemical and biogeochemical data, indicating that the plant-substrate relationship can be used to discover either the source of contamination or concealed mineralization (Benz, 2017; Dunn and Heberlein, 2020; Larsen et al., 1992; Nade et al., 2012; Oliva and Espinosa, 2007; Schaug et al., 1990).

1.2.1.2 Inverse Distance Weighted Interpolation

The inverse distance weighted (IDW) is a spatial prediction method that Shepard (1968) introduced. The IDW assumes that points close to one another are more alike than that farther away, and the local influence of each point diminishes with distance (Burrough et al., 2015; Ghezlbash et al., 2019). Therefore, the IDW method gives more weight to points that are closer to the prediction location (Figure 13). Let x_i be the sample points with the known corresponding value $u(x_i)$ for $1 \leq i \leq n$. The goal is to compute the value $u(x)$ of each given point x using the formula shown in Figure 13 (Shepard, 1968), where w is the relative weight, d is distance, and p is the power value. Mathematically, weights are proportional to the inverse of the distance that is raised to the power value p . Therefore, the weight decreases exponentially as distance increases. If $p=0$, the prediction value is equal to the mean of all data values in the neighbourhood, while a very large p -value gives approximately the same weight as the closest surrounding point. In geological software, the default p -value equals 2, although there is no justification for considering this value over other p -values (Vural, 2019). The IDW is a popular multivariate interpolation method for processing large geochemical datasets. This method is useful for creating element distribution maps and delineating geochemical anomalies (Cheng, 1999; Lima et al., 2003; Xie et al., 2010).

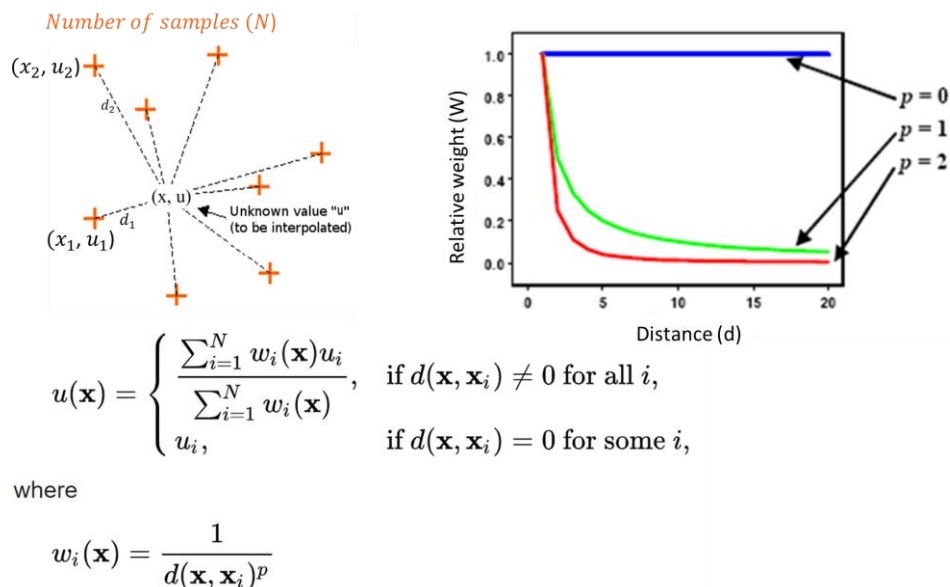


Figure 13. A simple schematic and formula showing the function of the inverse distance weighted (IDW) interpolation method (modified after Wikipedia).

1.3 Research Objectives and Outcomes

Biogeochemical exploration surveys have been widely used across the world to identify the presence of concealed mineralization using plant samples (Dunn, 2007b). However, there is a significant lack of data treatment, such as opening data closure, which results in biased and unreliable interpretations of biogeochemical data (Benz, 2017). The compositional nature of biogeochemical data, like any geochemical data, requires a systematic statistical approach to be interpreted effectively and meaningfully. Therefore, this research aims to show the importance of data preparation and the requisite steps before data analysis and interpretation. Also, it aims to attest to the significance and potential of robust multivariate statistical analysis to delineate zones of metal enrichment using biogeochemical exploration. To achieve the objectives of this study, three biogeochemical datasets are selected to evaluate data statistically. The datasets include the chemical analysis of different plant species and tissues collected over the early and advanced gold targets at the MBGP and YCGP.

No previous biogeochemical survey was conducted at the MBGP. This study is applied to identify geologically meaningful responses in plant samples associated with buried mineralization and examine the potential application of biogeochemical and statistical techniques

in mineral exploration. The results of the multivariate statistical analysis, such as PCA and IDW interpolation method, are applied to identify the plant-substrate relationship and find new vectors towards the extensions of gold mineralized zones. Also, the results of this study will be used as a supplementary exploration program to support previous exploration efforts and regional target generation.

The biogeochemical study over the YCGP has covered the entire property. It provides a unique opportunity to have a better understanding of the biogeochemical response in plant samples with respect to different lithologies. Also, datasets including multiple plant species are compared to identify the optimum plant medium representative of the study area. The implications of this research for Au prospectively using biogeochemical and statistical techniques are demonstrated using sets of systematic data preparation and robust multivariate statistical analysis.

This thesis is outlined in six chapters, including (1) an introduction and literature review; (2) a geological setting; (3) an application of multivariate data analysis to biogeochemical exploration at the Twin Lakes Deposit, Monument Bay Gold Project, Manitoba, Canada; (4) biogeochemical prospecting for gold at the Yellowknife City Gold Project, Northwest Territories, Canada: part 1- species optimization; (5) biogeochemical prospecting for gold at the Yellowknife City Gold Project, Northwest Territories, Canada: part 2- robust statistical analysis; and (6) summary and future research; as well as three appendices. Chapter 1, the introduction and literature review, describes the history and application of biogeochemical exploration to identify zones of metal enrichment. Also, it covers the application of data analysis to mineral exploration, the fundamental steps before statistical analysis, and the significance of robust statistical analysis in multi-element geochemical data interpretation. Chapter 2 describes the geological setting of the Archean greenstone-hosted orogenic gold deposit and the regional geology of two case studies conducted over the Monument Bay Gold Project and Yellowknife City Gold Project. Chapters 3 to 5 refer to the application of robust multivariate statistical analysis to biogeochemical exploration, covering the case studies conducted over the Monument Bay Gold Project and Yellowknife City Gold Project. The results of studies in chapters 3, 4, and 5 were published in *Chemical Geology* and *Applied Geochemistry*, respectively. The summary of this research and recommended future works can be found in chapter 6. Also, Appendices A to C

compare raw and transformed data for each biogeochemical dataset. The results of this research will assist geochemists in interpreting data effectively and uncovering latent information that may not be revealed unless robust data analysis is employed. Consequently, it will help to identify new Au targets at low cost and with significant reliability.

Chapter 2

2 Geological Setting

2.1 Archean Greenstone Hosted Orogenic Gold Deposits

The orogenic gold deposits are the primary source of gold globally. These deposits were mainly formed during the Archean to Phanerozoic at variable temperatures and pressures corresponding to the greenschist to amphibolite metamorphic facies (Gaboury, 2019; Goldfarb et al., 2005; Groves et al., 1998; Groves, 1993). Fluid sources, ligands, gold solubility, conduits, and the mechanisms for gold precipitation are the main parameters for the formation of orogenic deposits (Gaboury, 2019). Figure 14 indicates the proposed systematic analysis for the formation of orogenic gold deposits, including a linear succession of processes from bottom to top and in time.

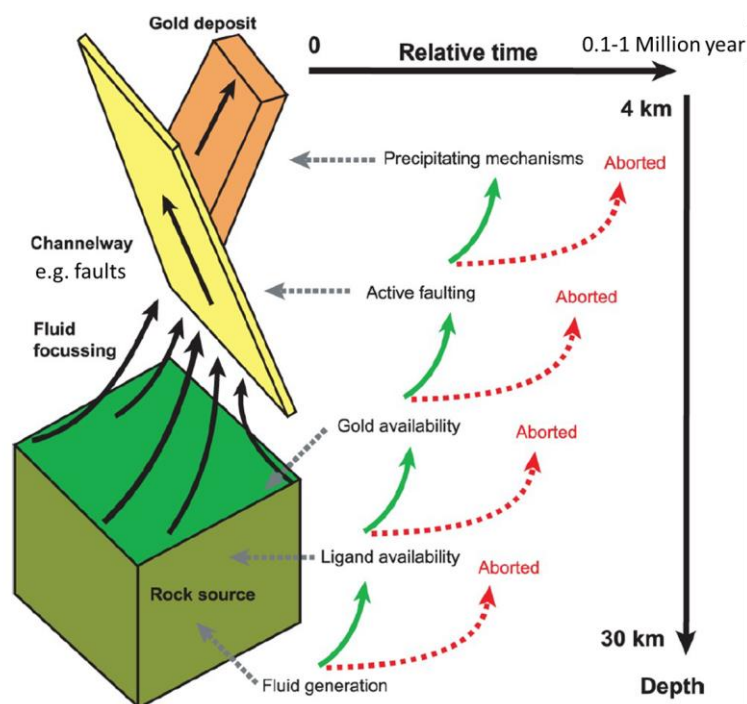


Figure 14. The conceptual representation of the critical factors controlling the formation of orogenic gold deposits. The succession of the process from bottom to top (fluid, ligand, gold, active fault system and efficient mechanism) and in time is required; otherwise, the mineralization system aborts (modified after Cox, 2016).

The primary origin of fluid at the orogenic gold deposit has been controversial since the oxygen and deuterium isotope data are located over the superposed field of magmatic and metamorphic fluids (Diamond, 2000). Magmatic fluids were suggested to have a felsic magma or granitic source (Xue et al., 2013). The origin of metamorphic fluids is the dehydration of seafloor rocks as a result of the metamorphic transition of greenschist to amphibolite at the temperature and pressure of $\sim 550^{\circ}\text{C}$ and $\sim 2\text{-}10$ Kbar, respectively (Phillips and Powell, 2010). Gold exists in three oxidization states of 0, 1+ and 3+. Under atmospheric conditions, gold is a non-reactive element that requires a ligand to increase its solubility and hydrothermal transportation. Hydrogen sulphide (HS^-) is suggested to be the preferred ligand for gold under hydrothermal conditions (Williams-Jones et al., 2009). The source of gold at orogenic gold deposits is not associated with a specific rock type and is still under discussion. It can be from basalts (Pitcairn et al., 2015), felsic magmas (Xue et al., 2013), or iron-rich formations (Lambeck et al., 2011). Recently, the primary pyrite formed as a result of bacterial reduction of sulphate on the seafloor was suggested as a primary source of gold (Pitcairn et al., 2015). At the same time, other studies by Large et al., 2007 and 2012, proposed that arsenic-bearing pyrites hosted in black shales are required for the development of orogenic gold deposits. Active structural discontinuities such as faults, shear zones, and folds act as conduits for the migration of fluids below the greenschist-amphibolite transition to the upper crust precipitation sites (Vearncombe and Zelic, 2015). Curvilinear faults, in particular, provide more permeability to transfer higher volumes of fluids (Gaboury et al., 2001). Finally, gold precipitates when CO_2 is removed from gold mineralizing fluids, resulting in acidic fluids (Phillips and Evans, 2004). A combination of these factors leads to an efficient mechanism of gold precipitation within pyrite.

Archean greenstone belts are the primary hosts to orogenic gold deposits. They include a sequence of metamorphosed mafic, ultramafic, and felsic volcanics associated with sedimentary rocks between granite and gneiss bodies within the Archean and Proterozoic cratons (Brandl et al., 2006). The well-known examples of greenstone belts in Canada are the Abitibi Greenstone Belt in the Superior Province, Ontario, and the Yellowknife Greenstone Belt in the Slave Province, Northwest Territories. At the Archean greenstone belt orogenic gold deposit, the mineral assemblage associated with quartz-dominated veins includes 3-5% iron sulphides and 5-15% carbonate minerals (Dubé, 2007;

Groves et al., 1998). The alteration minerals differ based on the host rock. Fuchsite, scheelite, albite, chlorite, and tourmaline can be mostly seen at greenschist metamorphic facies (Dubé, 2007). Gold mineralization shows significant enrichments of As, B, Bi, Hg, Sb, Te, and W (Groves et al., 1998).

Archean Greenstone-hosted orogenic gold deposits are a significant source of gold in the Superior and Slave provinces of the Canadian Shield. The Canadian Shield is mainly composed of Archean craton and Proterozoic orogens that make the Precambrian core of North America, dating 4.2 to 2.5 Ga (Card and Ciesielski, 1986). The Canadian Shield was first divided into different provinces and subprovinces based on their geological-geographical nature in 1939 (Card and Ciesielski, 1986). Later, a division based on the structural trend was proposed by Gill (1949). Wilson (1949) divided the Canadian shield based on the lithological and geochronological characteristics. He suggested that the Canadian shield was formed due to the successive accretion of orogenic belts around the central core formed by the Superior Province. Following that, studies by Stockwell (1964-1982), Douglas (1973), and Goodwin (1978) resulted in the subdivision of the Canadian shield into seven provinces according to the distinct structural trend, age, geological characteristics, and mineral deposit. Figure 15 shows the Canadian shield's final division, including the Nain, Grenville, Southern, Superior, Churchill, Slave and Bear provinces (The Canadian Encyclopedia).

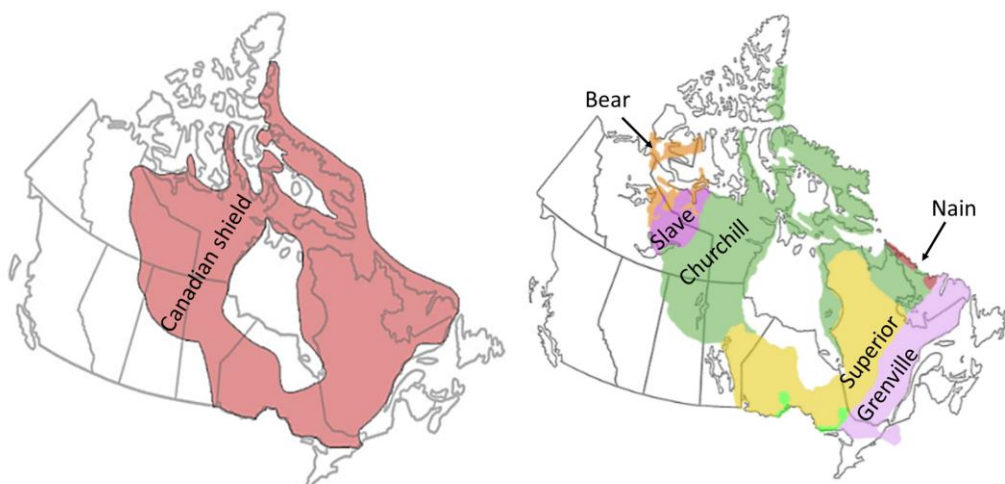


Figure 15. The Canadian Shield (left) and the seven geological provinces within it, including Nain, Grenville, Southern, Superior, Churchill, Slave and Bear provinces (modified after the Canadian Encyclopedia).

2.2 The Superior Province

The term “Superior Province” was proposed by Gill (1949). The Superior Province, the nucleus of the Canadian shield, contains the largest development of the exposed Archean craton dating 3.1-2.6 Ga years ago (Anhaeusser, 2014). It covers a 1572000 km² area, including northern Minnesota in the United States and central and north of Quebec, extending across central and southern Ontario to southwest Manitoba in Canada (Anhaeusser, 2014). The general composition of the Superior Province includes high-grade gneiss in the northwestern, pervasive metamorphic rocks in the northeastern, and metavolcanic-metasedimentary rocks in the southern parts (Card and Ciesielski, 1986). The Superior Province is divided into several linear subprovinces and domains based on lithological and structural characterization, accentuated by subparallel boundary faults (Figure 16) (Percival, 2007). These subprovinces and domains are generally grouped into the Western and Eastern Superiors. Western Superior Craton includes several terranes and domains that are stitched together during the Neoproterozoic period as a result of the formation and accretion of island arcs (Card and Ciesielski, 1986; Percival, 2007; Percival and Skulski, 2000). At the same time, the collision between terranes is responsible for the formation of Eastern Superior (Percival and Skulski, 2000). The subparallel faults slicing the Superior Province follow three major trends. In the northwestern and northeastern, faults have

west-northwest and northwest directions. While, in the southern parts, faulting occurs in an east-west direction (Percival, 2007).

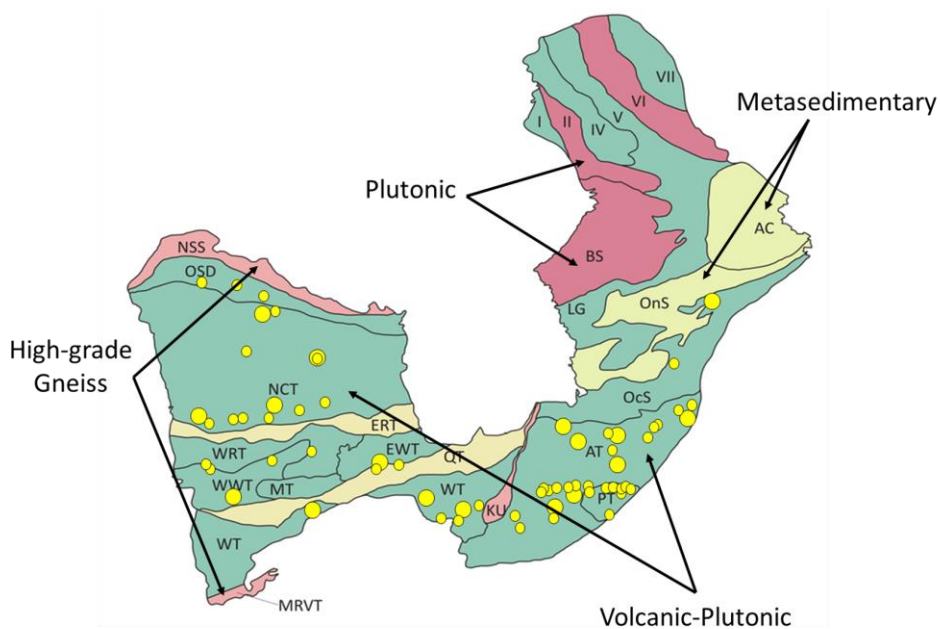


Figure 16. The Superior Craton is comprised of major subprovinces and domains, including NSS: Northern Superior Superterrane; OSD Oxford-Stull Terrane; NCT: North Caribou Terrane; ERT: English River Domain; WRT: Winnipeg River Domain; WWT: Western Wabigoon Terrane; EWT: Eastern Wabigoon Terrane; MT: Marmion Terrane; QT: Quetico Terrane; WT: Wawa Terrane; MRVT: Minnesota River Valley Terrane; KU: Kapuskasing Uplift; AT: Abitibi Terrane; PT: Pontiac Terrane; OcS: Opatoca Subprovince; AC: Ashuanipi Complex; OnS: Opinaca Subprovince; LG: La Grande Subprovince; BS: Bienville Subprovince; I: Inukjuak Domain; II Tikkerutuk Domain; IV: Lake Minto Domain; V: Goudalie Domain; VI Utsalik Domain; VII: Douglas Harbour Domain. Gold deposits of the Superior Province are shown in yellow circles (modified after Percival, 2007).

Five discrete orogenies, including the Northern Superior, Uchian, Central Superior, Shebandowanian, and Minnesotan, were involved in the development of the Western Superior (Percival, 2007). These orogenies with north-to-south directions assembled these terranes and domains. Research by Percival et al. (2006) indicated that before **Northern Superior Orogeny**

(2.72 Ga), the western Superior was many pieces of microcontinents separated by east-west trending oceanic crust (Percival, 2007). During 2.72 Ga, active subduction along the Northern Superior Superterrane (NSS) and North Caribou Terrane (NCT) resulted in the drifting of NSS (Figure 17).

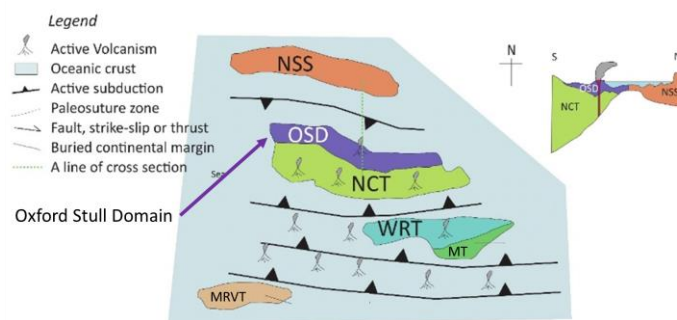


Figure 17. Before Northern Superior Orogeny (2.72 Ga), the Superior Craton was fragments of microcontinent separated by the E-W trending conduit-like ocean (modified after Percival et al., 2007).

Over time, the NSS joined the NCT and limited the Oxford Stull Domain (OSD). This event initiated the Superior Craton Formation. The two pieces of evidence for this event are the arc magmatism in OSD in 2.775-2.733 Ga and the south-over-north shear zone contact between NSS and NCT. During the **Uchlain Orogeny (2.72-2.70 Ga)**, the Winepig River Terrane (WRT) moved northward onto NCT and joined it (Figure 18).

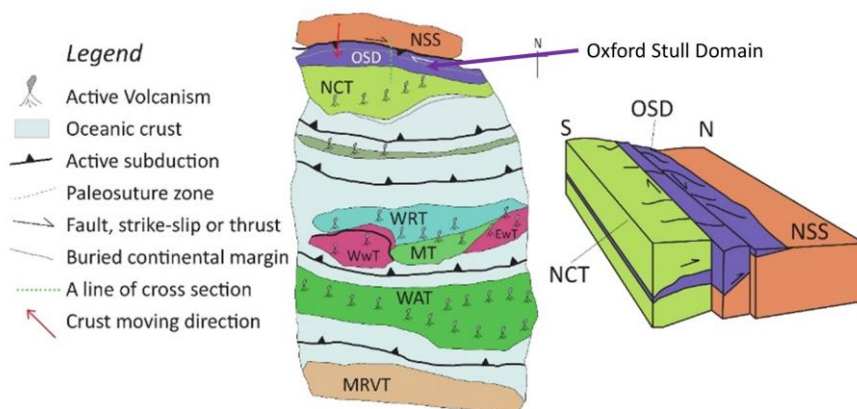


Figure 18. During the Uchlainn Orogeny, the NSS moves southward to NCT and limits OSD, initiating the formation of Superior Craton (modified after Percival et al., 2007).

The northeastward subduction of the younger Western Wabigoon Terrane (WWT) to the southwestern of the WRT was achieved during the **Central Superior Orogeny (2.70 Ga)** (Figure 19) (Cook et al., 2012). The **Shebandowanian Orogeny (2.69 Ga)** involves the accretion of the Wawa-Abitibi Terrane (WAT) to the southern margin of WWT (Figure 20) (Percival et al., 2012). The arc-related magmatism in WRT at 2.695 Ga is an indication of northward subduction. Cook et al. (2012) identified two deformations at the northern WAT during the Shebandowanian Orogeny. The first deformation (D1: 2.695 Ga) is the intra-arc deformation accompanied by calc-alkaline magmatism and the second one (D2: 2.685-2.680 Ga) is transpression deformation between WAT and WWT (Cook et al., 2012). **Minnesotan Orogeny (2.68 Ga)** is the last orogeny event marked by the Minnesota River Valley Terrane (MRVT) accretion with the composite Superior Cratone formed by the previous orogeny events (Figure 21).

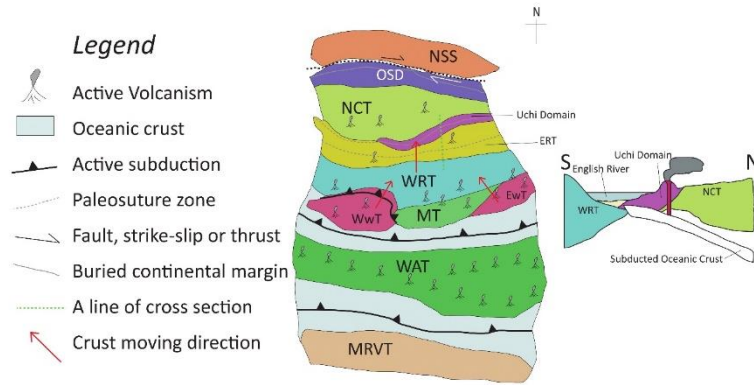


Figure 19. During Central Superior Orogeny, the WRT at the south subducted northward onto the NCT (modified after Percival et al., 2007).

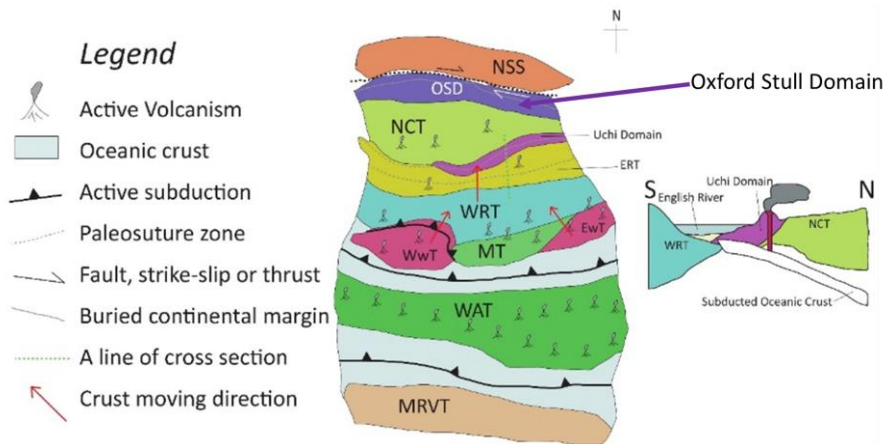


Figure 20. The WAT moved northward to collide with the composite Superior Craton during the Shebandowanian Orogeny (Percival et al., 2012).

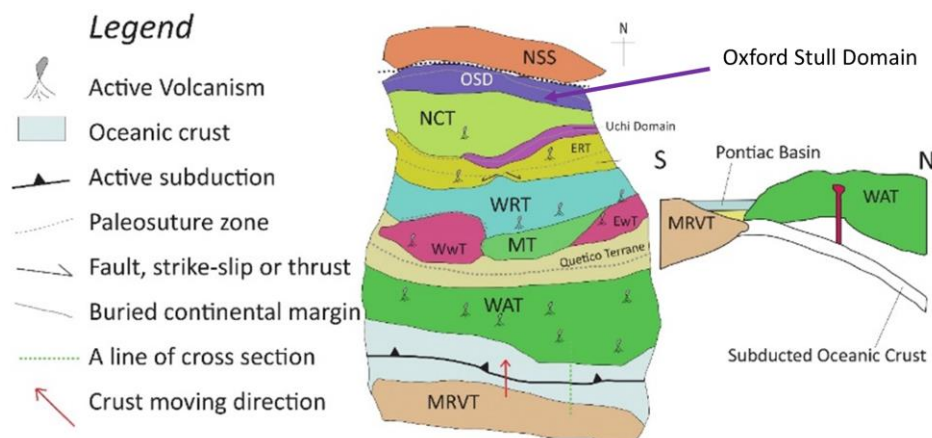
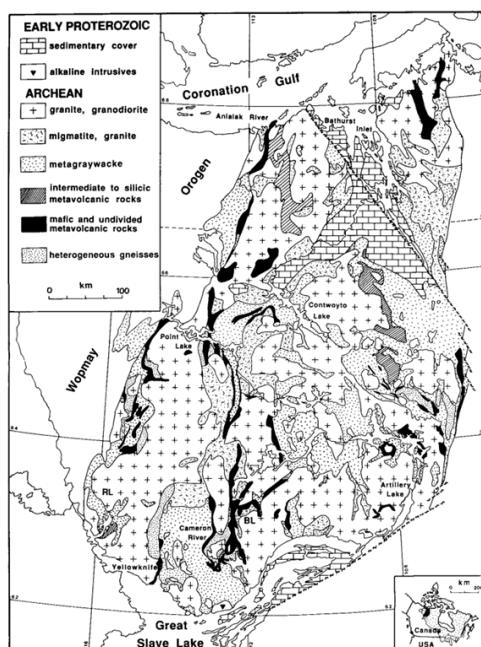


Figure 21. The MRVT moved northward to collide with the pre-mature craton during the final orogeny event, the Minnesotan Orogeny (modified after Cook et al., 2006).

Canada's largest gold deposits are located at the more than 35 different greenstone belts within the southeastern portion of the Superior Province (Figure 23) (Goldfarb et al., 2001). In the Superior Province, the orogenic lode-gold deposits are associated with Archean granite-greenstone terranes formed between 2.71 to 2.68 Ga (Dubé, 2007; Percival, 2007). The Abitibi Terrane (AT), Wawa Terrane (WT), and Oxford-Stull Domain (OSD) contain some of the largest Archean greenstone-hosted orogenic gold deposits in the Superior Province (Percival, 2007). The Monument Bay Gold Project (MBGP) is an economically promising Archean shear-hosted gold deposit located in the Oxford-Stull Domain (OSD), Superior Province.

2.3 The Slave Province

The Slave Province is an Archean age granite-greenstone terrane located in the northwestern part of the Canadian Shield (Kusky, 1989). According to Padgham (1985) and Kusky (1989), the Slave Province is formed as a result of a collisional tectonic model in which the accreted terranes are sutured (Helmstaedt and Padgham, 1986; Kusky, 1989; Padgham, 1985). Figure 22 shows the lithological map of the Slave province. Narrow north-trending swatch-shaped greenstone belts are concentrated in the central part of the Slave Province, creating a prominent line (Kusky, 1986). Greenstone belts to the west of this line are predominantly comprised of mafic volcanics and plutonic rocks, while those to the east consist of intermediate and felsic volcanic material (Padgham, 1985). Quartzofeldspathic gneisses are also limited to the west of the prominent line.



**Figure 22. Lithological map of the Slave Province, Modified after Henderson (1985)
(Henderson, 1985).**

Kusky (1989) divided the Slave Province into four tectonostratigraphic terranes: Anton, Sleepy Dragon, Contwoyto, and Hackett River volcanic terranes (Figure 23). It is proposed that these terranes are separated by high-strain zones recording large displacements (Henderson, 1985; Kusky, 1989). Anton Terrane composed rocks from the Yellowknife to the Anialik River. It hosts some of the oldest rocks in the Slave Province, including a tonalitic gneiss exposed in a basement culmination in Wopmay orogen (3.48 ± 6 Ga) and gray tonalitic rocks in a diatreme near Yellowknife (3.21 Ga) (Baadsgaard et al., 1980). Anton Terrane also includes quartzofeldspathic gneisses that are widely but sporadically distributed throughout the terrane (Easton, 1985) and primarily surrounded by younger granitoid. The Sleepy Dragon terrane is the smallest terrane which extends from northeast of Yellowknife to Point Lake. The rock composition includes intermediate to mafic quartzofeldspathic gneiss, banded and migmatitic gneisses, and chloritic granite (Krogh and Gibbins, 1978). The protolith to the Sleepy Dragon gneisses is granodiorite and tonalite. Covello et al. (1988) suggested that shallow-water sedimentary sequences near Detour Lake unconformably deposited on these gneisses (Kusky, 1989). The Contwoyto terrane consists of graywacke-mudstone turbidites composed of matrix, rock fragments (felsic volcanics, mafic volcanics, chert, granite), and feldspars (Henderson,

1985). These sediments are exposed in a series of westward-directed folds and thrusts (Bowring and Van Schmus, 1984). In many areas, the sediments of Contwoyto terrane are underlain by greenstone belt mafic volcanics (Kusky, 1988). According to Kusky (1988), the base of these greenstone belts is either truncated to unknown. There are also other greenstone belts in the Contwoyto terrane that are primarily composed of basaltic pillow lavas and exhibit both tholeiitic and calc-alkaline differentiation trends (Padgham, 1985). The volcanics of Contwoyto terrane are intruded by a series of granitoids, characterizing an accretionary prism tectonic setting (King et al., 1988). The Hackett River arc rocks are significantly different from the mafic volcanics of Contwoyto terrane, including a series of predominantly felsic volcanic piles and some synvolcanic granitoid rocks (Padgham, 1985).

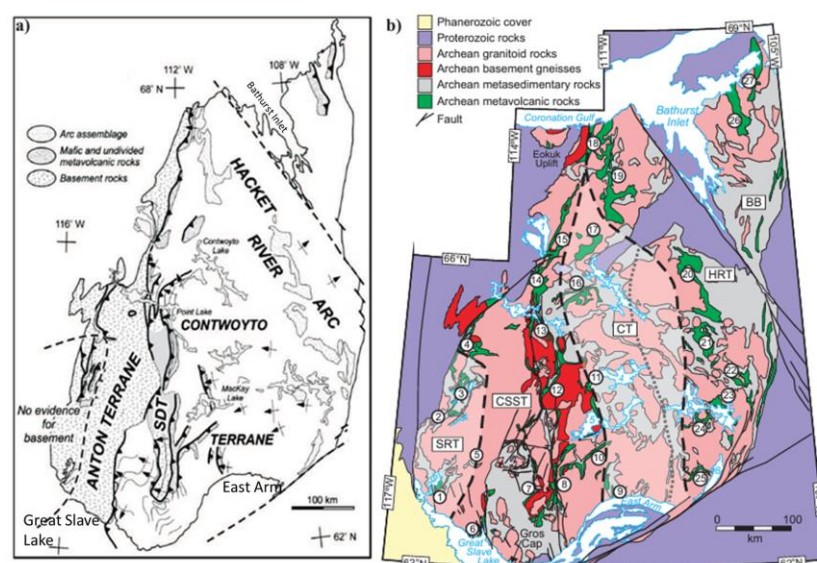


Figure 23. (a) The tectonostratigraphic terranes in the Slave Province, including Anton, Sleepy Dragon, Contwoyto, and Hackett River volcanic terranes proposed by Kusky (1989), (b) Modified terrane map proposed by Helmstaedt and Pehrsson (2012) (H. H. Helmstaedt, Pehrsson, Percival, Cook, and Clowes, 2012). BB: Bathurst Block, CSST: Central Slave superterrane, CT: Contwoyto Terrane, HRT: Hackett River Terrane) (modified after Padgham, 1985).

According to a modification by Helmstaedt and Pehrsson (2012), the slave province is subdivided into five tectonic terranes, including the Central Slave superterrane (CSST), Hackett River Terrane (HRT), Contwoyto Terrane (CT), Snare River Terrane (SRT), and Bathurst Block

(BB). Central Slave superterrane (CSST) includes the Sleepy Dragon terrane and some parts of the Anton terrane. The basement core of the Slave Province varies in the western part, where CSST is located (Bleeker, 2002). The southern portion of CSST is termed the Central Slave Basement Complex (CSBC) (3.4 to 2.85 Ga) (Bleeker et al., 2000), and the northern portion of CSST is called the Northern Slave Basement Complex (NSBC) (4.0 to 2.85 Ga) (Bleeker, 2002). These two basements were combined and overlapped by pre-Yellowknife Subgroup sequences by 2.58 Ga (Helmstaedt et al., 2012). The Hackett River Terrane (HRT), located in the eastern portion of the Slave province, is composed of calc-alkaline volcanic rocks dominated by felsic to intermediate rocks (Cairns et al., 2005; Lambert, 2005). The Contwoyto Terrane (CT), located between the CSST and HRT, is dominated by metasedimentary packages. The Snare River Terrane (SRT), located in the most western part of the Slave province, is a distinct crustal block that evolves independently from CSST (Bennett et al., 2005). According to Bennet (2005), the composition of the SRT includes a plutonic-gneiss core with highly metamorphosed supracrustal remnants encircled by a low-grade metamorphosed supracrustal belt (Bennett et al., 2005; Helmstaedt et al., 2012). Bathurst Block (BB) was not identified by Kusky's terrane map and is still poorly known. This portion of the Slave province contains mafic volcanic rocks similar to the Yellowknife Greenstone Belt (Sherlock et al., 2003).

2.4 Geology of Case Studies

2.4.1 The Monument Bay Gold Project (MBGP)

The Monument Bay Project (MBGP), spanning the border between northeastern Manitoba and northwestern Ontario, comprises 136 contiguous claims with 312,5 Km² of land in Manitoba (McCracken, 2016). Tectonically, the MBGP is located in the Oxford-Stull Domain (OSD), Situated between the Hudson Bay Terrane (HBT) and the North Caribou Terrane in the northwest of the Superior Province (Figure 24).

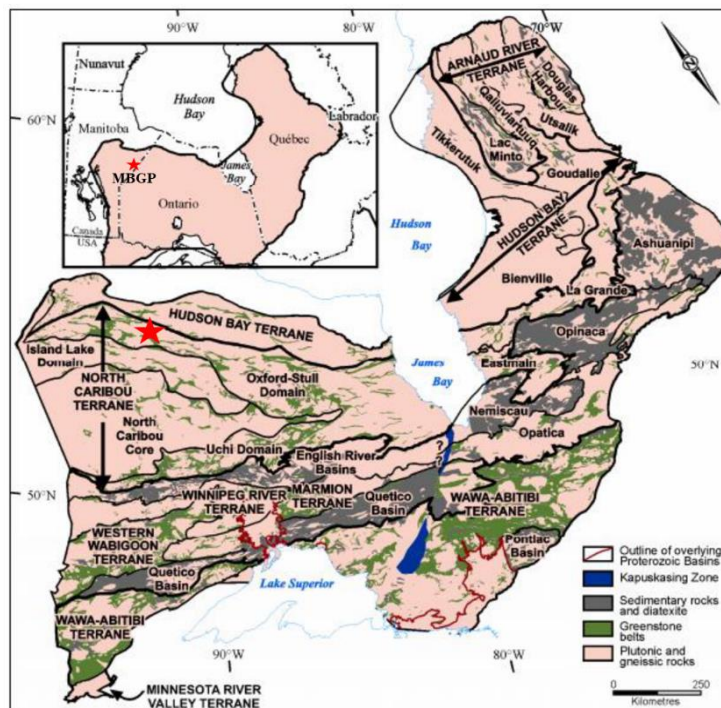


Figure 24. The location of MBGP in the Oxford-Stull Domain within the NW of the Archean Superior Province (modified after the Yamana technical report, unpublished).

The Oxford-Stull Domain (ODS) is an east-west trending ribbon-shaped granite-greenstone belt terrane that is delimited by the North Kenyon Fault in the north and the Stull-Wunnummin and God Lake Narrows Shera Zones in the south (Figure 24) (Percival, 2007). The ODS is dominated by a lode gold-bearing mélange of plutonic suites and some of the largest greenstone belts exposed across the Northwestern Superior Province. The Stull Lake Greenstone Belt (SLGB), which hosts the MBGP, is one of the largest greenstone belts in the NW of the Superior Province (Corkery et al., 1998). The SLGB preserves three volcano-sedimentary assemblages and plutonic rock suites, including Hayes River, Oxford Lake, and Cross Lake Assemblages (McCracken et al., 2016; Stone, 2005; Stone et al., 1998). These assemblages reveal the complex history of ductile deformation and tectonic segmentation occurring along the crustal-scale Stull-Wunnummin Shear Zone (SWSZ) (Skulski et al., 2000).

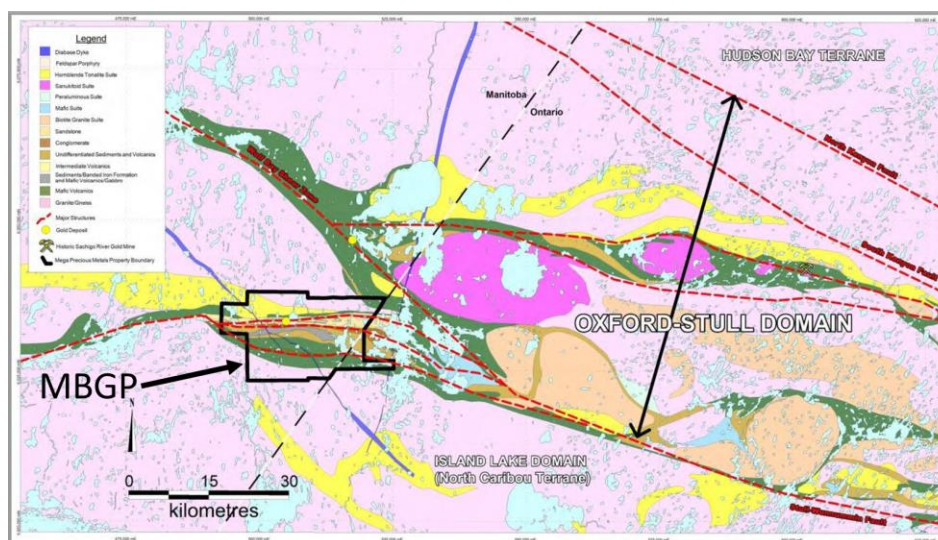


Figure 25. Regional Geology in the Oxford-Stull Domain (modified after Yamana technical report, nonpublished).

The Hayes River is the oldest assemblage dating back to ~2.85-2.83 Ga. The bedrock composition at the Hayes River Assemblage includes the northward younging pillowed tholeiitic basalts of oceanic to continental margin affinity (Skulski et al., 2000). The Hayes River assemblage is locally intruded by felsic volcanics, banded iron formations, sediments and synvolcanic gabbro bodies (Stone et al., 1998). The Oxford Lake Assemblage (~2.73-2.71 Ga) is subdivided into lower and upper units. The lower Oxford Lake is dominated by alc-alkaline to alkaline mature island arc to continental arc felsic to intermediate volcanics. The upper Oxford Lake is comprised of sedimentary Assemblage, including cross-bedded and graded arkose rocks and polymictic conglomerates (Stone, 2005). The Cross Lake Assemblage is the youngest major assemblage of supracrustal rocks in the OSD. It consists of the fluvial-alluvial polymictic conglomerates and cross-bedded sandstones that unconformably overlie the Oxford Lake Assemblage.

The exploration history at the OSD started with regional mapping and diamond drilling in 1936. Following that, multimedia geochemical, geophysical, and geological methods, including airborne electromagnetic (EM), magnetometer, very-low-frequency (VLF), induced polarization (IP) surveys, geological mapping, and diamond drill hole programs, were conducted to identify

and assess the alteration assemblages, vein morphology, and visible gold characterization (McCracken, 2016).

In 1996, the Manitoba Department of Energy and Mines, Mineral Resources Division conducted the first biogeochemical survey over Monument Bay as part of a belt-scale geochemical survey called Operation Superior Project (Fedikow et al., 1997). The goal of sampling vegetation in this survey was to use twigs chemistry to map the concealed bedrock, which resulted in a well-constrained biogeochemical database with multiple vegetation geochemical anomalies in proximity to the Twin Lakes Deposit (Fedikow et al., 1998).

The Monument Bay Project is divided into six distinct zones, including the Twin Lakes Zone (TL), Twin Lakes West Zone (TLW), Twin Lakes East (TLE), The South Limb Shear Zone (SLS), Mideast Zone (ME), and AZ Zone, of which the TL, ME, and AZ zones are the major exploration targets. These targets are located within the Twin Lakes Shear Zone (TLSZ) and South Limb Shear Zone (SLSZ), which are splays of the Stull-Wunnummin Shear Zone (SWSZ) (Figure 25). These zones encompass volcano-sedimentary assemblages of the Hayes, Oxford and Cross Lake Group.

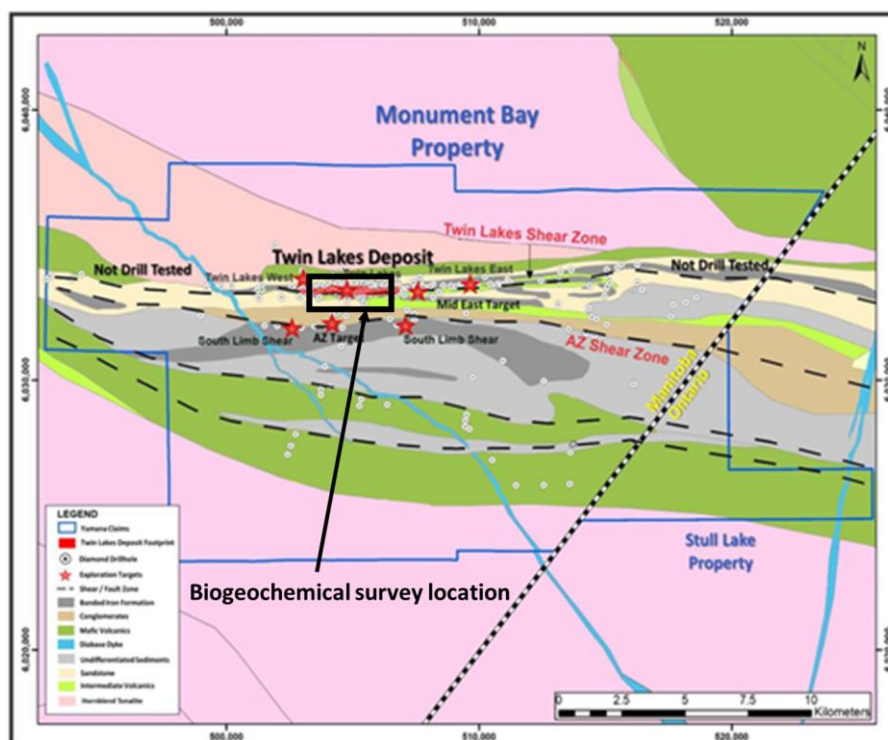


Figure 26. The regional geology map of Monument Bay Property and Stull Lake Property indicates the major structures and claim outlines. The red stars show the geographical distribution of six distinct zones at the MBGP (modified after Casali, 2020).

The Twin Lakes (TL) Deposit is located in the western part of the Stull Lake Greenstone belt and the margins of plutonic suites of the OSD. It is a highly prospective gold deposit hosted within the 200 m wide mylonitic TLSZ, which has a discontinuous mineralized strike length of over 4 km (Figure 26) (McCracken, 2016). The Oxford Lake Group is the main host rock for the Twin Lakes gold deposit. The rock assemblage in the Oxford Lake Group comprises felsic to intermediate metavolcanic tuffs intercalated with sediments, intermediate feldspar phyric volcanic flows, and late feldspar porphyritic dikes (McCracken, 2016). Three categories of gold mineralization have been identified in the TL Deposit (1) Quartz tourmaline+- pyrite-arsenopyrite-pyrrhotite veins; (2) Smoky quartz \pm pyrite-pyrrhotite-arsenopyrite-chalcopyrite veins; and (3) Quartz-albite-ankerite-scheelite \pm pyrite-arsenopyrite- sphalerite-chalcopyrite-galena-antimony (Hill, 2011b). Gold mineralization is most commonly observed with arsenopyrite and pyrite and associated with smokey grey quartz veins, which are the main host to high-grade gold mineralization in the TL Deposit (Hill, 2011a). This area was classified as an

Archean greenstone belt shear-hosted mesothermal gold deposit associated with deep crustal-scale faults and a large hydrothermal system (Goldfarb and Groves, 2015). Recent geochemical and petrological studies by Casali et al. (2020) and Hao et al. (2020a and 2020b) on the offcut core samples and inclusions using synchrotron micro-X-ray fluorescence and electron probe microanalysis (EPMA) indicate that gold grains are disseminated on edge or inside sulphide grains (Cavallin, 2019; Hao et al., 2020a). These studies also indicate that Au is associated with As and Fe in arsenopyrites, with Cu in chalcopyrite, and with Pb in galena. (Casali et al., 2020; Hao et al., 2020a, 2020b).

2.4.2 Yellowknife Greenstone Belt (YGB)

The YGB is one of several greenstone belts with primarily regional metamorphism to greenschist-amphibolite grades exposed in the southern segment of the Slave Province (R. J. Botor et al., 2019; Cousens et al., 2006; Cousens, 2000; Isachsen and Bowring, 1994). The YGB comprises the Central Slave Basement Complex (CSBC), overlaid by the Central Slave Cover Sequence and the Yellowknife Subgroup (Figure 27). The Central Slave Cover Sequence includes a sequence of fuchsitic quartzites, banded iron formations (BFI), and intermediate to felsic volcanic rocks that pervasively overlie the CSBC (Bleeker, 2002; Cousens, 2000). According to Bleeker and Hall (2007), the transition between the crystalline basement rocks of CSBC to quartzite of the Central Slave Cover Sequence is due to erosion (W Bleeker and Hall, 2007). The Yellowknife subgroup overlies the Central Slave Cover Sequence. This subgroup was deposited during multiple tectonic events, such as rifting and mafic volcanism, resulting in the formation of YGB (Bleeker, 2002; Bleeker and Hall, 2007; Botor, 2018; Ootes et al., 2011). The Yellowknife subgroup includes the Kam Group, Banting Group, and Duncan Lake Group. (Cousens et al., 2006; Cousens, 2000; Shelton et al., 2016). It is also locally intruded by ultramafic sills, which obscure the contact zone between the Central Slave Cover Sequence and Kam Group (Cousens et al., 2006).

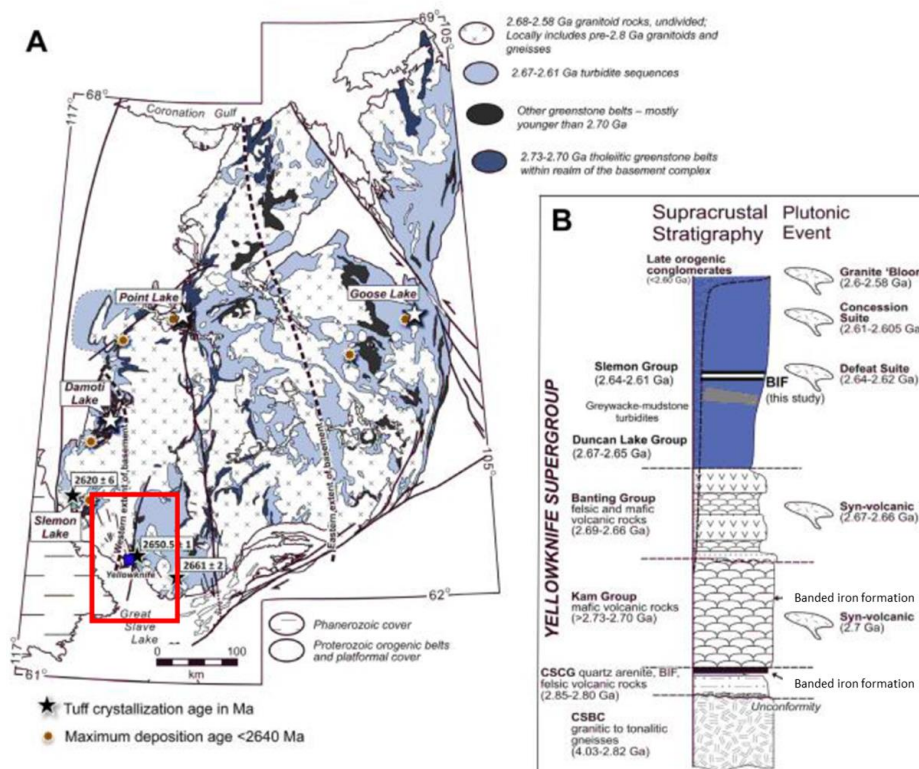
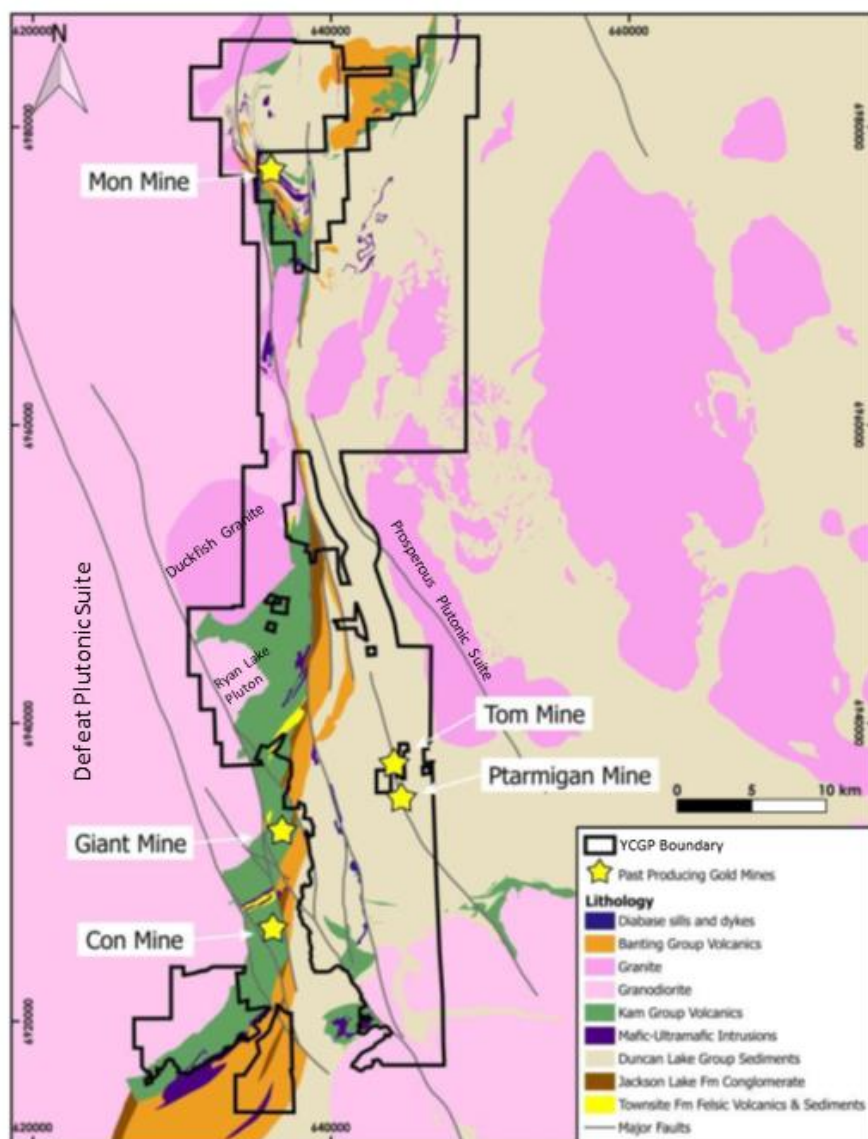


Figure 27. (A) The geological map of the Slave Province, modified after Hauggard et al. (2017). (B) The stratigraphic column of the Yellowknife Subgroup, host to the YGB (modified after Botor, 2018).

The Kam Group (2.721-2.701 Ga), comprising a large portion of the YGB, includes the Chan, Crestaurum, Townsite, and Yellowknife Bay formations from base to top. All conformable formations have a mafic to intermediate volcanic composition, mainly subalkaline basalts and basaltic andesites, excluding the Townsite Formation, which is composed of felsic to intermediate volcanic rocks (Armitage, 2021; Cousens et al., 2006). The Banting Group (2.685-2.660 Ga) is primarily comprised of sheared calc-alkaline intermediate to felsic volcanic and volcanoclastic sedimentary rocks (Armitage, 2021). The Kam and Banting groups are unconformably overlain by the youngest Archean rocks of the Jackson Lake Formation (>2.605 Ga) (Armitage, 2021; Cousens et al., 2006; Helmstaedt and Padgham, 1986; Henderson and Brown, 1966). Conglomerates of the Jackson Lake Formation have infilled the Yellowknife River Fault Zone (YRFZ), which is a faulted contact zone between the Kam Group and the

Banting/Duncan Lake Groups indicating post-faulting sediments deposition (Armitage, 2021; Falck, 1990; Martel and Lin, 2006).



**Figure 28. Regional geology of the YGB, Modified after NWT Helmstaedt and Hounsell
Compilation map (modified after Armitage, 2021).**

The YGB is intruded by the multiple felsic intrusive events, including the Ryan Lake pluton (2675 Ma), Defeat Plutonic Suite (ca. 2630-2615 Ma), Duckfish Granite (2608 Ma), and Prosperous Suite (2596 Ma) in succession (Figure 28) (Armitage, 2021; Henderson, 1985; Palmer et al., 2021). The most significant metamorphic event within the YGB occurred in

association with the intrusion of the Defeat Suite pluton and Prosperous suites. Although these plutonic suits have been weakly metamorphosed, they triggered the metamorphism grade at the YGB to the amphibolite facies (Shelton et al.; Thompson, 2006).

The YGB is conformably overlain by the dominantly sedimentary packages of the Duncan Lake Group (2680 Ma), including the Walsh Lake and Burwash Formations to the east (Armitage, 2021; Helmstaedt and Padgham, 1986; Henderson, 1985). The Walsh Lake and Burwash Formations of the Duncan Lake Group consist of a thick pile of greywacke and mudstone turbidites that conformably overlie the Banting Group (Figure 29) (Armitage, 2021; Helmstaedt and Padgham, 1986; Henderson, 1985; Martel and Lin, 2006).

There are diverse mineralization styles throughout the YGB, occurring as visible and refractory gold (Botor, 2018; Ootes et al., 2011). Visible gold is commonly observed in younger veins, associated with sphalerite, galena, chalcopyrite, pyrite, arsenopyrite, or molybdenite. While refractory gold is primarily bounded in the arsenopyrite (or arsenian pyrite) crystal lattice (Ootes et al., 2011; Shelton et al., 2016). Gold mineralization also can be seen as quartz lodes within the greywacke mudstone turbidites present in the younger sedimentary units and banded iron formations (Ootes et al., 2011). According to Van Hees et al. (2006), the origin of the turbidite-hosted gold resulted from the metamorphism process triggered by the Prosperous Pluton intrusion. In general, gold mineralization at the YGB is similar to other mesothermal, orogenic, quartz-carbonate or gold-only deposits, mainly hosted in shear zones that transect mafic volcanic and metasedimentary rocks (Goldfarb et al., 2005).

2.4.3 Yellowknife City Gold Project (YCGP)

The Yellowknife City Gold Project (YCGP) encompasses a prolific orogenic gold trend situated along shear zones and faults related to the north-south trending Archean Yellowknife Greenstone Belt (YGB). The YCGP extends for 10 to 60 km to the north, east, and south of the city of Yellowknife, Northwest Territories, Canada (Figure 29) (Armitage, 2021).

The YCGP is divided into three zones: Northbelt, Eastbelt and Southbelt (Figure 29). The Northbelt has the same characteristics and stratigraphy that underlies the historic Giant and Con mines, mainly hosted in quartz-carbonate-bearing shear zones that crosscut primarily mafic volcanic-dominated rocks (Groves et al., 1998; Ootes et al., 2011; Siddorn et al., 2006). There are four main targets within the Northbelt, including the Homer Lake target, Walsh Lake target,

Sam Otto target, and Ryan Lake target (Figure 29). There are several advanced and early prospects within each target.

The Homer Lake target is located at the northern end of the Yellowknife City Gold Property, associated with the metavolcanics of the Chan Formation and the linear intrusive quartz porphyry bodies. Homer Lakes hosts zones of polymetallic (Au, Ag, Pb, Zn) enrichment alongside porphyry-mafic contacts.

Mispickel prospect within the Walsh Lake target is a deformation zone hosted within the Walsh Lake target covered by turbiditic sediments of the Walsh Lake Formation that contains high gold grade intercepts. Shears at the Mispickel deposit contain several quartz veins with low to moderated arsenopyrite, pyrite, pyrrhotite, and visible gold.

The Sam Otto target includes the Sam Otto shear, Dave's pond, and Screamer Island prospects. The Sam Otto Shear is a prospective bulk tonnage target with the most extensive mineralization system yet discovered at the YCGP. The Sam Otto Shear is hosted in felsic to intermediate volcanics of the Banting Formation with intercalated sediments and mafic volcanics and finely disseminated pyrite and arsenopyrite. Dave's Pond is the strike extension of the Mispickel zone, located west of the sam Otto shear. Dave's Pond is a narrow shear-hosted quartz-carbonate veining prospect hosted within felsic to intermediate volcanics. Screamer Island is a new target of high-grade gold mineralization identified during a property-wide exploration program at the southern extension of the Sam Otto Shear, supporting the notion that the Sam Otto Shear is a large mineralization system.

The Ryan Lake target includes the Crestaurum, Barney shear and porphyry, Hébert-Brent, AES shear, and Shear 20 prospects. Crestaurum is a narrow discrete north-northeast trending shear zone that crosscuts the mafic volcanics of the Kam Group (Chan and Crestaurum Formations). Mineralization at the Crestaurum Shear comprises low to moderate pyrite, arsenopyrite, visible gold, stibnite, chalcopyrite, sphalerite, galena, and other minerals associated with the multi-stage quartz-carbonate veining. The Barney Shear is a north-south multi-kilometre-wide deformation zone within the Chan Formation affected by the northeast-trending crossing structure. Barney hosts mineralization within quartz-carbonate veins with several intervals with moderate to high levels of coarse sulphides, including arsenopyrite, pyrite, galena, chalcopyrite, pyrrhotite, and sphalerite (Armitage, 2021). The Barney porphyry, located beneath the barney shear, is a felsic intrusion that is associated with sulphides, precious metals and a

large amount of Mo (Armitage, 2021). The Hébert-Brent prospect is located within a flat plunging zone, hosted within the mafic volcanic and intrusive rocks cut by felsic porphyry dykes with no trace of mineralization. The Hébert-Brent prospect shows a replacement style gold mineralization associated with fine to medium-grained pyrite and needle arsenopyrite (Armitage, 2021). The AES Shear is a 5 km long gold structure located in proximity to the North Giant Extension (NGX) structure. The NGX structure is believed to be the northward continuation of the Giant ore system (Kelly, 1993). The high-grade quartz vein structure within the NGX at the south of the Northbelt shows a promising potential (Armitage, 2021). The Shear 20 is located alongside the contact of the Ryan Lake Pluton with volcanic rocks to the east. Drill holes targeted in the vicinity of these veins reveal an abundance of arsenopyrite, lesser pyrite, chalcopyrite, galena, and locally molybdenite (Armitage, 2021).

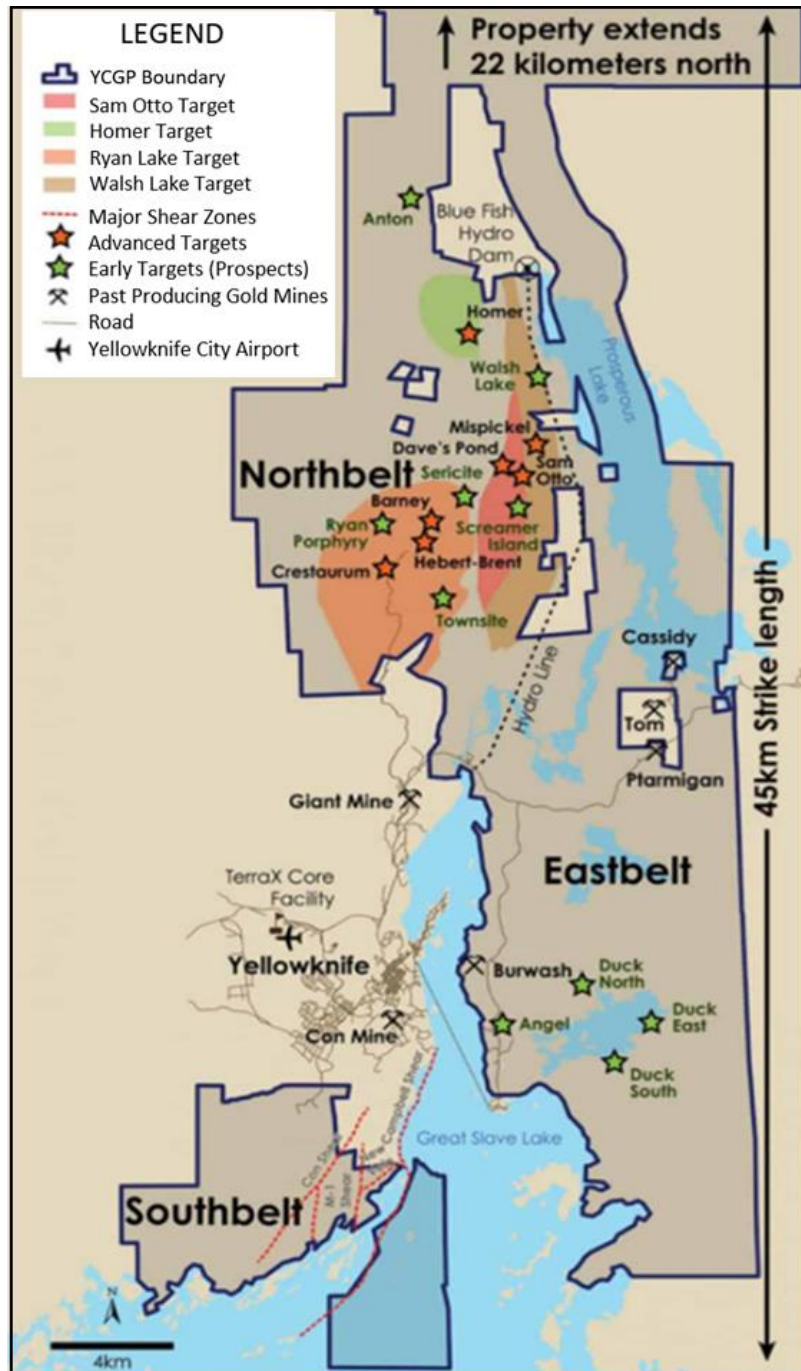


Figure 29. the Yellowknife City Gold Project (YCGP) advanced targets and new gold prospects within the Northbelt, including Sam Otto, Homer Lake, Ryan Lake, and Walsh lake targets, and within the Eastbelt, including the vicinity of the former Tom and Ptarmigan mines and Duck Lake target (modified after Botor, 2018).

Gold prospecting in the Eastbelt is still in the preliminary stage, and localized exploration has been conducted over the known showings, such as the Duck Lake target and historic Ptarmigan and Tom mines. Duck Lake veins, located south of the Eastbelt, crosscut folded Burwash Formation sediments. Gold mineralization at the Duck Lake target occurs in proximity to more prolific gold-producing plugs, including granite-tonalite-granodioritic intrusions, where high gold values are detected. West-northwest trending Ptarmigan and Tom quartz veins contain free visible gold within the irregularly shaped quartz bodies, hosted by amphibolite rade deformed turbidite rocks of Burwash formation (Richardson and Lentz, 2019).

The Southbelt encompasses the southern portion of the YCGP, immediately south of the historic gold mine. The Southbelt zone is underlain by the mafic volcanic intruded by felsic bodies, the same stratigraphy that host the Giant and Con mines. According to the Gold Terra, this part of the property stacked the southern strike extension of the YGB along the strike extension of the Campbell Shear (Armitage, 2021).

Chapter 3

3 Application of Multivariate Data Analysis to Biogeochemical Exploration at the Twin Lakes Deposit, Monument Bay Gold Project, Manitoba, Canada

Abstract

The Twin Lakes Deposit, located in the northwest of the Superior Province, is a promising Archean Greenstone-hosted orogenic gold deposit. Biogeochemical and statistical techniques were used for the first time in this area to assess the geochemical dispersion patterns of Au, As, Bi, Se, Sb, Tl, Fe, Co, Ni, Cr, Mo, Cd, Pb, Zn, Mn, K, P, B, Mg, Ca, Ba, and Cu in black spruce samples collected perpendicularly to the overall trend of shear-hosted gold mineralization. ICP-MS analysis of ashed black spruce bark, twigs, and needles has outlined a biogeochemical response of black spruce to concealed mineralization. Most elements are accumulated preferentially in twigs and bark, while B, K, Mg, Mn, and P are highly concentrated in needles. High Au and Tl enrichments were identified in all sample types compared to the background level. The scatter plot matrix demonstrated a positive bivariate relationship between Au and Fe, Mg, Cu, Mo, and Zn; and horizontal to slightly negative correlations with Ca, K, Mn, P, and B. Investigations on the spatial distribution pattern of Au and its pathfinder elements using a robust log-transformed inverse distance weighted (IDW) interpolation method revealed the presence of zones of gold enrichment in the north to the northwest of the survey, where Au is accompanied by Tl-As-Cd>Bi, Pb, Se>Sb. According to the Robust RQ-mode principal component analysis (PCA), two main components control the distribution of elements in black spruce, including (1) a geological factor that mostly reflects bedrock composition; and (2) a physiological factor that reflects the biological processing of essential elements. Of importance is that Au and its pathfinder elements, including As, Se, Tl, and to a lesser extent, Bi, Cd, and Pb were well-separated as a subgroup of the geological factor with a clear spatial relationship to gold mineralization. This study demonstrates a biogeochemical response in black spruce is associated with gold mineralization at the Monument Bay Gold Project using multivariate statistical methods. The results of this study are promising and can be extrapolated to wider surveys across the Monument Bay Gold Project to vector toward new gold mineralized zones or

extensions of the Twin Lakes gold deposit. The results also provide a suite of gold pathfinder elements that support exploration efforts and regional target generation.

3.1 Introduction

Orogenic gold deposits are the main source of gold production in the world (Gaboury, 2019; Tomkins, 2013). They are characterized mainly by carbonate \pm sulphide \pm sericite \pm chlorite alteration assemblages in greenschist-facies host rocks produced by low sulphide and high CO₂ ore fluids (Goldfarb et al., 2001). Abundant quartz \pm carbonate veins with crack-seal texture in orogenic gold deposits imply the source of the fluids is at supralithostatic pressures (Goldfarb et al., 2001), while the mineralized lodes formed at a wide range of upper to mid-crustal temperatures and pressures (200-650 °C and 1–5 kbar) (Groves, 1993). In Canada, the Superior Province is the largest and best-preserved Archean craton hosting greenstone-hosted orogenic gold deposits that constitute 86% of Canadian gold production (Dubé and Gosselin, 2007; Lydon and Goodfellow, 2007). A comprehensive compilation of the geology, tectonic evolution and metallurgy of orogenic gold deposits from the Superior Province is provided by Percival et al. (Percival et al., 2004; Percival, 2007).

This study demonstrates that analysis of biogeochemical samples and multivariate statistical analysis are robust and effective alternatives or supplements to other surficial sampling techniques in the early stages of exploration. In the biogeochemical method, the chemical characteristics of vegetation are examined to determine the presence and character of underlying mineralization (Dunn, 2007b). This method is beneficial since the extensive root systems of plants can uptake metals from the substrate and integrate the geochemical signature of the concealed outcrop. The concentration of metals of interest substantially varies in different tissues of various plants. Bark, twigs, foliage, and cones of spruce, pine, fir, birch, alder, and Labrador tea are found to significantly accumulate metals of interest in the boreal forest. Although some plant tissues are more optimal for accumulating metals, their consistency and practical purposes should be considered.

Biogeochemical data needs to be carefully evaluated from the statistical point of view, including univariate, bivariate, and multivariate analyses to identify the plant-substrate

relationship. In univariate statistics, each variable is examined separately, while the relationship between two variables is explored in bivariate statistics. The multivariate statistical technique is particularly useful when there is a large dataset with a high degree of correlation between the variables. Principal component analysis (PCA) is an adaptive multivariate data analysis method that reduces dimensionality, increases interpretability and minimizes information loss; therefore, a few components can describe the whole variability. Also, it can give an insight into the multidimensional patterns in the data that would be missed with univariate and bivariate analysis (Shtangeeva et al., 2009). There are several studies on the application of multivariate statistical analysis to biogeochemical data, indicating that the plant-substrate relationship can be used to discover either the source of contamination or concealed mineralization (Benz, 2017; Dunn and Heberlein, 2020; Larsen et al., 1992; Nude et al., 2012; Oliva and Espinosa, 2007; Schaug et al., 1990). This study uses a combination of biogeochemical and statistical knowledge to identify whether a geologically meaningful response exists in black spruce associated with buried mineralization at the Twin Lakes Deposit.

The Monument Bay Project, spanning the border between northeastern Manitoba and northwestern Ontario, consists of three exploration targets, including the Twin Lakes Deposit, the Mid-East target, and the AZ target. Over the past 70 years, various exploration techniques, including multimedia geochemical, geophysical and geological methods, have been used at the Monument Bay Project, working on the alteration assemblages, vein morphology, and visible gold characterization (McCracken, 2016). In 1996, the first biogeochemical survey over Monument Bay was conducted by the Manitoba Department of Energy and Mines, Mineral Resources Division as a part of a belt-scale geochemical survey called Operation Superior Project (Fedikow et al., 1997). The goal of sampling vegetation in this survey was to use twig chemistry to assist in mapping the concealed bedrock, which resulted in a well-constrained biogeochemical database with multiple vegetation geochemical anomalies in proximity to the Twin Lakes Deposit (Fedikow et al., 1998). In 2018, another biogeochemical survey was employed by Yamana Gold Inc., specifically over the Twin Lakes Deposit, to identify the biogeochemical response in black spruce and implement the results in a wider survey across the Monument Bay Project. Black spruce (*Picea mariana*) is selected as a suitable vegetation medium as it is ubiquitous within the study area. Also, it tends to enrich trace elements (Eccles, 1998; Nyade et al., 2013), especially Au and As in its tissues (Dunn, 2007b; Kovalevsky, 1987;

Warren and Delavault, 1950), as well as high values of other trace elements, including Bi, Cd, Hg, Ni, and Pb in bark tissue (Dunn, 2007b). This study aims to identify any geologically meaningful response in black spruce associated with buried mineralization at the Twin Lakes Deposit and examine the potential application of biogeochemical and statistical techniques as interdisciplinary approaches in mineral exploration.

3.2 Regional Geology:

The Monument Bay Project is an economically promising Archean shear-hosted gold deposit (Cavallin, 2019; Ghorbani et al., 2020), comprised of 35 contiguous, un-surveyed mining claims totalling 6692 ha, located approximately 570 km northeastern of Winnipeg (Hill, 2011a). The Monument Bay Project is underlain by granitoid crustal blocks of the Northern Superior Province that are bounded by east-trending, dextral strike-slip greenschist facies shear zones (Percival, 2007). The Oxford-Stull Domain (OSD), which hosts the Monument Bay Gold Project, is dominated by a lode gold-bearing mélange of plutonic suites and some of the largest greenstone belts exposed across the Northwestern Superior Province. The Stull Lake greenstone belt within the OSD preserves three volcano-sedimentary assemblages and plutonic rock suites, including, from oldest to youngest, the Hayes River, Oxford Lake, and Cross Lake assemblages that reveal the complex history of ductile deformation and tectonic segmentation occurring along the crustal-scale Stull-Wunnummin Shear Zone (SWSZ) (Figure 30A) (Skulski et al., 2000).

The Twin Lakes Deposit, Mid-East, and AZ zones are the major exploration targets at the Monument Bay project located within the Twin Lakes Shear Zone (TLSZ) and South Limb Shear Zone (SLSZ), which are splays of the SWSZ (Figure 30A). The Twin Lakes Deposit is a highly prospective gold deposit hosted within the 200 m wide mylonitic TLSZ, which has a discontinuous mineralized strike length of over 4 km (Figure 30B) (T. McCracken, 2016). The Oxford Lake Group, the main host rock for the Twin Lakes gold deposit, is comprised of felsic tuffs and intermediate feldspar-phyric flows. Three types of gold mineralization have been identified in this area (1) quartz-tourmaline±py-asp-po veins; (2) smoky quartz±po-asp-cpy veins; and (3) quartz-albite-ankerite-scheelite+py-asp-sph-cpy-gl-sb veins (Hill, 2011b). Gold mineralization is most commonly observed with arsenopyrite and pyrite and associated with smokey grey quartz veins, which are the main host to high-grade gold mineralization in the study

area (Hill, 2011a). The recent geochemical and petrological studies on offcut drills and inclusions using synchrotron micro X-ray fluorescence and electron probe microanalysis (EPMA) indicate that some gold grains are disseminated on edge or inside sulphide grains (Cavallin, 2019; Hao et al., 2020a). The results of these studies also indicate that Au is associated with As and Fe in arsenopyrites, with Cu in chalcopyrite, and with Pb in galena. (Casali et al., 2020; Hao et al., 2020a, 2020b).

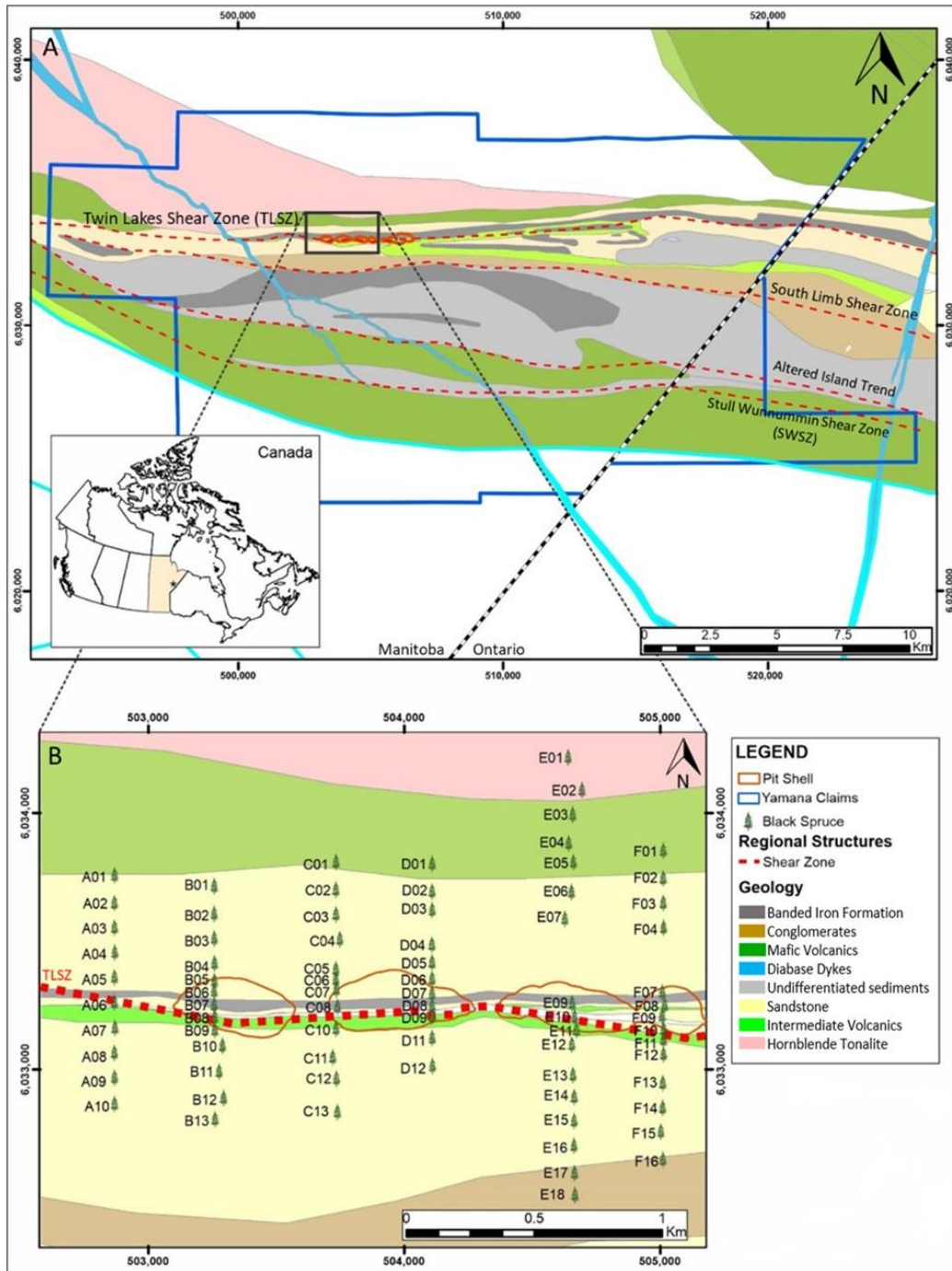


Figure 30. (A) Regional geology of the Monument Bay Project, northeastern Manitoba. Modified by the authors from Yamana Gold Inc. (unpublished), 2020. (B) Location of black spruce sampling sites within the Twin Lakes Gold Deposit.

3.1 Methodology

3.1.1 Sample Collection and Preparation

In June 2018, Yamana Gold Inc. embarked on a biogeochemical survey over the Twin Lakes Deposit to examine the biogeochemical response in black spruce related to concealed mineralization and find the sample medium with the best potential (bark vs twigs vs needles) for biogeochemical prospecting. Twigs and bark are found to be the optimum candidates for biogeochemical exploration (Dunn, 2001; Dunn, 2007b; Dunn et al., 1995). Needle samples were also taken as they are easy to collect and process. 85 black spruce were selected and collected across six almost 1 km long transects oriented perpendicular to the Twin Lakes shear zone, which hosts the deposit with a variable grid spacing of tighter intervals (50 m) over the Twin Lake Deposit and coarser resolution (100 m) distal to the projected surface expression of mineralization. Bark, needles, and twigs were taken from live and mature black spruce following detailed sampling guidelines designed by Dunn (2007) within a six-week period to minimize fluctuations in uptake due to seasonal changes (Dunn, 2007b). Samples were taken in June because high concentrations of Au commonly occur at this time, and the plant chemistry is more stable due to a slowdown in growth (Cohen et al., 1987; Stednick and Riese, 1987). No background samples were collected nearby the study area during the initial studies. Therefore, the median or 50 percentile value is used as it gives a useful estimation of the background value (Dunn, 2007b). Also, the iterative 2σ -technique was applied to define the geochemical background range (Matschullat et al., 2000; Reimann et al., 2005). This technique provides a normal distribution by discarding all the data values beyond the $\text{mean} \pm 2\sigma$ (σ : standard deviation). This calculation is repeated until all remaining values lie within this range, representing the background range. The geochemical background range can be useful for monitoring the environmental baseline in the future. The exact value of $\text{mean} + 2\sigma$ was interpreted as the upper background limit or threshold.

3.1.2 Analytical Analysis

The sample weight required for chemical analysis is a minimum of 400g (wet). Post-collection, samples were sorted and placed on a rack in a heated building overnight to dry out. Following that, samples were macerated to produce a homogeneous and representative

pulp. Subsequently, 100 g of all dried samples were weighed out and transferred into an ashing pan, followed by controlled ignition at 475 °C for 24 h. Afterward, a 0.25g aliquot was digested in 75% aqua regia using a digestion block operating at 115°C and then analyzed using ultra-low detection limit inductively coupled plasma-mass spectrometry (ICP-MS). Multi-element determinations were carried out using the ME-VEG41a package at ALS Global in Vancouver, Canada. The ashing process with a 2-4% average yield provides ~50 times concentration of trace elements relative to the unashed plant tissue. The results of the unashed samples were not included in this study as the concentration of elements of interest, such as gold and its pathfinder elements, were not detected in >90% of samples.

3.1.3 Processing Biogeochemical Data

Compositional data, such as biogeochemical data, are subjected to basic error-checking before being passed as a suitable dataset for analysis. SPSS 25.0. statistics software has been used to prepare data, treat extreme outliers, and censor datasets (Almasi et al., 2015; Keshavarzi et al., 2015; Lemenkova, 2019; Rastegarimehr et al., 2017). Excluding or removing data is a problematic approach when dealing with nondetects and outliers. Data exclusion leads to an upward bias in subsequent measures of location (e.g., mode, median, and mean) and then makes it impossible to compare a group of variables simultaneously. Therefore, winsorization was used to modify spurious outliers to the next highest or lowest values (Dixon, 1960). Also, censoring was applied to keep the majority of data intact and to not use zeros by replacing a nondetected value with a fraction of the detection limit (Benz, 2017). A number of methods were discussed by Sanford et al. 1993 to censor data. In this study, a one-half method detection level (1/2 MDL) (Carranza, 2011) was used for Au, Ba, and Tl, with less than 20% of data lower than the detection limit. For example, 0.1 ppb was substituted for nondetect Au values reported by the laboratory as <0.2 ppb. For elements with less than 20% of data higher than the detection limit, including K and Mn, the upper MDL was used. So, 50,000 was replaced by 50,000.1 ppm for Mn. The precision of data should be calculated to evaluate the measurement errors attributed to different stages of sampling, preparation and sub-sampling, and analytical processes (Heberlein et al., 2020). The precision of data was calculated using the percent average coefficient of variation (% $C_{V_{Avg}}$) introduced by Abzalov (2008). In this formula, N is the number of duplicated samples, and a

and b are the concentration of element i in the primary and duplicate samples, respectively. The $\%CV_{Avg}$ values below 20% indicate good data precision, between 20 and 30% acceptable precision, between 30 and 50% marginal precision, and over 50% poor precision. In this dataset, most of the elements are within the good and acceptable quality range (Table 2).

$$CV_{avg}(\%) = 100 \times \sqrt{\frac{2}{N} \sum_{i=1}^N \frac{(a_i - b_i)^2}{(a_i + b_i)^2}}$$

Table 2. Data precision results using the average coefficient of variation ($CV_{avg}(\%)$) shows a marginal range for B, while other elements have an acceptable to good range.

MBGP biogeochemical data			
Elements	$CV_{avg}(\%)$	Elements	$CV_{avg}(\%)$
Ba_ppm	30.28604	P_pct	17.95122
Pb_ppm	29.17392	B_ppm	15.89578
W_ppm	28.70921	Fe_ppm	15.59965
Cd_ppm	27.6957	Cr_ppm	14.66181
Sb_ppm	26.76239	K_pct	14.04437
Se_ppm	26.50746	Ni_ppm	12.94296
Au_ppm	25.36011	Mg_pct	12.35756
Bi_ppm	24.791	Co_ppm	9.208497
Tl_ppm	24.39897	Mn_ppm	7.647193
Ti_pct	22.27177	Cu_ppm	7.580757
Mo_ppm	21.13467	Zn_ppm	5.140985
As_ppm	19.70004	Ca_pct	1.70272

3.1.4 Principal Component Analysis (PCA)

PCA stands for principal component analysis and is a linear dimension reduction technique for large datasets. Mathematically, in PCA, it is assumed that there is an observation matrix of X whose rows and columns are observations (n) and variables (p), respectively. We denote the covariance matrix of X by S with the corresponding eigenvalue-eigenvector pairs of (λ_i, e_i) , $i=1, \dots, p$. The eigenvalues and eigenvectors are found in a way that satisfies $eS = \lambda S$ where e is a matrix and λ is a vector. The obtained e and λ are the matrix of eigenvectors and vector of eigenvalues, respectively. The i^{th} principal component is, then, given by $Y_i = e_{i1} X_1 + \dots + e_{ip} X_p$, satisfying $Var(Y_i) = \lambda_i$ and $Cov(Y_i, Y_j) = 0$, $i=1, \dots, p$ and $i \neq j$. The aforementioned eigenvectors

create a new set of axes for describing and demonstrating the entire distribution on bivariate scatterplots by reducing the dimensionality of the data set while losing only a minimal amount of the original information (Johnson and Wichern, 2002).

The principal component analysis permits a reduction in the number of variables to a smaller number with a minimum loss of information (Singh et al., 2017). PCA can be divided into R-mode, which focuses on the interrelationship between elements, and Q-mode, representing the correlation between samples (Chen, 2015; Neff, 1994). RQ-mode PCA was first described as a biplot method by Gabriel (1971) and then modified by Zou et al. (1983) for geochemical data (Zhou et al., 1983). In this method, both the variable (R) and the sample (Q) loading are assessed simultaneously on the same scale (Zhou et al., 1983). In this study, RQ-mode PCA was applied using ioGAS 7.3. to reveal and evaluate the elemental interrelationship and the associated samples simultaneously. The measure of sampling adequacy (MSA) using the Kaiser-Meyer-Olkin (KMO) test was performed as a prerequisite to multivariate analysis (Kaiser and Rice, 1974; Šorša et al., 2017). Adequate sample size, at least ten samples for each element, and a minimum sample-to-element ratio (N/P; P in math refers to a variable) of at least five to 20 are the main assumptions of the multivariate analysis (Comrey and Lee, 2013; Jolliffe and Cadima, 2016) since too many variables lead to inadequate variance stability and poor recovery of components (Osborne and Costello, 2004). The robust analysis was also applied as data were not normally distributed and included outliers (Grunsky, 2010). Then, the log-ratio transformation was applied due to the potential for closure and the skewed nature of biogeochemical data (Aitchison, 1982; Grunsky, 2010). Standardization was also performed on both log-normalized and normally distributed data using ioGAS 7.3. to ensure that each variable is weighted equally. Log-transformation of skewed data and standardization are frequently employed in multivariate statistical analysis (Aitchison, 1982; Benz, 2017; Chen, 2015; Cloutier et al., 2008; Güler et al., 2002; Nejadhadad et al., 2017; Schaug et al., 1990; Shtangeeva et al., 2009).

Table 3. Descriptive statistics of Min, Max, mean (average value), median (background value), and mean $\pm 2\sigma$ (background range) values in the black spruce bark, needles and twigs (DL: detection limits, σ : standard deviation, ppm: part per million, ppb: part per billion, pct: percent, σ : standard deviation).

Black Spruce Tissue	Bark				
Elements (DL)	Min	Max	Mean	Median	Mean \pm 2σ
Au_ppb (0.2)	>0.2	230	3.99	0.9	-1.435
As_ppm (0.01)	0.75	4.95	1.88	1.67	0.66-2.80
Bi_ppm (0.001)	0.026	0.484	0.13	0.11	0.03-0.16
Cd_ppm (0.001)	0.116	4.66	1.48	1.31	0.59-2.03
Pb_ppm (0.01)	4.62	87.7	22.91	20.65	6.71-29.62
Sb_ppm (0.01)	>0.1	0.97	0.46	0.45	0.15-0.61
Se_ppm (0.005)	0.107	1.045	0.52	0.5	0.21-0.73
Tl_ppm (0.002)	0.006	0.278	0.08	0.04	0.002-0.04
B_ppm (1)	99	408	244.4	224	113-356
K_pct (0.01)	0.6	2.94	1.42	1.39	0.77-1.89
Mg_pct (0.001)	0.29	1.6	0.8	0.78	0.39-0.98
Mn_ppm (0.1)	2220	20500	9664	8925	3002-13580
P_pct (0.001)	0.169	1.04	0.54	0.52	0.21-0.68
Zn_ppm (0.1)	886	3000	1796	1780	1187-2147
Cu_ppm (0.01)	25.8	149.5	67.7	64	35-83.3
Ba_ppm (0.1)	428	2570	1383	1280	624-1256
Ca_pct (0.1)	20.3	38.4	33.61	33.55	32.2-36.3
Co_ppm (0.002)	0.49	6.55	1.85	1.59	0.63-2.3
Cr_ppm (0.01)	1.27	241	10.4	5.85	2.14-8.33
Fe_ppm (1)	723	6700	2378	2200	782-3430
Mo_ppm (0.01)	0.2	30.2	1.15	0.68	0.33-0.88
Ni_ppm (0.04)	4.34	166.5	15.28	12.8	6.2-16.02
Black Spruce Tissue	Twigs				
Elements (DL)	Min	Max	Mean	Median	Mean \pm 2σ
Au_ppb (0.2)	>0.2	303	5.26	1.1	-2.62
As_ppm (0.01)	0.46	7.13	2.06	1.9	0.87-3.07
Bi_ppm (0.001)	0.02	0.268	0.11	0.1	0.04-0.16
Cd_ppm (0.001)	0.058	2.05	0.75	0.7	0.22-1.26
Pb_ppm (0.01)	3.59	42.1	12.19	10.6	4.7-18.3
Sb_ppm (0.01)	0.18	6.12	1.16	1	0.48-1.7
Se_ppm (0.005)	0.12	1.145	0.5	0.46	0.19-0.8
Tl_ppm (0.002)	0.02	1.47	0.24	0.11	0.002-0.1
B_ppm (1)	248	749	478	471	407-536
K_pct (0.01)	4.34	10.1	9.84	10.1	10.1
Mg_pct (0.001)	1.17	5.62	3.3	3.25	2.15-3.9
Mn_ppm (0.1)	5690	39500	20472	19675	7244-31244
P_pct (0.001)	1.31	4.67	2.94	2.87	2.06-3.61
Zn_ppm (0.1)	1740	4320	2647	2525	1797-3171
Cu_ppm (0.01)	61.1	282	142.1	139.5	98.6-170.9
Ba_ppm (0.1)	288	2480	1119	1095	438-1648
Ca_pct (0.1)	10.9	27.6	22.9	22.9	19.46-27.1
Co_ppm (0.002)	0.92	5.95	2.79	2.54	1.42-3.42

Cr_ppm (0.01)	3.39	55.4	16.61	16	7.53-23.74
Fe_ppm (1)	1500	8800	4234	4000	1909-5626
Mo_ppm (0.01)	0.41	7.39	1.81	1.59	0.72-2.2
Ni_ppm (0.04)	8.24	73.9	27.67	24.75	11.7-37.7
Black Spruce Tissue	Needles				
Elements (DL)	Min	Max	Mean	Median	Mean \pm 2σ
Au_ppb (0.2)	>0.2	2.7	0.38	0.2	0.2
As_ppm (0.01)	0.33	1.11	0.56	0.54	0.318-0.724
Bi_ppm (0.001)	0.003	0.137	0.02	0.02	0.01-0.22
Cd_ppm (0.001)	0.013	0.4	0.11	0.09	0.03-0.12
Pb_ppm (0.01)	0.87	5.61	1.94	1.71	0.82-1.94
Sb_ppm (0.01)	0.11	0.94	0.29	0.25	0.11-0.38
Se_ppm (0.005)	0.042	0.328	0.15	0.14	0.05-0.2
Tl_ppm (0.002)	0.002	1.11	0.07	0.03	0.003-0.017
B_ppm (1)	111	1390	582	554	238-839
K_pct (0.01)	5.24	10.1	10.01	10.1	10.1
Mg_pct (0.001)	1.2	5.52	2.64	2.45	1.67-2.8
Mn_ppm (0.1)	6470	50000.1	28328	26700	8795-45133
P_pct (0.001)	1.405	3.99	2.48	2.36	1.29-3.63
Zn_ppm (0.1)	812	3130	1833	1718	1334-2555
Cu_ppm (0.01)	15.6	73.1	34.7	33.2	19.99-42.76
Ba_ppm (0.1)	75.1	1025	474.4	443	96-726
Ca_pct (0.1)	15	30.1	24.48	23.1	20.05-29.14
Co_ppm (0.002)	0.122	1.845	0.41	0.3	0.152-0.449
Cr_ppm (0.01)	0.64	12.85	2.12	1.47	0.64-2.63
Fe_ppm (1)	458	3300	953	781	493-988
Mo_ppm (0.01)	0.12	15.1	0.7	0.32	0.1-0.38
Ni_ppm (0.04)	1.29	26.3	4.9	4.07	0.54-7.4

3.1 Results and Discussion

3.1.1 Summary of Statistics

Table 3 summarizes the biogeochemical data for 255 bark, needles, and twigs of 85 black spruce collected at the Twin Lakes Deposit, Monument Bay Project. Generally, in the spruce family, metals and trace elements are significantly concentrated in the bark and twigs (Dunn, 2007b). In the study area, the majority of elements have high values in the order of ashed twigs > bark > needles. However, B, K, P, Mg, and Mn are preferentially accumulated in needles, while Ba, Bi, Ca, Cd, and Pb are preferentially concentrated in the bark. The average concentration (mean), background value (median), and background range (mean \pm 2 σ) of elements are provided in Table 3. The comparison between the average values and background range

indicates all elements concentrations are within the background range, except Au, Tl, Cr, and Mo in the bark; Au and Tl in twigs; and Tl, Mo, and Pb in needles. The comparison between Au average and background level shows the average concentration of Au in both bark and twigs is four times, and in needles is two times higher than the background level. Gold average values in black spruce twigs and bark are higher than the upper background limit (threshold/ $\text{mean}+2\sigma$), showing significant enrichment of Au in these samples. Thallium average values in all sample types and Mo mean values in bark and needle samples are more than two times higher than the background levels. Calcium, P, Mg, and K indicate insignificant differences in average contents compared to the background values in all sample types. The average value of all other elements in bark and twigs shows slight enrichments compared to the background level. The difference between mean and background values of As, Bi, Cd, Pb, Sb, and Se in needle samples is less than bark and twigs, showing a physiological tendency not to concentrate these elements of interest.

3.1.2 Biogeochemical Distribution of Elements in Black Spruce:

Generally, plants can uptake two types of elements: essential and trace elements. Essential or nutritional elements are necessary for plant metabolism and growth cycle, which can be divided into two subgroups of macronutrients, including P, Mg, K, and Ca and micronutrients comprised of B, Co, Cu, Fe, Mn, Mo, Ni, and Zn. Elements such as Ba and Cr play no significant role in plants; however, experimentation has found trace levels can enhance plant growth under certain circumstances (Kabata-Pendias, 2001). The presence of trace elements such as Au, Bi, As, Cd, Pb, Sb, Se, and Tl in plants can reflect passive uptake due to either the presence of buried mineralization or contamination (Dunn, 2007b; Kabata-Pendias, 2001).

Element logarithmic mean contents in bark, needles and twigs are shown in Figure 31. Needles and twigs are the preferred targets for B, K, Mg, Mn, and P, which are essential elements for plants. Twigs and bark demonstrate a high capability to accumulate elements that are highly associated with lithology-mineralogy associations, including Au, As, Sb, Se, Tl, Zn, Cu, Co, Cr, Fe, and Ni (twigs>bark) and Bi, Cd, and Pb (bark>twigs). Elements such as Cu and Zn should be interpreted with caution since they can represent the lithology-mineralogy association as well as plant metabolism function (Dunn, 2007b). Although Ca is a plant nutrient, it prefers to accumulate in bark more than in other tissues.

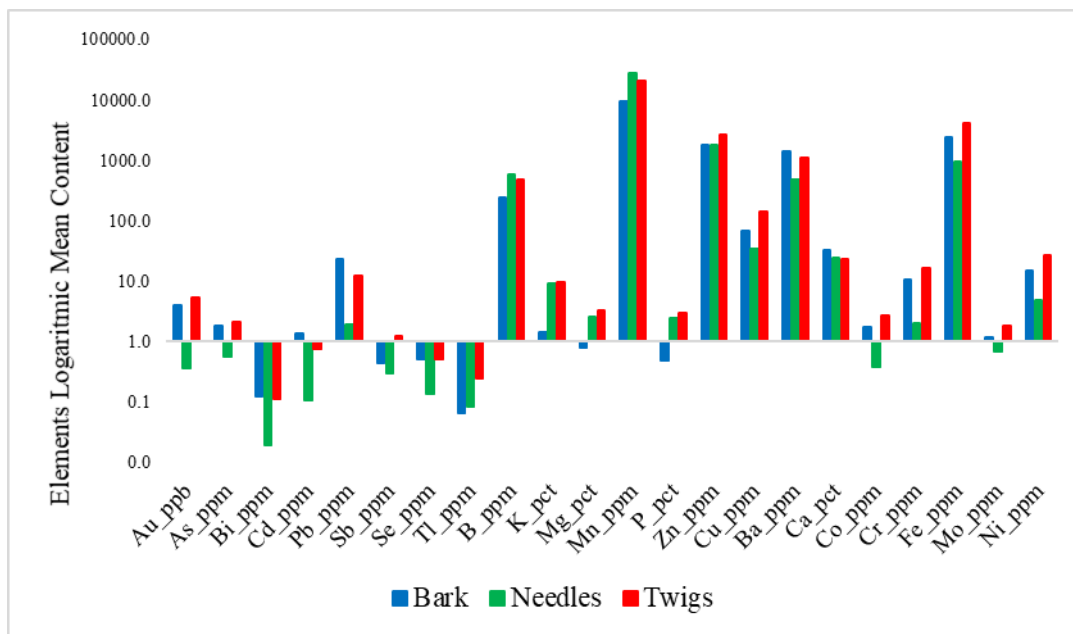


Figure 31. Comparison of the logarithmic mean values of selected elements in ashed bark (blue), needles (green), and twigs (red) collected at the Twin Lakes Deposit.

A scatter plot matrix (Figure 32) was used to visualize bivariate relationships and the correlation between Au and nutrient elements in black spruce samples. There is no meaningful relationship between Au and macronutrients as the regression line is almost horizontal to slightly positive except for Ca, which displays a minor negative correlation. Micronutrient metals including Cu, Fe, Mo, Ni and Zn are significantly associated with Au, which is highly likely due to the bedrock composition, while a slight negative correlation between Au with Mn and B can be seen. A notable association exists between Mg, P, and K with other nutrients, whereas Cu, Mn and B show no relationship to a slightly negative correlation. Calcium also indicates a clear negative correlation with other nutrients due to the difference in the target organ and antagonistic relationship (Kabata-Pendias, 2001; White and Broadley, 2003).

3.1.3 Element Associations:

Cobalt (Co): Generally, Co is associated with Ni, where the geological environment is dominated by mafic to ultramafic rocks. A co-distribution pattern between Au and Co can be seen adjacent to the mineralized zone.

Copper (Cu): The Cu average content appears significantly enhanced in comparison with other trace elements. Copper plays a fundamental role in plant metabolism (Yruela, 2005). Like most metal micronutrients, Cu is mostly concentrated in twigs. The range of Cu concentration in ashed black spruce varies between 15.6 ppm to 282 ppm, averaging 81 ppm. Samples with the highest Cu content mainly occur far from the Au conceptual pit shell. However, Cu content in some twigs samples is co-located over Au elevated zones due to its similar chemical and mineralogical association with Au in the study area (Antweiler et al., 1982; Hao et al., 2020 a and 2020b).

Iron (Fe): Iron is one of the most studied elements in plants since it is responsible for energy transformations necessary for syntheses and various life processes of the cell (Boardman, 1975; Price et al., 1972). From a mineral exploration perspective, high Fe content can represent ultramafic/mafic substrates (Dunn, 2007b). Iron is the main component of pyrite and arsenopyrite which are Au-bearing sulphides found in the study area. Iron is positively correlated with Au and highly enriched peripheral to Au-enriched zones.

Molybdenum (Mo): Molybdenum is one of the least essential micronutrients with chalcophile and lithophile properties that is mainly associated with felsic rock (Kabata-Pendias, 2001; Sigel and Sigel, 2002). Molybdenum mean values indicate that it is highly concentrated in twigs and bark than in needles. However, values up to 15 ppm were identified in needles, which is significantly higher relative to the background level. The highest Mo value is 20 ppm recorded in black spruce bark restricted to zones identified as overlying intermediate volcanic rocks.

Nickel (Ni): Nickel values in the ashed black spruce samples vary between 1.3 and 166.5 ppm, averaging 15 ppm. A positive correlation can be seen between Ni and Au. The distribution pattern of Ni shows a relative enrichment over and peripheral to the Au mineralized area, mainly associated with mafic rocks.

Manganese (Mn): Manganese, like other divalent cations, is mainly taken up metabolically rather than by passive absorption (Kabata-Pendias, 2001). Also, it has a strong affinity with Co geochemically (Kabata-Pendias, 2001). Needles can accumulate a high content of Mn in comparison to other tissues (Heenan and Campbell, 1980). A notable correlation between Mn and other essential elements such as Mg, Zn, B, and Cu is observed. Calcium and

Mn are negatively correlated because of accumulation in different plant organs. Fe and Mn show a strong correlation because they are highly concentrated in the plant and interrelated in their metabolic function (Kabata-Pendias, 2001). However, it is essential to note that excess Mn in plants can retain Fe in its inactive state due to their antagonistic relationship (Megonigal et al., 2004). A healthy plant should contain a Fe/Mn ratio ranging from 1.5 to 2.5. In black spruce, this ratio is 0.13, representing a significant Fe deficiency and Mn enrichment. Needles > twigs are the preferred organ for Mn accumulation. At the Twin Lakes deposit, a high concentration of Mn in black spruce samples is commonly associated with mafic volcanic rocks.

Zinc (Zn): The concentration of Zn in ashed black spruce samples varies between 886 and 3000 ppm, averaging 2100 ppm. Zinc can be considered an indicator metal associated with Au chemically (Antweiler et al., 1982). A strong correlation between Au and Zn has been reported in spruce needles over the 3Ts epithermal Au-Ag prospect in central British Columbia (Dunn et al., 2007). The mean concentration of Zn in black spruce in the study area shows a strong positive signature peripheral to the Au mineralized area, which is associated with mafic volcanic units.

Barium (Ba): Brooks stated that 220 ppm Ba in the ashed plant is moderately toxic (Shacklette et al., 1978). However, a biogeochemical survey conducted by Dunn and Hoffman in northern Saskatchewan showed that black spruce twigs and bark were enriched in Ba up to ~1000 ppm (Dunn and Hoffman, 1986). Patterns of Ba distribution in biogeochemical datasets can assist in delineating carbonate-rich zones because of the chemical affinities of Ba with Ca.

Chromium (Cr): Although the primary source of elevated Cr in plants is anthropogenic, plants growing on ultramafic and mafic substrates can accumulate significant Cr (Kabata-Pendias, 2001). Most of the Cr anomalies collected in the study area are located in proximity to mafic and ultramafic units. Some of the high Cr values (up to 240 ppm, identified in bark samples) are co-distributed with high Au values. Dunn et al. (1990) reported an association between Cr, Co, and Au at the Jasper Gold mine in northern Saskatchewan (Dunn et al., 1990).

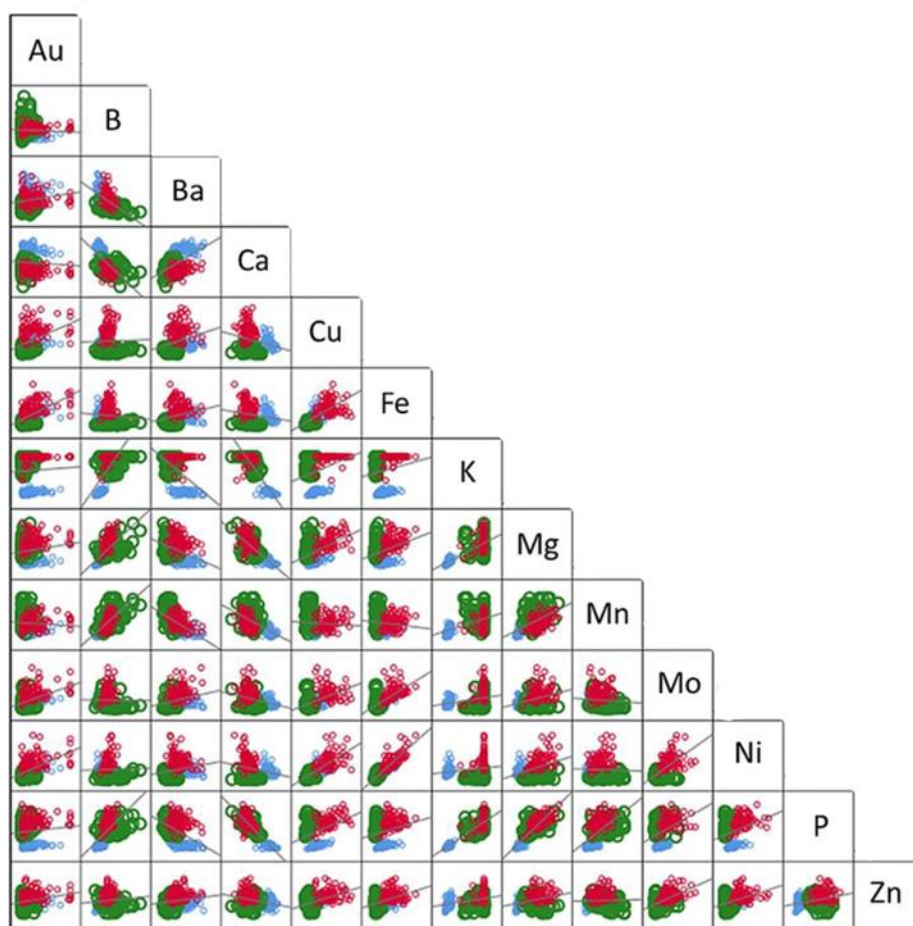


Figure 32. Scatter plot matrix of gold and nutrient elements for needles (green), twigs (red), and bark (blue). Scatter plot matrix demonstrates a strong bivariate relationship between Au and micronutrients metals, including Cu, Fe, Ni, Mo and Zn, indicating a plant-substrate relationship. While slightly negative to no meaningful correlation can be seen between Au and B, Ba, Ca, K, Mg, Mn and P due to differences in their chemistry and accumulation organ.

Gold (Au): Gold has no essential role in plant growth; therefore, any high gold values likely reflect the presence of concealed mineralization (Dunn, 2007b). Gold background levels of 5 to 10 ppb in ashed samples of black spruce have been reported (Dunn et al., 1995). The concentration of Au in black spruce tissue at the Twin Lakes Deposit varies between >0.2 to 303 ppb, with the highest concentration in twigs located over mineralization (Figure 33A). In this study, the distribution pattern of Au was substantiated by its pathfinder elements to avoid

reporting unreal anomalies. Gold pathfinder elements or indicators refer to elements, mostly non-ore (Rose and Hawkes, 1979), that are in association with gold and can be used to delineate zones of gold enrichment. Arsenic, Bi, Sb, Se, Cd, Pb, and Tl have been reported by many researchers as prospective pathfinder elements of gold (Dunn, 2007b; Kovalevsky, 1995; Kovalevsky and Kovalevskaya, 1989). A comparison of the distribution pattern of these elements assists in delineating zones of Au enrichment. A robust log-transformed inverse distance weighted (IDW) interpolation method is used to interpolate the spatial variation of Au and its pathfinder elements and reveal their interrelationship with respect to the geology beneath. The spatial distribution of gold is plotted on each gold pathfinder IDW map (Figure 33A-H). IDW is a popular approach to processing large geochemical datasets by estimating unknown hidden data from the known measured values (Burrough et al., 2015). As shown in Figure 33A, zones of gold enrichment are proximal to the TLSZ, more significantly to the north of the conceptual pit shell at the Twin Lakes Deposit. The comparison of elemental profiles in all six transects shows a high correlation between Au and Tl, As, Cd>Bi, Pb, Se>Sb (Figure 33A-H). Thallium shows the highest correlation with gold at the Twin Lakes deposit.

Arsenic (As): Whether the sample medium is rock, soil, water, or vegetation, As can be of great value as a pathfinder element for Au (Dunn, 2007b). The average concentration of As in ashed black spruce samples varies between ~0.3 to 7 ppm. As content in bark and needles is almost the same as the background level, with a slight enrichment in twigs. Twigs are the favoured target tissue for both As and Au. The As profile illustrated in Figure 33B shows the As-Au co-distribution pattern in the northwest portion of the survey, where high Au anomalies are identified in samples collected over and in proximity to the TLSZ and intermediate volcanic package. Another association between gold and As is identified in the east, where As is enriched peripheral to zones of Au enrichment.

Bismuth (Bi): Bismuth is one of the indicators for many types of mineralization, but its concentration in vegetation is lower than the detection limit (Dunn, 2007b). Therefore, high values of Bi need to be inspected closely to determine their significance. The concentration of Bi in the ashed black spruce bark samples collected in the study area is up to 484 ppb, specifically in the northwest, where gold is highly enriched, indicating its significant role as a gold pathfinder

element. There is also a Au-Bi association in the north and east portions of the survey. The correlation between Au and Bi can be observed in Figure 33C.

Cadmium (Cd): Cadmium can be highly absorbed by the root system due to its geochemical affinity with Zn and is less significantly utilized by metabolic reactions (Smeyers-Verbeke et al., 1978). Cadmium mean value in black spruce bark is higher than the twigs and needles. Geochemical and biochemical antagonisms between Cd and Fe, Zn, Cu, Se and Ca lead to Cd depletion in the black spruce samples (Kabata-Pendias, 2001). Cadmium in black spruce is captured by the cell wall components and therefore accumulates and stabilizes in the bark. It might be due to the barrier mechanism of the plant preventing circulating toxic elements. Hence, the highest concentration of Cd can be seen in bark and less in twigs>needles. Cadmium cannot always be considered a promising pathfinder element for gold mineralization. Yet, its spatial relationship to the elevated Au zones is sometimes of value in providing a focus for exploration efforts (Dunn, 2007b). Similar to Bi and As, there is a multi-site enrichment for Cd that is mainly restricted to intermediate volcanic units proximal to the zones of Au enrichment and TLSZ (Figure 33D).

Lead (Pb): Lead can mimic the biogeochemical and physiological behaviour of Ca and replace it metabolically. Therefore, Pb is more commonly accumulated in the bark. Same as Cd, due to the toxic effects of Pb, a barrier mechanism in black spruce tends to accumulate Pb in dead tissues such as bark rather than growing tissues such as twigs and needles. Elevated Pb content as a pathfinder of Au (Griffis and Agezo, 2000; Nude et al., 2012) is observed in black spruce samples peripheral to zones of Au enrichment, and to a lesser extent, over mineralization (e.g., the northwest portion of the survey area) (Figure 33E). Positive correlations between Au and Pb were observed in geochemical studies on sulphide grains (Hao et al., 2020a and 2020b). Bismuth and Pb distribution patterns are very similar (Figure 33C and E).

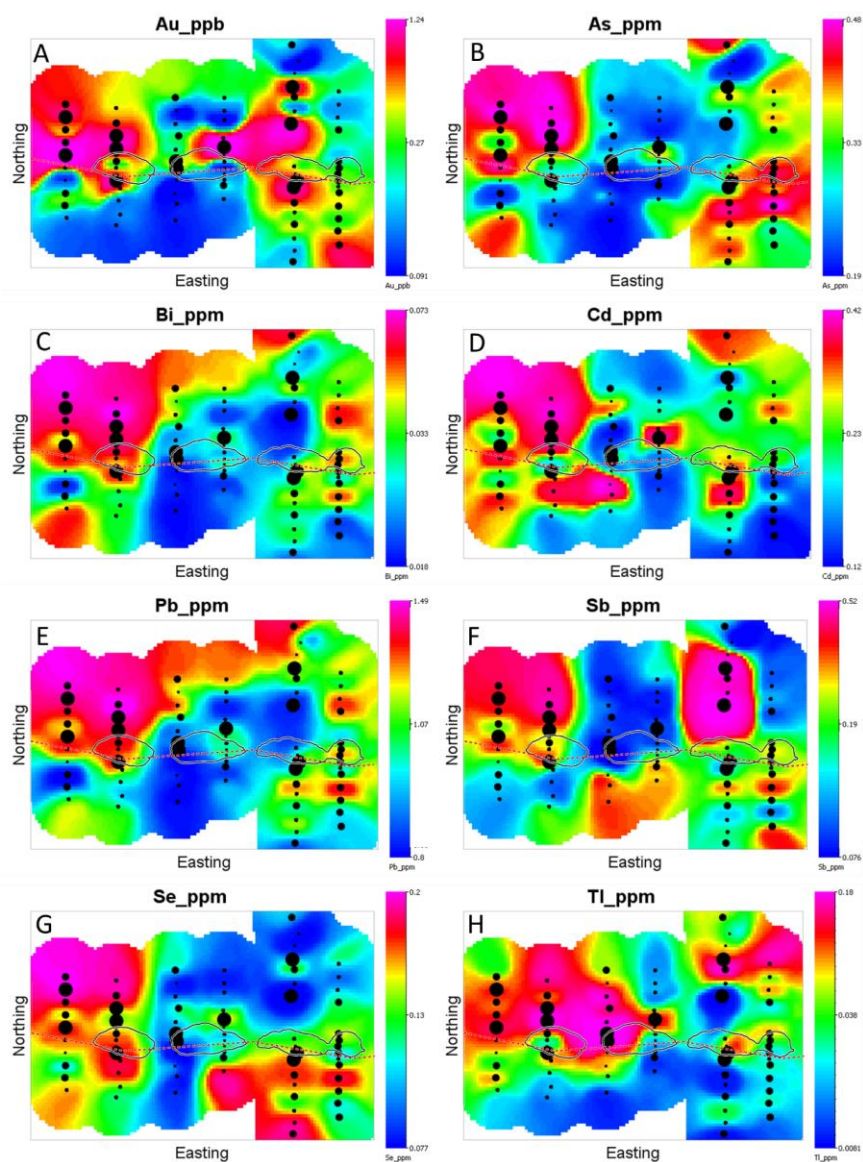


Figure 33. The IDW interpolation method exhibits the spatial distribution of gold pathfinder elements over and peripheral to the conceptual pit shell at the Twin Lakes Deposit. The conceptual pit shell is outlined in black. The red dotted line represents the Twin Lakes Shear Zone (TLSZ). The comparison of element profiles along six transects indicates a significant association between Au and As, Se, Bi, and Tl and a relative association with Sb, Cd and Pb. Small black dots indicate Au concentrations below the 80th percentile (<3 ppb). Medium circles represent values between the 81st to 97th percentile (3 to 10 ppb). Large circles represent values over the 98th percentile (11 to 303 ppb), respectively.

Antimony (Sb): Antimony is a common element in orogenic gold deposits (R. J. Goldfarb and Groves, 2015) that can be considered a pathfinder of gold (Dunn, 2007b). It is expected that 20-30% of Sb may have volatilized during the ashing process by controlled ignition at 475 °C (Dunn, 2007b). Black spruce samples collected above intermediate to mafic units have contiguous Sb values up to 6.1 ppm in twigs. Antimony anomalies have multiple coincidences with the zones of Au enrichment toward the northwest and east portions of the survey area, peripheral to the Twin Lakes Deposit (Figure 33F).

Selenium (Se): Selenium, in trace levels, plays a fundamental role in plant metabolism. However, its physiological significance is not well-understood (Combs Jr and Combs, 1986; Kabata-Pendias, 2001). Selenium resembles S and can substitute for S in biological processes (Kabata-Pendias, 2001). Geochemically, Se has chalcophilic and siderophilic tendencies and enters the lattice of sulphides (Dunn, 2007b). Therefore, high concentrations of Se in plant samples can reflect the presence of sulphide-bearing deposits. The solubility of Se depends on the redox regime, pH, and temperature. Selenium uptake by plants increases at higher pH, Eh and temperature >20°C (Alina Kabata-Pendias, 1998; Lindberg and Lannek, 1970). According to the studies by Pickering et al. (2000 and 2003) on the Se concentration and speciation in plants, foliage is the preferred sample medium in a biogeochemical survey that requires measurements of Se (Dunn, 2007b; Pickering et al., 2000; Pickering et al., 2003). It is probable that some of Se would be volatilized during the ashing process (Dunn, 2007b). Therefore, the Se content of ashed tissues may not represent the total Se of dry material. The spatial distribution map of Se shows zones of enrichment in samples collected in the west to the northwest over intermediate volcanic rocks, where Au is also enriched (Figure 33G). Other enrichments were also detected in the southern part of the survey, where no Au anomalies were identified (Figure 33G).

Thallium (Tl): Thallium is an important biogeochemical prospecting tool for Au. The high correlation between Tl and Au has been noted in several tree species close to mineralized areas (Warren et al., 1968). Thallium can be enriched in polymetallic deposits along with As and Sb (Warren et al., 1964). Geochemically, It can disperse during the oxidation of sulphides due to its high mobility, which makes it available to plant roots (Dunn, 2007b). Thallium is highly enriched over the TLSZ in association with intermediate volcanic units to the north. With respect

to all proposed pathfinders, Tl offers an exceptional occurrence, distribution pattern, and association with Au (Figure 33H).

3.1.4 Robust RQ-Principal Component Analysis (PCA)

PCA is a well-known method in the evaluation of multi-element associations and interrelationships related to geological processes (Chen, 2015). Robust RQ-mode PCA was applied to identify the main factors controlling the occurrence and distribution of major and trace elements in black spruce with respect to lithology over and peripheral to the Au mineralized zones at the Twin Lakes deposit.

Twenty-two elements (Au, As, Bi, Se, Sb, Tl, Fe, Co, Ni, Cr, Mo, Cd, Pb, Zn, Mn, K, P, B, Mg, Ca, Ba, and Cu) were selected for PCA analysis based on their significance from the exploration point of view and sample to variable (N/P) ratio of five. The Kaiser-Meyer-Olkin test result of 0.933 verified the appropriateness of our dataset for PCA. In RQ-PCA, elements (R) and samples (Q) loading were compared simultaneously at the same weight. Based on the Q mode of PCA, which acts like K-means clustering analysis, data are well clustered into three groups, indicating sample types (Figure 43). Generally, sample types (blue, green, and red coloured dots) with relatively large concentrations of certain elements (vectors) are co-located on the plot. In black spruce samples in the study area, most elements, including Fe, Co, Ni, Mo, Ti, Sb, and Cr, are accumulated in twigs; therefore, these element vectors plot close to twigs (red dots). Barium, K, Mg, Mn, P, and S are grouped close to needles (green dots), whereas Ca, Ba, Pb, and Cd are grouped near the bark (blue dots). The concentration of As, Au, and Bi in the bark and twigs are similar; therefore, they are located in the middle of the field for the blue and red dots.

The angle between elements and the length of the vectors should be considered in visualizing the variable plots obtained from PCA. The length of the vectors shows the influence of elements on the components, and the angle between elements indicates the power of interrelationship and correlation. All elements have almost the same length vectors because standardization leads to the same weight of variables. However, essential elements have a slightly longer, or put another way, more powerful vector than other elements. Moreover, each component contains sets of elements located close to each other, forming a small angle that

signifies a strong similar chemical association or distribution. Conversely, divergent and large angles (close to 180°) represent negative correlations, such as the angles between sets of the elements Ca-Ba and Zn-Mn-Cu-K-Mg-P-B. Sets of the elements Cd-Pb-As-Au-Bi-Se-Tl-Fe-Co-Ni-Mo-Ti-Sb-Cr meets Ca-Ba and Zn-Mn-Cu-K-Mg-P-B at almost 90° , which means they are not related (Figure 34).

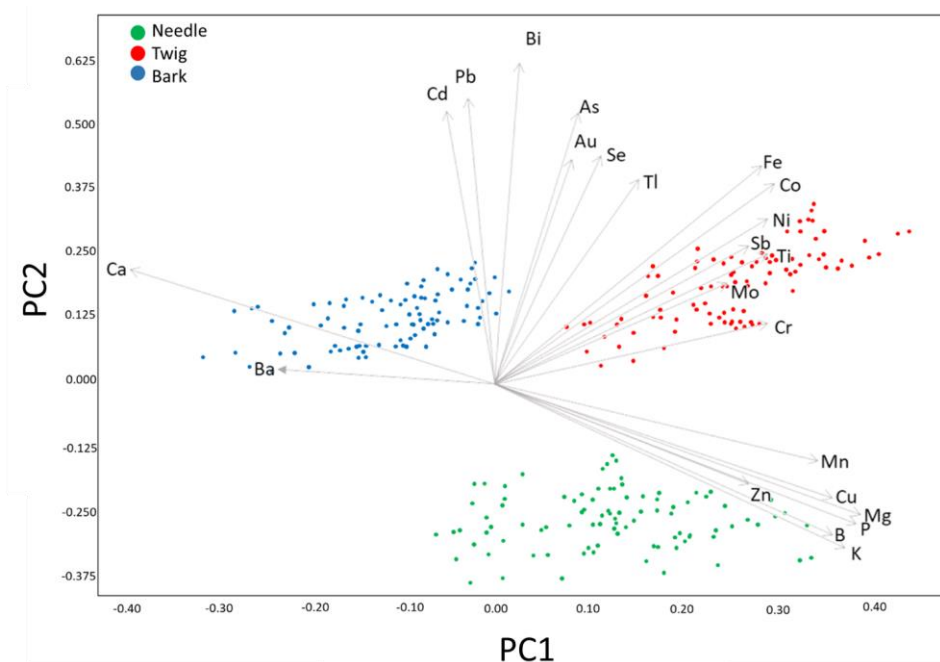


Figure 34. According to the robust RQ mode-PCA, two components control the distribution pattern of elements in black spruce samples. The geological/ mineralization/Fe factor represents the black spruce-substrate relationship, including elements that reflect bedrock composition, whereas the physiological factor contains a set of nutrition elements. Gold and its pathfinder elements, including As, Se, Tl, Bi, Pb and Cd, are a subset of geological/ mineralization/Fe, representing the association of bedrock with concealed mineralization. Also, a small angle between sets of nutrients or sets of metals demonstrates their strong correlation. The proximity of needles (green dots) to Mn, Cu, Mg, P, B, K and Zn indicates the high concentration of nutrients in needles, while Ca with structural function is close to bark samples (Blue dots).

Two components have been extracted with associated eigenvalues greater than one suggested by the Kaiser criterion (Kaiser, 1960). The first principal component (PC) is oriented

in the direction of maximum variance of the data. The second PC is orthogonal to the first PC, lying in the direction of the maximum remaining variance. PC 1 and 2 account for ~79% of the total variance in the dataset, representing the distribution pattern of elements in the black spruce tissues, their chemical affinity, and the plant-substrate relationship. Component 1, the “geological/ mineralization/Fe factor”, is characterized by high positive loadings for Cd, Pb, As, Au, Bi, Se, Tl, Fe, Co, Ni, Mo, Ti, Sb, and Cr, reflecting the chemistry of underlying bedrock with a signature suggestive of mineralization (~49% of total variance). The second component, the “physiological factor”, is defined by essential elements including Ca, Ba, K, P, Mg, Zn, Cu, and B, which explained ~30% of the total variance. PCA 2 can be divided into two subgroups of Ca-Ba and Zn-Mn-Cu-K-Mg-P-B, related to the accumulation of these essential elements in different tissues, as seen in Figure 34.

Black spruce samples collected over the Twin Lakes deposit show a high concentration of Fe-associated elements, including Fe, Co, Cr, Ti, Ni, and Mo. Dunn (1995) suggested that Fe-associated suites of elements in PCA can constitute an “iron factor” (Dunn, 1995). In gold mineralized zones, elements commonly associated with the iron factor include Au, As, Sb, and Cr (Dunn, 2007b). At the Twin Lakes Au Deposit, the iron factor can be equally considered a geological factor that includes Fe-associated and Au pathfinder elements. The small angle between the Au, As, and Fe vectors in Figure 34 confirms their association with substrate minerals such as pyrite (FeS_2) and arsenopyrite (FeAsS), which are the main Au-bearing minerals in the study area (Cavallin, 2019). Also, As has the smallest PCA angle with Au, indicating the strong relationship and the importance of arsenic as a pathfinder for Au. The presence of other Au pathfinder elements, including Se, Tl, and to a lesser extent Bi, Pb and Cd in black spruce within geological factor/iron factor suggests their dispersion is positively correlated with underlying Au mineralization (Lintern and Anand, 2017). Antimony has the least coincidence with zones of Au enrichment and the largest PCA angle with the Au vector among Au pathfinder elements at Twin Lakes.

The second component or physiological factor is defined by essential elements, including Ca, Ba, K, P, Mg, Zn, Cu and B, which explains ~27% of the total variance. Plant physiological functions have the largest contribution to this component. Generally, the chemical composition of black spruce needles with a very low concentration of metals is substantially different from

other tissues (Dunn, 2007b). Barium, K, P, Mg, Zn, Cu and B are mostly accumulated in needles and are interrelated, as evidenced by the small angle between these vectors. However, Ca clusters with a negative relationship to this component due to its structural function and accumulation in the bark. Barium has a geochemical association with Ca and can substitute it chemically; therefore, it has a similar negative loading within the physiological factor.

Although there is no one-to-one relationship in plant-substrate chemistry (Dunn, 2007b), a positive relationship between the vegetation responses and the concentrations of elements in the underlying bedrock was detected using multivariate data analysis at the Twin Lakes Deposit. The coincidence of Au with pathfinder elements in the northwest of the survey area attests to the robustness of biogeochemical and multivariate data analysis in delineating areas of Au enrichment and extracting the latent factors that might not be revealed using traditional data analysis.

3.2 Conclusions

It has been observed that a biogeochemical exploration using bark and twigs is a good tool for delineating elevated zones of Au mineralization undercover, which were already identified using other geological and geophysical methods in proximity to the TLSZ. Although the absolute concentration for Au is very low (\leq ppb), there is sufficient contrast in the data to be able to extract geologically meaningful patterns. The robust log-transformed inverse distance weighted grid image indicates that the spatial distribution of gold pathfinders has given rise to increased uptake of gold pathfinder elements with coincident Au enrichment either over the mineralization or at its margins. RQ-mode PCA plots derived from the correlation matrix of the selected elements suggest the existence of two factors: geological and physiological factors. The geological factor includes Fe-associated elements (iron factor) in the gold mineralization area with a high concentration in bark and twigs (Fe, Cr, Co, Ni, Mo, Sb, Au, As, Pb, Cd, Bi, Tl and Se). The physiological factor includes nutrient elements with a high concentration in needles (Mg, K, P, B, Cu, and Mn) except Ca and Ba, with negative loadings in this factor due to their accumulation in the bark. PCA clearly illustrates the Au-As association, representing its role as a gold pathfinder element at the Twin Lakes deposit. The Tl-As-Cd group significantly, and the Bi-Pb-Se group to a lesser extent, are shown to be best as gold pathfinder elements due to their

high statistical associations. There is also a response in Sb, but its statistical association is not strong. The biogeochemical survey conducted over the Twin Lakes Deposit provides valuable information to ascertain the potential of the property and specific zones as an exploration target by revealing zones of Au mineralization. Biogeochemical surveys could enhance exploration practices, especially in areas that are not easily accessible by traditional geological survey methods. Besides, this type of survey is quite beneficial in terms of time efficiency and the low cost of sample acquisition and preparation. Furthermore, these biogeochemical data can be later used in environmental surveys, indicating the baseline metal concentrations at the Monument Bay Project before mine development.

Chapter 4

4 Biogeochemical Prospecting for Gold at the Yellowknife City Gold Project, Northwest Territories, Canada: Part 1 - Species Optimization

Abstract

The Yellowknife City Gold Project (YCGP), located close to the city of Yellowknife, Northwest Territories, Canada, is exploring and drilling the extension of the Au-bearing shear zones that host the Giant and Con Mines. A biogeochemical survey was conducted over the Crestaurum and Barney deposits, which are hosted within two well-known high Au-grade shear zones at the YCGP. A total of 625 needle samples were collected from the alder (*Alnus incana*) (n=76), Labrador tea (*Ledum groenlandicum*) (n=40), black spruce (*Picea mariana*) (n=189), and juniper (*Juniperus*) (n=320), and analyzed using ICP-MS. Robust statistical analyses were applied to biogeochemical data to (1) identify the biogeochemical response in plant samples with respect to the underlying mineralogy, (2) detect the most preferred plant species in the study area, and (3) identify Au pathfinder elements and subsequently zones of Au enrichment. Principal component analysis (PCA) and K-means clustering analysis were employed to achieve these objectives. The preliminary statistical analysis showed that plant samples can successfully accumulate anomalous Au values up to 147 ppb. Also, it showed that black spruce and Labrador tea can accumulate higher concentrations of Au than alder and juniper. According to the PCA, mineralization/geological (PC1) and physiological (PC2) factors control the distribution of elements in plant samples. According to K-means clustering, plant samples were classified into three clusters based on the vegetation type and their affinity to accumulate suites of elements. Black spruce samples were identified as the optimum sample media for biogeochemical exploration at the YCGP as they were clustered in proximity to the mineralization/geological factor (PC1) responsible for loading vectors of Au, Ag, As, Se, Bi, Pb, Cu, Co, Fe, Zn, Cd, Tl, and Cr. Au is strongly correlated with its pathfinder elements (Ag, As, Se, Bi, Tl and Sb), specifically in the south of the Crestaurum Shear. The presented results in this study demonstrate that zones of Au enrichment can be detected using biogeochemical and robust statistical methods.

4.1 Introduction

The Yellowknife City Gold Project (YCGP) is located within the well-studied Archean-age Yellowknife Greenstone Belt (YGB) in the southwest corner of the Slave Craton (Armitage, 2021; Cousens, 2000). The YCGP encompasses 791 square km of contiguous land to the north, south, and east of the city of Yellowknife in the Northwest Territories, Canada (Armitage, 2021; Botor, 2018). Interest in explorations of the Yellowknife City Gold Property commenced in the 1930s in sediment-hosted quartz veins of the Burwash Formation due to the presence of the nearby Giant (8.1 Moz @ 16.0 g/t Au) and Con (6.1 Moz @ 16.1 g/t Au) Mines (Armitage, 2021; Shelton et al.). Although these mines were closed in the early 2000s, an unexplored, highly prospective district-scale land position in the north portion of the YCGP was actively explored (Shelton et al.). The Northbelt was originally explored in 2013 by Gold Terra to assess the continuity of the shear zones and associated mineralization related to the Giant and Con Mines. This area is interpreted to represent the northern extension of the Giant Mine structure (North Giant Extension: NGX) (Kelly, 1993b). Gold Terra has subsequently expanded the potential and prospective geology of the project by the acquisition of the Southbelt (extension of the Campbell and Con shears) and Eastbelt (contiguous with the Northbelt). Since these acquisitions, various exploration techniques, including multimedia geochemical, geophysical, and geological surveys, have been carried out for Au exploration in an attempt to better understand alteration assemblages and Au mineralization (Armitage, 2021; Baragar, 1966; Cassidy, 2007; Cousens et al., 2006; van Hees et al., 1999).

Starting in 2015, Gold Terra expanded and delineated Au potential at the YCGP using biogeochemistry. The application of plant biogeochemistry to mineral prospecting is a well-established approach in mineral exploration (Dunn, 2007b), using chemical analysis of vegetation to measure the presence and character of underlying mineralization [3]. In Canadian boreal forests, coniferous trees (e.g. spruce, pine, fir, and juniper) and shrubs (e.g. alder, willow, and Labrador tea) are widespread and able to accumulate relatively high concentrations of metals (Cohen et al., 1987; Dunn, 1981; Dunn, 2007b). These species are considered the preferred sample medium to provide reconnaissance biogeochemical mapping of concealed bedrock. According to surveys conducted by Dunn and others in 2001 and 2002 for the Yellowknife

EXTECH program, black spruce (*Picea mariana*) and Labrador tea (*Ledum groenlandicum*) demonstrated a high ability to uptake anomalous concentrations of Au and its pathfinder elements (As and Sb) (Dunn, 2001; Dunn, 2007b; Dunn et al., 2002). Generally, a Pathfinder element for Au refers to a non-ore element associated with Au, and its spatial relationship to ore systems is of value in providing vectors during exploration efforts. Arsenic, Bi, Se, Sb, Cd, Pb, Hg, Zn, Cu, and Tl have been reported widely in the literature as well-known pathfinders for Au (Aitchison, 1982; Anand et al., 2019; Boyle, 1979; Dunn, 2007b; Dunn et al., 2005; Erdman and Olson, 1985; Ghorbani et al., 2020; Ghorbani et al., 2022a; Ghorbani et al., 2022b; Girling et al., 1979; Kovalevsky and Kovalevskaya, 1989; Lintern and Anand, 2017; Reid et al., 2008; Warren and Horsky, 1986).

In order to understand the geochemical processes dominating the plant-substrate relationship, biogeochemical data should be treated, assessed, and analyzed statistically using the same procedures that would be applied to any set of geochemical exploration data. Precision of data is a critical component in assessing geochemical data quality before data interpretation. Abzalov (2008) introduced the average coefficient of variation, defined as CV_{avg} (%), to calculate the measurement errors in geochemical data (Abzalov, 2008). The compositional nature of geochemical data must also be considered in advance of any statistical interpretations. The compositional nature of geochemical data is expressed as part of some whole such as (part per billion) ppb, (part per million) ppm, or weight percentage (wt.%). It means that the sum of the elemental composition in any geochemical sample of interest (e.g., rock, water, or plant) is constant. The constant sum or data closure problem is the most important limitation related to the compositional data that may lead to bias in correlations between two variables (Rollinson, 1992). This issue can be addressed using logarithms of ratios (Aitchison, 1982; Buccianti and Grunsky, 2014; Filzmoser et al., 2009a).

The present study was conducted to (1) identify the biogeochemical characterization of Au and its pathfinders in plants that retain a record of the concealed mineralization setting and (2) apply robust statistical techniques to evaluate multi-element associations and reveal their interrelationships in plants with respect to the geology beneath, both of which assist in delineating zones of Au enrichment at the YCGP. Multivariate statistical analyses are well-known robust methods to evaluate the associations, correlations, and trends between variables (elements) and observations (any geochemical sample such as plants or rocks). Principal

component analysis (PCA) and K-means clustering are recognized as practical geostatistical approaches in geochemical prospecting for buried mineralization (Benz, 2017; Dunn and Heberlein, 2020; Ghorbani et al., 2022a; Ghorbani et al., 2022b; Pratas, Prasad, Freitas, and Conde, 2005; Zuo, 2011). PCA is a linear dimension reduction technique for large datasets and a well-known method for identifying multi-element associations and interrelationships related to geological processes (Chen, 2015). K-means clustering is also an unsupervised data classification technique that is useful for identifying the controls on element variations (Hartigan, 1975). The combination of these methods provides insights into the dominant geochemical processes controlling the distribution of elements in plant samples in respect of the underlying mineralization. Also, it highlights the robustness of biogeochemical and statistical techniques for follow-up studies.

4.2 Regional Geology of the YCGP

Orogenic Au deposits (Bohlke, 1982), also known as lode-Au deposits, are an important source of Au worldwide. These deposits are dominantly associated with metamorphic terranes formed at variable depths ranging from 2 to 20 km and associated temperature-pressure regimes of 200 to 700 °C and <1-5 kbar, respectively (Groves et al., 1998). Generally, orogenic Au deposits occur at or above the brittle-ductile transition in compressional settings where hot Au-bearing fluids from deeper levels are the source of the mineralization (Goldfarb et al., 2005; Groves et al., 1998). Gold in orogenic deposits is commonly hosted in quartz-carbonate veins and iron-enriched sulphidized wall rocks (Dubé, 2007). Silver, As, B, Bi, Mo, Sb, Te, W, and sometimes anomalous Cu, Pb, and Zn, may accompany Au in orogenic Au systems (Dubé and Gosselin, 2007; Groves et al., 1998).

The Yellowknife City Gold Project (YCGP) extends for 10 to 60 km to the north, east, and south of the city of Yellowknife, Northwest Territories, Canada (Armitage, 2021). This project is located in the southern part of the Slave Province (Figure 35). The Slave Province is an Archaean granite-greenstone terrane containing several ore deposits, including base metals, Ag, and Au (2.7 to 2.55 Ga) (Isachsen and Bowring, 1997; Ootes et al., 2011). In Particular, the YCGP encompasses a prolific orogenic Au trend situated along shear zones and faults related to the north-south trending Archean Yellowknife Greenstone Belt (YGB). The YGB is one of several greenstone belts with primarily low-grade greenschist facies metamorphism exposed in

the southern portion of the Slave Province (R. J. Botor et al., 2019; Cousens et al., 2006; Cousens, 2000; Isachsen and Bowring, 1994). The YGB consists of a north-south trending metavolcanic sequence of mafic to felsic volcanics of the Kam and Banting Groups, which are unconformably overlain by a conglomerate package of the Jackson Lake Formation (Armitage, 2021; Cousens et al., 2006; Helmstaedt and Padgham, 1986; Henderson and Brown, 1966) (Figure 35). The YGB is intruded by the Ryan Lake pluton, Defeat Plutonic Suite, Duckfish Granite, and the Anton Complex to the west (Armitage, 2021; Henderson, 1985) and is conformably overlain by the dominantly sedimentary packages of Duncan Lake Group, including the Walsh Lake and Burwash Formations to the east (Armitage, 2021; Helmstaedt and Padgham, 1986; Henderson, 1985).

The Kam Group, from base to top, includes the Chan, Crestaurum, Townsite, and Yellowknife Bay (host of the Giant and Con Mines) Formations. All conformable formations have a mafic to intermediate volcanic composition, mainly subalkaline basalts and basaltic andesites, excluding the Townsite Formation, which is composed of felsic to intermediate volcanic rocks (Armitage, 2021; Cousens et al., 2006). The Banting Group is primarily comprised of sheared calc-alkaline intermediate to felsic volcanic and volcanoclastic sedimentary rocks (Armitage, 2021). The Jackson Lake Formation is the youngest. Conglomerates of the Jackson Lake Formation have infilled the Yellowknife River Fault Zone (YRFZ), which is a faulted contact zone between the Kam Group and the Banting/Duncan Lake Groups indicating post-faulting sediments deposition (Armitage, 2021; Falck, 1990; Martel and Lin, 2006). The Walsh Lake and Burwash Formations of the Duncan Lake Group consist of a thick pile of greywacke and mudstone turbidites that conformably overlie the Banting Group (Armitage, 2021; Helmstaedt and Padgham, 1986; Henderson, 1985; Martel and Lin, 2006). Gold mineralization at the YGB is similar to other mesothermal, orogenic, quartz-carbonate or Au-only deposits, which are mainly hosted in shear zones that transect mafic volcanic and metasedimentary rocks (Goldfarb et al., 2005).

The YCGP is divided into three zones, including the Northbelt, Eastbelt and Southbelt (Figure 35). The Northbelt has the same characteristics and stratigraphy that underlies the historic Giant and Con mines, mainly hosted in quartz-carbonate-bearing shear zones that crosscut primarily mafic volcanic-dominated rocks (Groves et al., 1998; Ootes et al., 2011; Siddorn et al., 2006). This study covers the two well-known Au-bearing shear zones within the

northern portions of the property, including the Crestaurum and Barney Shears. Crestaurum is a narrow discrete north-northeast trending shear zone that crosscuts the mafic volcanics of the Kam Group (Chan and Crestaurum Formations). Mineralization at the Crestaurum Shear is characterized by low to moderate pyrite, arsenopyrite, visible Au, stibnite, chalcopyrite, sphalerite, galena, and other minerals associated with multi-stage quartz-carbonate veining (Armitage, 2021). The Barney Shear is a north-south multi-kilometre wide deformation zone within the Chan Formation affected by a northeast-trending crossing structure. The Barney Shear hosts mineralization within quartz-carbonate veins with several intervals characterized by moderate to high levels of coarse sulphides, including arsenopyrite, pyrite, galena, chalcopyrite, pyrrhotite, and sphalerite (Armitage, 2021).

4.3 Methodology

4.3.1 2015 Biogeochemical Survey

In 2015, a biogeochemical survey was conducted over the Crestaurum and Barney Shears, located in the north portion of the YCGP. The objective of this survey was to identify the optimum sampling medium for biogeochemical exploration at the YCGP and evaluate whether there is a plant-substrate relationship that is related to mineralization using statistical techniques. To achieve these objectives, 625 new growth needle and leaf samples, including field duplicates and standards, were taken from the dominant vegetative cover in the study area, including 320 juniper (*Juniperus*), 189 black spruce (*Picea mariana*), 76 alder (*Alnus incana*), and 40 Labrador tea (*Ledum groenlandicum*) samples. Samples were collected at 10 m station spacing along 25 m spaced cut lines oriented perpendicular to the Crestaurum shear; and at 10 m station spacing along 50 m spaced cut lines oriented perpendicular to the Barney shear, respectively. Needle and leaf samples were collected by snipping 25 cm lengths of branches, representing about the seventh growth season (Armitage, 2021), from chest height and around the circumference of trees. A minimum of 200 g wet sample of each plant was required for chemical analysis (Dunn, 2007b). The majority of samples in the study area were taken from areas of bedrock outcrop covered by thin (< 30 cm) organic-rich soils with sparse tree cover to slightly more forested areas [54]. Bedrock outcrop is commonly exposed to the surface over the entirety of the survey area (Palmer et al., 2021). Forested soils are thicker than the bedrock outcrop soils and are mainly covered by trees such as black spruce, consisting of a thin organic layer overlying poorly

developed soils and sometimes thin tills (< 2m) (Kerr and Knight, 2002; Wolfe and Morse, 2017).

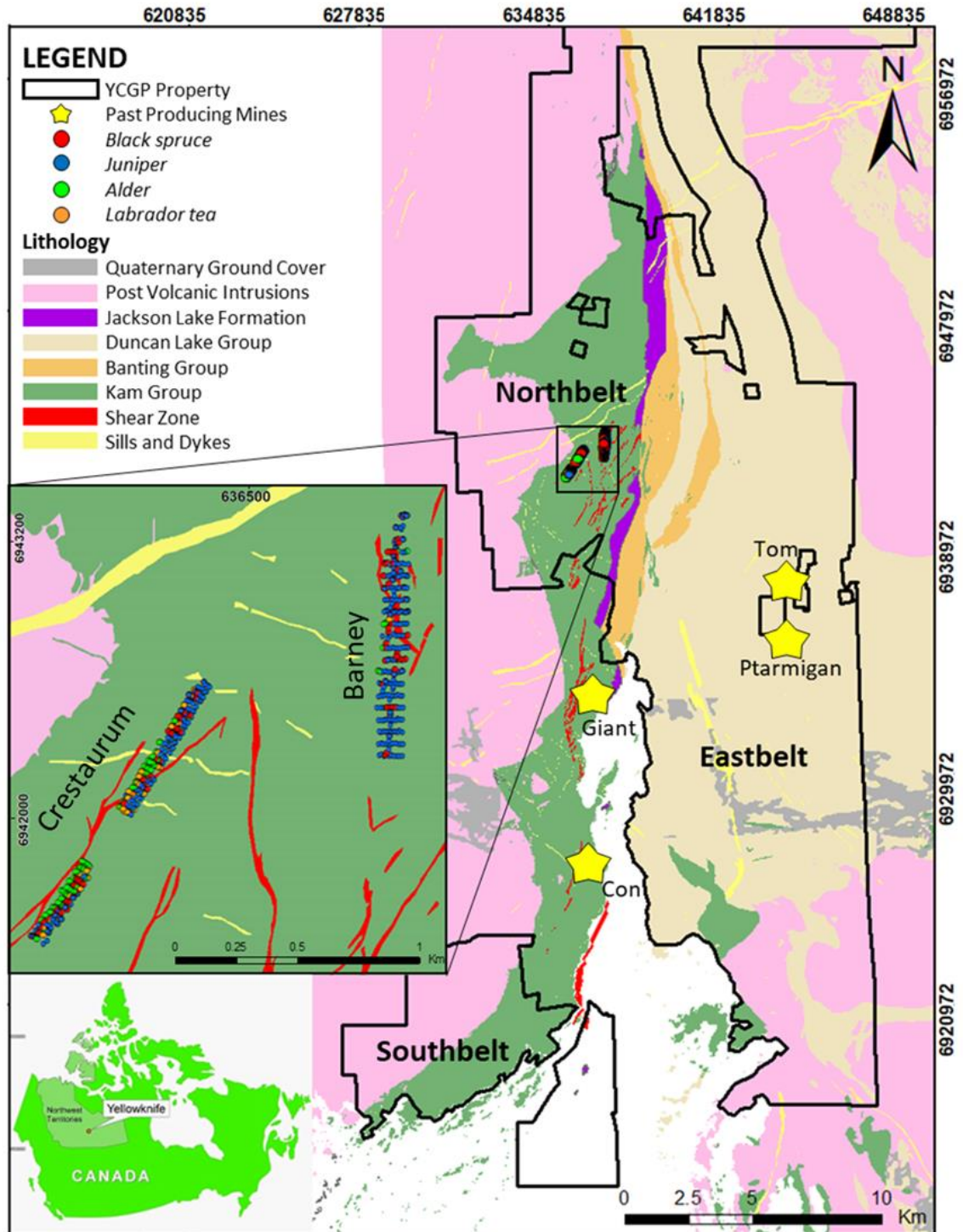


Figure 35: Regional geology of the Yellowknife City Gold Project (YCGP) and the location of samples collected at the 2015 biogeochemical survey (Ghorbani et al., 2022a).

Post-collection, needle and leaf samples were placed on a rack in a heated building overnight to dry out. Samples were prepared at ALS Labs in Vancouver, where the twigs and leaves were carefully separated and milled using a Wiley Mill to 100% passing 1mm. Subsequently, 100 g of all dried samples were weighed out and transferred into an ashing pan, followed by controlled ignition at 475 °C for 24 h. Then 0.25-gram aliquots of each ashed sample were digested in 75% aqua regia (1HNO₃:3HCl) using digestion. The final solution was analyzed by inductively coupled plasma-mass spectrometry (ICP-MS) using the ME-VEG41a package for ashed vegetations at ALS Global, Vancouver, British Columbia, Canada. A merged biogeochemical dataset including elements Au, As, Ag, As, B, Bi, Ca, Cd, Co, Cr, Cu, Fe, K, Mg, Mn, Mo, Ni, P, Pb, S, Sb, Se, Tl, and Zn was imported into the geochemical analysis software, ioGAS, for further data validation, including control of analytical data quality, data treatment, censoring, log-ratio transformation, multivariate data analysis and interpretations.

4.3.2 Data Preparation and Assessment

A systematic approach was applied to interpret biogeochemical data effectively and meaningfully. First, the precision of data was evaluated to identify the measurement errors attributed to different stages of field sampling, lab sub-sampling, preparation, and analytical processes (Heberlein et al. 2020). The precision of data was computed using the average coefficient of variation, CV_{avg} (%), to assess the effect of the measurement error and the quality of biogeochemical data (Table 4) (Ghorbani et al., 2022a). In the following formula, N is the number of duplicated pairs, and a and b are the concentration of element i in the original and duplicate samples, respectively (Abzalov, 2008).

$$CV_{avg}(\%) = 100 \times \sqrt{\frac{2}{N} \sum_{i=1}^N \frac{(a_i - b_i)^2}{(a_i + b_i)^2}}$$

Then, a 1/2 detection limit was used to censor values below the lower limit of detection (LLD) with a fraction of the detection limit (Carranza, 2011). As biogeochemical data are compositional data, a log-ratio transformation was employed to address the closure problems (Aitchison, 1982; Buccianti and Grunsky, 2014; Chen, 2015; Demšar, Harris, Brunsdon, Fotheringham, and McLoone, 2013; Filzmoser et al., 2009a; Grunsky and de Caritat, 2020).

Robustification was also applied using M-estimator to mitigate the effect of outliers. This method reduces the weight of the observation with a significant error to cope with outliers (Filzmoser and Hron, 2008; Filzmoser et al., 2009a; Stanimirova et al., 2007).

Robust RQ-mode principal component analysis (PCA) and K-means clustering were applied to identify the elemental association in the needle and leave samples and their inter-relationship with different vegetation types over the Crestaurum and Barney Shears. PCA is a linear dimension reduction technique for large datasets that transforms original data into a new lower-dimensional representation using a linear projection with a minimum loss of information (Demšar et al., 2013; Singh et al., 2017). RQ-mode PCA was introduced by Zou et al. (1983) to geochemical data, signifying the interrelationship between elements (R-mode) and the combinations of samples (Q-mode) that explain variation among variables simultaneously (Chen, 2015; Neff, 1994; Zhou et al., 1983). K-means clustering analysis is a simple and powerful unsupervised algorithm that has been widely used in data mining to discover the hidden spatial pattern and structure of unlabelled samples (Xu et al., 2021; Zuo, 2017). In this method, samples are classified into different clusters, exhibiting all samples in the same cluster with relatively similar characterization.

4.3.3 Data Precision

This study expresses the average coefficient of variation ($CV_{avg}(\%)$) as the total measurement error. A high total measurement error can obscure meaningful geochemical patterns and consequently undermine the biogeochemical technique to identify underlying mineralization (Abzalov, 2008). Coefficient of variation values below 20% indicate good data precision; between 20% and 30% acceptable precision; between 30% and 50% marginal precision; and over 50%, poor precision. In 2015 biogeochemical data, most elements are within the good and acceptable quality range (Table 4). Cadmium, Tl, Se, Au, and S are found within the marginal range (Table 4). These elements must be used with caution as their distribution patterns are likely to be influenced by noise caused by poor reproducibility (Dunn and Heberlein, 2020; Heberlein et al., 2020).

Table 4: Calculation of data precision results using the average coefficient of variation ($CV_{avg}(\%)$) indicate a marginal range for Cd, Tl, Se, Au, and S in 2015 biogeochemical data.

2015 Biogeochemical data					
Elements	CV _{avg} (%)	Elements	CV _{avg} (%)	Elements	CV _{avg} (%)
Cd_ppm	48.06	Sb_ppm	22.6	Zn_ppm	11.08
Tl_ppm	47.44	Ni_ppm	22.17	P_pct	9.94
Se_ppm	39.59	Pb_ppm	20.78	As_ppm	9.89
Au_ppm	33.52	Ba_ppm	19.11	Fe_ppm	9.62
S_pct	30.5	Mo_ppm	17.82	Co_ppm	9.27
Mn_ppm	27.97	K_pct	17.09	B_pct	9.19
Mg_pct	23.98	Cr_ppm	15.66	Cu_ppm	7.63
Bi_ppm	23.93	Ag_ppm	14.01	Ca_pct	1.43

4.4 Results and Discussion

4.4.1 Summary of Statistics

Table 5 provides the statistical summary applied to 625 black spruce, alder, Labrador tea, and juniper samples. In this study, Au, its associated pathfinder elements, including Ag, As, Bi, Sb, Se, Tl, Pb, and Tl, as well as a suite of other elements, including Cr, Fe, Ni, Mn, Zn, Co, Ca, Cu, Cd, P, K, S, Mg, B, and Mo, were selected to identify potential biogeochemical responses in plants to subsurface variations in geology. The results of the univariate statistical analysis show that the lowest (0.4 ppb) and highest (147 ppb) Au values were identified in juniper needles. The average Au concentration for all vegetation types is ~9 ppb. Black spruce samples with average Au values of 18.6 ppb demonstrate an enhanced ability to accumulate Au and reflect the plant-substrate relationship compared to Labrador tea, alder, and juniper with lower average Au contents of 12.86 ppb, 5.3 ppb, and 4 ppb, respectively. In addition to Au, the average concentration of most elements, including Ag, As, Bi, Sb, Se, Tl, Pb, Tl, Cr, Fe, Ni, Mn, Co, Cu and Cd, are elevated in black spruce in comparison to other vegetation types, with the exception of Mo, K, Zn, S, and Mg, which are accumulated more in alder samples. Boron and Ca have higher values in Labrador tea and juniper compared to other vegetations.

In order to have a better understanding of the depletion and enrichment of each element, the average concentration of each element in all sample types was compared with a background level. In this study, no suitable background samples were collected as the entire area of the survey is underlain by a similar geology. Therefore, the median or 50th percentile was used as background (Dunn, 2007b). The average concentrations of Au in plant samples (9.1 ppb) collected at the YCGP are almost two times higher than the background level (4.4 ppb). Particularly, black spruce and Labrador tea are highly enriched in Au. Mean Au content in black

spruce (18.61 ppb) is more than four times and in Labrador tea (12.86 ppb) is more than two times higher than the background level (4.4 ppb). Alder is slightly enriched in Au (5.3 ppb), while juniper is depleted (3.9 ppb) compared to the background value (4.4 ppb). Comparing the Ag and Bi mean values to the background levels shows no difference to slight enrichments in alder and juniper. Silver is enriched up to 40 times in black spruce. Silver and Bi are accumulated more than two times in Labrador tea samples. Arsenic, Pb, Sb, Se, Cr, Fe, Mn, Cu, Cd, and Zn values are enriched in all sample types compared to the background level. Thallium values in black spruce, juniper, and Labrador tea are three times more than the background level. Cobalt is accumulated at twice the background level in black spruce and alder. Juniper and alder have accumulated Ni two times higher than the background level. No significant difference was identified for Ca in juniper between the mean content and background value, while Ca is depleted in the other vegetation types. Molybdenum shows more than five times enrichment in alder, while black spruce and Labrador tea contain the same mean Mo content as the background value.

Table 5: Descriptive statistics of Min, Max, mean and median values of element concentrations for 625 vegetation samples collected at the YCGP. The number of collected samples for each plant species is shown in brackets. Also, the average concentration of elements in different vegetation types, including alder, black spruce, juniper, and Labrador tea, are provided. The Median or 50th percentile is considered the background level.

Sample Type	All Vegetation Samples				Alder	Black Spruce	Juniper	Labrador Tea
Elements	Min	Max	Mean	Background	Mean			
Au_ppb	0.4	147	9.1	4.4	5.3	18.61	3.92	12.86
Ag_ppm	0.02	6.08	0.64	0.05	0.06	1.98	0.04	0.13
Bi_ppm	0	0.282	0.03	0.02	0.01	0.07	0.02	0.04
As_ppm	1.94	185	19.15	10.1	13.85	40.22	6.72	29.02
B_ppm	76	1620	323	219	589	447	149	626
Ca_pct	13.55	26	24.3	26	21.78	23.31	25.97	21.15
Cd_ppm	0.02	8.27	0.82	0.62	0.6	1.09	0.77	0.41
Co_ppm	0.29	64.3	4.76	2.2	5.09	10.08	1.7	3
Cr_ppm	0.52	24.8	3.88	2	1.98	8.23	1.67	4.62
Cu_ppm	12.45	338	93.9	52.7	103	191	28	144
Fe_ppm	459	15400	2466	1300	1406	5263	1043	2650
K_pct	1.21	11	7.42	7.66	10.83	9.41	5.02	10.78
Mg_pct	0.2	7.69	2.33	1.99	5.44	2.71	1.17	3.89
Mn_ppm	261	27000	6185	4040	7977	10524	2562	11271
Mo_ppm	0.11	36.7	1.57	0.81	4.6	0.8	1.41	0.83
Ni_ppm	1.01	196.5	25.2	14	20	33.57	21.1	29.63
P_pct	0.29	1.001	0.94	1	1	1	0.88	1
Pb_ppm	1.19	170	7.56	3.91	3.51	15.81	3.43	9.22
S_pct	0.04	3.31	0.76	0.61	1.54	0.99	0.36	1.39
Sb_ppm	0.3	44.6	2.87	1.35	1.98	5.95	1.04	4.65
Se_ppm	<0.01	1.185	0.16	0.1	0.09	0.32	0.07	0.18
Tl_ppm	<0.001	6.73	0.16	0.03	0.04	0.4	0.03	0.18
Zn_ppm	87	8790	1344	456	3608	2423	432	843

Au concentration in vegetation types collected over the Crestaurum and Barney Shears are compared in Figures 36 and 37. Needle samples collected over the Crestaurum shear contain higher Au values than those collected over the Barney Shear in all vegetation types except alder, which contains similar Au values in both localities (Figure 36). High Au values (89 to 147 ppb) were identified in all vegetation types located in close proximity to each other over the south of the Crestaurum Shear. Black spruce indicates a significant Au enrichment in both shears compared to other vegetation species (Figure 37).

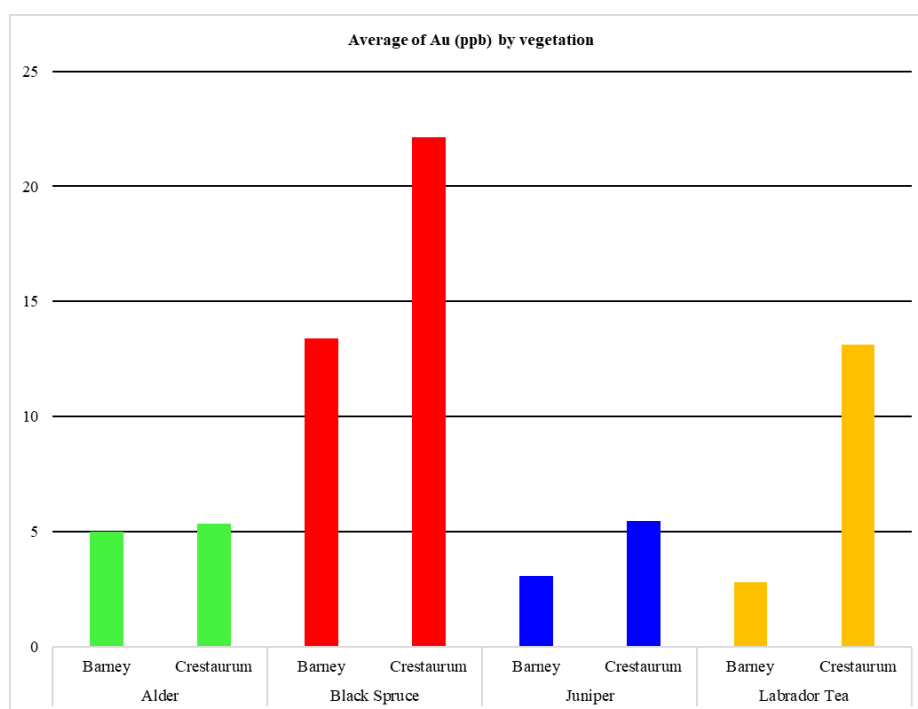


Figure 36: The comparison of the average concentration of Au (ppb) in ash in foliage by different vegetation species collected over the Barney and Crestaurum Shears.

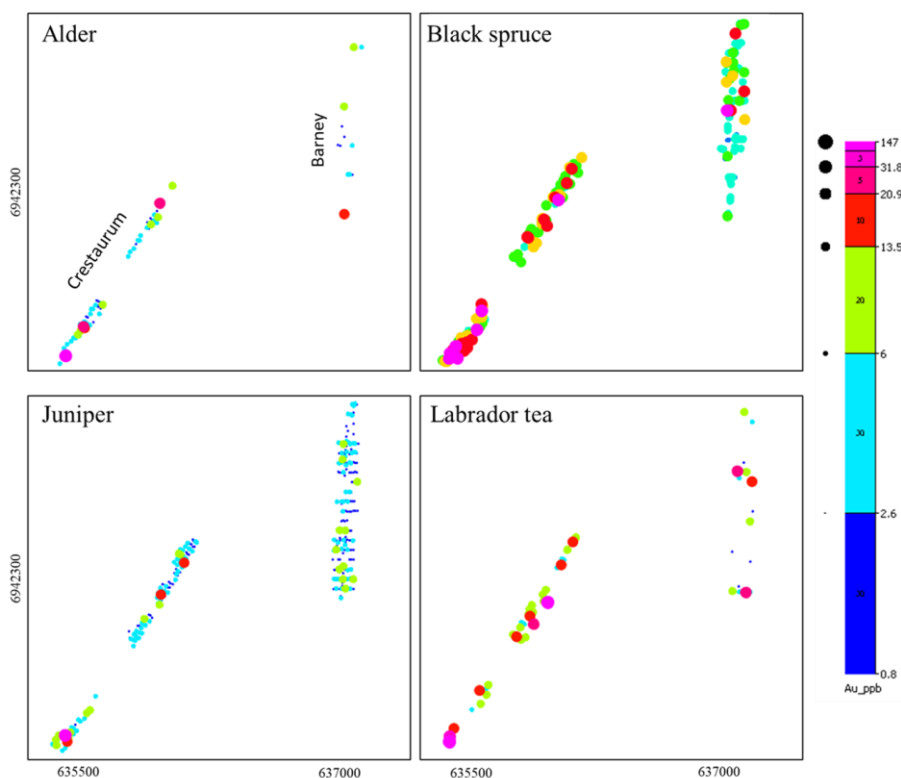


Figure 37: The concentration of Au in alder, juniper, black spruce, and Labrador tea foliage samples collected over the Crestaurum and Barney Shear. Anomalous Au values up to 147 ppb (in ash) were identified in all vegetation types located over the southern portion of the Crestaurum shear. Black spruce needles show a significant Au enrichment compared to other vegetation.

4.4.2 Robust RQ-Mode Principal Component Analysis (PCA)

The biogeochemical study at the YCGP was carried out to document element concentrations and spatial variations in plant samples. A robust RQ-mode principal component analysis (PCA) inspection of this data was applied to identify the geochemical processes dominating the element distribution in vegetation samples in the survey area (Figure 38). PC1, PC2, and PC3 with eigenvalues greater than one account for ~83% of the total variance covering the most important data information. PC1 and PC2 are the main geochemical factors controlling the distribution of elements in vegetation samples collected in the 2015 biogeochemical survey.

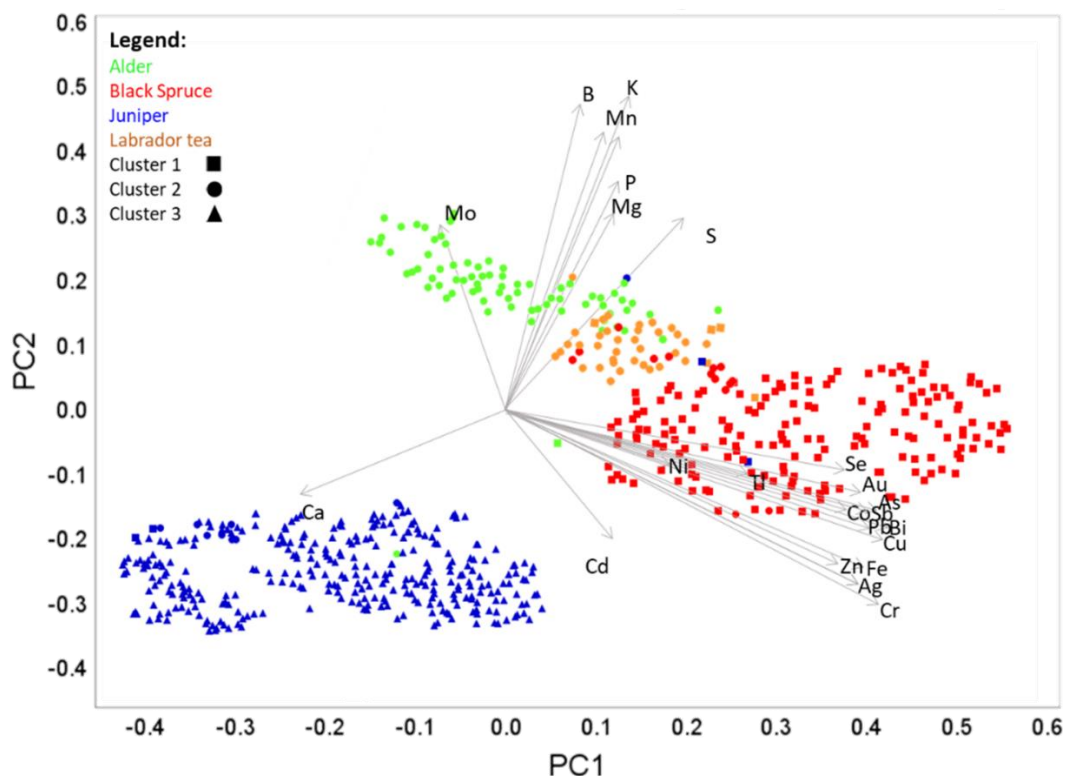


Figure 38: Graphical representation of the robust RQ-mode principal component analysis (PCA) and K-means clustering applied to the 2015 biogeochemical sample. The PCA results indicate that the mineralization/geological factor (PC1) and physiological factor (PC2) are the contributing factors controlling the distribution of elements in plant samples collected at YCGP. PC3 includes only Mo, which is positively loaded in PC2. Based on the K-means clustering, samples are grouped into three clusters shown by square, circle, and triangle shapes, demonstrating the plant-substrate relationship with respect to the lithology/mineralogy beneath.

PC1 (~65% of total variance) consists of a set of elements that primarily represent the bedrock composition, including Au, Ag, As, Se, Bi, Pb, Cu, Co, Fe, Zn, Cd, Ti, and Cr. The association of Fe, Co, Cr, Ti, and Ni with Au, As, and Sb in one component of the PCA demonstrates a strong plant-substrate relationship in the Au mineralized area (Dunn, 1995; Ghorbani et al., 2022a). Therefore, the biogeochemical signature controlling PC1 is termed the mineralization/geological factor. The loadings of PC1 are vectored close to black spruce samples shown in red (Figure 38). PC2 (~13% of total variance) is dominated by elements that are considered essential elements for plant metabolism. This component has a strong negative

loading for Ca and strong positive loadings for B, Mn, Mg, K, P, and Mo. The plant physiological factor reflects the biogeochemical response (PC2) that controls the occurrence and distribution of essential elements in plant samples. The loadings of PC2 are positively vectored toward alder (green) and Labrador tea (orange) samples. Alder and Labrador tea have broader leaves than black spruce and juniper needles. Therefore, they indicate more physiological features related to the presence of essential elements such as Mg, K, and P. Calcium is negatively loaded to PC2, likely because of its structural function in plant metabolism and tendency to accumulate in bark than needles and leaves (Dunn, 2007b). PC3 is responsible for ~5% of the total variance, including only Mo, which is also positively loaded in PC2. PC3 loading is proximal to the alder samples (green), indicating a significant association between Mo and alder samples.

4.4.3 K-Means Clustering Analysis

K-means clustering analysis was applied to the 625 needle samples collected in the study area. According to Figure 38, needle samples are grouped into three clusters based on their vegetation type and affinity to the specific suites of elements. Clusters are presented in different shapes: cluster 1 = squares, cluster 2= circles, and cluster 3= triangles (Figure 38). Cluster 1 is dominated by the majority of the black spruce samples (red squares), located proximal to the set of elements that compose PC1 (mineralization/geological factor). Therefore, black spruce can be considered the preferred sample medium to reflect a plant-substrate relationship by accumulating higher concentrations of metals, Au, and associated pathfinder elements. Cluster 2 includes samples from Labrador tea (orange circles) and alder (green circles). Labrador tea samples (orange circles) are clustered between PC1 and PC2, slightly more toward PC2, signifying the influence of both the mineralization/geological and physiological factors on the biogeochemistry of Labrador tea samples. Labrador tea is the second most preferred plant species for the biogeochemical survey at the YCGP. Alder samples (green circles) are located proximal to PC2 and PC3, where sets of elements responsible for the physiological factor are located. The association of alder and PC3, where the Mo vector is loaded, is related to the tendency of alders to accumulate Mo (Dunn, 2007b). The requirement of Mo in alder and the presence of anomalous values of Mo in alder have been reported in studies by Becking (1961), Dunn (1984), and Dunn et al. (1990). Juniper samples (blue triangles) are predominantly associated with

cluster 3, which is loaded negatively to PC1. These samples contain low values of Au and are considered the least suitable media for biogeochemical prospecting of Au compared to other vegetations in the study area. Also, the Ca vector near the juniper samples can be attributed to the higher concentration of Ca in junipers compared to the other vegetation types.

The PCA and K-means clustering indicate that mineralization/geological and physiological factors are the dominant biogeochemical signatures controlling the distribution of elements in plants at the YCGP. Also, black spruce was identified to be the best sample medium for biogeochemical reconnaissance prospecting for Au in the study area. In black spruce, Au is associated significantly with As and Sb ($R^2 > 0.8$) and somewhat less with Bi and Pb ($R^2 > 0.63$). These associations demonstrate the robustness of the plant-substrate relationship since mineralization in the region consists of low to moderate abundances of sulphides such as pyrite, arsenopyrite, stibnite, and galena at the Crestaurum and Barney shears (Armitage, 2021). Also, a high Au-Mo association ($R^2: 0.56$) was identified in black spruce. This relationship may be related to the presence of late felsic intrusions with strong Au \pm Mo mineralization (Armitage, 2021). It has been claimed that Mo is a successful biogeochemical indicator of mineralization because plant tissues do not establish significant barriers to Mo uptake (Dunn, 2007b).

The PCA and K-means clustering analysis indicate that Ag, As, Bi, Sb, Se, and Tl are the best pathfinders of Au in the current study. Also, black spruce > Labrador tea were identified as the best vegetation media for Au prospecting in the study area. All pathfinder elements are significantly enriched in the southern portion of the Crestaurum Shear, where high Au concentrations are identified (Figure 37). The association of Au with As and Sb is related to the sulphide mineralization hosted within the mafic volcanics. Many studies reported the presence of As-bearing and Sb-bearing minerals such as pyrite, arsenopyrite, and stibnite within the Crestaurum and Barney Shears (Armitage, 2021; Botor, 2018). Also, positive associations between Au and Ag can possibly be related to the presence of porphyry-style mineralization with high Au and Ag content intersecting the Barney shear (Armitage, 2021). Thallium is a useful pathfinder of Au in biogeochemical exploration. A strong association between Au, Tl, As, and Sb is observed in polymetallic deposits (Dunn, 2007b). Also, a significant association between Au and Tl is identified in spruce samples located at the Highland Valley mine in Southern British Columbia (Dunn, 2007b; Warren and Horsky, 1986). Significant correlations between Au and Ag, Bi, Se and, to a lesser extent, As and Tl were observed north of the Barney Shear. Samples

collected from the north of the Barney shear are located precisely over the mineralized shear (Figure 35), where Au and its pathfinder elements are similarly enriched. These associations illustrate a crystal-clear example of the plant-substrate relationship and the robustness of the biogeochemical technique in delineating zones of Au enrichment. The results of this study can be applied to a wider survey across the YCGP to look for extensions of the advanced targets and possibly elucidate new targets at low cost and with significant reliability.

4.5 Conclusion

The outcomes of the biogeochemical prospecting for Au at the Crestaurum and Barney Shears using biogeochemical and robust statistical techniques were found to be positive and reliable. Statistical analysis indicates that black spruce needle samples can accumulate a significant amount of Au, up to 147 ppb in ash. Black spruce > Labrador tea are confirmed as the optimum sample media among all plant species collected for this study. The comparison between Crestaurum and Barney Shear indicated that foliage samples collected over the Crestaurum Shear are more enriched in Au in all plant samples except for alder, with the same Au values in both shears. Principal component analysis and K-means clustering analysis are used to discover the plant-substrate relationship and elemental association. Three factors controlling the geochemical distribution in plant samples are identified using PCA. PC1 includes a strong association between Au, Ag, As, Se, Bi, Pb, Cu, Co, Fe, Zn, Cd, Tl, and Cr, representing the mineralization/geological factor. Well-known Au pathfinder elements, including Ag, As, Se, Sb, Bi, and Tl, are attributed to PC1, indicating the mineralization association. PC2 includes essential elements for plant metabolism, including B, Ca, Mn, Mg, K, P, and Mo. Ca is negatively loaded into PC2 due to its structural function. PC2 represents physiological factors. PC3 consists of only Mo, significantly associated with alder samples. K-means clustering classifies samples into three clusters based on the vegetation type and their tendency to accumulate specific sets of elements. Black spruce samples are grouped into cluster 1, where PC1 or the mineralization/geological factor is vectored. This result verifies the ability of black spruce to provide insight into the geochemistry and composition of the underlying lithologies. Labrador tea and alder samples are classified into cluster 2, while juniper samples are grouped in Cluster 3. Au is strongly accompanied by its pathfinder elements, especially in the south of the Crestaurum Shear. The association of Au with its pathfinder elements indicates the reliability of

the results and a strong plant-substrate relationship. The positive result of this survey verifies the robustness of the combined use of biogeochemical and statistical analysis, which can be used in a broader survey across the YCGP to find extensions to the advanced and early-stage Au targets.

Chapter 5

5 Biogeochemical Prospecting for Gold at the Yellowknife City Gold Project, Northwest Territories, Canada: Part 2, Robust Statistical Analysis

Abstract

The Yellowknife City Gold Project (YCGP) is a promising Au district located in proximity to the city of Yellowknife, Northwest Territories, Canada. Positive results of a short biogeochemical survey in 2015 over the Crestaurum and Barney shears (Part 1) resulted in a broad survey over the early and advanced Au targets across the YCGP (Part 2). This survey uses a systematic two-phase statistical approach, including process discovery and process validation, to evaluate the multi-element biogeochemical dataset and identify the geochemical process controlling elemental occurrence and distribution in black spruce needles. To achieve these objectives, 2788 black spruce needle samples were collected across the Northbelt and Eastbelt of the YCGP and analyzed by ICP-MS using a multi-element determinations package for unashed vegetation. Following that, a biogeochemical dataset including Au, As, Ag, Bi, Ca, Cd, Co, Cr, Cu, Fe, K, Mg, Mn, Mo, Ni, P, Pb, S, Sb, Se, Tl, and Zn were prepared and analyzed using univariate and multivariate statistical analyses, including principal component analysis (PCA) and inverse distance weighted (IDW) interpolation method. The univariate statistical analysis showed that the average Au value in the black spruce needle is higher than the background level in all targets. Contiguous anomalous Au values were identified in needle samples collected proximal to the Ptarmigan and Tom mines (~10 ppb) and Ryan Lake target (3.8 ppb). According to the robust RQ mode-PCA, PC1 and PC2 control the distribution pattern of elements in black spruce needles. PC1 includes two sets of elements indicating geochemical/mineralization factor (Au, As, Sb, Fe, Pb, and Mo) and physiological factor (Cu, Ca, Zn, K, S, P, and Mg). On the other hand, PC2 differentiates these two factors with more emphasis on the influence of the geochemical/mineralization factor. The IDW interpolation method indicates zones of Au enrichments at the YCGP are associated with different sets of pathfinder elements based on the bedrock composition and mineralization style. According to the IDW, elevated Au values associated with shear zones hosted within mafic/ultramafic bodies are accompanied by As, Sb, Pb, and Cu, while those located proximal to late felsic bodies are accompanied by Ag, As, Se,

Hg, and Tl. Zones of Au enrichment located along the faulted contacts between the felsic-intermediate metavolcanics and sulphide metasediments are accompanied by Bi, Se, Hg, and Zn. The results of this study attest to the robustness of multivariate statistical analysis in detecting zones of Au enrichment using biogeochemical exploration.

5.1 Introduction

The Yellowknife City Gold Project (YCGP) encompasses 791 square km of contiguous land to the north, south, and east of the city of Yellowknife in the Northwest Territories, Canada (*Yellowknife City Gold project, The Last Undeveloped High-Grade Gold Camp in Canada*, 2015). The YCGP is located within the Archean-age Yellowknife Greenstone Belt (YGB) in the southwest corner of the Slave Craton, which is one of the best exposed and well-researched greenstone belts in Canada (Cousens, 2000). The first Au discovery in the Yellowknife camp was in sediment-hosted quartz veins of the Burwash Formation in 1934. The Au discoveries within the metavolcanic rocks that hosted the Giant and Con Mines were made in 1935. The north portion of the YCGP is believed to be comprised of an unexplored, highly prospective district-scale mineralization system representing the northern extension of the Giant Mine structure (NGX) (Kelly, 1993b). Therefore, an exploration program on the Northbelt portion of the YCGP commenced in 2013 to assess the continuity of the shear zones and associated mineralization related to the Giant Mine. Following that, the potential and prospective geology of the project were expanded to the Southbelt (extension of the Campbell and Con shears) and Eastbelt (contiguous with the Northbelt).

Starting in 2015, Gold Terra Resource Corp. conducted a short reconnaissance biogeochemical survey to expand and delineate Au potential at the YCGP. This survey aimed to use the chemical analysis of vegetation to measure and confirm the presence and character of underlying mineralization at the YCGP (Ghorbani et al., 2022a). In this survey, over 600 plant samples, including mountain alder (*Alnus incana*), Labrador tea (*Ledum groenlandicum*), black spruce (*Picea mariana*), and juniper (*Juniperus*) were collected over the Crestaurum and Barney deposits, which are hosted by high Au grade shear zones on the YCGP. Multivariate statistical analyses were applied to the biogeochemical dataset, and the returned results show a significant biogeochemical response in plant samples with respect to the underlying mineralogy. The statistical analysis demonstrates that plant samples, black spruce and Labrador tea, in particular,

can successfully accumulate anomalous Au values up to 147 ppb in ash. Also, Ag, As, Se, Bi, Tl and Sb were found to be Au pathfinder elements in plant samples, confirming what had been previously determined in other petrological, mineralogical, and geochemical studies (Armitage, 2021; Ghorbani et al., 2022a). Previous biogeochemical surveys conducted by Dunn and others in 2001 and 2002 for the Yellowknife EXTECH program have also demonstrated a high ability of black spruce and Labrador tea to uptake anomalous concentrations of Au and its pathfinder elements (As and Sb) (Dunn, 2001 and 2007; Dunn et al., 2002).

Positive outcomes of the 2015 survey resulted in a broad reconnaissance biogeochemical survey across the YCGP in 2017. This biogeochemical survey was conducted over different drilled and early-stage targets across the Northbelt and Eastbelt using the preferred sample medium (black spruce) identified as such in the 2015 biogeochemical survey. This survey aims to use robust statistical analysis to assess the multi-elemental association and, more importantly, the biogeochemical characterization of Au and its pathfinders in black spruce with respect to the geology beneath. The results of this survey help to determine the geochemical processes dominating the plant-substrate relationship over various lithologies and mineralization settings across the YCGP.

A systematic two-phase approach is required to achieve these objectives, including process discovery and process validation. These steps were suggested by Grunsky and Caritat (2020) to evaluate multi-element geochemical datasets and identify geochemical processes that may not be crystal clear unless robust data analysis is employed (Grunsky and de Caritat, 2020). The initial process discovery step evaluates the associations, correlations, and trends between variables (elements) and observations (any geochemical sample such as plants or rocks). In the process validation step, the observed patterns and associations are tested to verify whether they are valid and applicable to building a model or not. Advanced analytics in process discovery and validation involves the use of several robust multivariate statistical analyses such as principal component analysis (PCA) and inverse distance weighted (IDW) interpolation. These methods are known as practical geostatistical approaches in geochemical prospecting for concealed mineralization (Bartier and Keller, 1996; Benz, 2017; Dunn and Heberlein, 2020; Ghorbani et al., 2022b; Pratas et al., 2005; Yasrebi et al., 2016; Zuo, 2011). PCA is an unsupervised dimension reduction method that describes the distribution of multivariate data using a new set

of data axes known as components (Shepard, 1968). In geochemical studies, each component is a linear combination of all the geochemical variables that can represent a contributing geochemical factor (Burrough et al., 2015). A comprehensive implication of PCA to geological data analysis is presented by Davis (1986). The inverse distance weighted (IDW) is a spatial prediction method that Shepard (1968) introduced. IDW assumes that points close to one another are more alike than that farther away, and the local influence of each point diminishes with distance (Burrough et al., 2015; Ghezelbash et al., 2019). Therefore, the IDW method gives more weight to points that are closer to the prediction location. Mathematically, weights are proportional to the inverse of the distance that is raised to the power value p . Therefore, the weight decreases exponentially as distance increases. If $p=0$, the prediction value is equal to the mean of all data values in the neighbourhood, while a very large p -value gives approximately the same weight as the closest surrounding point. In geological software, the default p -value equals 2, although there is no justification for considering this value over other p -values (Vural, 2019). IDW is also a popular multivariate interpolation method in processing large geochemical datasets. This study provides insight into the dominant geochemical processes controlling the distribution of elements in plant samples in respect of the underlying lithology and mineralization.

5.2 General Geological Setting:

Orogenic Au deposits (Bohlke, 1982), also known as lode-Au deposits, are a common worldwide source of Au. These deposits are dominantly associated with metamorphic terranes formed at variable depths ranging from 2 to 20 km and associated temperature-pressure regimes of 200 to 700 °C and <1-5 kbar, respectively (Groves et al., 1998). Gold in orogenic deposits is commonly hosted in quartz-carbonate veins and Fe-enriched sulphidized wall rocks (Dubé, 2007) and associated with Ag, As, B, Bi, Mo, Sb, Te, W, and sometimes with Cu, Pb, and Zn (Dubé and Gosselin, 2007; Groves et al., 1998).

The Yellowknife City Gold Project (YCGP) encompasses orogenic Au mineralization along shear zones and faults related to the north-south trending Archean Yellowknife Greenstone Belt (YGB). The YGB is one of several greenstone belts with primarily low-grade greenschist facies metamorphism exposed in the southern portion of the Slave Province (Botor et al., 2019; B. Cousens et al., 2006; Cousens, 2000; Isachsen and Bowring, 1994). The YGB is in many ways analogous to the more comprehensively studied Abitibi Greenstone Belt in Ontario and

Quebec (Robert, 1990). The YGB is composed of metavolcanic rocks of the >2.70 Ga Kam Group and the 2.69 to 2.66 Ga Banting Group (Armitage, 2021; B. Cousens et al., 2006; Helmstaedt and Padgham, 1986; J. F. Henderson and Brown, 1966) (Figure 39). The Con and Giant deposits are hosted by dominantly mafic rocks of the Kam Group. The YGB is intruded in the west by the Ryan Lake pluton, Defeat Plutonic Suite, Duckfish Granite and the Anton Complex (Armitage, 2021; J. B. Henderson, 1985) and is conformably overlain by the dominantly sedimentary packages of the Duncan Lake Group of turbidites, including the Walsh Lake and Burwash Formations, to the east (Armitage, 2021; Helmstaedt and Padgham, 1986; J. B. Henderson, 1985). The Kam and Banting groups are separated by the Hay-Duck Fault, also called the Yellowknife River Fault Zone (YRFZ). The YRFZ is a major crustal fault, typically an important feature of terranes that host mesothermal Au deposits (Dubé, 2007). The Jackson Lake Formation contains conglomerate grading upwards to sandstone and then argillite; it is localized proximal to the Hay-Duck Fault and is interpreted as an analogue to the more widely known Timiskaming Conglomerate in the Abitibi (Siddorn and Halls, 2002). Gold mineralization at the YGB is similar to other mesothermal, orogenic, quartz-carbonate or Au-only deposits, which are mainly hosted in shear zones that transect mafic volcanic and metasedimentary rocks (Goldfarb et al., 2005).

The YCGP is divided into three zones, including the Northbelt, Eastbelt and Southbelt (Figure 39). This study covers the north and east portions of the property. The Northbelt has the same characteristics and stratigraphy that underlies the historic Giant and Con mines, mainly hosted in quartz-carbonate-bearing shear zones that crosscut primarily mafic volcanic-dominated rocks (Groves et al., 1998; Ootes et al., 2011; Siddorn et al., 2006). Within the Northbelt, samples were collected from both advanced and early Au targets, including the Ryan Lake target, Sam Otto target, Walsh Lake target, and Homer Lake target. (Figure 39).

The Crestaurum Shear, Barney Shear, Townsite, AES Shear, and Shear 20 were studied within the Ryan Lake target. Crestaurum is a narrow discrete north-northeast trending shear zone that crosscuts the mafic volcanics of the Kam Group (Chan and Crestaurum Formations). Mineralization at the Crestaurum Shear comprises low to moderate pyrite, arsenopyrite, visible gold, stibnite, chalcopyrite, sphalerite, galena, and other minerals associated with the multi-stage quartz-carbonate veining. The Barney Shear is a north-south multi-kilometre-wide deformation zone within the Chan Formation affected by the northeast-trending crossing structure. Barney

hosts mineralization within quartz-carbonate veins with several intervals with moderate to high levels of coarse sulphides, including arsenopyrite, pyrite, galena, chalcopyrite, pyrrhotite, and sphalerite. The AES Shear is a 5 km long Au structure located in proximity to the North Giant Extension (NGX) structure. The NGX structure is believed to be the northward continuation of the Giant ore system (Kelly, 1993). The high-grade quartz vein structure within the NGX at the south of the Northbelt shows a promising potential (Armitage, 2021). The Shear 20 is located along the contact of the Ryan Lake Pluton with volcanic rocks to the east. Drill holes targeted in the vicinity of these veins reveal an abundance of arsenopyrite, lesser pyrite, chalcopyrite, galena, and locally molybdenite (Armitage, 2021). The Sam Otto Shear is a prospective bulk tonnage target with the most extensive mineralization system yet discovered at the YCGP. The Sam Otto Shear is hosted in felsic to intermediate volcanics of the Banting Formation with intercalated sediments and mafic volcanics and finely disseminated pyrite and arsenopyrite. Screamer Island is a new target of high-grade Au mineralization identified during a property-wide exploration program at the southern extension of the Sam Otto Shear, supporting the notion that the Sam Otto Shear is a large mineralization system. Mispickel is a deformation zone hosted within the Walsh Lake target covered by turbiditic sediments of the Walsh Lake Formation that contains high Au-grade intercepts. Shears at the Mispickel deposit contain several quartz veins with low to moderate arsenopyrite, pyrite, pyrrhotite, and visible Au. The Homer Lake target is located at the northern end of the Yellowknife City Gold Property, associated with the metavolcanics of the Chan Formation and the linear intrusive quartz porphyry bodies. Homer Lakes hosts zones of polymetallic (Au, Ag, Pb, Zn) enrichment along porphyry-mafic contacts.

Gold prospecting in the Eastbelt is still in the preliminary stage; however, a few Au enrichment zones have been identified at the new Duck Lake target, as well as in proximity to the historic Ptarmigan and Tom mines. Duck Lake veins, located south of the Eastbelt, crosscut folded Burwash Formation sediments. Gold mineralization at the Duck Lake target occurs in proximity to more prolific Au-producing plugs, including granite-tonalite-granodioritic intrusions, where high Au values are detected. West-northwest trending Ptarmigan and Tom quartz veins contain free visible Au within the irregularly shaped quartz bodies.

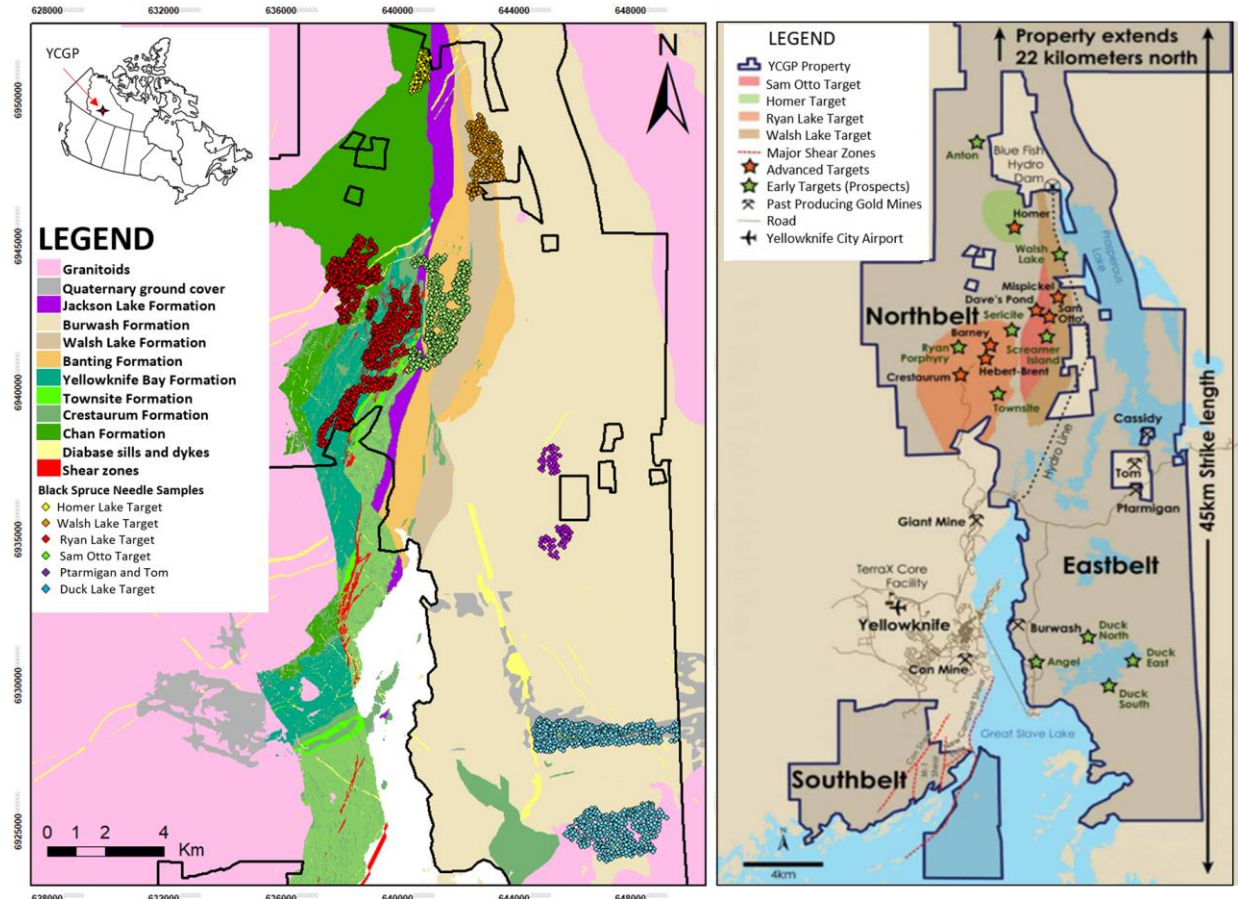


Figure 39. (Right) the Yellowknife City Gold Project (YCGP) advanced and new Au targets within the Northbelt, including Sam Otto, Homer Lake, Ryan Lake, and Walsh lake targets, and within the Estbelt, including the vicinity of the former Ptarmigan and Tom mines and Duck Lake target (Armitage, 2021). (Left) Regional geology of the YCG and the location of needle samples collected at the 2017 biogeochemical survey. From north to south: Yellow dots (Homer Lake target), Orange dots (Walsh Lake target), Red dots (Ryan Lake target), Green dots (Sam Otto target), Purple dots (Ptarmigan and Tom), and Blue dots (Duck Lake target).

5.3 Methodology

5.3.1 Reconnaissance Biogeochemical Survey

In 2017, a total of 2788 black spruce needle samples were collected, including 1945 samples across the Northbelt and 843 samples across the eastern portion of the YCGP. The majority of needle samples in the study area were collected from areas of bedrock outcrop covered by thin (< 30 cm) organic-rich soils with sparse tree cover to slightly more forests [54]. Forested soils are thicker than the bedrock outcrop soils and are mainly covered by trees such as black spruce, consisting of a thin organic layer overlying poorly developed soils and sometimes thin tills (< 2m) (Kerr and Knight, 2002; Wolfe and Morse, 2017).

Quality control measures included collecting and inserting field duplicate and control samples at a frequency of approximately one in 22 samples and 70 samples, respectively. Preparation was conducted at ALS Labs in Vancouver, where the twigs and leaves were carefully separated and milled using a Wiley Mill to 100% passing 1mm. After drying and milling, a one-gram aliquot of each milled sample was then digested for eight hours in nitric acid (HNO₃), followed by three hours of heating in a graphite heating block. Subsequently, samples were cooled and brought up to volume with 22% hydrochloric acid (HCl). The resulting solution was completely mixed and analyzed by inductively coupled plasma mass spectrometry (ICP-MS) using the ME-VEG41 multi-element determinations package for unashed vegetations at ALS Global, Vancouver, British Columbia, Canada.

A merged biogeochemical dataset including elements Au, As, Ag, As, Bi, Ca, Cd, Co, Cr, Cu, Fe, K, Mg, Mn, Mo, Ni, P, Pb, S, Sb, Se, Tl, and Zn was imported into the geochemical analysis software, ioGAS.7.4 for further data validation, including control of analytical data quality, data treatment, censoring, centred log-ratio (CLR) transformation, and multivariate data analysis.

5.3.2 Data Preparation and Assessment

It is required to prepare and assess the geochemical data carefully as it influences the data interpretations profoundly. Biogeochemical data are compositional, which means they are mainly reported as a proportion of some whole such as weight percent (wt. %) or part per million (ppm). Therefore, the sum of the elemental composition in samples is a constant,

resulting in the constant sum or data closure problem in compositional data. This issue is the most important limitation related to compositional data that may lead to bias in correlations between two variables (Rollinson, 1992).

In general, biogeochemical data are not normally distributed, only occur in real positive number space, and have a closure problem. The presence of outliers in biogeochemical data is frequent as a result of human or instrument error. In the literature, log-ratio transformation and robustification are used as popular solutions to address these issues (Aitchison, 1982; Buccianti and Grunsky, 2014; Chen, 2015; Demšar et al., 2013; Filzmoser et al., 2009a; Ghorbani et al., 2022b; Grunsky and de Caritat, 2020). Log-ratio transformation opens the closed system and provides a better insight into realistic relationships among variables (Carranza, 2011; Filzmoser et al., 2012). Robustification uses M-estimator to reduce the weight of the observation with a significant error and cope with outliers (Filzmoser and Hron, 2008; Filzmoser et al., 2009a; Stanimirova et al., 2007).

In this study, the distribution pattern of each element in each target was evaluated using probability plots to identify the geochemical background. No missing values were found in the 2017 biogeochemical data. 1/2 method detection limit was used for elements with less than 20% data values below the detection limit (Carranza, 2011). The Maximum likelihood estimation using probability plotting was used for >20% of data values below the detection limit to find the probability distribution that best explains the observed data (Carranza, 2011). The precision of data is a critical part of systematic data assessment to identify and avoid possible measurement errors. These errors can be caused at different stages of sampling, preparation and sub-sampling, and analytical processes (Heberlein et al., 2020) and lead to biased interpretations. In this study, the average coefficient of variation (CV_{avg} (%)) was calculated using

$$CV_{avg}(\%) = 100 \times \sqrt{\frac{2}{N} \sum_{i=1}^N \frac{(a_i - b_i)^2}{(a_i + b_i)^2}}$$

where N is the number of sample pairs, and a_i and b_i are the concentration of element of interest in the primary and duplicate samples of i^{th} sample pair, respectively (Abzalov, 2008).

Process discovery and process validation were applied to identify multi-element associations in biogeochemical data and the plant-substrate relationship (Grunsky and de Caritat, 2020). The process discovery was examined using robust RQ-mode principal component analysis (PCA) to identify the element association in the needle samples collected over early and advanced Au targets at the YCGP. PCA is a linear dimension reduction technique that transforms original data into a new lower-dimensional representation using a linear projection with a minimum loss of information (Demšar et al., 2013; Singh et al., 2017). RQ-mode PCA signifies the interrelation between elements (R-mode) and the combinations of samples (Q-mode) that explain variation among variables at the same time (Chen, 2015; Neff, 1994; Zhou et al., 1983).

Process validation was also evaluated using the robust log-transformed inverse distance weighted (IDW) interpolation method to reveal the plant-substrate relationship and identify the zone of Au enrichment within the Northbelt and Eastbelt at the YCGP. The IDW interpolation method estimates the data values for unknown adjacent samples using the known measured data values (Burrough et al., 2015) using a spatial variation of Au and associated pathfinders in each target. This method helps to find the extension of the previous mining area and introduce the new prospecting zones. For this purpose, Au anomalies were prioritized according to the strength of their Au responses (i.e., samples with Au contents over the 99th or 98th percentile threshold) and their pathfinder elements signature.

5.3.3 Data Precision

The average coefficient of variation ($CV_{avg}\%$) was used to express the total measurement error. High total measurement errors can obscure meaningful geochemical patterns and consequently undermine the biogeochemical technique to identify underlying mineralization (Abzalov, 2008). Coefficient of variation values below 20% indicate good data precision; between 20% and 30% acceptable precision; between 30% and 50% marginal precision; and over 50%, poor precision. After data QA/QC, only Se was found within the marginal range. Other elements were categorized within the acceptable to good precision (Table 6). Higher $CV_{avg}\%$ value can be attributed to the low concentrations of these elements in needle samples.

Table 6. Precision of data using the average coefficient of variation ($CV_{avg}\%$) indicates a marginal range for Se in the 2017 biogeochemical data. Other elements are within an acceptable to a good range of precision.

2017 biogeochemical data			
Elements	$CV_{avg}\%$	Elements	$CV_{avg}\%$
Se_ppm	32.73	Ag_ppm	18.54
Cr_ppm	28.61	Hg_ppm	17.06
Pb_ppm	26.98	Mn_ppm	15.66
Sb_ppm	26.06	Fe_ppm	15.52
Au_ppm	25.98	S_pct	10.7
Cd_ppm	25.58	Zn_ppm	10.55
Mo_ppm	24.56	Ca_pct	9.63
Ni_ppm	22.79	Mg_pct	8.31
Tl_ppm	21.75	Cu_ppm	7.44
Bi_ppm	21.21	K_pct	6.32
Co_ppm	20.02	P_pct	5.11
As_ppm	18.92		

5.4 Results and Discussion

5.4.1 Summary of Statistics

Table 7 provides the descriptive statistics, including minimum, maximum, mean, median, and background values for Au, As, Ag, As, Bi, Ca, Cd, Co, Cr, Cu, Fe, Hg, K, Mg, Mn, Mo, Ni, P, Pb, S, Sb, Se, Tl, and Zn in black spruce needle samples collected across the YCGP. Figure 40 compares the average concentration of elements in black spruce needles, normalized to background values. Generally, the Au background level in plant samples is reported as one ppb Au (Dunn, 2007b), but it is significantly lower in most environments (Dunn, 1995). At the YCGP, the average Au values in black spruce needles show ~15% to 80% enrichment compared to their background levels. The highest to lowest Au enrichment is observed in the samples collected at Ptarmigan and Tom > Duck Lake > Homer Lake > Sam Otto > Ryan Lake > Walsh Lake. Contiguous anomalous Au values, up to 10 ppb, are detected at the Eastbelt property, where the Ptarmigan Mine is located. Anomalous Au values at the Ryan Lake target are limited to the Crestaurum deposit and shear 20 areas. High Au values at the Duck Lake target are seen in samples collected from the contact zone between the felsic bodies and metasediments of the Burwash Formation. Arsenic mean values show 5%

enrichment at the Ryan Lake samples and 80% enrichment at the Ptarmigan and Tom samples compared to the background values. Ryan lake also shows a slight enrichment in As values, while no enrichment is observed in the other targets. Needle samples collected over the Ptarmigan Mine and Ryan Lake target (NGX and the contact between felsic intrusion to the mafic volcanics) show anomalous As values up to 5-10 ppm. Thallium is depleted in all targets except Homer Lake and Sam Otto, with 40 to 50% enrichments. Bismuth shows 50% to 80% enrichment in all targets except for Homer Lake and Ptarmigan and Tom. 4% to 6% Se enrichment is observed in needle samples collected at Walsh Lake and Ptarmigan and Tom. At the Ryan Lake target, Mo is more than three times higher than the background level. Also, it shows 12%, 35%, and 45% enrichments in Walsh Lake, Sam Otto, and Ptarmigan and Tom. Studies indicate that strong Au ± Mo mineralization at the Ryan Lake target (Crestaurum and Barney shear) is related to late felsic intrusion into the mafic bodies (Armitage, 2021). Mean Ag, Cd, and Pb show enrichment only in Ptarmigan and Tom areas. High values of Ag, up to 109 to 258 ppb, are accumulated in needle samples collected at the Homer Lake and Ryan Lake targets. Lead enrichment at the Ptarmigan and Tom is 2.5 times higher than the background level. Anomalous Zn and Pb values are identified in the Homer Lake target, indicating the presence of high-grade polymetallic showings related to the intrusion of felsic bodies into mafic volcanics. All targets are depleted in Co compared to the background levels, while it shows no difference at the Ryan Lake target. Chromium and Fe mean values show no difference in all targets compared to the background values, while they are more than two times higher than the background level in Ptarmigan and Tom. Mean Hg values indicate no enrichment compared to the background level at all targets. The highest Hg values are identified in Walsh Lake Sam Otto targets (~50 ppb). Essential elements, including Zn, Ca, S, Cu, Mg, K, and P, show no significant difference compared to the background levels in all targets. Slight variation in these elements in needle samples is due to their essential role in plant metabolism. Nickel, Sb, and Mn are depleted in all targets.

Table 7. Descriptive statistics of minimum, maximum, mean, median, and the background level of elements concentration in 2788 black spruce needle samples collected at six different targets, including Duck Lake and former Ptarmigan and Tom Mines at the Eastbelt and Ryan Lake, Sam Otto, Walsh Lake and Homer Lake targets at the Northbelt are provided. Ppb: part per billion, ppm: part per million, pct: percent, BG: background.

Elements Univariate	Duck Lake				
	Min	Max	Mean	Median	BG
Au (ppb)	>0.1	2.5	0.132	0.1	0.1
As (ppm)	0.06	1.22	0.304	0.27	0.396
Tl (ppm)	0.001	0.124	0.008	0.004	0.009
Bi (ppm)	>0.0005	0.05	0.001	0.001	0.001
Cd (ppm)	>0.0005	0.09	0.008	0.005	0.009
Sb (ppm)	0.01	0.15	0.021	0.02	0.026
Hg (ppm)	0.009	0.055	0.023	0.022	0.023
Se (ppm)	0.0025	0.072	0.014	0.013	0.015
Mo (ppm)	0.005	0.35	0.011	0.01	0.011
Ag (ppm)	>0.002	0.081	0.02	0.017	1.064
Pb (ppm)	0.005	1.24	0.044	0.04	0.045
Co (ppm)	0.005	1.445	0.089	0.061	0.606
Cr (ppm)	0.01	0.95	0.102	0.08	0.101
Ni (ppm)	0.02	4.25	0.493	0.33	0.573
Cu (ppm)	0.53	2.14	1.015	0.99	1.026
Zn (ppm)	21.6	188	82.7	81.4	90.533
Fe (ppm)	13	92	24.1	22	22.152
Ca (pct)	0.44	2.1	1.044	1.02	1.068
K (pct)	0.23	0.68	0.359	0.35	0.364
S (pct)	0.02	0.33	0.083	0.08	0.079
Mg (pct)	0.026	0.146	0.075	0.074	0.08
Mn (ppm)	56.2	4120	1236	1160	1459
P (pct)	0.06	0.185	0.105	0.103	0.108

Elements Univariate	Homer Lake				
	Min	Max	Mean	Median	BG
Au (ppb)	>0.1	0.9	0.131	0.1	0.1
As (ppm)	0.04	0.41	0.143	0.13	0.143
Tl (ppm)	0.001	1.605	0.091	0.032	0.06
Bi (ppm)	>0.0005	0.009	0.002	0.001	0.002
Cd (ppm)	>0.0005	0.174	0.011	0.004	0.013
Sb (ppm)	0.01	0.04	0.02	0.02	0.027
Hg (ppm)	0.009	0.033	0.018	0.017	0.018

Se (ppm)	0.0025	0.033	0.01	0.008	0.01
Mo (ppm)	0.005	0.04	0.008	0.01	0.009
Ag (ppm)	0.003	0.109	0.023	0.019	0.029
Pb (ppm)	>0.01	0.08	0.035	0.03	0.041
Co (ppm)	0.004	0.595	0.093	0.043	0.283
Cr (ppm)	0.03	0.75	0.12	0.09	0.115
Ni (ppm)	0.02	2.57	0.32	0.18	0.47
Cu (ppm)	0.72	1.48	1.061	1.05	1.105
Zn (ppm)	23.8	239	104.9	96.5	126.055
Fe (ppm)	13	75	20.9	19	19.518
Ca (pct)	0.55	2.06	1.101	1.08	1.134
K (pct)	0.18	0.48	0.294	0.29	0.3
S (pct)	0.04	0.17	0.072	0.07	0.07
Mg (pct)	0.039	0.14	0.074	0.07	0.078
Mn (ppm)	50.9	2980	931.2	811	1421
P (pct)	0.049	0.125	0.07	0.069	0.07

Elements Univariate	Ptarmigan and Tom				
	Min	Max	Mean	Median	BG
Au (ppb)	>0.1	9.9	0.739	0.1	0.405
As (ppm)	0.06	10.3	0.846	0.21	0.429
Tl (ppm)	0.001	0.08	0.009	0.003	0.013
Bi (ppm)	>0.0005	0.123	0.01	0.005	0.017
Cd (ppm)	>0.0005	0.697	0.038	0.0105	0.033
Sb (ppm)	0.01	0.05	0.019	0.02	0.022
Hg (ppm)	0.013	0.037	0.021	0.022	0.022
Se (ppm)	0.005	0.051	0.014	0.011	0.013
Mo (ppm)	0.005	0.14	0.027	0.01	0.018
Ag (ppm)	0.004	0.081	0.023	0.017	0.021
Pb (ppm)	>0.01	2.97	0.2	0.06	0.079
Co (ppm)	0.009	0.631	0.136	0.088	0.22
Cr (ppm)	0.03	6.99	0.59	0.145	0.229
Ni (ppm)	0.11	2.75	0.594	0.445	0.85
Cu (ppm)	0.58	3.86	1.234	1.135	1.197
Zn (ppm)	16.1	127.5	59.215	56.4	63.607
Fe (ppm)	16	890	78.902	32.5	34.5
Ca (pct)	0.44	1.68	0.873	0.83	0.962
K (pct)	0.2	0.54	0.356	0.35	0.361
S (pct)	0.04	0.22	0.073	0.07	0.07
Mg (pct)	0.032	0.129	0.076	0.073	0.076
Mn (ppm)	120.5	3150	856	778	988
P (pct)	0.047	0.179	0.103	0.0995	0.104

Elements Univariate	Ryan Lake				
	Min	Max	Mean	Median	BG
Au (ppb)	>0.1	3.8	0.158	0.1	0.133
As (ppm)	0.06	5.06	0.407	0.33	0.386
Tl (ppm)	0.001	0.579	0.034	0.017	0.087
Bi (ppm)	>0.0005	0.052	0.002	0.001	0.001
Cd (ppm)	>0.0005	0.066	0.005	0.003	0.006
Sb (ppm)	0.005	0.27	0.032	0.03	0.038
Hg (ppm)	0.007	0.038	0.019	0.018	0.019
Se (ppm)	0.0025	0.135	0.012	0.01	0.012
Mo (ppm)	>0.005	3.39	0.037	0.01	0.01
Ag (ppm)	>0.001	0.258	0.022	0.018	0.026
Pb (ppm)	0.005	2.55	0.055	0.04	0.055
Co (ppm)	0.001	1.09	0.053	0.025	0.054
Cr (ppm)	0.01	2.87	0.137	0.11	0.127
Ni (ppm)	0.02	4.18	0.204	0.11	0.31
Cu (ppm)	0.64	2.28	1.118	1.1	1.127
Zn (ppm)	15.2	171.5	78.1	76.3	86
Fe (ppm)	13	220	30.8	26	27
Ca (pct)	0.28	2.24	1.175	1.16	1.233
K (pct)	0.17	0.61	0.3	0.29	0.307
S (pct)	0.03	0.29	0.079	0.08	0.079
Mg (pct)	0.028	0.168	0.077	0.075	0.081
Mn (ppm)	20.8	3410	815.5	715	1233
P (pct)	0.047	0.169	0.075	0.069	0.068

Elements Univariate	Sam Otto				
	Min	Maxi	Mean	Median	BG
Au (ppb)	>0.1	1.4	0.131	0.1	0.1
As (ppm)	0.06	1.56	0.229	0.19	0.243
Tl (ppm)	0.001	0.713	0.015	0.007	0.011
Bi (ppm)	>0.0005	0.019	0.002	0.001	0.001
Cd (ppm)	>0.0005	0.044	0.005	0.003	0.006
Sb (ppm)	0.005	0.07	0.02	0.02	0.023
Hg (ppm)	0.009	0.05	0.022	0.021	0.023
Se (ppm)	0.0025	0.048	0.013	0.011	0.013
Mo (ppm)	>0.005	0.82	0.013	0.01	0.01
Ag (ppm)	>0.001	0.071	0.018	0.015	0.022
Pb (ppm)	0.01	0.23	0.04	0.04	0.041
Co (ppm)	0.002	0.454	0.058	0.036	0.107
Cr (ppm)	0.01	0.77	0.119	0.09	0.105

Ni (ppm)	0.02	1.5	0.255	0.19	0.444
Cu (ppm)	0.51	2.04	1.025	1.01	1.041
Zn (ppm)	24.8	172	79.7	78	85
Fe (ppm)	12	117	24.4	23	23
Ca (pct)	0.49	2.11	1.125	1.08	1.172
K (pct)	0.18	0.51	0.322	0.32	0.307
S (pct)	0.005	0.21	0.067	0.06	0.068
Mg (pct)	0.034	0.176	0.071	0.067	0.072
Mn (ppm)	28.9	4190	897.7	849	1094
P (pct)	0.05	0.158	0.087	0.0835	0.087

Elements Univariate	Walsh Lake				
	Min	Max	Mean	Median	BG
Au (ppb)	>0.1	0.7	0.113	0.1	0.1
As (ppm)	0.03	0.55	0.135	0.12	0.147
Tl (ppm)	0.001	0.145	0.012	0.006	0.03
Bi (ppm)	>0.0005	0.009	0.001	0.001	0.001
Cd (ppm)	>0.0005	0.056	0.005	0.003	0.005
Sb (ppm)	0.01	0.05	0.017	0.02	0.02
Hg (ppm)	0.009	0.046	0.022	0.022	0.023
Se (ppm)	0.0025	0.057	0.012	0.011	0.011
Mo (ppm)	>0.005	0.18	0.011	0.01	0.01
Ag (ppm)	>0.001	0.091	0.014	0.012	0.022
Pb (ppm)	0.01	0.15	0.038	0.03	0.041
Co (ppm)	0.006	0.903	0.118	0.073	35.8
Cr (ppm)	0.02	0.85	0.134	0.11	0.119
Ni (ppm)	0.02	12.35	0.445	0.3	0.705
Cu (ppm)	0.57	2.99	0.996	0.96	1.018
Zn (ppm)	13	150	69.6	68	80
Fe (ppm)	14	130	22.8	21	22
Ca (pct)	0.55	1.8	1.024	0.99	0.767
K (pct)	0.21	0.6	0.332	0.32	0.329
S (pct)	0.03	0.27	0.076	0.07	0.075
Mg (pct)	0.029	0.137	0.078	0.075	0.085
Mn (ppm)	117	3950	1137.6	1030	1414
P (pct)	0.057	0.225	0.091	0.088	0.093

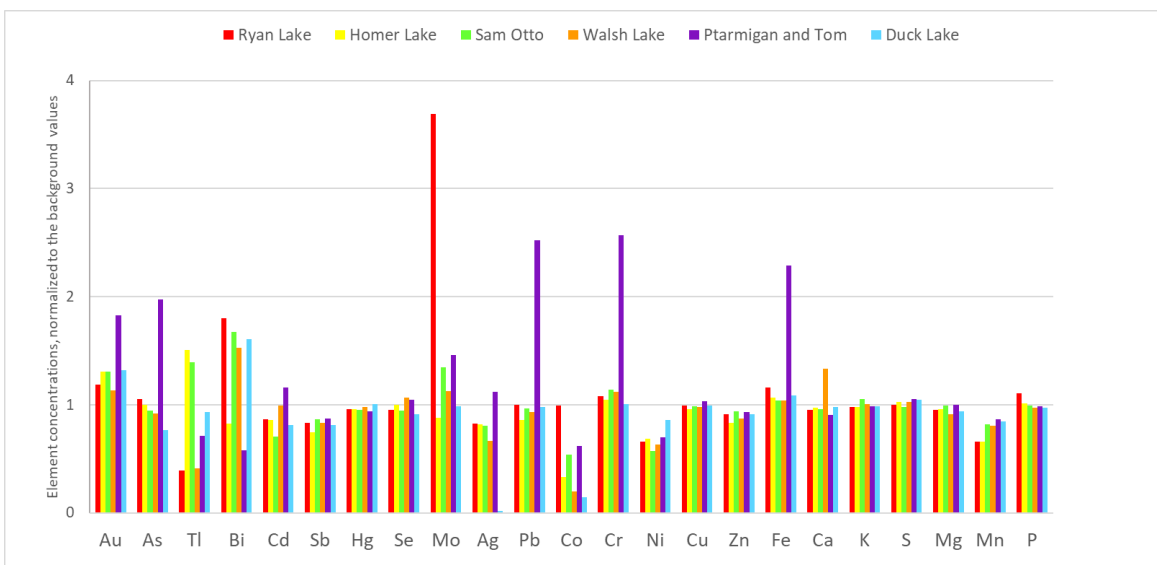


Figure 40. Average concentration of elements, normalized to the background level, in black spruce needle collected from the early and advanced Au targets, including Ptarmigan and Tom mines (purple), Duck Lake target (blue), Homer Lake target (Yellow), Ryan Lake target (red), Sam Otto target (green), and Walsh Lake target (orange). Gold shows enrichment in all targets.

5.4.2 Principal Component Analysis

Statistical analyses, including robust RQ-mode PCA and IDW interpolation, were applied to identify the geochemical factors controlling the elemental variation in black spruce needles. Understanding the occurrence and distribution pattern of Au and its pathfinder elements helps to identify zones of Au enrichment more effectively and reliably. Robust RQ-mode PCA was employed to transform the X-selected elements into a few meaningful components containing distinct elemental associations. Figure 41 shows a PCA biplot graph, including two corresponding principal components (PC1 and PC2). Element loadings are shown as vectors. The closer loading plots indicate strong associations. Needle samples in the biplot PCA graph are shown with circles in different colours representing different Au targets, including yellow circles (Homer Lake target), orange circles (Walsh Lake target), red circles (Ryan Lake target), green circles (Sam Otto target), purple circles (Tom and Ptarmigan mines), and blue circles (Duck Lake target). Also, the size of the circles indicates the relative concentration of Au in samples.

Robust RQ-mode Principal Component Analysis

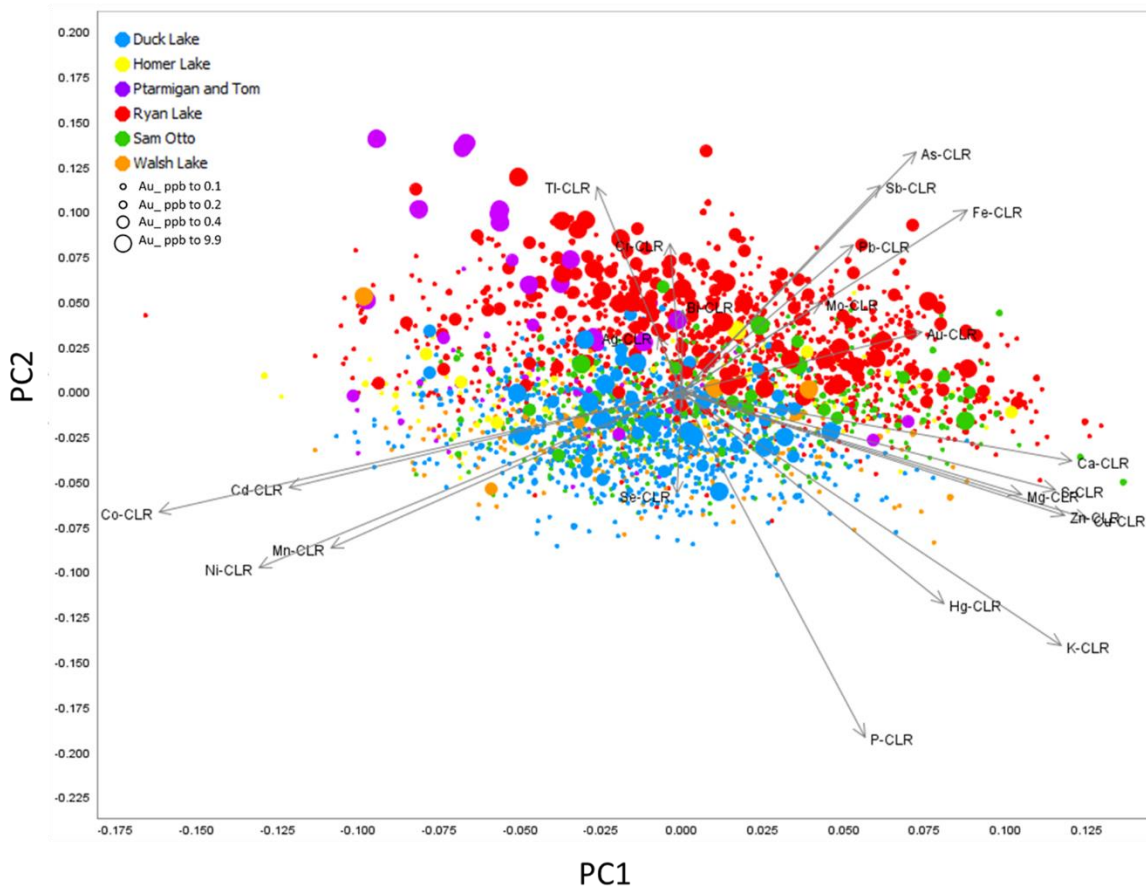


Figure 41. According to the robust RQmode-PCA, PC1 and PC2 control the distribution pattern of elements in black spruce samples. PC1 indicates geochemical/mineralization and physiological factors contribute to elemental variation in black spruce needle samples. Strong associations of Au with As, Sb, Pb, Mo, and Fe clearly illustrate the plant-substrate relationship. PC2 emphasizes the influence of the geochemical/ mineralization factor. Also, it provides valuable information about the associated pathfinders for Au, including As, Sb, Pb, Tl, Ag, and Bi. Needle samples collected in early and advanced targets are presented in different colours: Duck lake target in blue, Homer lake target in yellow, Ptarmigan and Tom in purple, Ryan Lake target in red, Sam Otto target in green, and Walsh Lake target in orange. Gold values are displayed as circles of different sizes. Larger circles represent higher Au values. Samples with higher Au values are primarily associated with needle samples collected from the Ryan Lake target and Ptarmigan and Tom mines and are proximal to the geochemical/mineralogical factor.

PC1 and PC2 account for 73.5% of the total variance of the data. Therefore, they represent the main factors controlling the distribution of elements in black spruce needles. PC1 (51% of the variation) shows positive loadings of Cu, Ca, Zn, K, S, P, Mg, Fe, Hg, Au, As, Sb, Pb, and Mo. PC1 indicates that the distribution of elements in plants is influenced by mineralogical/geochemical factor (Au, As, Sb, Fe, Pb, and Mo) and physiological factor (Cu, Ca, Zn, K, S, P, and Mg). Positive loadings of Au, As, Sb, Fe, Pb, and Mo in PC1 are significantly associated with needle samples collected across the Northbelt, including the majority of Ryan Lake and Sam Otto targets (red and green circles, respectively), which reflects the ability of plants to reveal the bedrock composition (Dunn, 2007b; Z. Ghorbani et al., 2022b). Arsenic, Sb, and Mo are the well-known geochemical signatures accompanying Au in greenstone-hosted quartz-carbonate vein orebodies (Armitage, 2021). Also, high concentrations of Au, As, Sb, and Mo have been reported at the Ryan Lake target (Armitage, 2021). The association of Au with Fe, As, Sb, and Pb can be attributed to the presence of arsenopyrite, stibnite, and galena in the mineralization structure at the Crestaurum and Barney shears and Shear 20 areas. Also, strong Au \pm Mo mineralization identified in proximity to the Crestaurum and the Ryan Lake targets is related to the late felsic intrusion. In the other direction of PC1, negative loadings of Co, Ni, Mn, and Cd, are located. These elements are enriched in needle samples located over the mafic volcanic of the Homer Lake target (yellow circles) and metasediments of the Burwash Formation (blue circles). The associations of Co, Ni, and Mn can be related to the similar geochemical characteristics of these elements. These elements are highly enriched in samples collected at Homer Lake and Duck Lake targets, shown with yellow and blue circles. The association of Co, Ni and Mn in granodiorite that intruded the metasediments of the Burwash Formation (blue circles) and mafic volcanic of the Homer Lake target (yellow circles) is related to similar geochemical characteristics of these elements.

PC2 (22.5% of variation) displays positive loadings of As, Sb, Tl, Fe, Cr, Pb, Mo, Bi, Au and Ag that are inversely associated with P, K, Mn, Cu, Zn, Co, Mg, S, and Ca. PC2 clearly discriminates the mineralogical/geochemical factor versus the physiochemical factor in needle samples. According to PC1 and PC2, Au is strongly associated with As, Sb, and Pb and less associated with Tl, Bi and Ag. These elements can be considered Au pathfinder elements at the

YCGP. Figure 42 indicates PC loadings for PC 1 to 4. PC 3 accounts for 6% of the total variance, including the negative loadings of Tl and Ag. PC 4 accounts for 5% of total variability, but the majority of elements have an absolute loading below 0.4.

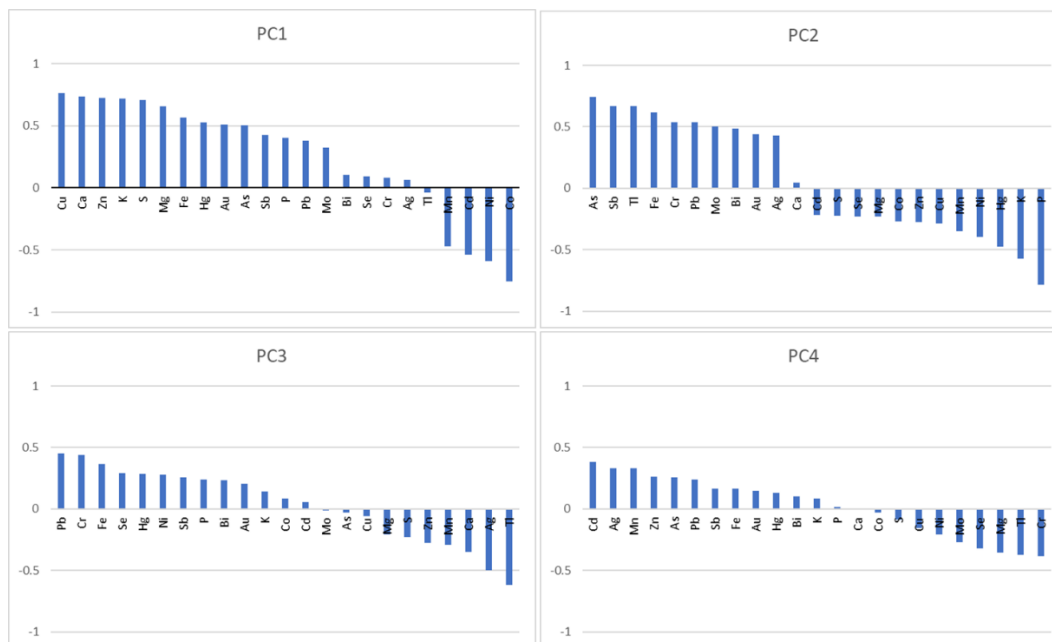


Figure 42. Loading of PC 1 to 4 illustrates each PC's elemental correlation. PC1 to 4 accounts for 84.5% of the total variance. PC 1 and 2 are the main components representing the contributing factors controlling the distribution of elements in black spruce needles. The majority of elements in PC3 and PC4 have an absolute loading below 0.4; therefore, they were excluded from the interpretations.

5.4.3 Robust Inverse Distance Weighted (IDW) Interpolation

Following process discovery, process validation was conducted to identify the plant-substrate relationship and zones of Au enrichment using the robust inverse distance weighted (IDW) interpolation method. IDW helps to reveal new information that cannot be obtained from raw data. It is vital to be skeptical of single-point Au anomalies that are not substantiated by pathfinder elements to avoid the nugget effect. Therefore, the distribution patterns of Au and its associated pathfinder elements (Ag, As, Bi, Cu, Hg, Pb, Sb, Se, Zn, and Tl) were studied simultaneously using the IDW interpolation method. Mercury and Se were not identified as Au pathfinders in process discovery using PCA. However, they were included in process validation

to evaluate their relationship with Au due to their potential to be Au pathfinders. Selenium was also identified as a strong Au pathfinder in the 2015 biogeochemical data conducted over the Northbelt (Ghorbani et al., 2022b).

According to IDW interpolation results, Au in each target is accompanied by different sets of pathfinder signatures depending on the bedrock composition and mineralization style (Figure 43). At the YCGP, zones of Au enrichment are found to be (1) commonly associated with shear zones within mafic/ultramafic host lithologies (As, Sb, Pb, Cu); (2) proximal to late felsic bodies intruded into mafic volcanics or sedimentary rocks (Ag, As, Se, Hg, Tl); and (3) commonly located along the faulted contacts between felsic-intermediate metavolcanics and sulphide metasediments (Bi, Se, Hg, Zn). A summary of the spatial distributions of Au and its associated pathfinder elements at each prospect is provided in Table 8.

Table 8. The comparison between early and advanced Au targets at the YCGP. According to the results of IDW interpolation, Au is accompanied by different sets of pathfinder elements with respect to the underlying lithology/mineralogy. * Contiguous anomalous Au values are detected at Duck Lake target, Ptarmigan Mine, and Ryan Lake target.

Location	EASTBELT		NORTHBELT				
	*Duck Lake	*Ptarmigan	*Ryan Lake		Sam Otto	Walsh Lake	Homer Lake
Au prospects	Duck Lake South	Ptarmigan	AES South and townsite (NGX)	Shear 20 and Crestaurum	Sam Otto and Screamer Island	Mispickel	Homer Lake
Formation	Burwash	Burwash	Crestaurum	Chan and Crestaurum	Banting	Walsh Lake	Chan
Bedrock composition	Metasediments+ Felsic intrusion		Mafic/felsic volcanic	Mafic volcanic + Felsic intrusion	Felsic to intermediate volcanics	Sulfidic metasediments	Mafic volcanic + Felsic intrusion
Au pathfinders	As, Se, Hg > Ag, Zn	As, Se, Bi, Ag, Pb, Cu	As, Bi, Sb, Pb > Ag, Cu	Tl, Ag, Sb > As	Hg, Bi, Pb, Sb, Se	Ag, Pb, Tl, Bi, Se, Cu	Tl, Ag, Zn, Bi, Cu

5.4.4 Northbelt Au prospecting:

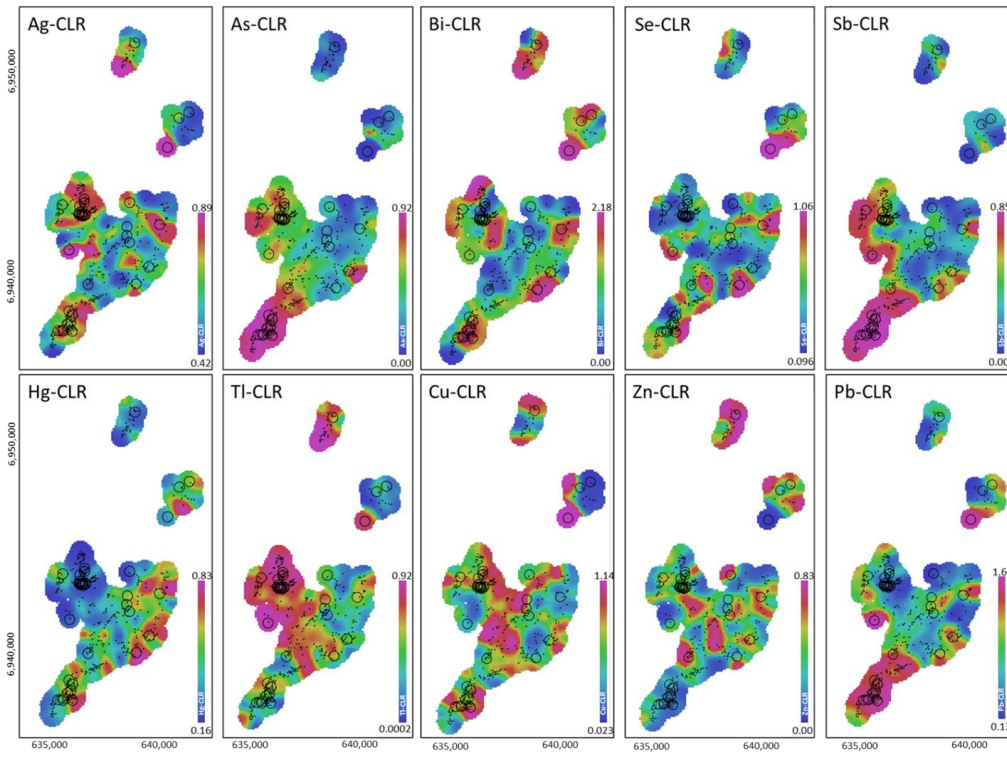
The IDW interpolation maps of Au pathfinder elements in Northbelt are shown in Figure 43. The Ryan Lake target consists of many new and previously known Au-bearing structures, of which the AES Shear, Townsite, Crestaurum Shear, Shears 17, 18, and 20 targets were studied

for the 2017 biogeochemical survey. In proximity to the NGX, where the Townsite Formation and AES Shear are located, strong signatures of As, Bi, Sb, Pb, Cu, and slightly less strong signatures of Ag in black spruce needles are observed. Strong association of Au with As and Sb is likely related to the presence of arsenopyrite and possibly stibnite associated with Au mineralization. The Au pathfinder signature in the needle samples differs near Shear 17,18, 20 localities and Crestaurum Shear, where Au is notably associated with Tl, Bi, Ag, Sb, and to a lesser extent with Pb, Cu, and As. This can be related to the contact between the late felsic bodies and the mafic volcanics of the Chan Formation, resulting in mineralization hosted both in the intrusions and the surrounding mafic volcanics. Associated sulphide mineralization in these localities also includes significant values of silver and chalcopyrite.

Anomalous Au values at the Sam Otto target are located along with the faulted contact (Yellowknife River Fault Zone: YRFZ) that separates the felsic-intermediate volcanics of the Banting Formation from sediments of the Jackson Formation. To the south of this target, where the Screamer Island zone is situated, positive signatures of Hg, Bi, Pb, Sb, Se and, to a lower degree, As are detected.

At the Walsh Lake target, two high Au values are identified. One is located within the Mispickel Zone and is accompanied by strong signatures of Tl, Bi, Se, and Cu. The other high Au value is within the Burwash Formation. However, no signature of pathfinder elements is identified.

Only one needle sample containing high Au content is identified at the Homer Lake target, within the contact zone between the Chan Formation mafic metavolcanics and the overlying Jackson Formation sediments. Zinc is strongly associated with Au and Tl, less so in this sample. Homer Lake samples are highly enriched in Ag, Tl, Zn, and Bi, which is likely related to the presence of two groups of metal showings, including Ag-Pb-Zn and Au-Cu, proximal to the Homer Lake target.



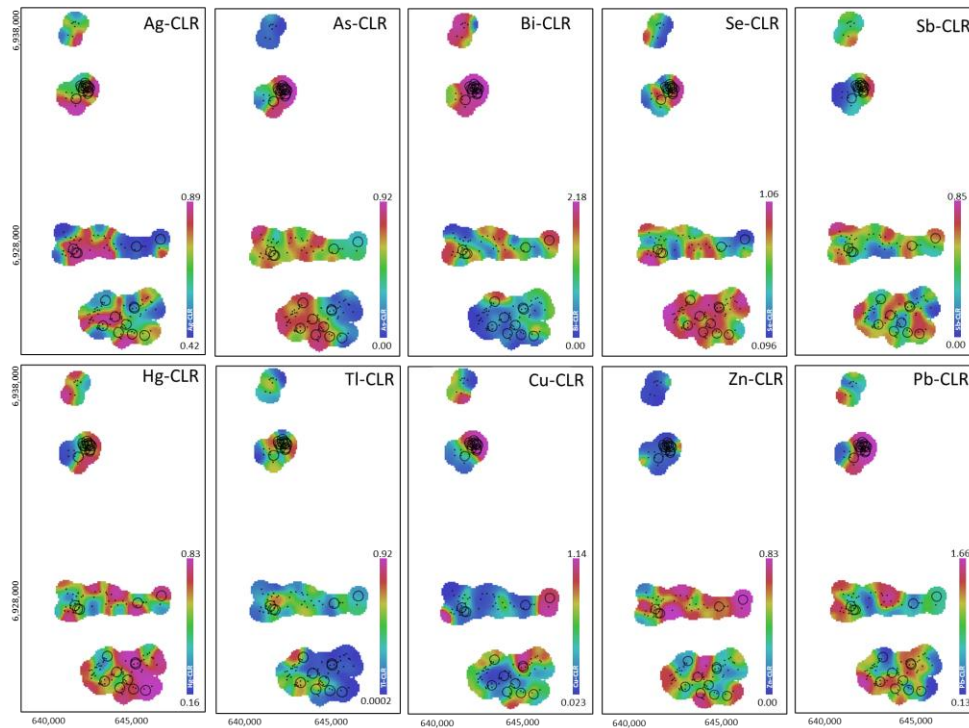


Figure 43. Robust center log-ratio (CLR) transformed inverse distance weighted (IDW) interpolation maps of Au pathfinder elements in Northbelt (upper) and Eastbelt (lower). Anomalous Au concentrations above 98 percentiles are shown with bigger circles. Contiguous high Au values are associated with shear zones within mafic/ultramafic host lithologies, including North Giant Extension (NGX) and shear 17, 18, and 20. High concentrations of As, Sb, Pb, and Cu, and to a lesser extent, Ag and Bi, are observed in these areas. Also, zones of Au enrichment are observed proximal to late felsic bodies intruded into mafic volcanics (Ryan Lake target) and sedimentary rocks (Duck Lake target). Gold in these zones is accompanied by high values of Ag, As, Se, Hg, and Tl. Elevated values of Au also can be seen along the faulted contacts between the felsic-intermediate metavolcanics and sulphide metasediments (Walsh Lake and Sam Otto target), where strong correlations between Au and Bi, Se, Hg, and Zn are identified. High concentrations of Ag, Bi, Tl, Cu, and Zn at the Homer Lake target are seen. The Ptarmigan area is enriched in all pathfinder elements of Au except Zn.

5.4.5 Eastbelt Au prospecting:

Figure 43 illustrates the IDW interpolation maps of Au pathfinder elements in Eastbelt. The strongest anomaly in the 2017 survey area consists of more than ten black spruce needle samples with Au values in the 99th percentile, hosted adjacent to the Ptarmigan mine area within Burwash Formation sediments. Au anomalies in the Ptarmigan mine area are coincident with almost all pathfinder element anomalies, including Ag, As, Hg, Se, Sb, and Pb.

At the Duck lake south target, several Au anomalies in black spruce needles were detected that are located in the contact zone of the Felsic intrusion with the Burwash sediments. This zone also shows elevated Ag, As, Hg, Se, Sb, and Pb values in black spruce needles. Similar anomalies have also been recorded in the surface rock samples, which confirms the plant-substrate relationship (Armitage, 2021). At the Duck Lake north target, elevated values of Ag, Hg, Se, and Pb are observed proximal to the faulted zone intruded by a diabase dyke/sill. Strong Ag and Zn signatures are also observed in samples collected at Duck Lake north.

In the process validation step, the spatial patterns and associations of Au and its pathfinder elements were investigated statistically to determine if these features are valid or simply coincidental associations. The process validation using the robust IDW interpolation method confirmed the strong Au response in black spruce where mineralization occurs. Also, it indicated that the association of Au with its pathfinders varies across the YCGP with respect to the lithology beneath. Mineralized shear zone structures, early intrusion-related metal enrichment, and hydrothermal fluids within proximal metasediments are found to be the contributing factors in Au enrichment in the substrate and subsequently in needle samples collected at the YCGP.

In the process validation step, the spatial patterns and associations of Au and its pathfinder elements were investigated statistically to determine if these features are valid or simply coincidental associations. The process validation using the robust IDW interpolation

method confirmed the strong Au response in black spruce where mineralization occurs. Also, it indicated that the association of Au with its pathfinders varies across the YCGP with respect to the lithology beneath. Mineralized shear zone structures, early intrusion-related metal enrichment, and hydrothermal fluids within proximal metasediments are found to be the contributing factors in Au enrichment in the substrate and subsequently in needle samples collected at the YCGP.

5.5 Conclusion

This study outlines the importance of a systematic approach in statistical data analysis in order to find a geochemical pattern in 2788 unashed black spruce needles collected at the YCGP. Identifying the dominant geochemical factors related to mineral exploration (process discovery), as well as validating them using a systematic, robust, and defensible approach (process validation), can extract useful information from geochemical data. In process discovery, the robust RQ-mode PCA was applied to reveal the factors controlling the elemental distribution and associations in black spruce needles. PC1 and PC2 were found to be the main components of the PCA, accounting for 74% of the total variance of data. According to PC1, the geochemical occurrence, distribution, and associations of elements in needle samples were influenced by the geochemical/mineralization and physiological factors. The geochemical/mineralization factor includes positive loadings of Au, As, Sb, Fe, Pb, and Mo, reflecting the presence of underlying mineralization. The physiological factor shows positive loadings of essential elements for plant metabolism, including Cu, Ca, Zn, K, S, P, and Mg. PC2 includes positive loadings of elements associated with geochemical/mineralization factor (As, Sb, Tl, Fe, Cr, Pb, Mo, Bi, Au and Ag) and negative loadings of essential elements, indicating the contribution and significance of the geochemical process in controlling the distribution of elements in needle samples. The reliability of identified zones of Au enrichments at the YCGP was substantiated by Au pathfinder elements using the process validation, where the observed patterns and associations are tested to develop

tools for predictive geochemical mapping. The IDW maps demonstrated that the association of Au and its pathfinder elements varies depending on the bedrock composition and mineralization style. Three zones of Au enrichment were identified. Anomalous Au values were identified in areas associated with underlying shear zones hosted within mafic/ultramafic lithologies. Gold is accompanied by As, Sb, Pb, and Cu in these areas. Strong correlations of As and Sb with Au are likely related to the presence of arsenopyrite, stibnite, chalcopyrite, and galena associated with Au mineralization. Also, high Au levels were identified in needle samples collected proximal to late felsic lithologies, accompanied by Ag, As, Se, Hg, and Tl. This can be related to the contact between the late felsic bodies and the mafic volcanics, resulting in mineralization hosted both in the intrusions and the surrounding mafic volcanics. Gold is also enriched in needles in samples located along the faulted contacts between the felsic-intermediate metavolcanics and sulphide metasediments. Gold is associated with Bi, Se, Hg, and Zn in these areas. Similar associations have also been recorded in the surface rock samples collected at the YCGP, which confirms the plant-substrate relationship. Through the interpretation of the results, contiguous high Au values with strong signatures of Au pathfinders are identified at the Ptarmigan, Ryan Lake (North Giant Extension), and Duck Lake targets.

Although unashed needle samples may not be the optimum sample media for biogeochemical exploration, yet strong biogeochemical responses were identified. The implications of this research for Au prospectivity using biogeochemical and statistical techniques at the YCGP indicate strong patterns that are useful for prioritizing Au exploration in certain regions at the Northbelt and Eastbelt. To be more constructive, a field validation program is recommended to cover unmapped areas across the YCGP and ground-truth the anomalous Au values detected by this research.

Chapter 6

6 Summary

Over a long time, plants evolved physically and chemically to adapt to the environment they overlie and accumulate elements essential for their metabolism. It is believed the selection of certain elements by plants depends on the geochemistry of the environment they overlie (Kabata-Pendias, 2001). The use of plants to understand the characteristics of lithology beneath is called the biogeochemical method. This research aims to apply the biogeochemical method to verify whether plants can reflect the chemistry of underlying bedrock and consequently use this information to identify zones of metal enrichment. To accomplish this, three biogeochemical datasets were selected for this research. The chemical analysis of over 3000 plant samples, including bark, needles, and twigs, collected in these surveys results in large biogeochemical datasets with various measurement errors related to the different stages of sampling, preparation and sub-sampling, and analytical processes. Therefore, the next objective of this research begins here, when data appears. Identifying thresholds and evaluating multi-element interrelationships and correlations is an inevitable objective in any geochemical survey, from mineral exploration to environmental assessment. However, data treatment is a frequently missing piece in dealing with geochemical data, leading to bias and unreliable interpretations. Therefore, geochemical data are subjected to basic error-checking and validation before being passed as a suitable dataset for analysis.

The major obstacles in geochemical data include censored values, non-normal distribution, and the constant-sum problem. Exploratory data analysis (EDA) is applied to validate data and address these obstacles. The EDA uses numerical (summary of statistics) and visualization (univariate and multivariate data analysis) methods to identify missing values and outliers, as well as data distribution and structures. According to previous studies, fabrication or

data substitution by a fraction of the detection limit for each undetected value causes bias and poor correlation (Grunsky and de Caritat, 2020). Also, the skewed nature of geochemical data requires log-ratio transformation to normalized data. The constant-sum problem also produces spurious correlations as a result of the closed number system. Hence, robust data analysis has been developed to proactively maintain data quality without reporting artificial anomalies and correlations. Data assessment using robust multivariate statistical analysis assists in evaluating data structure and verifying whether they are valid and applicable to building a model or not.

The following data processing and preparation were applied to the biogeochemical datasets using EDA:

- Biogeochemical data were treated using univariate data analysis. Treatments include determining missing values, censored values, and outliers. Data with missing values were entirely removed from the dataset. The fraction of the detection limit substituted data with less than 20% data values below the detection limit. Maximum likelihood estimation (using QQ or probability plots) was used for 20-50% of data values below the detection limit. This method provides more consistent results than simple arbitrary substitution by using the normal distribution to reproduce mean and skewness. Extreme outliers were replaced with the next highest/lowest values using winsorization.

- The spatial distribution of elements was evaluated individually to identify the level of skewness. Data with skewness values greater than 1 or less than -1 were considered strongly skewed. Therefore center log-ratio (CLR) transformations were applied to normalize data distribution and cope with outliers. The center-log ratio (CLR) transformation was selected among the several types of log transformation

as it better suits biogeochemical data and provides a better insight into elemental associations.

- **Data quality:** The average coefficient of variance ($C_{v_{avg}}$) was used to evaluate the precision of the data. This method measures the possible errors related to different stages of sampling, preparation and sub-sampling, and analytical processes.

- **Background value:** The average iterative 2σ -method was applied to calculate the missing background values. This method discards data values beyond the mean $\pm 2\sigma$ (σ : standard deviation) to provide a normal distribution. This calculation is repeated until all remaining values lie within this range, representing the background range.

After data preparation, a systematic two-phase approach, including process discovery and process validation, was applied to the datasets to extract the maximum hidden information (Grunsky and de Caritat, 2020). In this research, this approach was used to evaluate multi-element geochemical datasets and identify geochemical processes that may not be crystal clear unless robust data analysis is employed.

- **Process discovery:** The process discovery investigates the associations and trends between variables and observations using multivariate statistical analysis. Robust RQ-mode principal component analysis (PCA) and K-means clustering are well-known methods in the evaluation of multi-element associations and interrelationships related to geological processes. PCA is an adaptive multivariate data analysis method that reduces dimensionality, increases interpretability and minimizes information loss; therefore, a few components can describe the whole

variability. Also, it can give an insight into the multidimensional patterns in the data that would be missed with univariate and bivariate analysis. RQ-mode PCA signifies the interrelation between elements (R-mode) and the combinations of samples (Q-mode) that explain variation among variables at the same time. K-means clustering analysis is a simple and powerful unsupervised algorithm that has been widely used in data mining to discover the hidden spatial pattern and structure of unlabelled samples.

- **Process validation:** In the process validation step, the observed patterns and associations are tested to develop tools for predictive geochemical mapping. The inverse distance weighted (IDW) interpolation is a spatial prediction method useful for creating element distribution maps and delineating geochemical anomalies. The IDW assumes that data values in samples close to one another are more alike than that farther away and therefore predicts unknown hidden values using the adjacent known measured values.

The biogeochemical data were treated as mentioned above and assessed using process discovery, and process validation to (1) examine the potential application of biogeochemical and statistical techniques as interdisciplinary approaches in mineral exploration; (2) determine geologically meaningful responses in plant samples associated with buried mineralization; (3) identify the dominant geochemical processes controlling the distribution of elements in plant samples in respect of the underlying mineralization; (4) develop tools for predictive geochemical mapping to identify zones of Au enrichment. Exploratory data analysis (EDA), including univariate and multivariate statistical analysis, was applied to fulfill the objectives of this research.

The results of the statistical analysis of the biogeochemical surveys conducted at the MBGP and YCGP indicate that plant samples can successfully reflect the geochemistry of the bedrock they overlie. As expected, black spruce is the preferred sample media for biogeochemical exploration in the Canadian boreal forests. High concentrations of Au and its pathfinder elements are identified in black spruce samples collected at the MBGP and YCGP. Gold and its pathfinder elements, including As, Bi, Se, Sb, and Tl, strongly correlate in both study areas. However, the strength of correlations and pathfinder elements varies with respect to the underlying lithology. The comparison of black spruce sample tissue (twigs vs. bark vs. needle) collected at the MBGP indicates that twigs (303 ppb) >bark (230 ppb) in ash can accumulate higher concentrations of Au than needles (2.7 ppb) in ash. This is because needles are metabolically active organs with a barrier mechanism that avoids the accumulation of Au. Although only needle samples were collected at the YCGP, high values of Au up to 147 ppb in ash were identified.

According to the robust RQ-mode PCA, two factors control the geochemical distribution of elements in plant samples at the MBGP and YCGP: the geochemical/mineralization (PC1) factor and the physiological factor (PC2). PC1 includes a strong association between Au, Ag, As, Se, Bi, Pb, Cu, Co, Fe, Zn, Tl, and Cr, representing the plant-substrate relationship. PC2 or physiological factor includes essential elements for plant metabolism, including B, Ca, Mn, Mg, K, and P. Boron, Mn, Mg, K, and P are mainly associated with needles. While Ca is negatively correlated to the PC2 due to its structural function in plant samples.

According to the regional geology, both study areas are located in archean greenstone-hosted orogenic gold deposits. However, the host rocks differ. At the MBGP, the rock assemblage of the host rock is mainly comprised of felsic to intermediate metavolcanic tuffs intercalated with sediments, intermediate feldspar phyric volcanic flows, and late feldspar porphyritic dikes. Also, Au mineralization is associated with pyrite- arsenopyrite- sphalerite-

chalcopyrite- galena- antimony. The robust multivariate statistical analysis results on biogeochemical data indicate that Au is accompanied by Tl-As-Cd> Bi, Pb, Se, and Sb, reflecting the underlying mineralogy. High Au values are also identified in the north to the northwest part of the Twin Lake Shear Zone (TLSZ), where the dominant lithology is metasediments associated with mafic volcanics. Arsenic, Tl, Cd, Bi, Pb, Se, and Sb are also enriched in these areas. High Au values are also identified in a small area southeast of the property, where metasediments are associated with metaconglomerates. Gold is only associated with As, Se, and Sb in this area.

The YCGP is dominantly hosted by metavolcanic rocks in the Northbelt that is conformably overlain by the dominantly sedimentary packages to the east. At the YCGP, same as the MBGP, Au is correlated with As, Sb, Pb, Se, Bi, and Tl, as well as Cu, Zn, Ag and Hg. However, the strength of correlation and sets of Au pathfinders varies based on the lithology beneath. According to the robust Inverse distance weighted (IDW) interpolation method, elevated Au values associated with shear zones hosted within mafic/ultramafic bodies are accompanied by As, Sb, Pb, and Cu. Strong correlations of As and Sb with Au are likely related to the presence of arsenopyrite, stibnite, chalcopyrite, and galena associated with Au mineralization. Gold in samples located proximal to late felsic bodies is accompanied by Ag, As, Se, Hg, and Tl. This can be related to the contact between the late felsic bodies and the mafic volcanics, resulting in mineralization hosted both in the intrusions and the surrounding mafic volcanics. Associated sulphide mineralization in these localities also includes significant values of Ag. Zones of Au enrichment located along the faulted contacts between the felsic-intermediate metavolcanics and sulphide metasediments are accompanied by Bi, Se, Hg, and Zn. Similar associations have also been recorded in the surface rock samples collected at the YCGP, which confirms the plant-substrate relationship (Armitage, 2021). Cadmium indicates no association with Au at the YCGP. Through the interpretation of the results, contiguous high Au values with

strong signatures of Au pathfinders are identified at the Ptarmigan, Ryan Lake (North Giant Extension), and Duck Lake targets.

This research demonstrates the application of the biogeochemical technique as an efficient and cost-effective tool that can be used as an alternative or supplement to other surficial sampling techniques in the early stages of exploration. The exploratory data analysis combined with the robust techniques ensures consistent data interpretations and predictions. The results of these case studies imply that robust multivariate statistical analyses such as PCA and IDW interpolation are practical and reliable tools for revealing elemental association in plant samples with respect to the underlying mineralizations. Also, the results indicate the necessity of the systematic data treatment approach in order to avoid artificial correlations and biased interpretations. This research demonstrates that robust statistical analysis can be used to develop tools for predictive geochemical mapping in order to identify zones of Au enrichment.

6.1 Future Work

For future research, a field validation program is recommended to cover unmapped areas across the Monument Bay Gold Project (MBGP) and Yellowknife City Gold Project (YCGP) and ground-truth the anomalous Au values detected by this research. Due to the fact that biogeochemical surveys are quite beneficial in terms of time efficiency and the low cost of sample acquisition and preparation, a comprehensive survey over the entire MBGP is recommended. Missing background samples was one of the most severe limitations of this study. Therefore, it is suggested to collect background samples from different parts of black spruce and even other plant species. Furthermore, these background samples can be later used in environmental surveys, indicating the baseline metal concentrations at the Monument Bay Project before mine development.

A biogeochemical survey using needle samples could provide valuable information to identify the zone of Au enrichment at the YCGP. However, it is known by previous research that the barrier mechanism in needle tissue prevents Au absorption. The comparison between black spruce bark vs twigs vs needles at the MBGP notably demonstrated the ability of twigs and bark in Au accumulation. Therefore a biogeochemical survey using twigs or bark samples was suggested to confirm the results from needle samples and to find new zones that could not be identified using needles. Additionally, the physio-geochemical properties of soil highly influence the elemental distribution in plant samples. Therefore, besides future biogeochemical surveys, parallel soil surveys are recommended to better understand contributing factors that control the elemental distribution and association in plants with respect to the chemistry of underlying lithology.

Current implementations of statistics with ioGAS and SPSS provided a reliable perspective on geochemical data distribution. However, more effective results can be concluded from advanced data analysis using machine learning software in geosciences, such as Orange data mining. Also, future studies should provide more focus on increasing the reliability of high dimensional and low sample size datasets by reducing variables or finding the best components and variables.

Finally, considering the historical release of thousands of kilograms of arsenic trioxide particulates from Giant Mine into the atmosphere, collecting samples also is critical to assess the As dispersion to the environment closely. The presence of arsenic in the form of arsenite (As^{3+}) is challenging due to its bioavailability and mobility. Therefore, a study on the As speciation also is suggested to monitor and examine the spatial distribution and speciation of As at the YCGP.

References

- Abbas, G., et al. "Arsenic Uptake, Toxicity, Detoxification, and Speciation in Plants: Physiological, Biochemical, and Molecular Aspects." *International journal of environmental research and public health* 15, no. 1 (2018): 59.
- Abzalov, M. "Quality Control of Assay Data: A Review of Procedures for Measuring and Monitoring Precision and Accuracy." *Exploration and Mining Geology* 17, no. 3-4 (2008): 131-44.
- Adriano, D.C. "Trace Elements in Terrestrial Environments: Biogeochemistry, Bioavailability, and Risks of Metals". Vol. 860: Springer, 2001.
- Aitchison, J. "The Statistical Analysis of Compositional Data." *Journal of the Royal Statistical Society: Series B (Methodological)* 44, no. 2 (1982): 139-60.
- Almasi, A., et al. "Prospecting of Gold Mineralization in Saqez Area (Nw Iran) Using Geochemical, Geophysical and Geological Studies Based on Multifractal Modelling and Principal Component Analysis." *Arabian Journal of Geosciences* 8, no. 8 (2015): 5935-47.
- AMGEN scholars program, How to Interpret Histograms. "<https://amgenscholars.com/>. Accessed 10 December 2022."
- Anand, R.R., et al. "Gold and Pathfinder Elements in Ferricrete Gold Deposits of the Yilgarn Craton of Western Australia: A Review with New Concepts." *Ore Geology Reviews* 104 (2019): 294-355.
- Anhaeusser, C.R. "Archaean Greenstone Belts and Associated Granitic Rocks—a Review." *Journal of African Earth Sciences* 100 (2014): 684-732.

- Antweiler, J. C., et al. "Gold in Exploration Geochemistry." *Precious Metals in the Northern Cordillera* 10 (1982): 33-44.
- Archibold, O.W. *Ecology of World Vegetation*. Springer Science & Business Media, 2012.
- Armitage, A. "Amended Technical Report on the Resources Estimates for the Yellowknife City Gold Project, Yellowknife, Northwest Territories, Canada, Terrax Minerals Inc.": TerraX Minerals Inc., 2021.
- Baadsgaard, Z.N., et al. "Boulders from the Basement, the Trace of an Ancient Crust." *Selected studies of Archean gneisses and lower Proterozoic rocks, southern Canadian Shield.–Spec. Pap.(Geol. Soc. Amer.)* 182 (1980): 169-75.
- Babula, P., et al. "Uncommon Heavy Metals, Metalloids and Their Plant Toxicity: A Review." *Organic farming, pest control and remediation of soil pollutants* (2009): 275-317.
- Bakhat, H.F., et al. "Arsenic Uptake, Accumulation and Toxicity in Rice Plants: Possible Remedies for Its Detoxification: A Review." *Environmental Science and Pollution Research* 24, no. 10 (2017): 9142-58.
- Baragar, W.R.A. "Geochemistry of the Yellowknife Volcanic Rocks." *Canadian Journal of Earth Sciences* 3, no. 1 (1966): 9-30.
- Bartier, P.M., et al. "Multivariate Interpolation to Incorporate Thematic Surface Data Using Inverse Distance Weighting (Idw)." *Computers & Geosciences* 22, no. 7 (1996): 795-99.
- Becking, J.H. "A Requirement of Molybdenum for the Symbiotic Nitrogen Fixation in Alder (*Alnus Glutinosa* Gaertn.)." *Plant and Soil* (1961): 217-27.

- Bennett, V., et al., "Geology and U Pb Geochronology of the Neoproterozoic Snare River Terrane: Tracking Evolving Tectonic Regimes and Crustal Growth Mechanisms." *Canadian Journal of Earth Sciences* 42, no. 6 (2005): 895-934.
- Benz, D. "Multivariate Statistical Analysis of Lodgepole Pine Outer Bark Samples for Metallic Mineral Exploration within the Southern Nechako Plateau, British Columbia, Canada." University of Northern British Columbia, 2017.
- Bleeker, W, and B. Hall. "The Slave Craton: Geological and Metallogenic Evolution, in W. D. Goodfellow, Ed., *Mineral Deposits of Canada: A Synthesis of Major Deposit-Types, District Metallogeny, the Evolution of Geological Provinces, and Exploration Methods*: ." 849-79, 2007.
- Bleeker, W. "Archaean Tectonics: A Review, with Illustrations from the Slave Craton." *Geological Society, London, Special Publications* 199, no. 1 (2002): 151-81.
- Bleeker, W., et al. "Why the Slave Province, Northwest Territories, Got a Little Bigger." (2000).
- Boardman, N.K. *Trace Elements in Photosynthesis*. Vol. 199: Academic Press, New York, (1975).
- Bohlke, J.K. "Orogenic (Metamorphic-Hosted) Gold-Quartz Veins." *US Geological Survey Open-File Report* 795 (1982): 70-76.
- Botor, R.J.L, et al. "New Insights into Gold Mineralization at the Yellowknife City Gold Project, Northwest Territories from Synchrotron Micro-Xrf and Pxr." *Microscopy and Microanalysis* 25, no. S2 (2019): 834-35.

- Botor, R.J.L. "Understanding New Trends on Gold Mineralization at the Yellowknife City Gold Project, Northwest Territories, Using Synchrotron X-Ray Spectroscopy." (2018).
- Bowring, S.A., and W.R. Van Schmus. "U-Pb Zircon Constraints on Evolution of Wopmay Orogen." NWT Geological Association of Canada/Mineralogical Association of Canada 47 (1984).
- Boyle, R.W. "The Geochemistry of Gold and Its Deposits (Together with a Chapter of Geochemical Prospecting for the Element)." (1979).
- Brandl, G., et al. "Archaean Greenstone Belts." In *The Geology of South Africa*, 9-56: Geological Society of South Africa/Council for Geoscience Johannesburg/Pretoria, 2006.
- Brooks, R.R. "Geobotany and Biogeochemistry in Mineral Exploration." (1972).
- Brooks, R.R. "Plants That Hyperaccumulate Heavy Metals." *Plants and the chemical elements: biochemistry, uptake, tolerance and toxicity* (1994): 87-105.
- Brooks, R.R. "Statistics in Biological Prospecting." *Biological systems in mineral exploration and processing*. Ellis Horwood, Hertfordshire, UK, Part 7 (1995): 491-520.
- Brooks, R.R., et al. "Detection of nickeliferous rocks by analysis of herbarium specimens of indicator plants." *Journal of Geochemical Exploration* 7 (1977): 49-57.
- Brundin, N. "Method of Locating Metals and Minerals in the Ground, U.S. Patent 2,158,980." (1939).
- Buccianti, A., and E. Grunsky. "Compositional Data Analysis in Geochemistry: Are We Sure to See What Really Occurs During Natural Processes?": Elsevier, (2014).

Burrough, P.A., et al. Principles of Geographical Information Systems. Oxford university press, 2015.

Cairns, S., et al. "Neoproterozoic Decoupling of Upper-and Mid-Crustal Tectonothermal Domains in the Southeast Slave Province: Evidence from the Walmsley Lake Area." Canadian Journal of Earth Sciences 42, no. 6 (2005): 869-94.

Cannon, H.L., and H.L. Cannon. "Advances in Botanical Methods of Prospecting for Minerals. I: Advances in Geobotanical Methods." (1979).

Cannon, H.L., et al. "Metal Absorption by Equisetum (Horsetail)." US Geol. Surv. Bull.(US);(United States) 1278 (1968).

Cannon, H.L.. The Development of Botanical Methods of Prospecting for Uranium on the Colorado Plateau. US Government Printing Office, (1960).

Card, K.D., and A. Ciesielski. "Subdivisions of the Superior Province of the Canadian Shield." Geoscience Canada 13, no. 1 (1986).

Carr, M.H., and K.K Turekian. "The Geochemistry of Cobalt." Geochimica et Cosmochimica Acta 23, no. 1-2 (1961): 9-60.

Carranza, E.J.M. "Analysis and Mapping of Geochemical Anomalies Using Logratio-Transformed Stream Sediment Data with Censored Values." Journal of Geochemical Exploration 110, no. 2 (2011): 167-85.

Casali, J. "Hydrothermal Alteration Footprint of the Monument Bay Project, Manitoba, Canada." (2020).

Casali, J., et al. "Application of Large-Scale Synchrotron X-Ray Fluorescence 2d Mapping of Alteration Styles to Understand Gold Mineralization at the Monument Bay Project, Stull Lake Greenstone Belt, Manitoba, Canada." *Microscopy and Microanalysis* 26, no. S2 (2020): 3216-18.

Cassidy, K.F. "Gold in the Yellowstone Greenstone Belt, Northwest Territories: Results of the Extech Iii Multidisciplinary Research Project. Cd Anglin, H. Falck, Df Wright, and Ej Ambrose, Editors. Pp. 448. Geological Association of Canada, Mineral Deposits Division, Special Publication No. 3 (Dvd Included). 2006. Isbn 1-897095-09-0. Price Can 76.00, Memberpricecan 57.00." *Economic Geology* 102, no. 1 (2007): 159-60.

Cavallin, H.E., et al. "Application of Synchrotron Spectroscopy to Understanding Gold Mineralization at the Monument Bay Project, Stull Lake Greenstone Belt, Manitoba, Canada." *Microscopy and Microanalysis* 25, no. S2 (2019): 802-03.

Chandrakar, V., et al., "Arsenic-Induced Metabolic Disturbances and Their Mitigation Mechanisms in Crop Plants: A Review." *Biologia* 71, no. 4 (2016): 367-77.

Chen, S. *Principal Component Analysis of Geochemical Data from the Ree-Rich Maw Zone, Athabasca Basin, Canada*. Citeseer, 2015.

Cheng, Q. "Multifractality and Spatial Statistics." *Computers & Geosciences* 25, no. 9 (1999): 949-61.

Chung, C.F. "Estimation of Covariance Matrix from Geochemical Data with Observations Below Detection Limits." *Mathematical geology* 25, no. 7 (1993): 851-65.

- Cloutier, V., et al. "Multivariate Statistical Analysis of Geochemical Data as Indicative of the Hydrogeochemical Evolution of Groundwater in a Sedimentary Rock Aquifer System." *Journal of Hydrology* 353, no. 3-4 (2008): 294-313.
- Cohen, A.C. "Progressively censored sampling in the three parameter log-normal distribution." *Technometrics* 18, no. 1 (1976): 99-103.
- Cohen, A.C. "Tables for Maximum Likelihood Estimates: Singly Truncated and Singly Censored Samples." *Technometrics* 3, no. 4 (1961): 535-41.
- Cohen, D.R., et al.,. Biogeochemistry: A Geochemical Method for Gold Exploration in the Canadian Shield, In: R.G. Garrett, Ed., *Geochemical Exploration 1985*, *Journal of Geochemical Exploration* 29: 49–73. 1987.
- Combs J.R., et al. *The Role of Selenium in Nutrition*. Academic Press, Inc., 1986.
- Comrey, A.L., and H.B. Lee. *A First Course in Factor Analysis*. Psychology press, 2013.
- Cook, F.A., et al. "Tectonic Styles in Canada: Lithoprobe Perspective on the Evolution of the North American Continent." *Tectonic Styles in Canada: The Lithoprobe Perspective: Special Paper 49* (2012): 467-98.
- Corkery, M.T., et al. "Geology of the Little Stull Lake Area (Part of Nts 53k/10 and/7)." *Report of Activities* (1998): 111-18.
- Cousens, B.L. "Geochemistry of the Archean Kam Group, Yellowknife Greenstone Belt, Slave Province, Canada." *The Journal of geology* 108, no. 2 (2000): 181-97.

- Cousens, B.L., et al. "Regional Correlations, Tectonic Settings, and Stratigraphic Solutions in the Yellowknife Greenstone Belt and Adjacent Areas from Geochemical and Sm-Nd Isotopic Analyses of Volcanic and Plutonic Rocks ". (2006).
- Cox, S.F. "Injection-Driven Swarm Seismicity and Permeability Enhancement: Implications for the Dynamics of Hydrothermal Ore Systems in High Fluid-Flux, Overpressured Faulting Regimes—an Invited Paper." *Economic Geology* 111, no. 3 (2016): 559-87.
- Davis, J.C., and R.J. Sampson. "Statistics and Data Analysis in Geology." Vol. 646. New York: Wiley (1986).
- De La Espina, S.M.D. et al. "Detection by Bismuth Staining of Highly Phosphorylated Nucleo-Proteins in Plants. Determination of Its Specificity by X-Ray Microanalysis, Sds-Page and Immunological Analysis." *Biology of the Cell* 77 (1993): 297-306.
- Demšar, U., et al. "Principal Component Analysis on Spatial Data: An Overview." *Annals of the Association of American Geographers* 103, no. 1 (2013): 106-28.
- Diamond, L.W. "Fluid Chemistry of Orogenic Lode Gold Deposits and Implications for Genetic Models." *Gold in 2000* 13 (2000): 141.
- Dixon, W.J. "Simplified Estimation from Censored Normal Samples." *The Annals of Mathematical Statistics* (1960): 385-91.
- Dragon 6 user's manual
"http://www.taletе.mi.it/help/dragon_help/index.html?analysis_of_pca_results.htm.
Accessed 10 December 2022."

- Dubé, B. "Greenstone-Hosted Quartz-Carbonate Vein Deposits." *Mineral Deposits in Canada: A Synthesis of Major Deposit-Types, District Metallogeny, the Evolution of Geological Provinces, and Exploration Methods* (2007): 49-73.
- Dubé, B., and P. Gosselin. "Greenstone-Hosted Quartz-Carbonate Vein Deposits." *Geological Association of Canada, Mineral Deposits Division* (2007): 49-73.
- Dunn, C.E. "Biogeochemical Exploration for Gold in the La Ronge Belt, 1985." *Development* 1984 (1985): 89.
- Dunn, C.E. "Biogeochemical Investigations in Northern Saskatchewan: Preliminary Data on Tungsten, Gold, Platinum, Rare-Earths and Uranium." *Summary of investigations* (1983) Saskatchewan Geological Survey, Saskatchewan Energy Mines, Misc. Rep 83 (1983): 106-22.
- Dunn, C.E. "Biogeochemical Prospecting for Metals. Chapters 19 and 20." Eds. Brooks, RR, Dunn, CE, & Hall, *GEM Biological Systems in Mineral Exploration and Processing*, Ellis Horwood, Hemel Hempstead (UK), Toronto, NY (1995).
- Dunn, C.E. "New Perspectives on Biogeochemical Exploration." *Milkereit*, 2007. *Proceedings of Exploration* 7 (2007a): 249-61.
- Dunn, C.E. "The Biogeochemical Expression of Deeply Buried Uranium Mineralization in Saskatchewan, Canada." In *Developments in Economic Geology*, 437-52: Elsevier, 1981.
- Dunn, C.E. "The Massive Wollaston Uranium Biogeochemical Anomaly in the Boreal Forest of Northern Saskatchewan, Canada." Paper presented at the Proceedings of the symposium on uranium exploration methods, (1982).

- Dunn, C.E. Biogeochemistry in Mineral Exploration: Handbook of Exploration and Environmental Geochemistry Series (M. Hale, Series Editor), Volume 9. And Economic Geology, Vol. 102, No. 7, 2007, Pp. 1354-1354. (2007b).
- Dunn, C.E., and D.R. Heberlein. "A Geochemical Investigation of Halogens in Spruce Treetops and Integration with Existing Multi-Element Data—Blackwater/Trek Regions, Central British Columbia (Nts 093c, 093f)." (2020).
- Dunn, C.E., and E. Hoffman. "Multi-Element Study of Vegetation from a Zone of Rare-Earth Rich Allanite and Apatite in Northern Saskatchewan, Canada." Applied geochemistry 1, no. 3 (1986): 375-81.
- Dunn, C.E., and E.M Cameron. "Detailed Biogeochemical Studies for Uranium in the Nea/Iaea Athabasca Test Area." Uranium exploration in the Athabasca Basin, Saskatchewan, Canada. Ottawa (1983): 259-72.
- Dunn, C.E., and G.E. Ray. "A comparison of lithogeochemical and biogeochemical patterns associated with gold mineralization in mountainous terrain of southern British Columbia." Economic Geology 90, no. 8 (1995): 2232-2243.
- Dunn, C.E., and R.S. Angélica. Evaluation of Biogeochemistry as a Tool in Mineral Exploration and in Monitoring Environmental Mercury Dispersion in the Tapajos Gold District, Amazonia, Brazil. Natural Resources Canada, (2000).
- Dunn, C.E., et al. "Biogeochemical Survey of the Drybones Bay Area, Northwest Territories (Nts 85i/4) Using Outer Bark of Black Spruce." (2001).

- Dunn, C.E., et al. "Biogeochemical Survey, Baie Verte Area, Newfoundland: Black Spruce Twigs, Parts of Nts 12h/16 and 12i/1." Natural Resources Canada, Geological Survey of Canada, (1995).
- Dunn, C.E., et al. "Comparisons of Biogeochemical Data Obtained by Different Methods, and the Influence of Airborne Dust from Gold Mining and Milling, Yellowknife, Northwest Territories, Geological Survey of Canada, Open File.", (2002).
- Dunn, C.E., et al. "Halogens in Surface Exploration Geochemistry: Evaluation and Development of Methods for Detecting Buried Mineral Deposits." Geoscience BC, Report 8 (2005): 69.
- Dunn, C.E., et al. "Halogens in Surface Exploration Geochemistry: Evaluation and Development of Methods for Detecting Buried Mineral Deposits." Geoscience BC, Report 10 (2007): 2007-10.
- Dunn, C.E., et al. "Patterns of Metal Enrichment in Vegetation in Relation to Geology and Gold Mineralization: Star Lake Area, Saskatchewan." (1990).
- Dunn, C.E., et al. "Reconnaissance Biogeochemical Survey, Southeastern Cape Breton Island, Nova Scotia: Black Spruce Bark, Parts of Nts 11f, G, J, K." Natural Resources Canada, Geological Survey of Canada, (1992).
- DuToit, S.H.C, et al. Graphical Exploratory Data Analysis. Springer Science & Business Media, (2012).
- Easton, R.B. "The Nature and Significance of Pre-Yellowknife Supergroup Rocks in the Point Lake Area, Slave Structural Province, Canada." Evolution of Archean supracrustal sequences. Edited by Ayres LD, Thurston PC, Card KD, Weber W.. Geological Association of Canada, Special Paper 28 (1985): 153-67.

Eccles, D.R. Biogeochemical Orientation Survey over the Mountain Lake Diatreme, Alberta. Alberta Geological Survey, (1998).

Egozcue, J.J., et al. "Isometric Logratio Transformations for Compositional Data Analysis." *Mathematical geology* 35, no. 3 (2003): 279-300.

Erdman, J.A., and J.C. Olson. "The Use of Plants in Prospecting for Gold: A Brief Overview with a Selected Bibliography and Topic Index." *Journal of Geochemical Exploration* 24, no. 3 (1985): 281-304.

Falck, H. "Volcanic and Sedimentary Rocks of the Yellowknife Bay Formation, Giant Section, Yellowknife Greenstone Belt, Nwt." Carleton University, (1990).

Fedikow, M., et al. "Of98-5: Operation Superior: Multimedia Geochemical Survey Results from the Edmund Lake and Sharpe Lake Greenstone Belts, Northern Superior Province, Manitoba.", (1998).

Fedikow, M., et al. "Operation Superior: 1996 Multimedia Geochemical Data from the Max Lake Area (Nts 63i/8, 9 and 53l/5, 12); Manitoba Department of Energy and Mines, Mineral Resources Division, Open-File Report Of97-1, 34p. And 1 Disk.", (1997).

Filzmoser, P., and K. Hron. "Outlier Detection for Compositional Data Using Robust Methods." *Mathematical Geosciences* 40, no. 3 (2008): 233-48.

Filzmoser, P., et al. "Interpretation of Multivariate Outliers for Compositional Data." *Computers & Geosciences* 39 (2012): 77-85.

- Filzmoser, P., et al. "Principal Component Analysis for Compositional Data with Outliers." *Environmetrics: The Official Journal of the International Environmetrics Society* 20, no. 6 (2009a): 621-32.
- Filzmoser, P., et al. "Univariate Statistical Analysis of Environmental (Compositional) Data: Problems and Possibilities." *Science of the Total Environment* 407, no. 23 (2009b): 6100-08.
- Fisher, R.A. et al. "Studies in Crop Variation. Ii. The Manurial Response of Different Potato Varieties." (1923).
- Gaboury, A.C. et al. "Predictive Distribution of Fault-Fill and Extensional Veins: Example from the Sigma Gold Mine, Abitibi Subprovince, Canada." *Economic Geology* 96, no. 6 (2001): 1397-405.
- Gaboury, D. "Parameters for the Formation of Orogenic Gold Deposits." *Applied Earth Science* 128, no. 3 (2019): 124-33.
- Gabriel, K.R. "The Biplot Graphic Display of Matrices with Application to Principal Component Analysis." *Biometrika* 58, no. 3 (1971): 453-67.
- Gallego, S.M., et al. "Unravelling Cadmium Toxicity and Tolerance in Plants: Insight into Regulatory Mechanisms." *Environmental and Experimental Botany* 83 (2012): 33-46.
- Ghezelbash, R. "Incorporation of Principal Component Analysis, Geostatistical Interpolation Approaches and Frequency-Space-Based Models for Portraying the Cu-Au Geochemical Prospects in the Feizabad District, Nw Iran." *Geochemistry* 79, no. 2 (2019): 323-36.

- Ghorbani, Z., et al. "Application of Multivariate Data Analysis to Biogeochemical Exploration at the Twin Lakes Deposit, Monument Bay Gold Project, Manitoba, Canada." *Chemical Geology* (2022a): 120739.
- Ghorbani, Z., et al. "Biogeochemical Exploration at the Twin Lakes Au Deposit Using Synchrotron Radiation Micro X-Ray Fluorescence and X-Ray Absorption near-Edge Structure Spectroscopy." *Microscopy and Microanalysis* 26, no. S2 (2020): 1272-75.
- Ghorbani, Zohreh, Alan Sexton, Lisa L Van Loon, and Neil R Banerjee. "Biogeochemical Prospecting for Gold at the Yellowknife City Gold Project, Northwest Territories, Canada Part 1-Species Optimization." *Applied Geochemistry* (2022b): 105423.
- Ghosh, P., et al. "Phosphorus Solubilization and Plant Growth Enhancement by Arsenic-Resistant Bacteria." *Chemosphere* 134 (2015): 1-6.
- Gill, J.E. "Natural Divisions of the Canadian Shield." *Trans. Roy. Soc. Canada, 3d Ser., Sec. IV* 43 (1949): 61-69.
- Ginzburg, I.I. *Principles of Geochemical Prospecting: Techniques of Prospecting for Non-Ferrous Ores and Rare Metals*. Elsevier, 2013.
- Girling, C.A., et al. "Plants as Indicators of Gold Mineralization at Watson Bar, British Columbia, Canada." *Economic Geology* 74, no. 4 (1979): 902-07.
- Goldfarb, R.J., and D.I. Groves. "Orogenic Gold: Common or Evolving Fluid and Metal Sources through Time." *Lithos* 233 (2015): 2-26.
- Goldfarb, R.j., et al. "Distribution, Character and Genesis of Gold Deposits in Metamorphic Terranes." *Society of Economic Geologists*, 2005.

- Goldfarb, R.J., et al. "Orogenic Gold and Geologic Time: A Global Synthesis." *Ore geology reviews* 18, no. 1-2 (2001): 1-75.
- Goodwin, A.M. "Archean Crust in the Superior Geotraverse Area: Geologic Overview." Paper presented at the Proceedings of the 1978 Archean Geochemistry Conference. Department of Geology, University of Toronto, Toronto, Ont, 1978.
- Griffis, R.J., and F.L. Agezo. *Mineral Occurrences and Exploration Potential of Northern Ghana*. Minerals Commission, 2000.
- Groves, D.I. "The Crustal Continuum Model for Late-Archaean Lode-Gold Deposits of the Yilgarn Block, Western Australia." *Mineralium deposit* 28, no. 6 (1993): 366-74.
- Groves, R.J., et al. "Orogenic Gold Deposits: A Proposed Classification in the Context of Their Crustal Distribution and Relationship to Other Gold Deposit Types." *Ore geology reviews* 13, no. 1-5 (1998): 7-27.
- Grunsky, E.C. "The Interpretation of Geochemical Survey Data." *Geochemistry: Exploration, Environment, Analysis* 10, no. 1 (2010): 27-74.
- Grunsky, E.C., and P. de Caritat. "State-of-the-Art Analysis of Geochemical Data for Mineral Exploration." *Geochemistry: Exploration, Environment, Analysis* 20, no. 2 (2020): 217-32.
- Güler, C., et al. "Evaluation of Graphical and Multivariate Statistical Methods for Classification of Water Chemistry Data." *Hydrogeology journal* 10, no. 4 (2002): 455-74.
- Hao, C., et al. "Epma Characterization of Gold Associated with Different Sulfide Textures at the Monument Bay Deposit, Manitoba, Canada." *Microscopy and Microanalysis* 26, no. S2 (2020a): 2182-84.

- Hao, C., et al. "Multi-Scale Sr-MicrXRF Imaging and Characterization of Gold Mineralization at the Monument Bay Deposit, Stull Lake Greenstone Belt, Manitoba, Canada." *Microscopy and Microanalysis* 26, no. S2 (2020b): 1256-59.
- Hartigan, J.A. *Clustering Algorithms*. John Wiley & Sons, Inc., 1975.
- Haugaard, R., et al. "Neoarchaean Banded Iron Formation within a ~ 2620 Ma Turbidite-Dominated Deep-Water Basin, Slave Craton, Nw Canada." *Precambrian Research* 292 (2017): 130-51.
- Heberlein, D.R. et al. "Halogens and Other Volatile Compounds in Surface Sample Media as Indicators of Mineralization. Part 2: Mount Washington Epithermal Au-Cu-Ag Prospect, Vancouver Island, Bc (Nts 092f/14)."
- Heenan, D.P., and L.C. Campbell. "Transport and Distribution of Manganese in Two Cultivars of Soybean (*Glycine Max* (L.) Merr.)." *Australian journal of agricultural research* 31, no. 5 (1980): 943-49.
- Helmstaedt, H, and W.A. Padgham. "A New Look at the Stratigraphy of the Yellowknife Supergroup at Yellowknife, Nwt—Implications for the Age of Gold-Bearing Shear Zones and Archean Basin Evolution." *Canadian Journal of Earth Sciences* 23, no. 4 (1986): 454-75.
- Helmstaedt, H.H., et al. "Geology and Tectonic Evolution of the Slave Province—a Post-Lithoprobe Perspective." *Tectonic Styles in Canada: The LITHOPROBE Perspective: Geological Association of Canada Special Paper 49* (2012): 379-466.
- Henderson, J.B. *Geology of the Yellowknife-Hearne Lake Area, District of Mackenzie: A Segment across an Archean Basin*. Vol. 414: Geological Survey of Canada, 1985.

Henderson, J.F., and I.C. Brown. Geology and Structure of the Yellowknife Greenstone Belt, District of Mackenzie. Department of Mines and Technical Surveys, 1966.

Hill, B. "Mega Precious Metals Inc.: Updated Preliminary Assessment Study – Monument Bay Gold Project, Manitoba, Canada." (2011a).

Hill, B. Updated Preliminary Assessment Study – Monument Bay Gold Project, Manitoba, Canada. Rolling Rock Resources Corporation, (2011b).

Hotelling, H. "Analysis of a Complex of Statistical Variables into Principal Components." Journal of educational psychology 24, no. 6 (1933): 417.

Hron, Karel, Matthias Templ, and Peter Filzmoser. "Imputation of Missing Values for Compositional Data Using Classical and Robust Methods." Computational Statistics & Data Analysis 54, no. 12 (2010): 3095-107.

Isachsen, C. E., and S. A. Bowring. "Evolution of the Slave Craton." Geology 22, no. 10 (1994): 917-20.

Isachsen, C.E., and S.A. Bowring. "The Bell Lake Group and Anton Complex: A Basement–Cover Sequence beneath the Archean Yellowknife Greenstone Belt Revealed and Implicated in Greenstone Belt Formation." Canadian Journal of Earth Sciences 34, no. 2 (1997): 169-89.

Ismael, M.A. et al. "Cadmium in Plants: Uptake, Toxicity, and Its Interactions with Selenium Fertilizers." Metallomics 11, no. 2 (2019): 255-77.

Johnson, R. A., et al. Applied Multivariate Statistical Analysis. Vol. 5: Prentice hall Upper Saddle River, NJ, 2002.

- Jolliffe, I.T., and J. Cadima. "Principal Component Analysis: A Review and Recent Developments." *Philosophical Transactions of the Royal Society A: Mathematical, Physical and Engineering Sciences* 374, no. 2065 (2016): 20150202.
- Kabata-Pendias, A. *Trace Elements in Soils and Plants (Third Edition)*, (Crc Press, Oca Raton), 432 Pp. (2001).
- Kabata-Pendias, A., and H. Pendias. "Trace Elements in the Biological Environment. *Wyd. Geol.*" INC, Warsaw (1979).
- Kabata-Pendias, A., and H. Pendias. *Trace Elements in Soils and Plants (Second Edition)*, (Crc Press, Boca Raton), 365 Pp. (1992).
- Kabata-Pendias, A.,. "Geochemistry of Selenium." *Journal of environmental pathology, toxicology and oncology: official organ of the International Society for Environmental Toxicology and Cancer* 17, no. 3-4 (1998): 173-77.
- Kaiser, H.F. "The Application of Electronic Computers to Factor Analysis." *Educational and psychological measurement* 20, no. 1 (1960): 141-51.
- Kaiser, H.F., and J. Rice. "Little Jiffy, Mark Iv." *Educational and psychological measurement* 34, no. 1 (1974): 111-17.
- Keith, L. "Throwaway Data." *Environmental Science and Technology* 28, no. 8 (1994): 389A.
- Kelly, J.A. "Exploration Proposal, Northbelt Gold Property, Yellowknife Area. Internal Report, Nebex Resources Ltd., 30 P."(1993).

- Kerr, D.E., and R.D. Knight. An Overview of Gold Grain Distribution and Geochemistry of Till, Yellowknife Greenstone Belt, Northwest Territories. Natural Resources Canada, Geological Survey of Canada, (2002).
- Keshavarzi, B., et al. "Chemical Speciation, Human Health Risk Assessment and Pollution Level of Selected Heavy Metals in Urban Street Dust of Shiraz, Iran." *Atmospheric Environment* 119 (2015): 1-10.
- Khalid, S., et al. "Enhancing Cleanup of Environmental Pollutants." Cham: Springer (2017): 97-140.
- King, J.E., et al. "Deformation and Plutonism in the Western Contwoyto Lake Map Area, Central Slave Province, District of Mackenzie, Nwt." *Current research, Part C: Geological Survey of Canada Paper* (1988): 161-76.
- Kitayev, N.A., and R.I. Zhukova. "Relationship between the Concentrations of Gold in Soil, Forest Bedding and the Bark of Trees." *Sov Geol Geophys* 21, no. 12 (1980): 118-21.
- Kovalevskiy, A.L. "Biogeochemical Exploration for Mineral Deposits, Published for the Usdi and the Nsf, Amerind Publ." Co. Pvt. Ltd., New Delhi 136 (1979).
- Kovalevsky, A.L. Barrier-Free Biogeochemical Prospecting, In: R.R. Brooks, C.E. Dunn and G.E.M. Hall, Eds., *Biological Systems in Mineral Exploration and Processing* (Ellis Horwood, Uk), Pp. 283–299. (1995).
- Kovalevsky, A.L. *Biogeochemical Exploration for Mineral Deposits*. (Vnu Press, Utrecht), 224 Pp. (1987).

- Kovalevsky, A.L., and O.M. Kovalevskaya. Biogeochemical Haloes of Gold in Various Species and Parts of Plants, *Applied Geochemistry* 4: 369–374. (1989).
- Krogh, T.E., and W. Gibbins. "U-Pb Isotopic Ages of Basement and Supracrustal Rocks in the Point Lake Area of the Slave Structural Province, Canada." Paper presented at the Geol. Assoc. Can. Abstr, (1978).
- Kusky, T.M. "Accretion of the Archean Slave Province." *Geology* 17, no. 1 (1989): 63-67.
- Kusky, T.M. "Are Greenstone Belts in the Slave Province, Nwt Allochthonous?" Paper presented at the Workshop on Tectonic Evolution of Greenstone Belts, (1986).
- Kusky, T.M. "Thrusting between the Cameron River Greenstone Belt and the Sleepy Dragon Metamorphic Complex, District of Mackenzie." *Contrib. Geol. Northwest Territ* 3 (1988): 97-102.
- Lambeck, A. "Are Iron-Rich Sedimentary Rocks the Key to the Spike in Orogenic Gold Mineralization in the Paleoproterozoic?". *Economic Geology* 106, no. 3 (2011): 321-30.
- Lambert, M.B. Back River Volcanic Complex: An Archean Stratovolcano, Nunavut-Northwest Territories. Geological Survey of Canada, (2005).
- Larsen, E.H., et al. "Atmospheric Deposition of Trace Elements around Point Sources and Human Health Risk Assessment. Ii: Uptake of Arsenic and Chromium by Vegetables Grown near a Wood Preservation Factory." *Science of the Total Environment* 126, no. 3 (1992): 263-75.
- Lemenkova, P. "Numerical Data Modelling and Classification in Marine Geology by the Spss Statistics." *International Journal of Engineering Technologies* 5, no. 2 (2019): 90-99.

- Li, Y. "Factors Influencing Leaf Chlorophyll Content in Natural Forests at the Biome Scale." *Frontiers in Ecology and Evolution* 6 (2018): 64.
- Lima, A., et al. "Multifractal Idw Interpolation and Fractal Filtering Method in Environmental Studies: An Application on Regional Stream Sediments of (Italy), Campania Region." *Applied geochemistry* 18, no. 12 (2003): 1853-65.
- Lindberg, P.E., and N. Lannek. "Amounts of Selenium in Swedish Forages, Soils and Animal Tissues." *Trace Element Metabolism in Animals*. Livingstone, Edinburgh (1970): 421-26.
- Link, R.F., and G.S. Koch. "Some Consequences of Applying Lognormal Theory to Pseudolognormal Distributions." *Journal of the International Association for Mathematical Geology* 7, no. 2 (1975): 117-28.
- Lintern, M.J., and R.R. Anand. "Dispersion of Gold and Other Metals by Trees, Gravels and Soils near Boddington Gold Deposit, Western Australia." *Journal of Geochemical Exploration* 181 (2017): 10-21.
- Lungwitz, E.E. "The Lixiviation of Gold Deposits by Vegetation and Its Geological Importance." *Mining Journal (London)* 69 (1900): 500-02.
- Lydon, J.W., and W.D. Goodfellow. "An Overview of the Economic and Geological Contexts of Canada's Major Mineral Deposit Types." *Geological Association of Canada, Mineral Deposits Division* (2007): 3-48.
- Markert, B. "Progress Report on the Element Concentrations Cadastre Project (Eccp) of Intercol/Iubs, International Union of Biological Sciences, 25th General Assembly, Paris, 54 Pp.", (1994).

- Martel, E., and S. Lin. "Structural Evolution of the Yellowknife Greenstone Belt, with Emphasis on the Yellowknife River Fault Zone and the Jackson Lake Formation." *Geological Association of Canada Mineral Deposits Division* (2006): 95-115.
- Matschullat, J., et al. "Geochemical Background—Can We Calculate It?". *Environmental geology* 39, no. 9 (2000): 990-1000.
- McCracken, T. "Technical Report and Update Resource Estimate on the Monument Bay Project, Northern Manitoba (Ni 43-101). Project No: 131-24294-00_Rpt-02_R3. Yamana Gold Inc.", (2016).
- McCracken, T., and D. Thibault "Technical Report and Resource Estimate Update on the Monument Bay Project, Northern Manitoba. Wsp Canada Inc. Unpublished.". (2016.).
- Megonigal, J.P., et al. "Anaerobic Metabolism: Linkages to Trace Gases and Aerobic Processes." *Biogeochemistry*, (2004).
- Mengell, K., and E.A. Kirkby. *Principles of Plant Nutrition*. (International Potash Institute, Horgen), (1987).
- Natural Resources Canada. "Government of Canada." Natural Resources Canada. / Gouvernement du Canada, July 22, 2022. <https://www.nrcan.gc.ca/maps-tools-and-publications/publications/minerals-mining-publications/mining-sector-performance-report/18912>. Accessed 10 December 2022."
- Neff, H. "Rq-Mode Principal Components Analysis of Ceramic Compositional Data." *Archaeometry* 36, no. 1 (1994): 115-30.

- Nejadhadad, M., et al. "The Use of Univariate and Multivariate Analyses in the Geochemical Exploration, Ravanj Lead Mine, Delijan, Iran." *Minerals* 7, no. 11 (2017): 212.
- Nude, P.M., et al. "Identifying Pathfinder Elements for Gold in Multi-Element Soil Geochemical Data from the Wa-Lawra Belt, Northwest Ghana: A Multivariate Statistical Approach." *International Journal of Geosciences* 3, no. 01 (2012): 62.
- Nyade, P.K., et al. "Use of Surficial Geochemical Methods to Locate Areas of Buried Uranium Mineralization in the Jacque's Lake Area of the Central Mineral Belt, Labrador, Canada." *Canadian Journal of Earth Sciences* 50, no. 11 (2013): 1134-46.
- Odhiambo, B.D. "The Place of Geobotany in Geology." *Int. J. Geobot. Res* 6 (2016): 27-36.
- Okulitch, A.V. *Proposals for Time Classification and Correlation of Precambrian Rocks and Events in Canada and Adjacent Areas of the Canadian Shield*. Geological Survey of Canada, (1988).
- Oliva, S.R., and A.J. Fernández Espinosa. "Monitoring of Heavy Metals in Topsoils, Atmospheric Particles and Plant Leaves to Identify Possible Contamination Sources." *Microchemical Journal* 86, no. 1 (2007): 131-39.
- Ootes, L., et al. "The Timing of Yellowknife Gold Mineralization: A Temporal Relationship with Crustal Anatexis?". *Economic Geology* 106, no. 4 (2011): 713-20.
- Osborne, J.W., and A.B. Costello. "Sample Size and Subject to Item Ratio in Principal Components Analysis." *Practical Assessment, Research, and Evaluation* 9, no. 1 (2004): 11.

- Padgham, W.A. "Observations and Speculations on Supracrustal Successions in the Slave Structural Province." *Evolution of Archean Sequences*. Geological Association of Canada, Special Paper 28 (1985): 133-51.
- Palmer, M.J., et al. "Mineralogical, Geospatial, and Statistical Methods Combined to Estimate Geochemical Background of Arsenic in Soils for an Area Impacted by Legacy Mining Pollution." *Science of The Total Environment* 776 (2021): 145926.
- Percival, J.A. "Geology and Metallogeny of the Superior Province, Canada." 903-28: Geological Association of Canada, Mineral Deposits Division., (2007).
- Percival, J.A., et al. "Tectonic Evolution of the Western Superior Province from Natmap and Lithoprobe Studies." *Canadian Journal of Earth Sciences* 43, no. 7 (2006): 1085-117.
- Percival, J.A., and T. Skulski. "Tectonothermal Evolution of the Northern Minto Block, Superior Province, Quebec, Canada." *The Canadian Mineralogist* 38, no. 2 (2000): 345-78.
- Percival, J.A., et al. "Geology and Tectonic Evolution of the Superior Province, Canada." *Tectonic styles in Canada: The Lithoprobe Perspective*, Special Paper 49 (2012): 321-78.
- Percival, J.A., et al. "Panlithoprobe Workshop Iv: Intra-Orogen Correlations and Comparative Orogenic Anatomy." *Geoscience Canada* 31, no. 1 (2004).
- Phillips, G.N., and K.A. Evans. "Role of CO_2 in the Formation of Gold Deposits." *Nature* 429, no. 6994 (2004): 860-63.
- Phillips, G.N., and R. Powell. "Formation of Gold Deposits: A Metamorphic Devolatilization Model." *Journal of Metamorphic Geology* 28, no. 6 (2010): 689-718.

- Piccinin, R.C.R., et al. "A Screen of Some Native Australian Flora and Exotic Agricultural Species for Their Potential Application in Cyanide-Induced Phytoextraction of Gold." *Minerals Engineering* 20, no. 14 (2007): 1327-30.
- Pickering, I.J., et al. "Chemical Form and Distribution of Selenium and Sulfur in the Selenium Hyperaccumulator *Astragalus Bisulcatus*." *Plant physiology* 131, no. 3 (2003): 1460-67.
- Pickering, I.J., et al. "Reduction and Coordination of Arsenic in Indian Mustard." *Plant physiology* 122, no. 4 (2000): 1171-78.
- Pitcairn, I.K., et al. "Metabasalts as Sources of Metals in Orogenic Gold Deposits." *Mineralium Deposita* 50, no. 3 (2015): 373-90.
- Pratas, J., et al. "Plants Growing in Abandoned Mines of Portugal Are Useful for Biogeochemical Exploration of Arsenic, Antimony, Tungsten and Mine Reclamation." *Journal of geochemical exploration* 85, no. 3 (2005): 99-107.
- Price, C.A., et al. "Functions of Micronutrients in Plants." *Micronutrients in agriculture, 1972 - agris.fao.org 1972* (1972): 231-42.
- Raab, A., et al. "Uptake, Translocation and Transformation of Arsenate and Arsenite in Sunflower (*Helianthus Annuus*): Formation of Arsenic-Phytochelatin Complexes During Exposure to High Arsenic Concentrations." *New phytologist* 168, no. 3 (2005): 551-58.
- Rastegarimehr, M., et al. "Distribution, Source Identification and Health Risk Assessment of Soil Heavy Metals in Urban Areas of Isfahan Province, Iran." *Journal of African Earth Sciences* 132 (2017): 16-26.

- Reading scatterplots., "<https://www.mathbootcamps.com/reading-scatterplots/>. Accessed 10 December 2022."
- Reid, N. "Spinifex Biogeochemical Expressions of Buried Gold Mineralisation: The Great Mineral Exploration Penetrator of Transported Regolith." *Applied Geochemistry* 23, no. 1 (2008): 76-84.
- Reimann, C., et al. "Background and Threshold: Critical Comparison of Methods of Determination." *Science of the total environment* 346, no. 1-3 (2005): 1-16.
- Reimann, C., et al. *Statistical Data Analysis Explained: Applied Environmental Statistics with R*. John Wiley & Sons, (2011).
- Rengel, Z., et al. "Uptake of Zinc and Iron by Wheat Genotypes Differing in Tolerance to Zinc Deficiency." *Journal of Plant Physiology* 152, no. 4-5 (1998): 433-38.
- Richardson, M.W., and D.R. Lentz. "Characterization of Auriferous Quartz Veins of the Ptarmigan and Tom Gold Deposits, Yellowknife, Northwest Territories." *Atlantic Geology* 55 (2019).
- Robert, F. "Structural Setting and Control of Gold-Quartz Veins of the Val D'or Area, Southeastern Abitibi Subprovince: University of Western Australia Special Publication, V. 24." (1990).
- Rollinson, H.R. "Another Look at the Constant Sum Problem in Geochemistry." *Mineralogical Magazine* 56, no. 385 (1992): 469-75.
- Rose, Arthur. *Geochemistry in mineral exploration*. No. 622.1 R 795. (1979).

- Sanford, R.F., et al. "An Objective Replacement Method for Censored Geochemical Data." *Mathematical Geology* 25, no. 1 (1993): 59-80.
- Schaug, J., et al. "Multivariate Analysis of Trace Element Data from Moss Samples Used to Monitor Atmospheric Deposition." *Atmospheric Environment. Part A. General Topics* 24, no. 10 (1990): 2625-31.
- Scott, D.W. "Sturges' Rule." *Wiley Interdisciplinary Reviews: Computational Statistics* 1, no. 3 (2009): 303-06.
- Shacklette, H.T. "Element Content of Bryophytes, United States Geological Survey." (1965).
- Shacklette, H.T., et al. "Trace Elements in Plant Foodstuffs." *Toxicity of heavy metals in the environment, Part 1* (1978): 25-43.
- Sharma, P., and R.S. Dubey. "Lead Toxicity in Plants." *Brazilian journal of plant physiology* 17, no. 1 (2005): 35-52.
- Shelton, K.L., et al. "Nwt Open File 2016-02 Ore Petrography, Fluid Inclusion and Stable Isotope Studies of Gold and Base-Metal Sulphide Mineralization in a Northern Portion of the Yellowknife Greenstone Belt." (2016).
- Sheoran, V., et al. "Phytomining of Gold: A Review." *Journal of Geochemical Exploration* 128 (2013): 42-50.
- Shepard, D. "Proceedings of the 1968 23rd Acm National Conference." ACM New York, NY, USA, (1968).

- Sherlock, R.L., et al. Volcanic Stratigraphy, Structural Geology, and Gold Mineralization in the Wolverine-Doris Corridor, Northern Hope Bay Volcanic Belt, Nunavut. Natural Resources Canada, Geological Survey of Canada, (2003).
- Shtangeeva, I, et al. "Multivariate Statistical Analysis of Nutrients and Trace Elements in Plants and Soil from Northwestern Russia." *Plant and soil* 322, no. 1-2 (2009): 219-28.
- Siddorn, J., et al. "The Giant-Con Gold Deposits: Preliminary Intergrated Structural and Mineralization History." In *Gold in the Yellowknife Greenstone Belt, Northwest Territories: Results of the Extech Iii Multidisciplinary Research Project*, 213-31: Geological Association of Canada, (2006).
- Siddorn, J.P., and H.C. Halls. "Variation in Plagioclase Clouding Intensity in Matachewan Dykes: Evidence for the Exhumation History of the Northern Margin of the Sudbury Igneous Complex." *Canadian Journal of Earth Sciences* 39, no. 6 (2002): 933-42.
- Sidney, F. Principal Component Analysis "<https://community.alteryx.com/t5/Data-Science/Tidying-up-with-PCA-An-Introduction-to-Principal-Components/ba-p/382557>. Accessed 12 Dec, 2022"
- Sigel, A., and H. Sigel. *Metals Ions in Biological System: Volume 39: Molybdenum and Tungsten: Their Roles in Biological Processes*. CRC Press, (2002).
- Sinclair, A.J. "Selection of Threshold Values in Geochemical Data Using Probability Graphs." *Journal of geochemical exploration* 3, no. 2 (1974): 129-49.
- Singh, C.k., et al. "Multivariate Statistical Analysis and Geochemical Modeling for Geochemical Assessment of Groundwater of Delhi, India." *Journal of Geochemical Exploration* 175 (2017): 59-71.

- Skulski, T., et al. "Geological and Geochronological Investigations in the Stull Lake–Edmund Lake Greenstone Belt and Granitoid Rocks of the Northwestern Superior Province." Report of activities (2000): 117-28.
- Smeyers-Verbeke, J., et al. "Cd Uptake by Intact Wheat Plants." *Plant, Cell & Environment* 1, no. 4 (1978): 291-96.
- Šorša, A., et al. "Urban Geochemistry: Sisak in Croatia, a Long-Lasting Historical, Urban and Industrial City." *Geochemistry: Exploration, Environment, Analysis* 17, no. 2 (2017): 159-63.
- Stanimirova, I., et al. "Dealing with Missing Values and Outliers in Principal Component Analysis." *Talanta* 72, no. 1 (2007): 172-78.
- State of Canada's Forests 2004-2005: The Boreal Forest." Natural Resources Canada, Canadian Forest Service, Headquarters, Planning, Operations and Information Branch, Ottawa. 96pp (2005).
- Stednick, J.D., and W.C. Riese. "Temporal Variation of Metal Concentrations in Biogeochemical Samples over the Royal Tiger Mine, Colorado, Part II. Between-Year Variation." *Journal of Geochemical Exploration* 27, no. 1-2 (1987): 53-62.
- Stednick, J.D., et al. "Temporal Variation of Metal Concentrations in Biogeochemical Samples over the Royal Tiger Mine, Colorado, Part I: Within Year Variation." *Journal of Geochemical Exploration* 29, no. 1-3 (1987): 75-88.
- Stockwell, C.H. "Fourth Report on Structural Provinces, Orogenies, and Time-Classification of Rocks of the Canadian Precambrian Shield." Part II. Geological Studies. Geological Survey of Canada, Paper 64, no. 17 (1964): 1-7.

- Stone, D. Geology of the Northern Superior Area, Ontario. Ministry of Northern Development & Mines, Ontario Geological Survey, (2005).
- Stone, D., et al. "Geology of the Ellard Lake-Pasquatchai River and Stull Lake Areas, Northern Superior Province." Summary of Field Work and Other Activities, Ontario Geological Survey Miscellaneous Paper 169 (1998): 136-42.
- The Canadian Encyclopedia, [Www.Thecanadianencyclopedia.ca/En/Article/Shield](http://www.thecanadianencyclopedia.ca/en/article/shield). Accessed 24 January 2022."
- Thió-Henestrosa, S., and J.A. Martín-Fernández. "Dealing with Compositional Data: The Freeware Codapack." *Mathematical Geology* 37, no. 7 (2005): 773-93.
- Thompson, P.H. "Metamorphic Constraints on the Geological Setting, Thermal Regime, and Timing of Alteration and Gold Mineralization in the Yellowknife Greenstone Belt, Nwt, Canada." *Geological Association of Canada Mineral Deposits Division* (2006): 142-72.
- Thoresby, P., and I. Thornton. "Heavy Metals and Arsenic in Soil, Pasture Herbage and Barley in Some Mineralised Areas in Britain: Significance to Animal and Human Health." Paper presented at the Trace substances in environmental health; proceedings of University of Missouri annual conference, (1979).
- Tlustos, P., et al. "The Accumulation of Arsenic in Radish Biomass When Different Forms of as Were Applied in the Soil." *Rostlinna Vyroba-UZPI (Czech Republic)* (1998).
- Tomkins, A.G. "A Biogeochemical Influence on the Secular Distribution of Orogenic Gold." *Economic Geology* 108, no. 2 (2013): 193-97.
- Tukey, J.W. *Exploratory Data Analysis*. Vol. 2: Reading, MA, (1977).

- Van Hees, E.H. et al. "Metasedimentary Influence on Metavolcanic-Rock-Hosted Greenstone Gold Deposits: Geochemistry of the Giant Mine, Yellowknife, Northwest Territories, Canada." *Geology* 27, no. 1 (1999): 71-74.
- Van Hees, E.H., et al. "21. Genesis of the Ptarmigan Gold Deposit: Is It of Magmatic Affinity?". (2006).
- Vearncombe, J., and M. Zelic. "Structural Paradigms for Gold: Do They Help Us Find and Mine?". *Applied Earth Science* 124, no. 1 (2015): 2-19.
- Viladevall, M., et al. "Biogeochemical Exploration Using the Thola Shrub in the Andean Altiplano, Bolivia." *Geochemistry: Exploration, Environment, Analysis* 12, no. 1 (2012): 33-44.
- Vural, A. "Evaluation of Soil Geochemistry Data of Canca Area (Gümüşhane, Turkey) by Means of Inverse Distance Weighting (Idw) and Kriging Methods-Preliminary Findings." *Bulletin of the Mineral Research and Exploration* 158, no. 158 (2019): 195-216.
- Warren, H.V. *Biogeochemical Prospecting for Lead*. Vol. 395: Elsevier, Amsterdam, (1978).
- Warren, H.V., and R.E. Delavault. "Gold and Silver Content of Some Trees and Horsetails in British Columbia, Geological Society of America Bulletin 61: 123–128.". (1950).
- Warren, H.V., and S.J. Horsky. "Thallium, a Biogeochemical Prospecting Tool for Gold." *Journal of Geochemical Exploration* 26, no. 3 (1986): 215-21.
- Warren, H.V., et al. "The Role of Arsenic as a Pathfinder in Biogeochemical Prospecting." *Economic Geology* 59, no. 7 (1964): 1381-85.

- Warren, H.V., et al. Arsenic Content of Douglas-Fir as a Guide to Some Gold, Silver and Base Metal Deposits, Canadian Mining and Metallurgy Bulletin 61: 860–867." (1968).
- White, P.J., and M.R. Broadley. "Calcium in Plants." Annals of botany 92, no. 4 (2003): 487-511.
- Williams-Jones, A.E., et al. "Gold in Solution." Elements 5, no. 5 (2009): 281-87.
- Wilson, J.T. "The Origin of Continents and Precambrian History." Royal Society of Canada Transactions 43 (1949): 157-84.
- Wold, S., et al. "Principal Component Analysis." Chemometrics and intelligent laboratory systems 2, no. 1-3 (1987): 37-52.
- Wolfe, S.A., and P.D. Morse. "Lithalsa Formation and Holocene Lake-Level Recession, Great Slave Lowland, Northwest Territories." Permafrost and Periglacial Processes 28, no. 3 (2017): 573-79.
- Xie, S., et al. Geochemical Multifractal Distribution Patterns in Sediments from Ordered Streams." Geoderma 160, no. 1 (2010): 36-46.
- Xu, H., et al. "Discovering Hidden Spatial Patterns and Their Associations with Controlling Factors for Potentially Toxic Elements in Topsoil Using Hot Spot Analysis and K-Means Clustering Analysis." Environment International 151 (2021): 106456.
- Xue, I.C. et al. "No Mass-Independent Sulfur Isotope Fractionation in Auriferous Fluids Supports a Magmatic Origin for Archean Gold Deposits." Geology 41, no. 7 (2013): 791-94.

Yamana Gold Provides Update on Its Generative Exploration Program and on Plans to Unlock Value from Advanced and Advancing Exploration Projects in the Program and Lay the Foundation for Its Next Generation of Mines in This Decade (News Release)." (2020).

Yasrebi, A.B., et al. "Application of an Inverse Distance Weighted Anisotropic Method (Idwam) to Estimate Elemental Distribution in Eastern Kahang Cu-Mo Porphyry Deposit, Central Iran." *International Journal of Mining and Mineral Engineering* 7, no. 4 (2016): 340-62.

Yruela, I. "Copper in Plants." *Brazilian Journal of Plant Physiology* 17, no. 1 (2005): 145-56.

Zhao, F.J. et al. "Arsenic Uptake and Metabolism in Plants." *New Phytologist* 181, no. 4 (2009): 777-94.

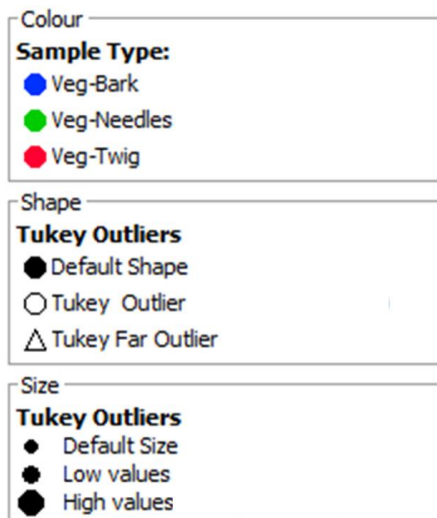
Zhou, D., et al. "Dual Extraction of R-Mode Andq-Mode Factor Solutions." *Journal of the International Association for Mathematical Geology* 15, no. 5 (1983): 581-606.

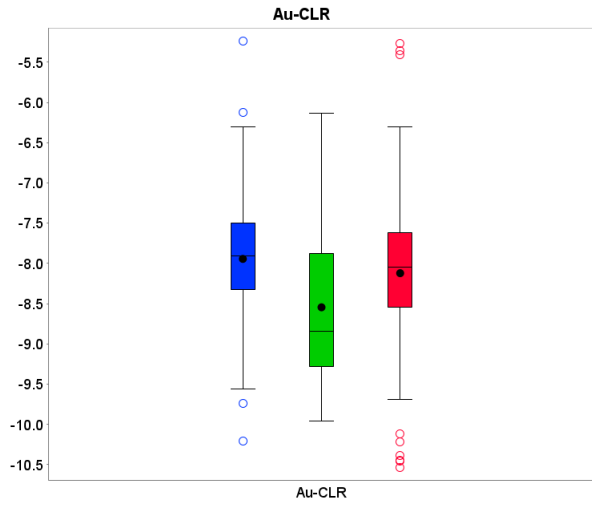
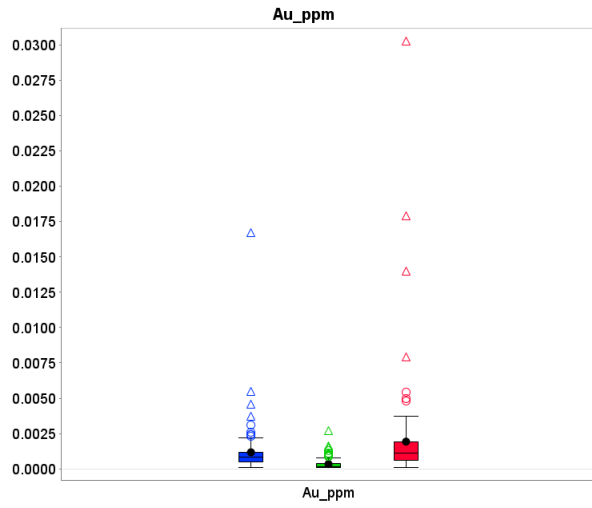
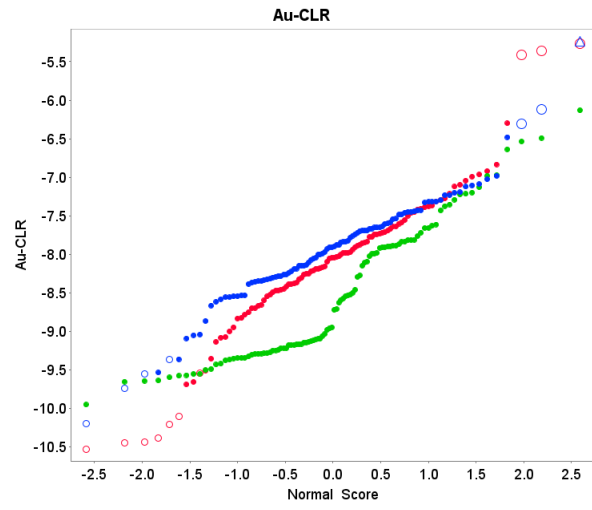
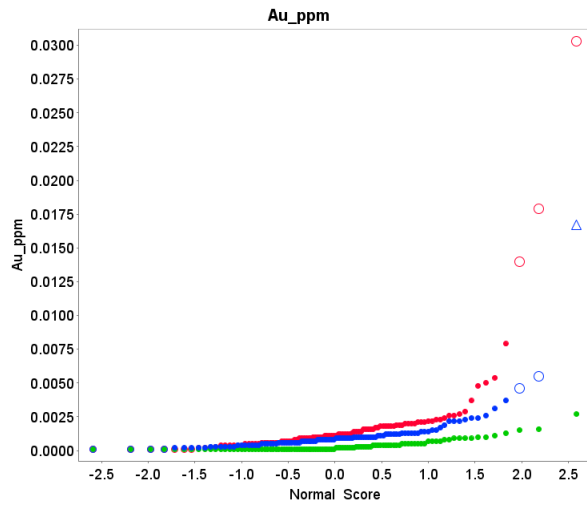
Zuo, R. "Decomposing of Mixed Pattern of Arsenic Using Fractal Model in Gangdese Belt, Tibet, China." *Applied geochemistry* 26 (2011): S271-S73.

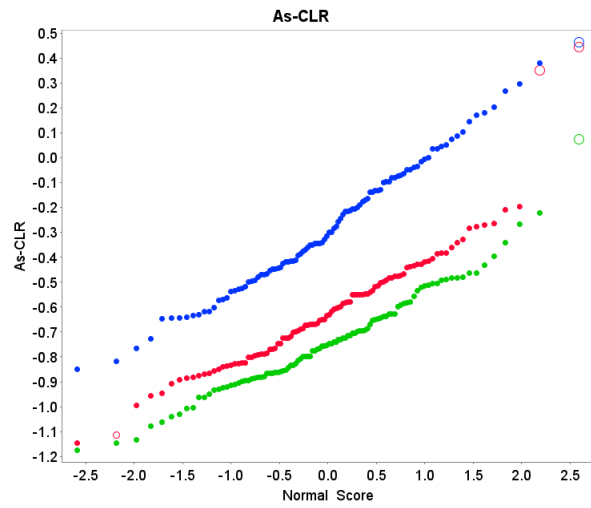
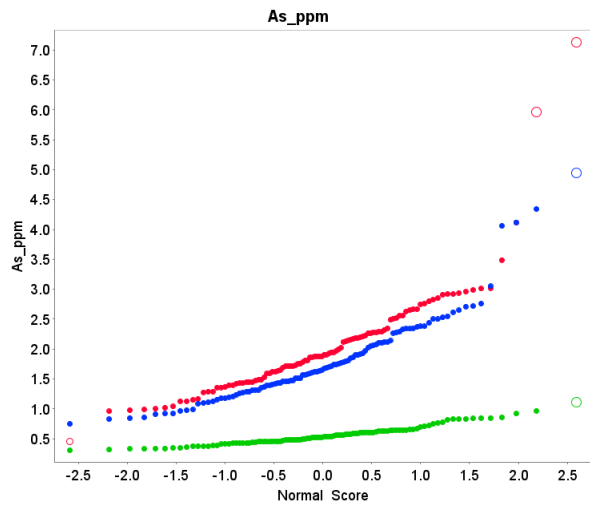
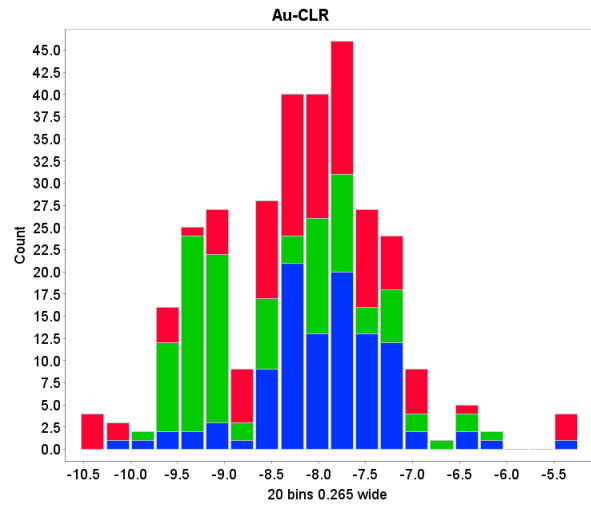
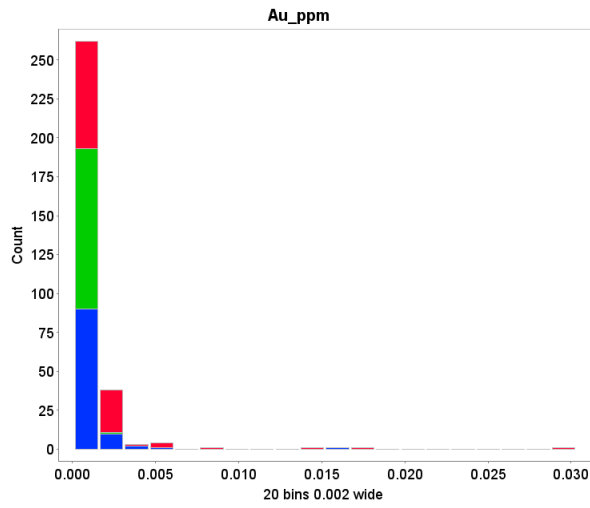
Zuo, R. "Machine Learning of Mineralization-Related Geochemical Anomalies: A Review of Potential Methods." *Natural Resources Research* 26, no. 4 (2017): 457-64.

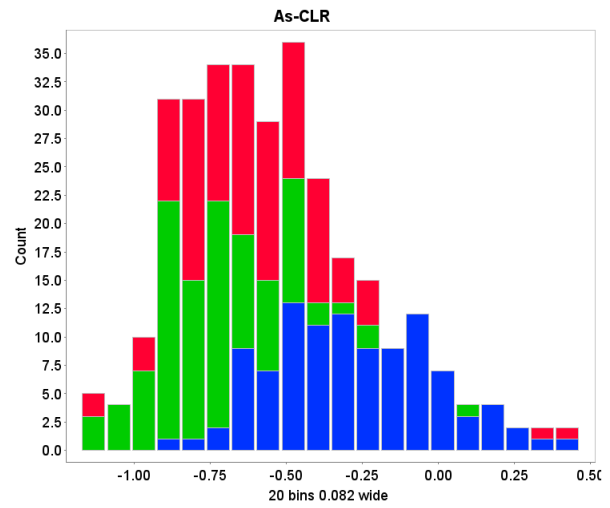
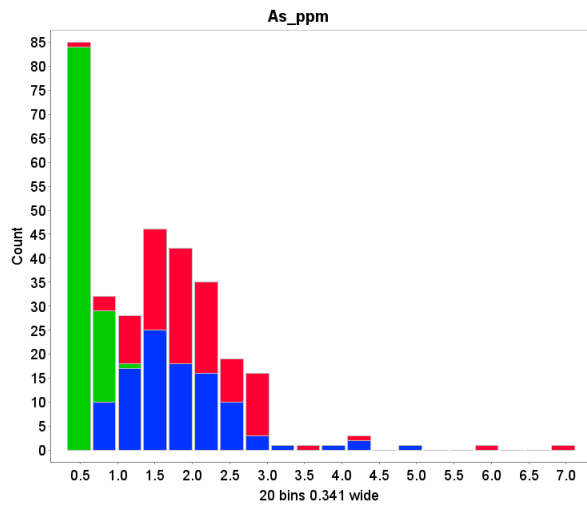
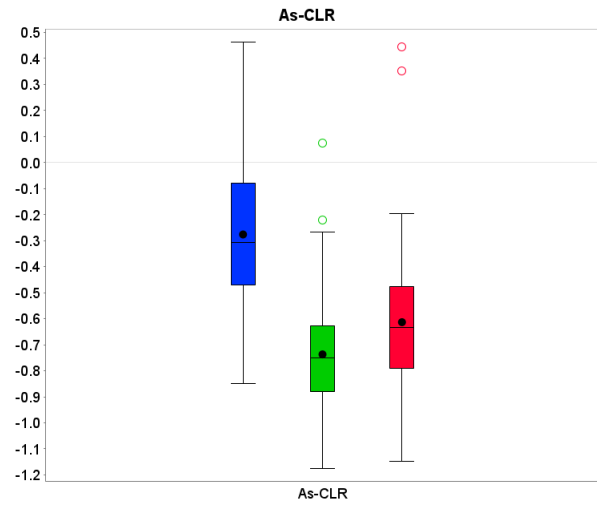
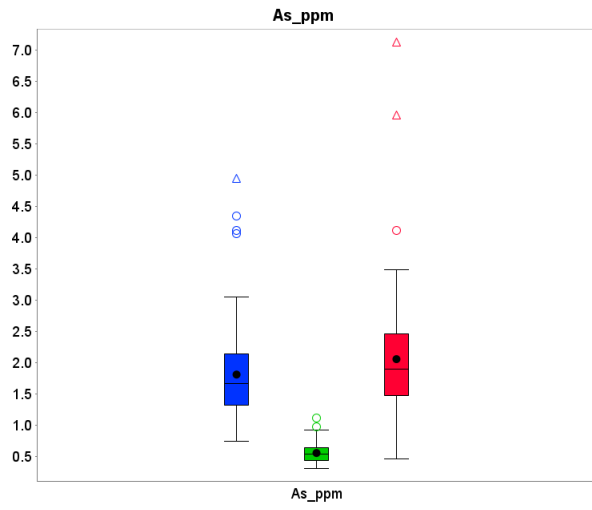
Appendix A

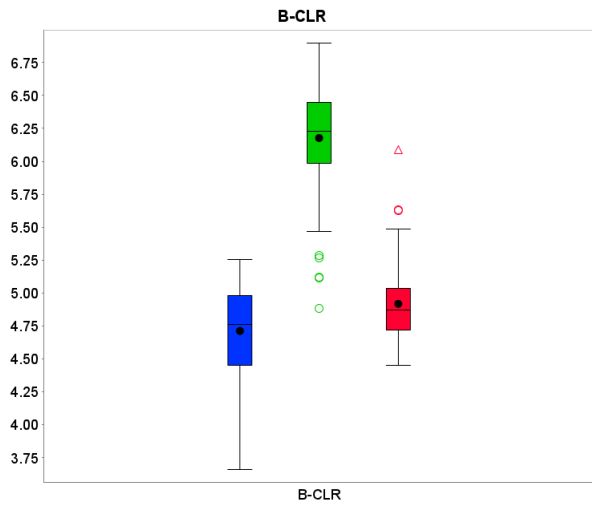
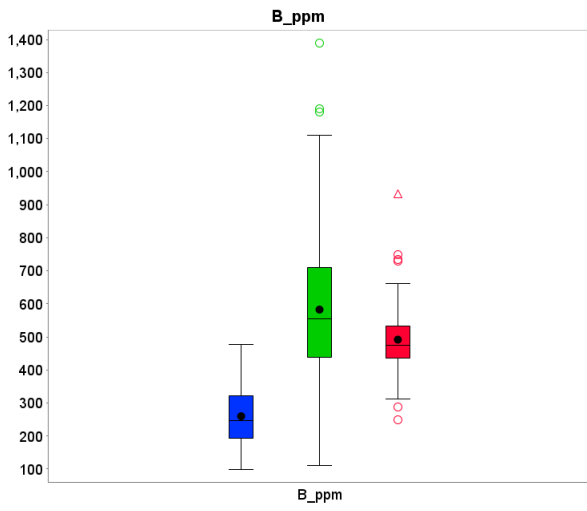
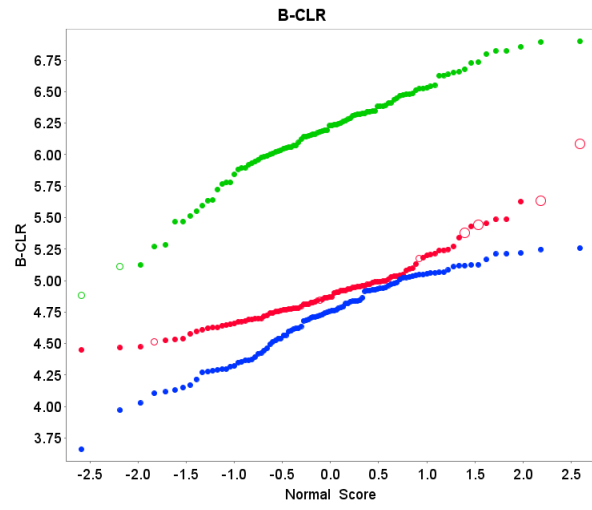
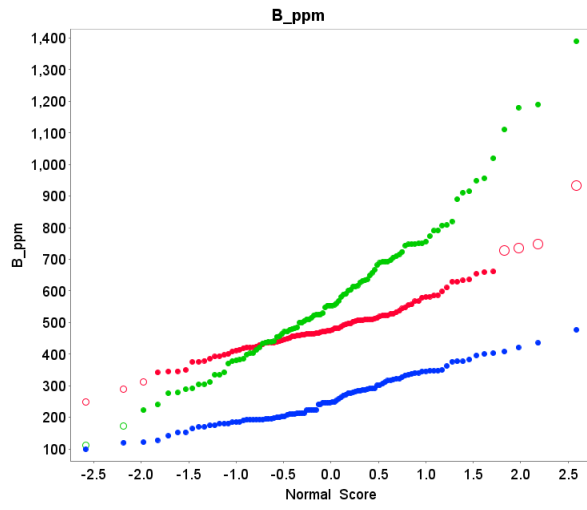
Appendix A compares the raw and transformed data of the Monument Bay Gold project (MBGP) using probability plots, scatter plots and histograms. The plots on the right demonstrate the raw data distribution for each element. On the left side, data distribution is normalized using center log-ratio (CLR) transformation. Tukey method was used to show the outliers (circles) and extreme or far outliers (triangles). The figure below shows the legend.

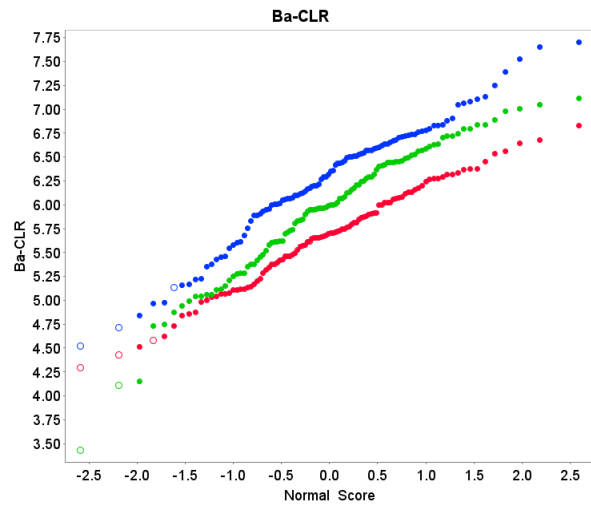
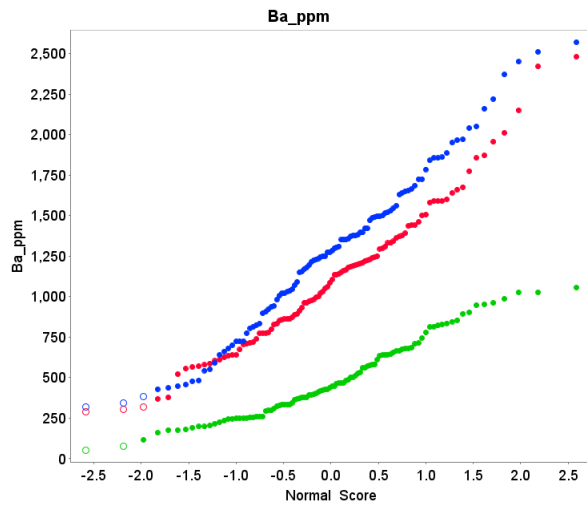
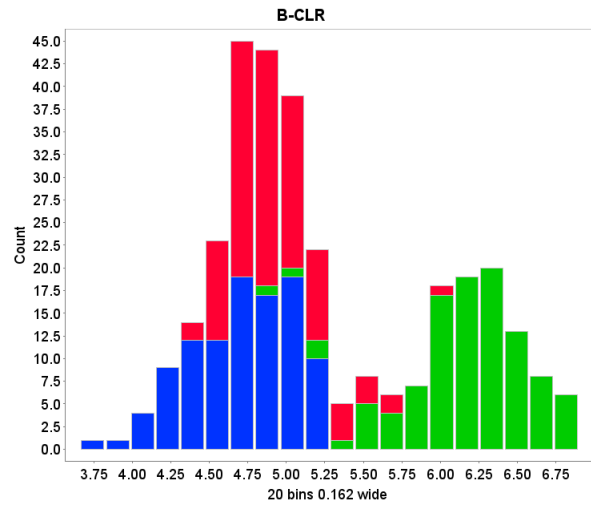
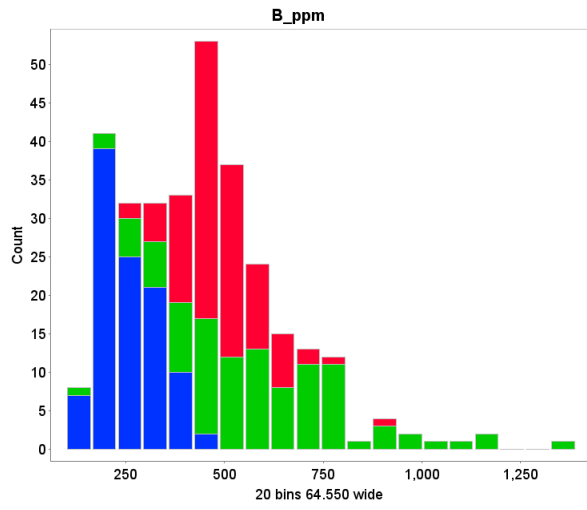


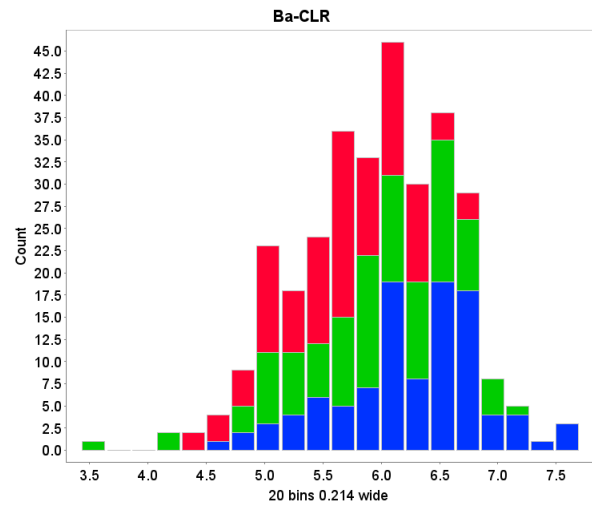
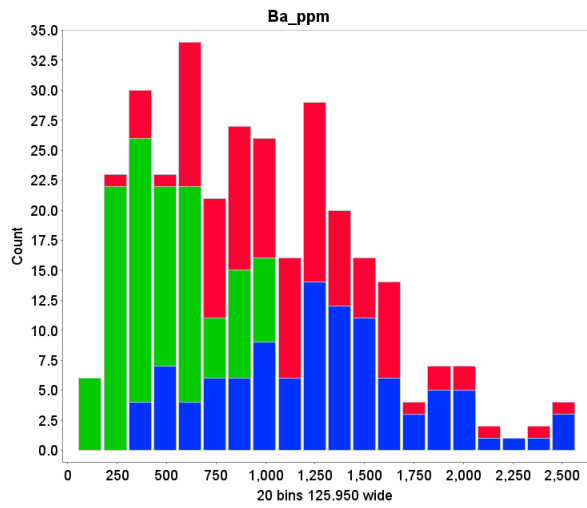
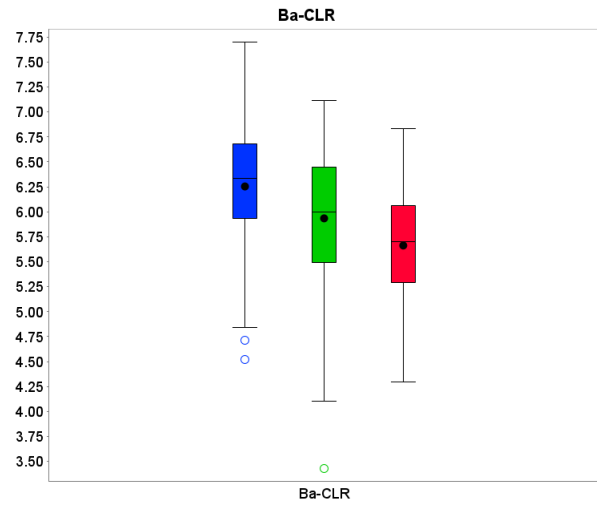
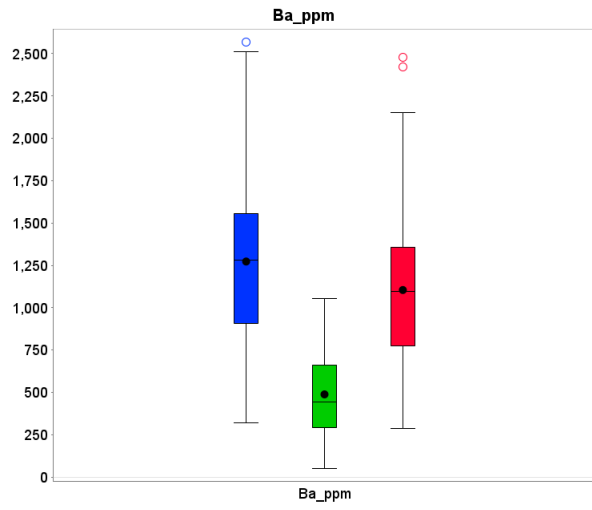


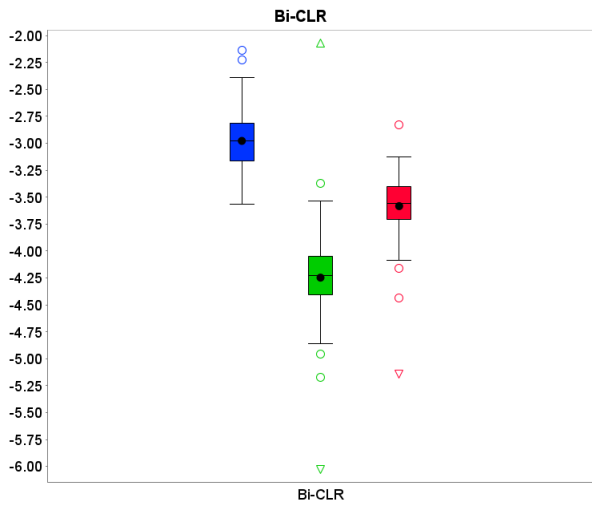
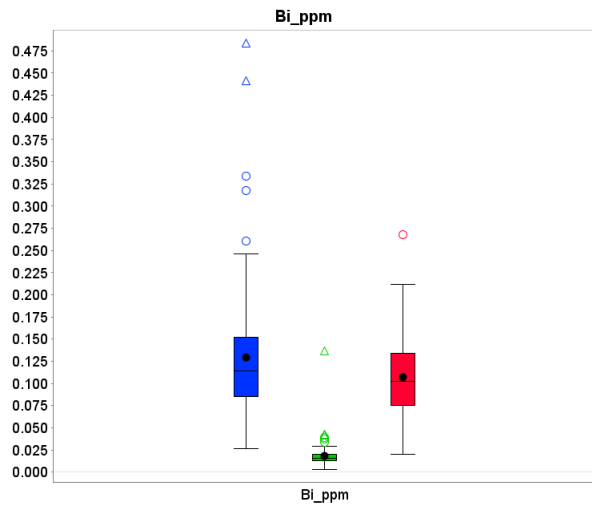
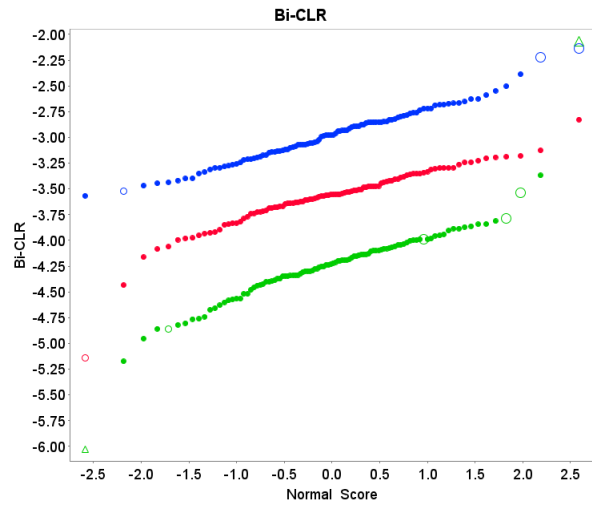
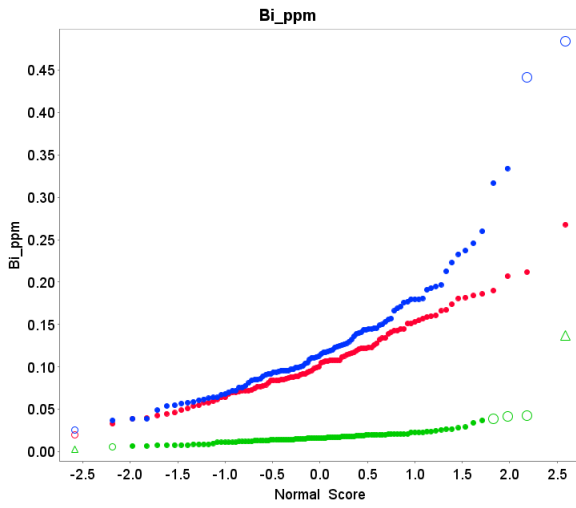


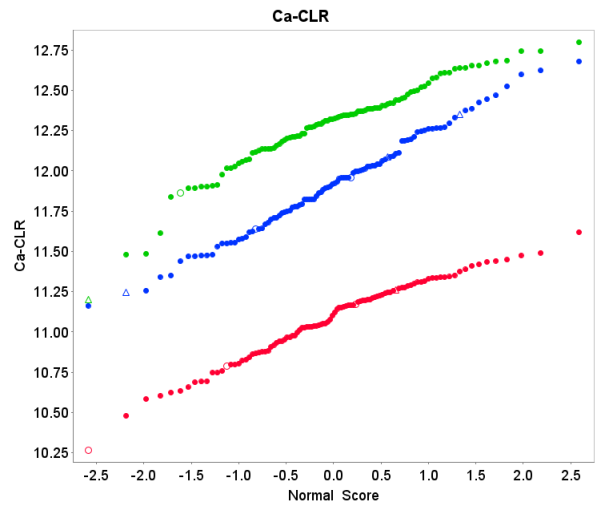
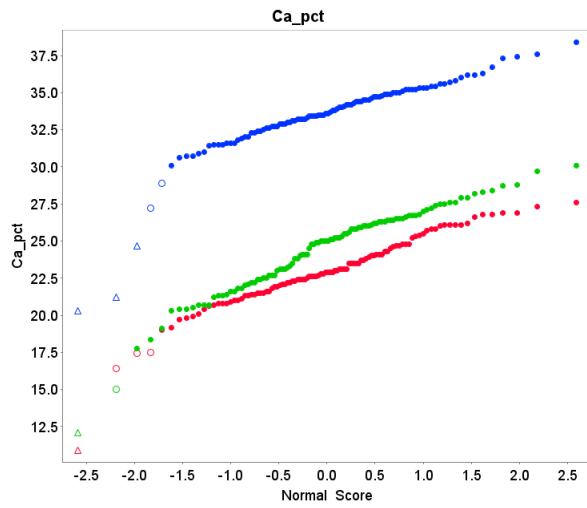
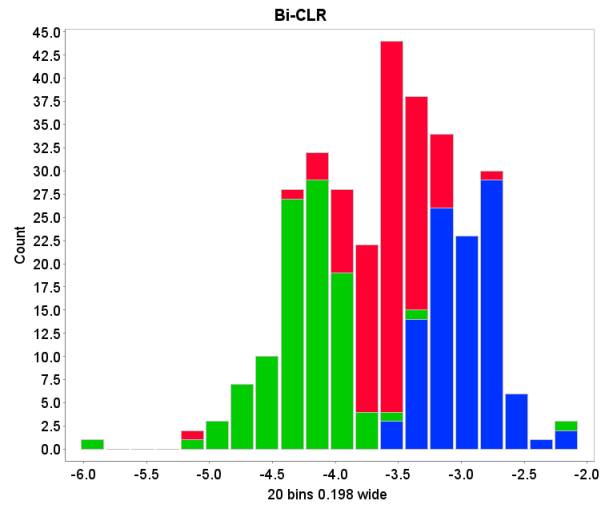
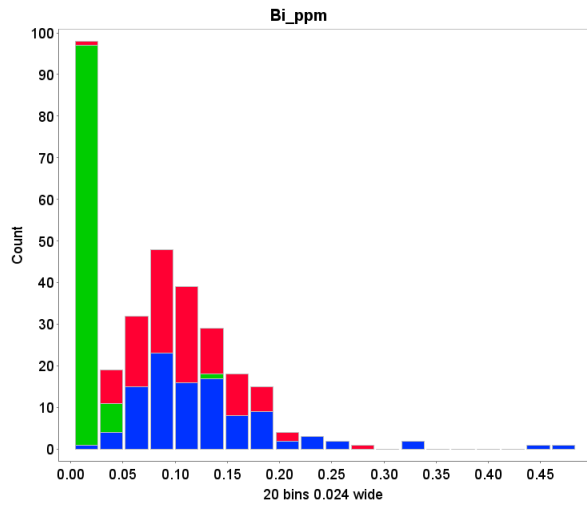


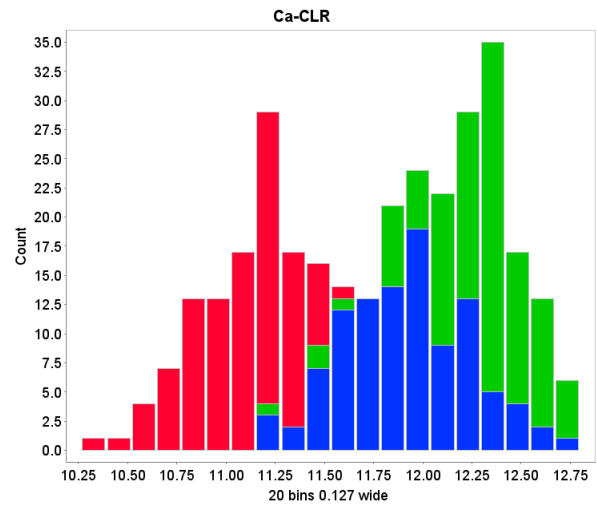
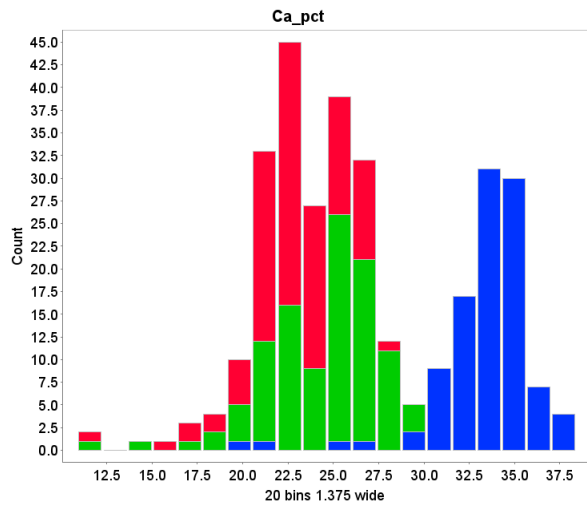
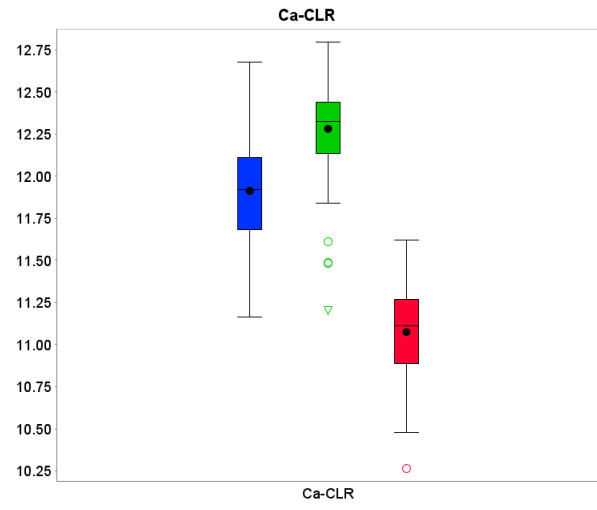
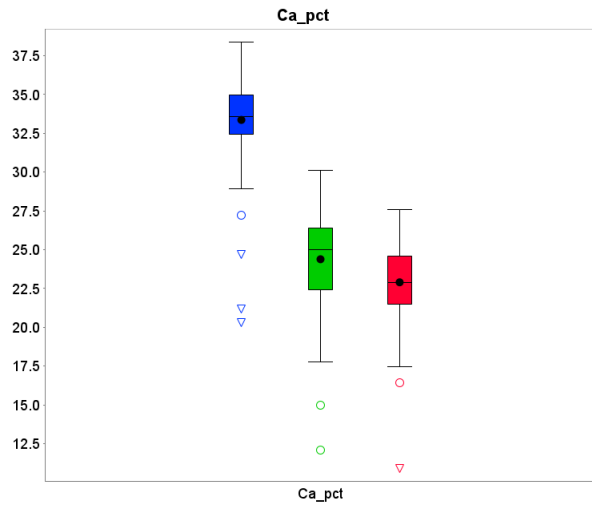


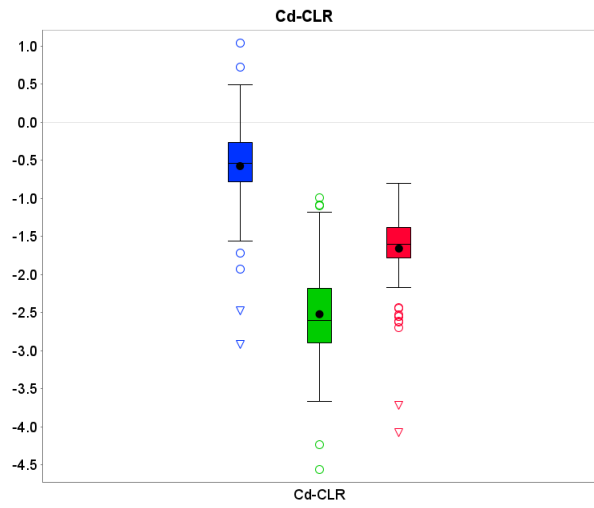
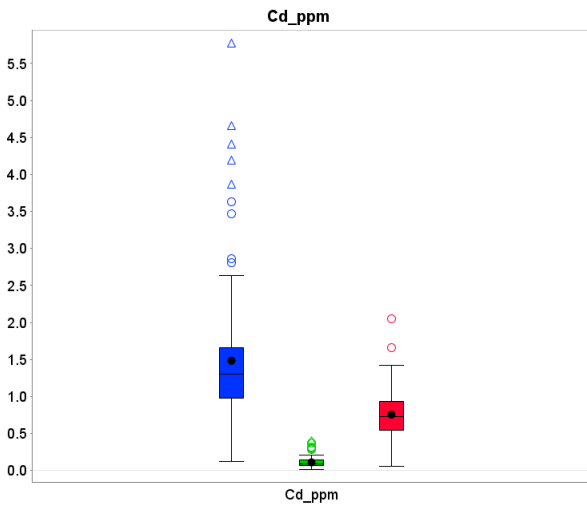
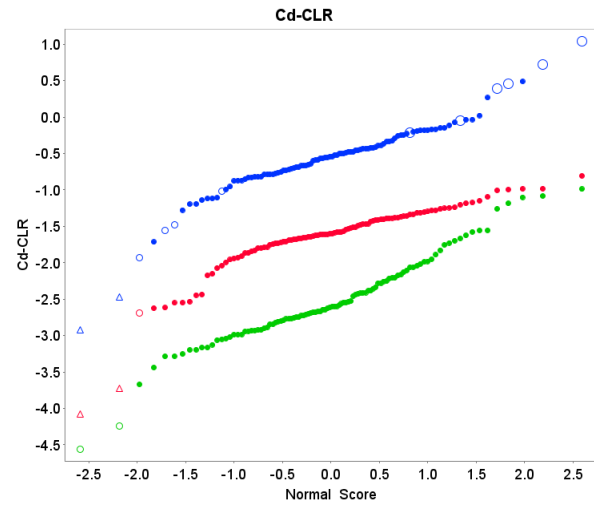
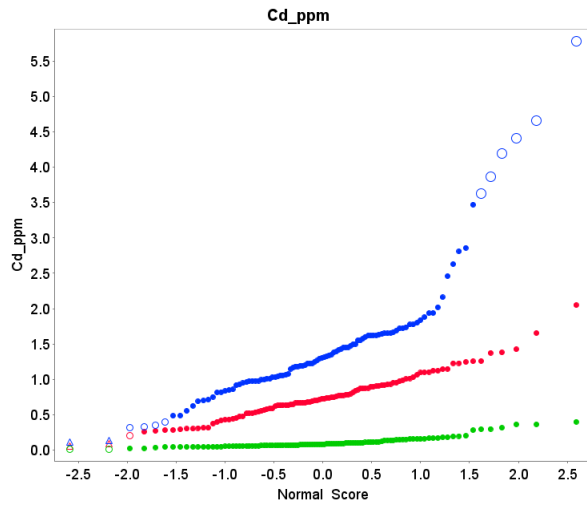


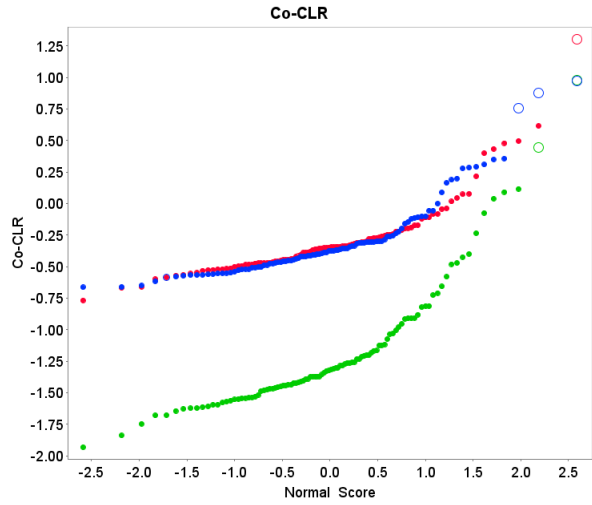
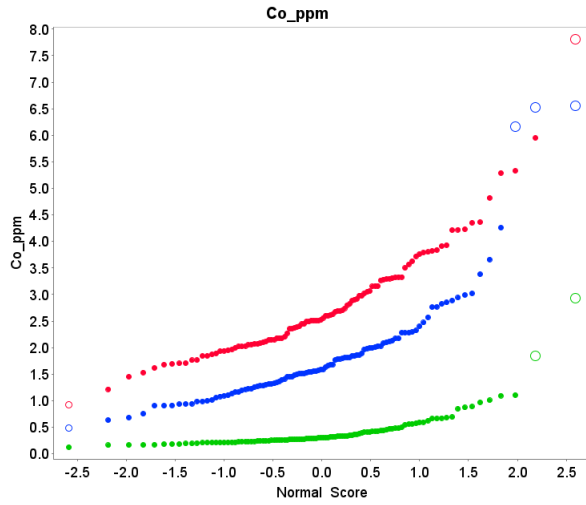
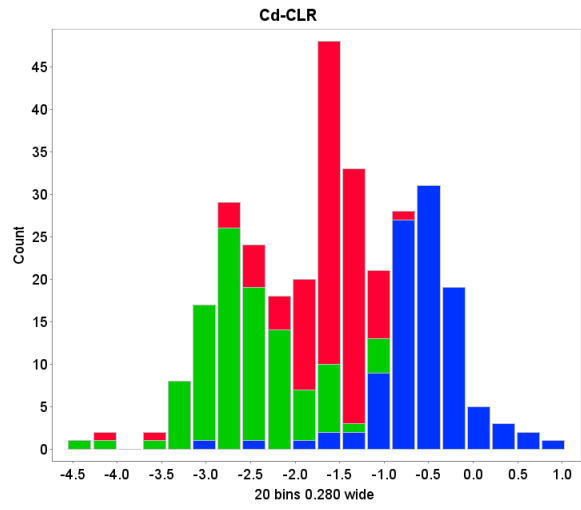
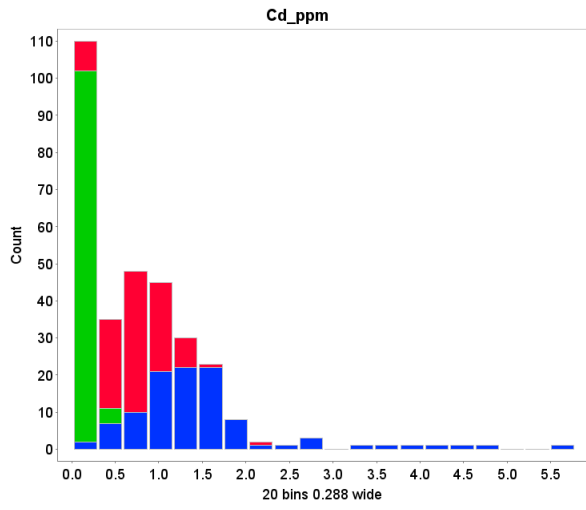


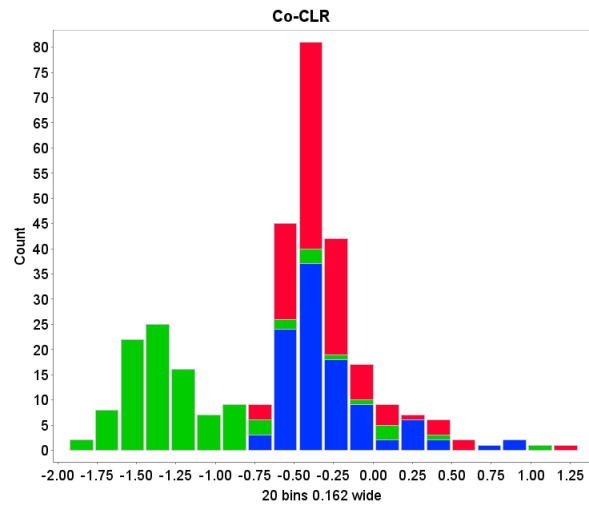
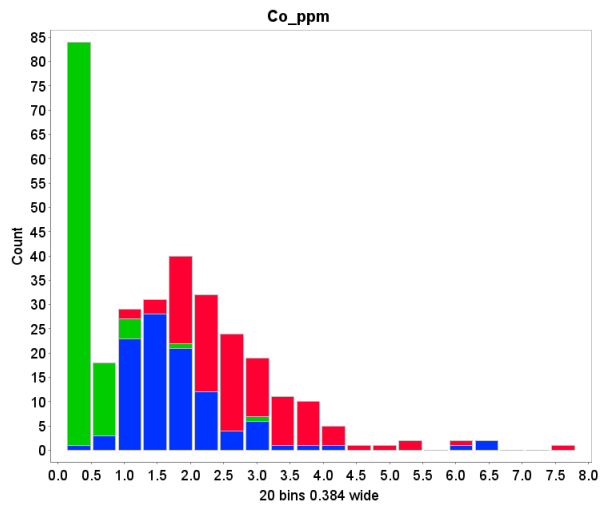
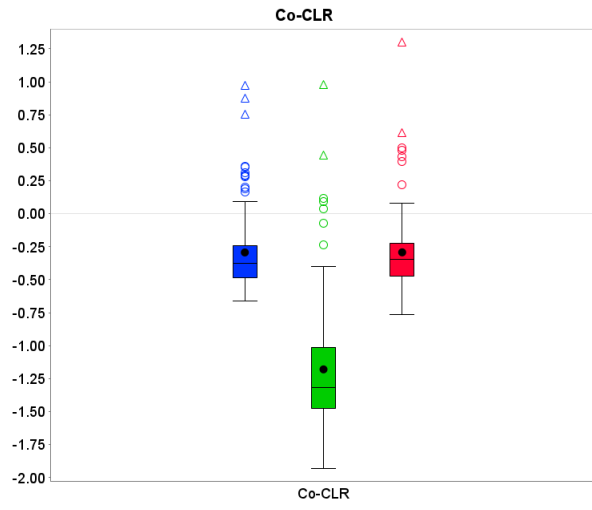
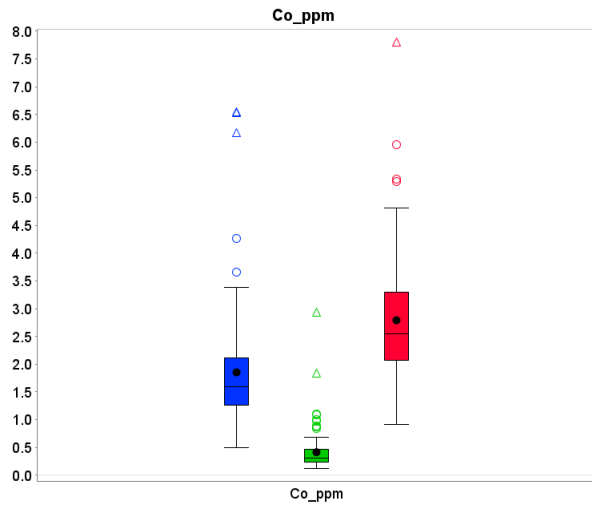


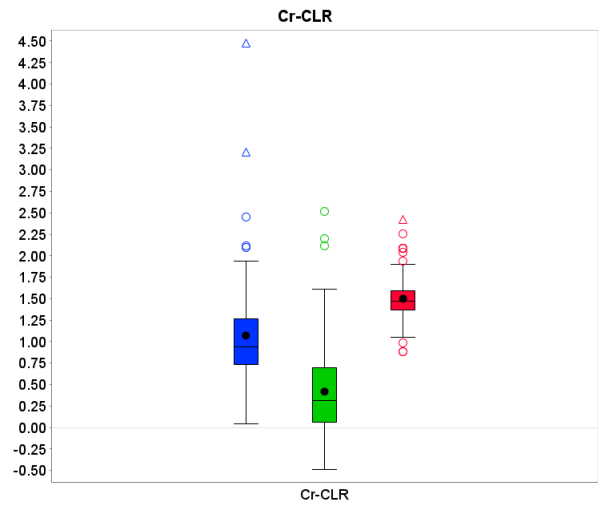
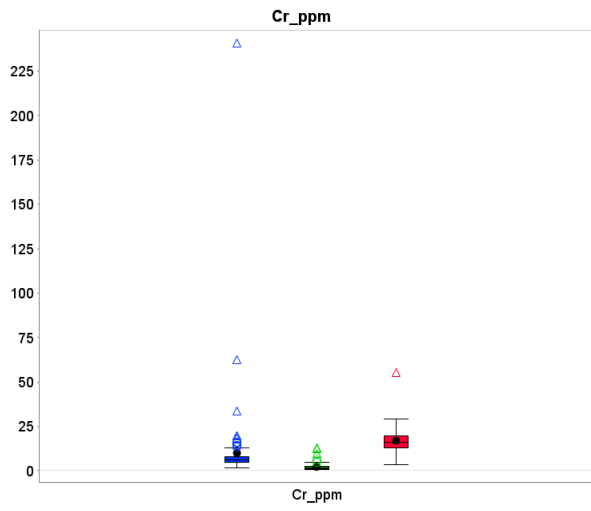
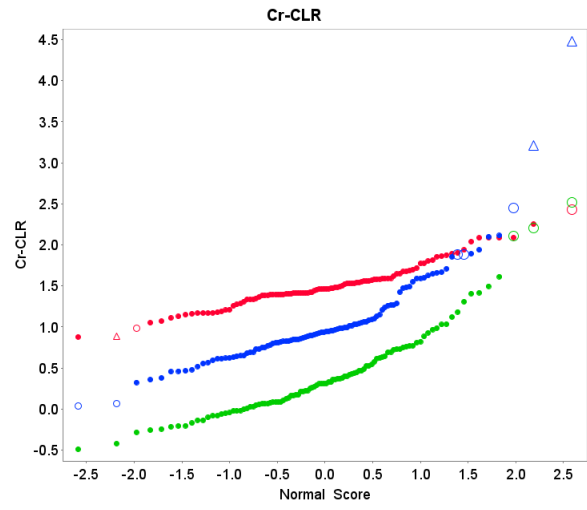
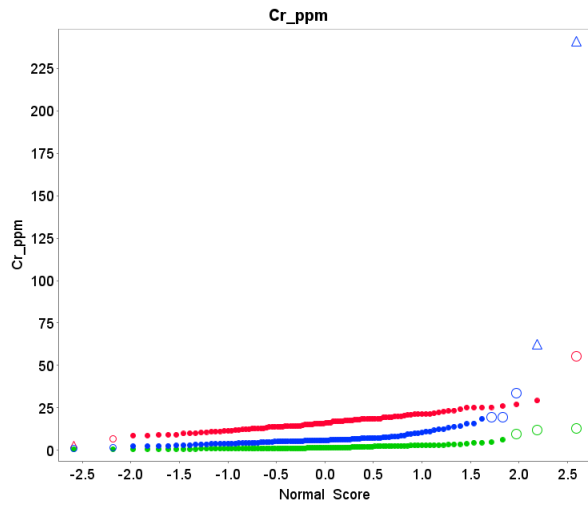


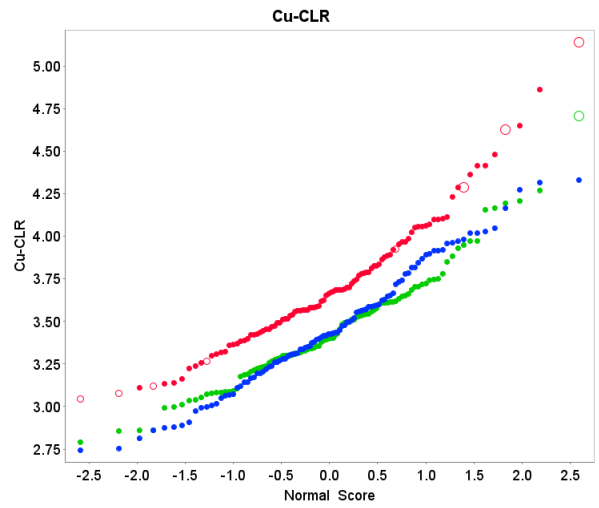
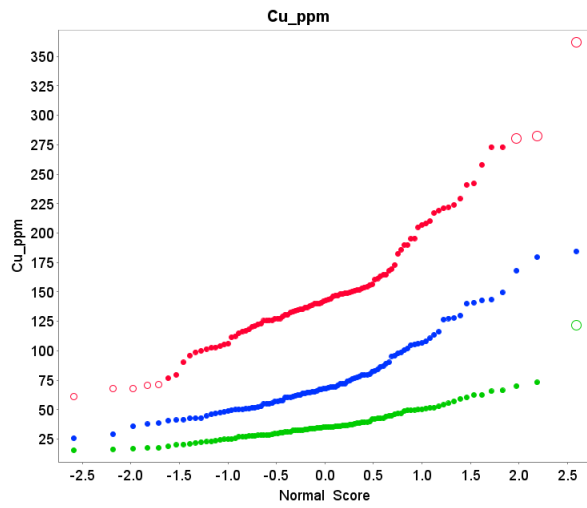
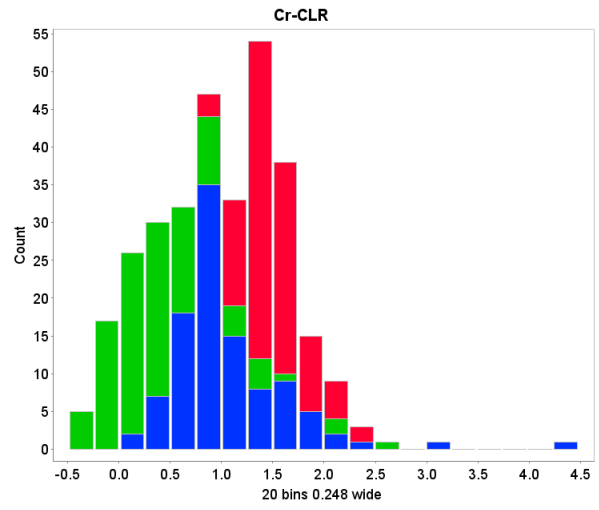
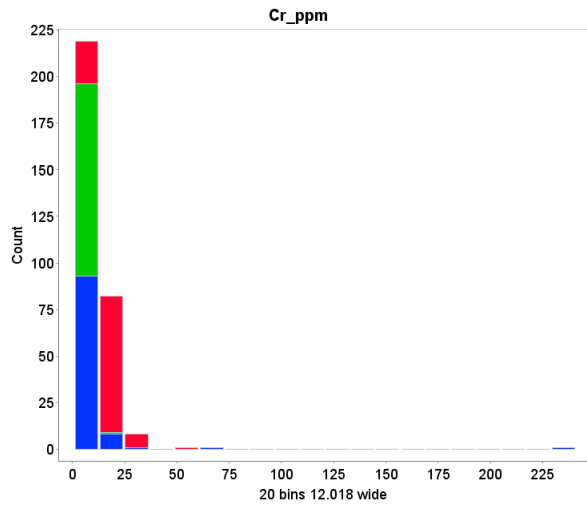


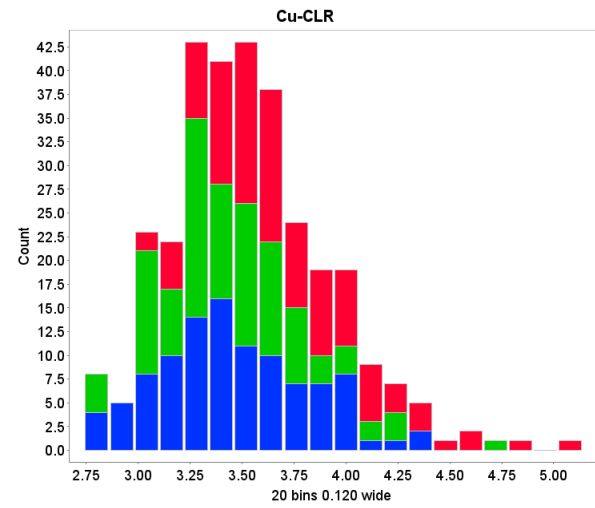
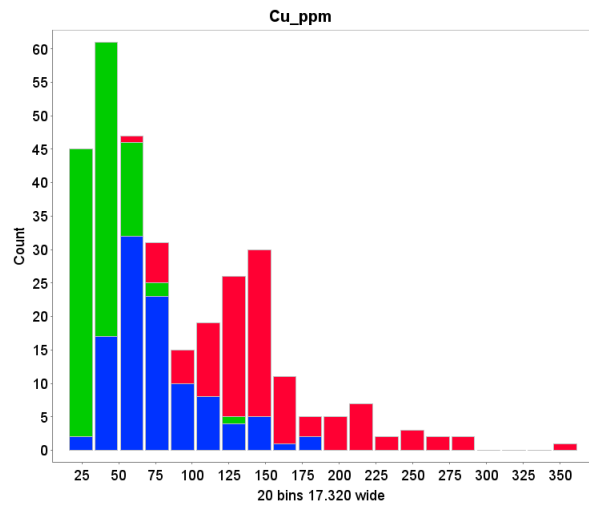
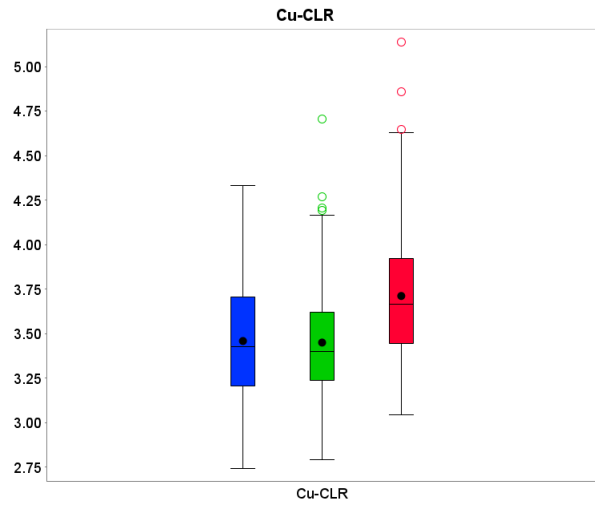
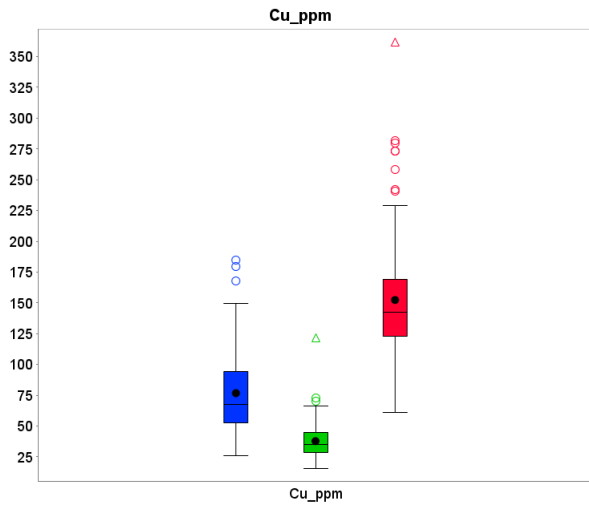


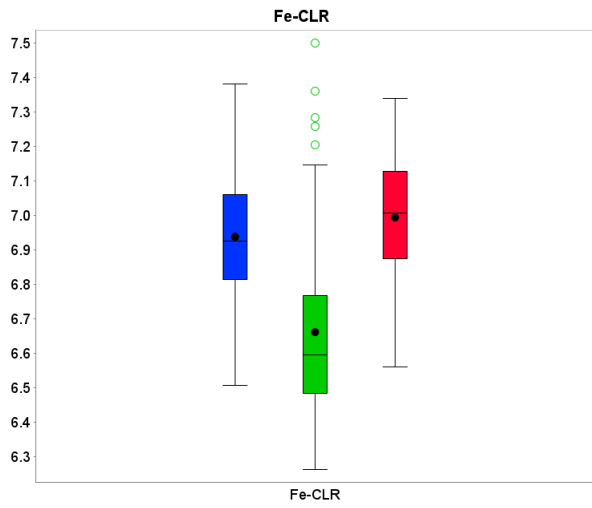
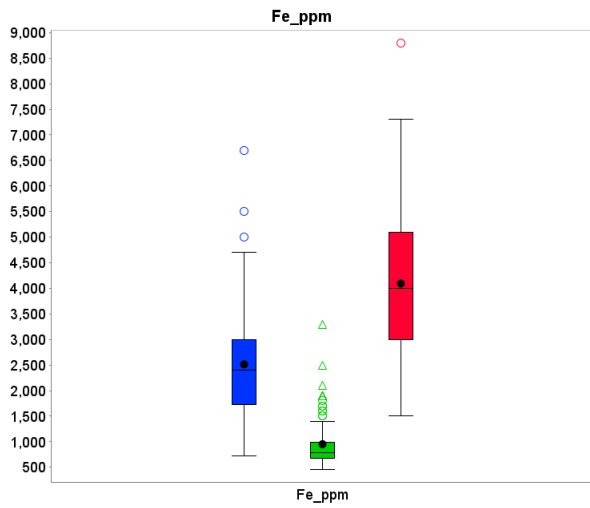
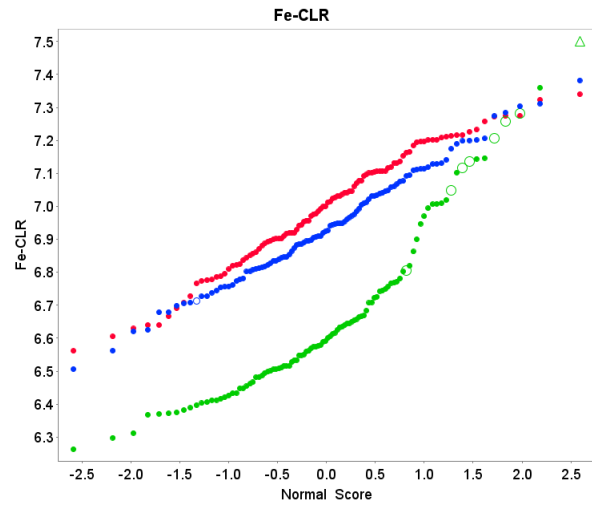
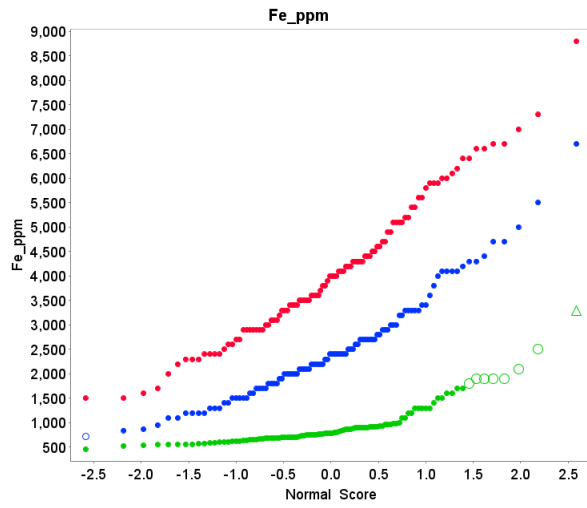


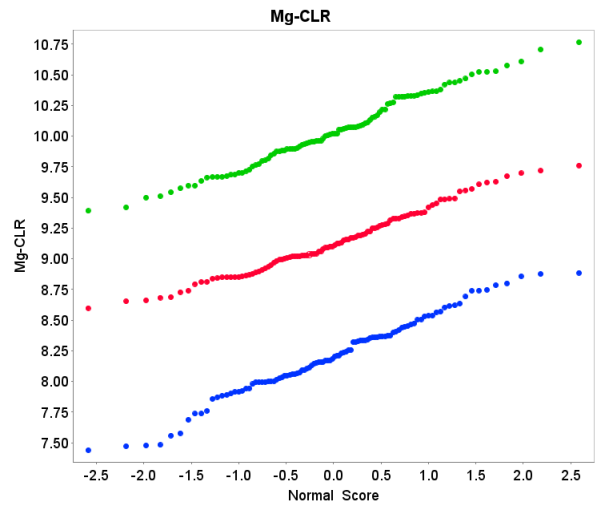
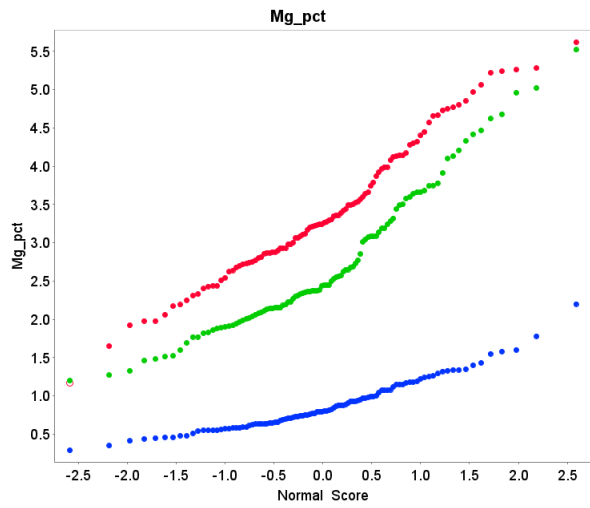
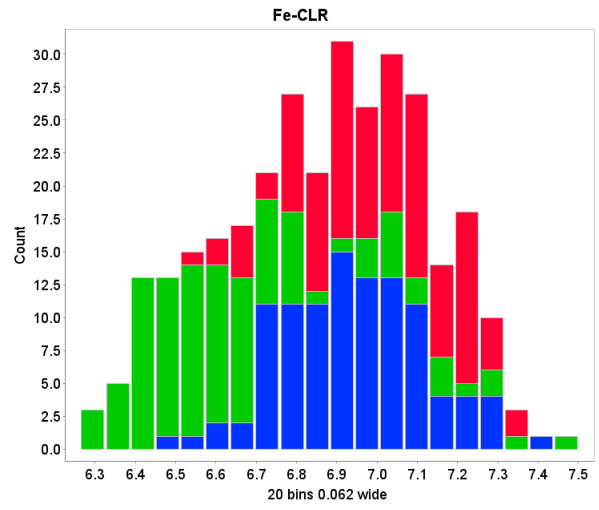
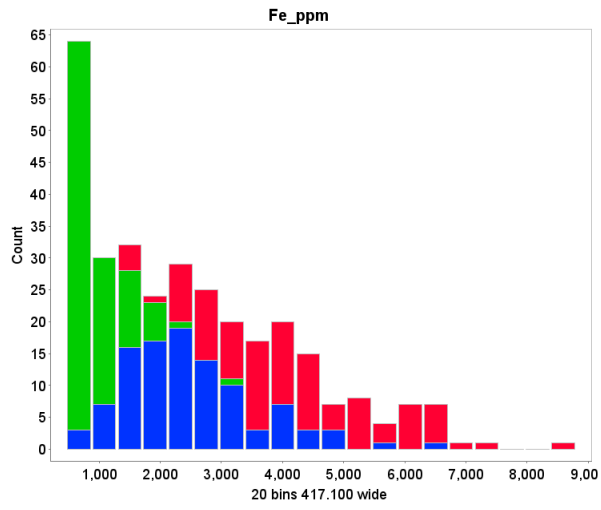


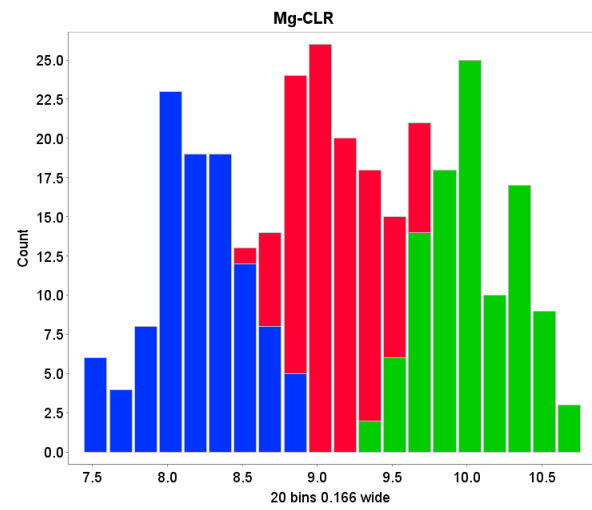
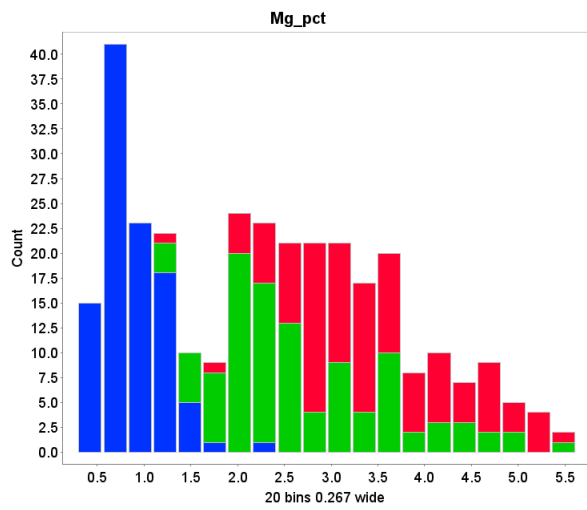
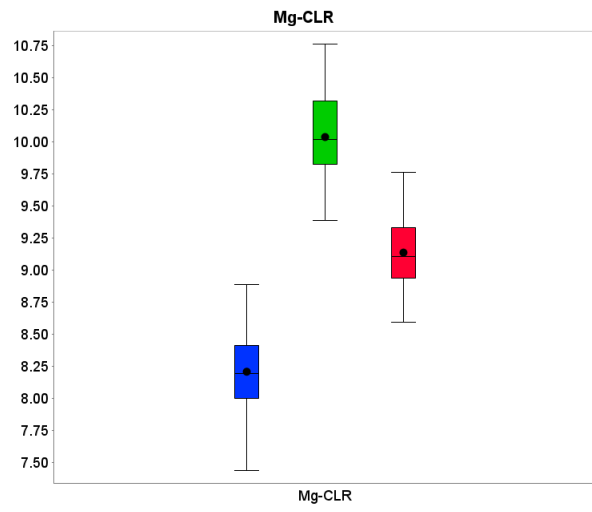
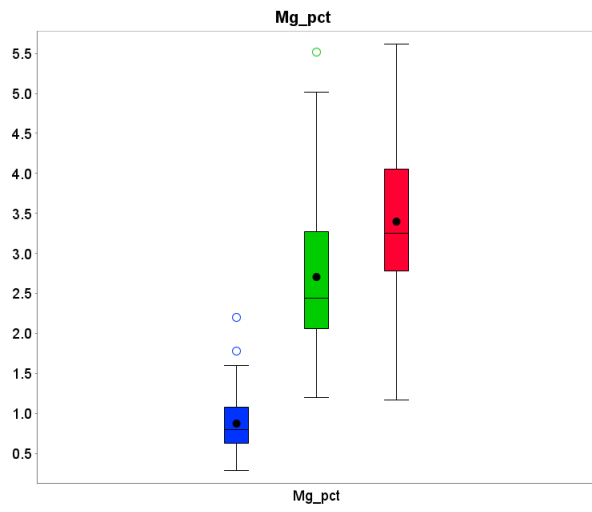


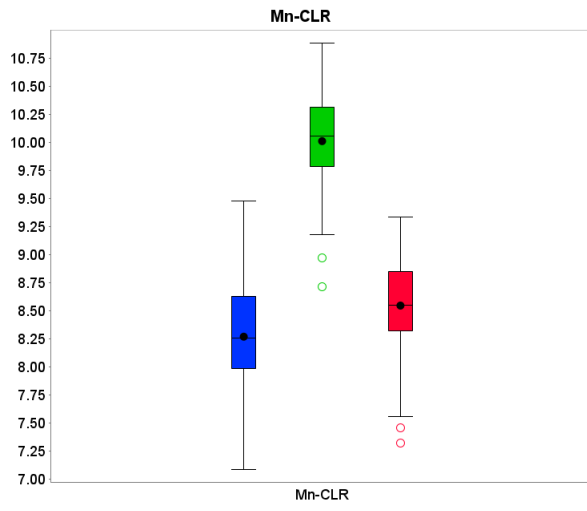
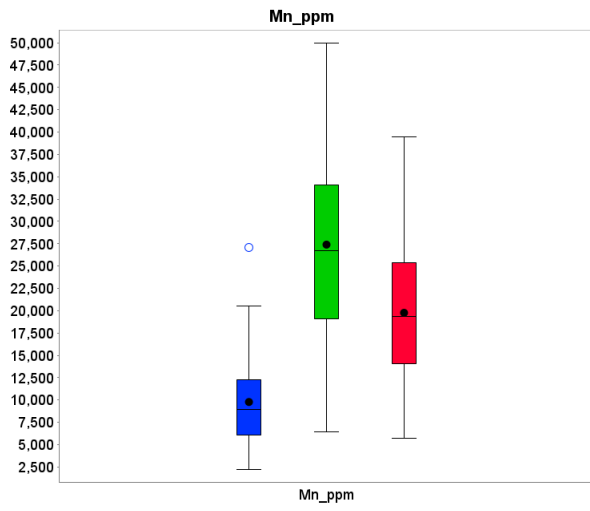
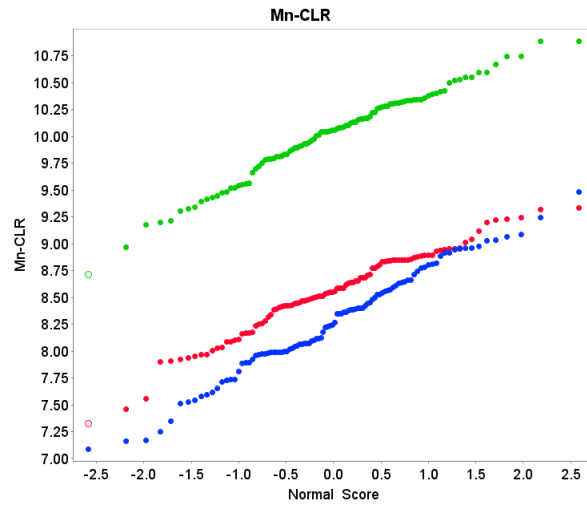
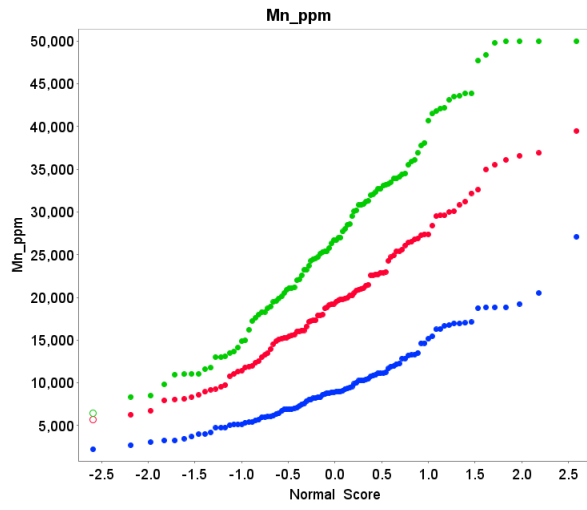


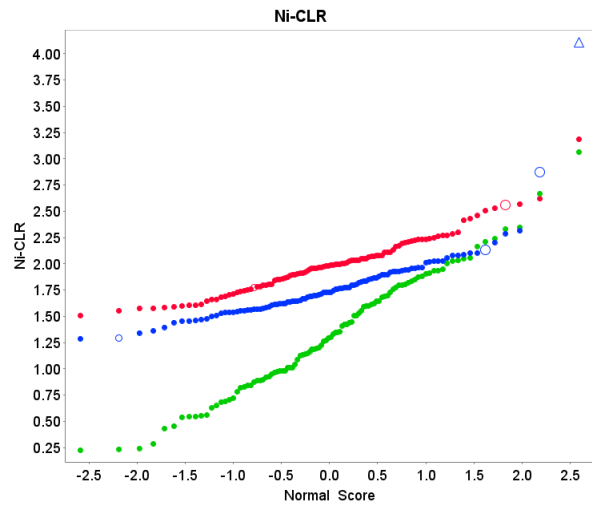
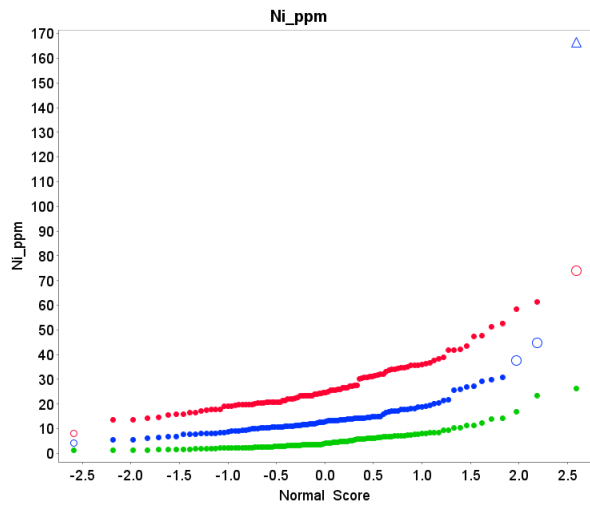
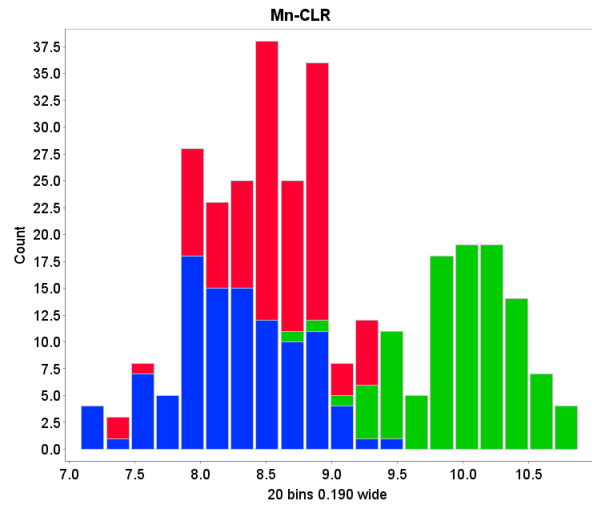
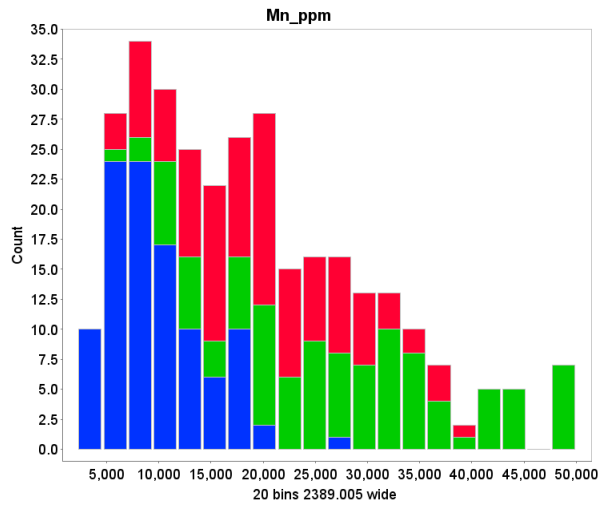


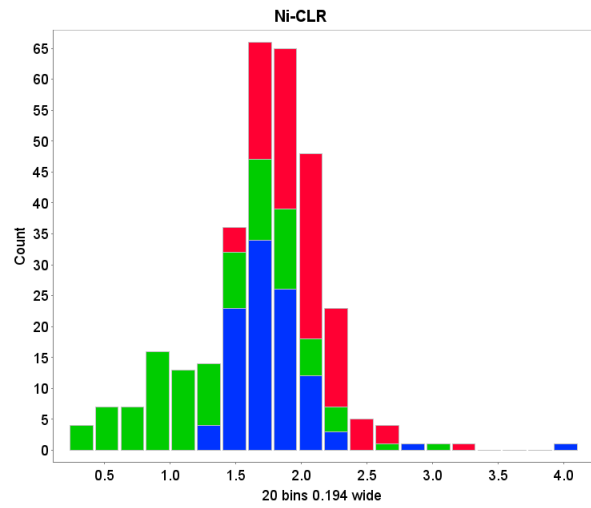
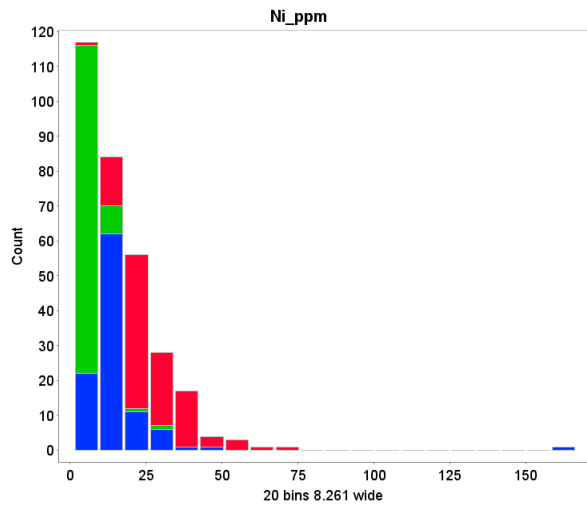
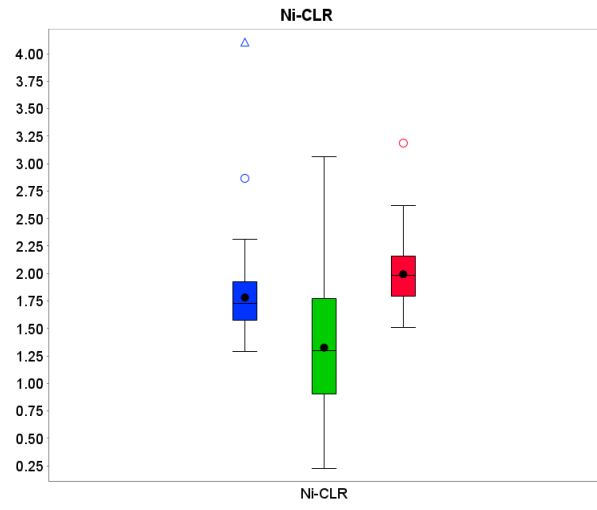
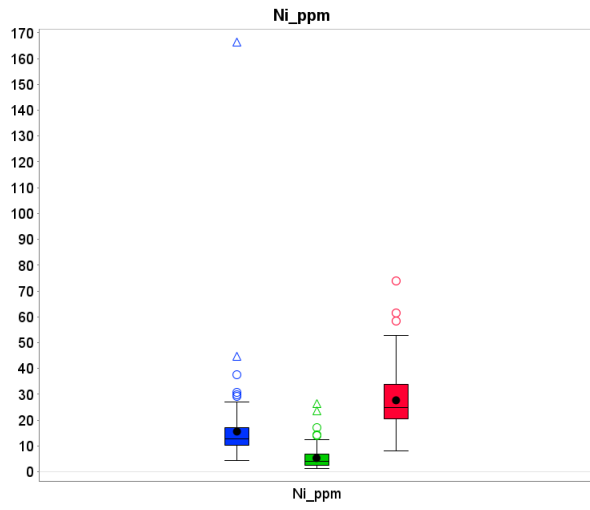


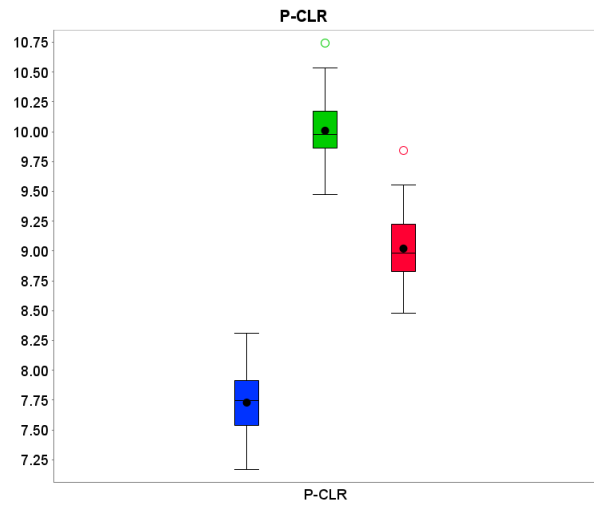
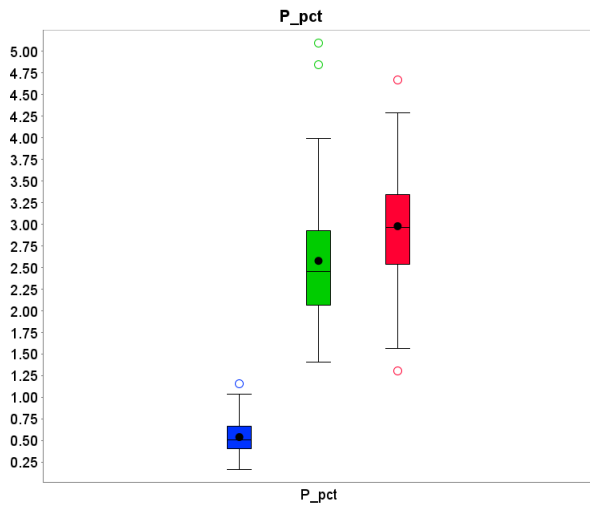
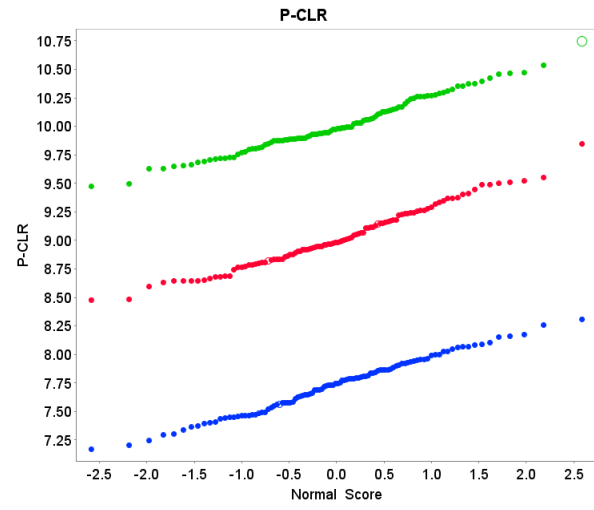
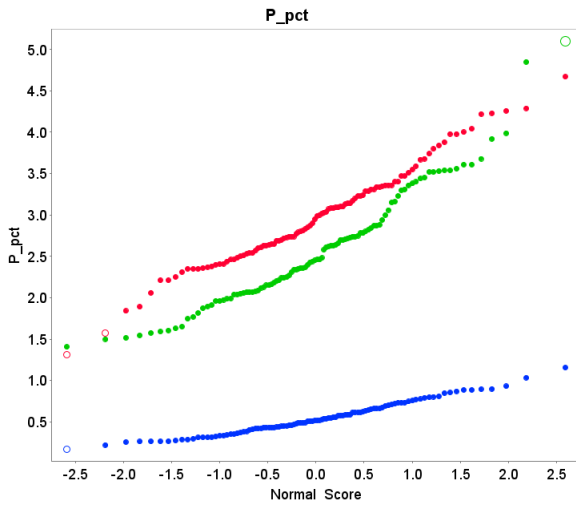


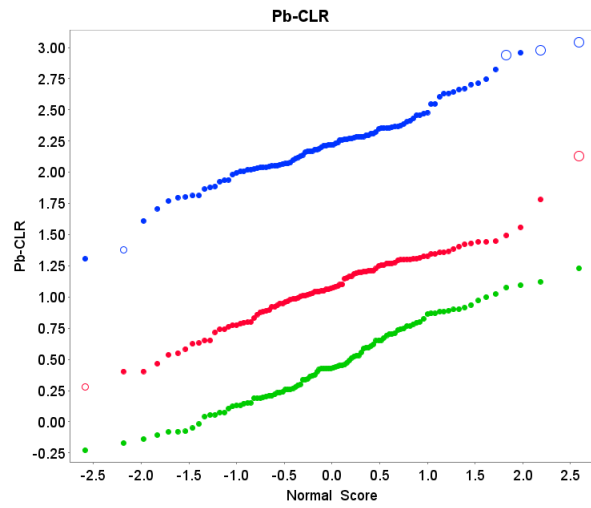
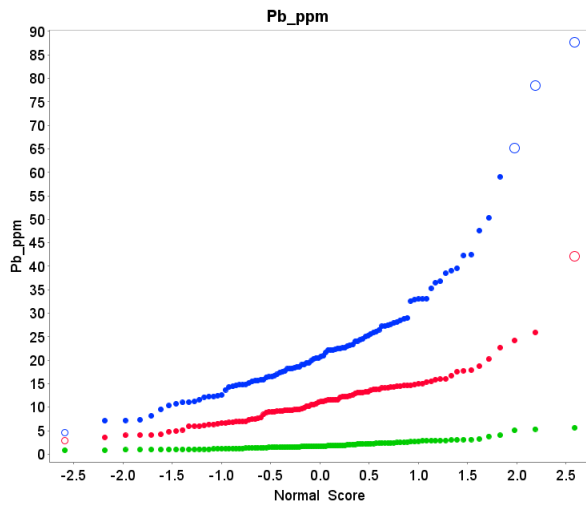
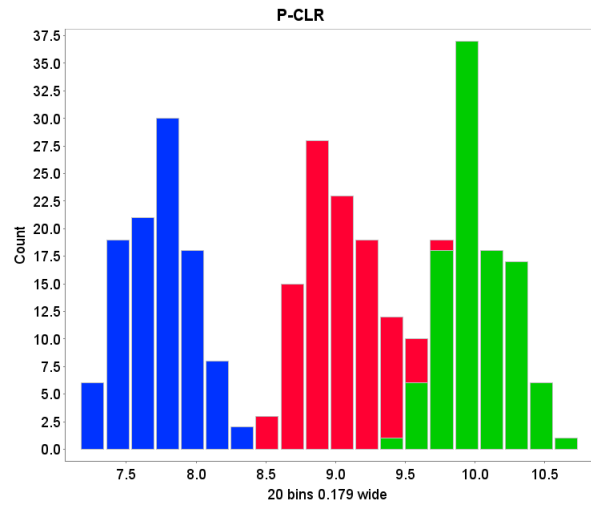
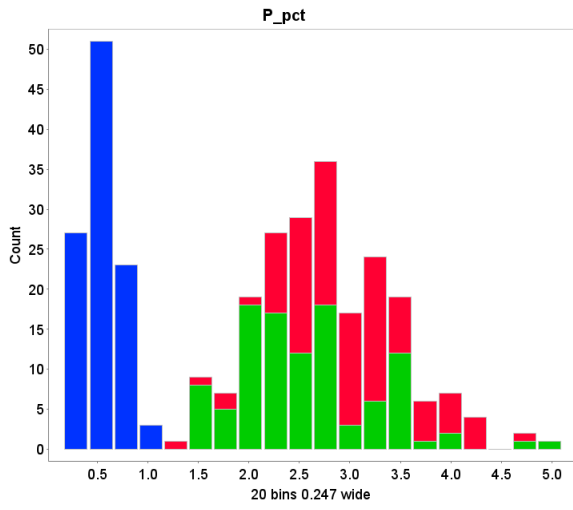


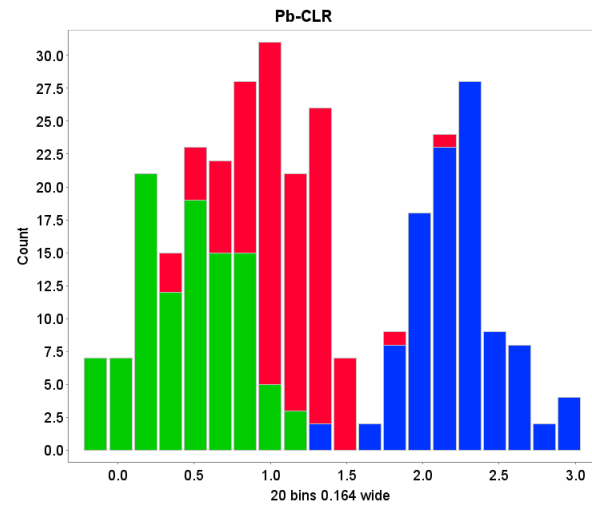
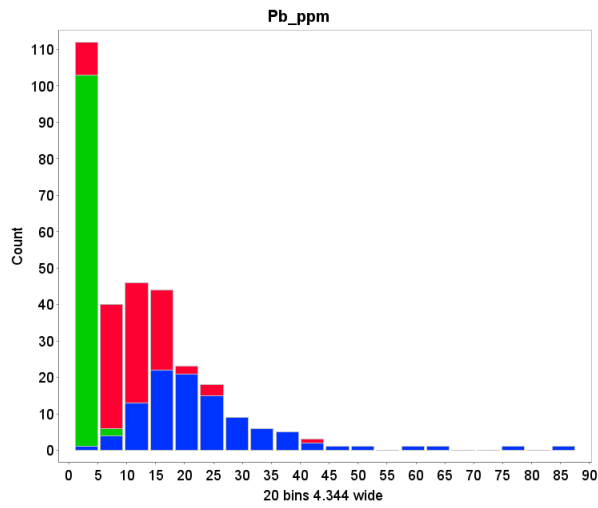
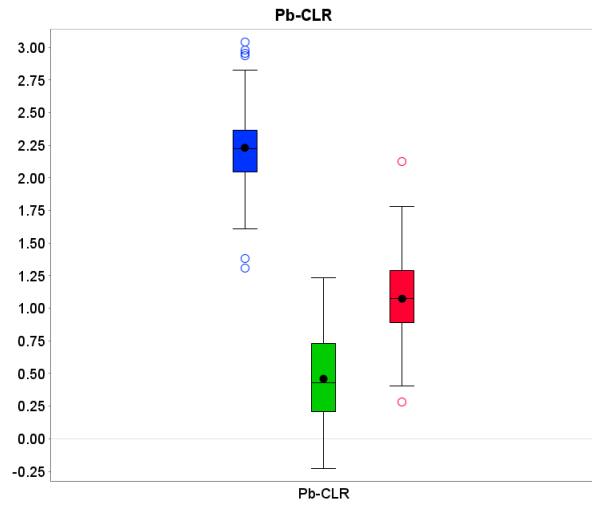
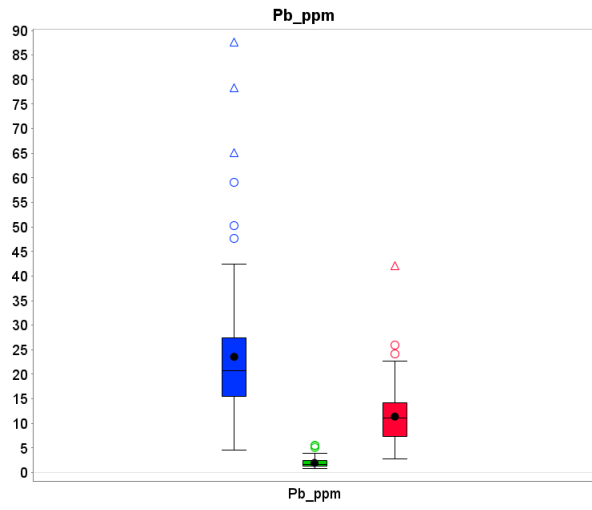


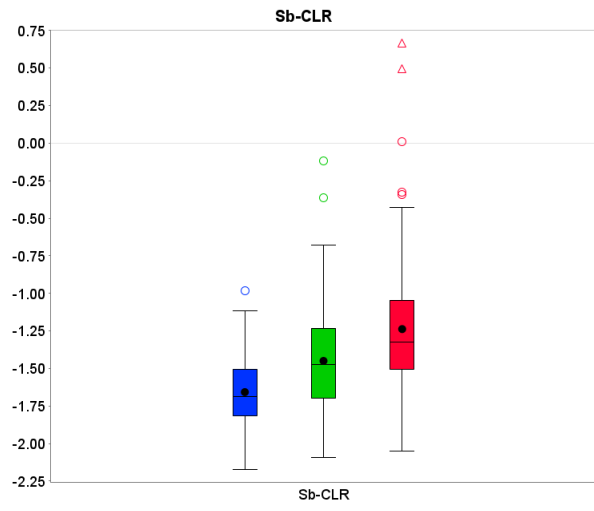
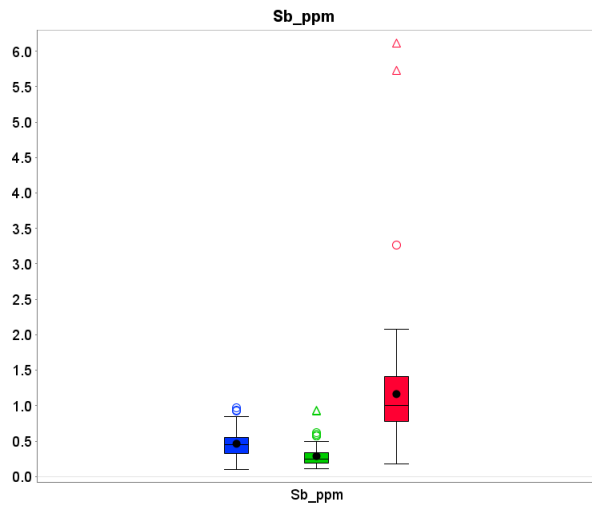
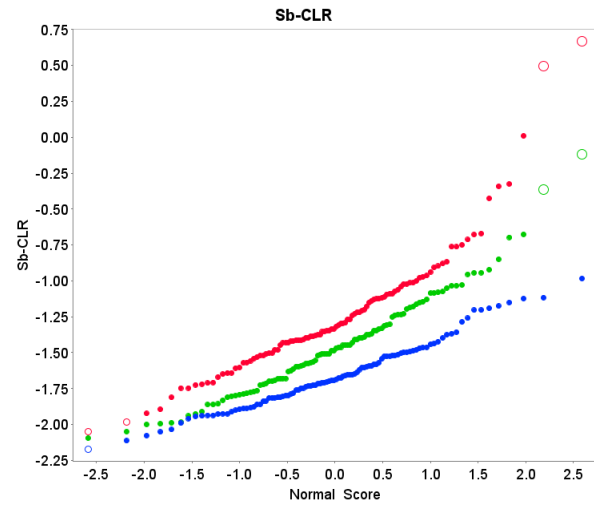
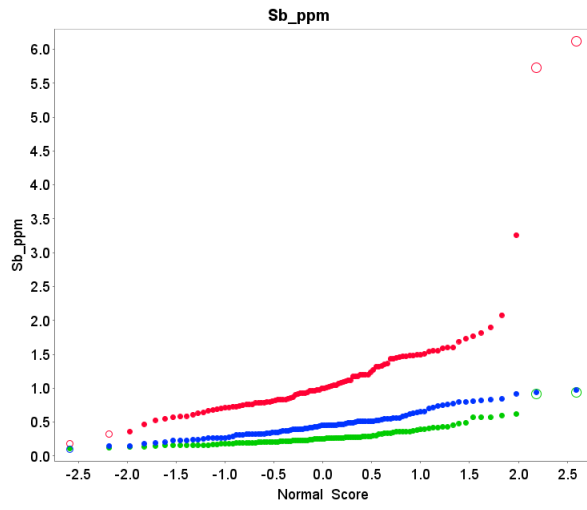


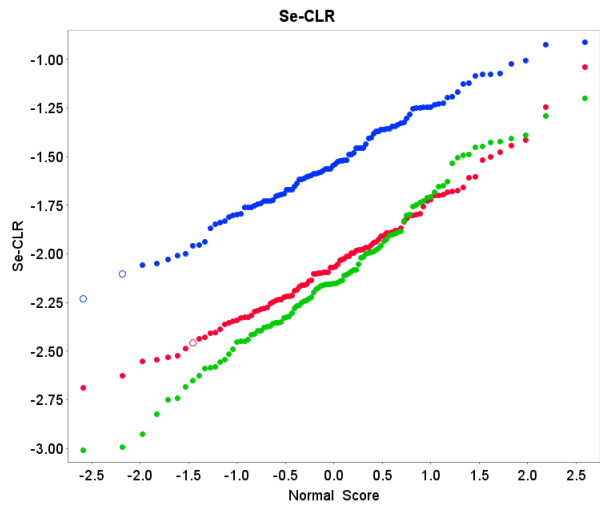
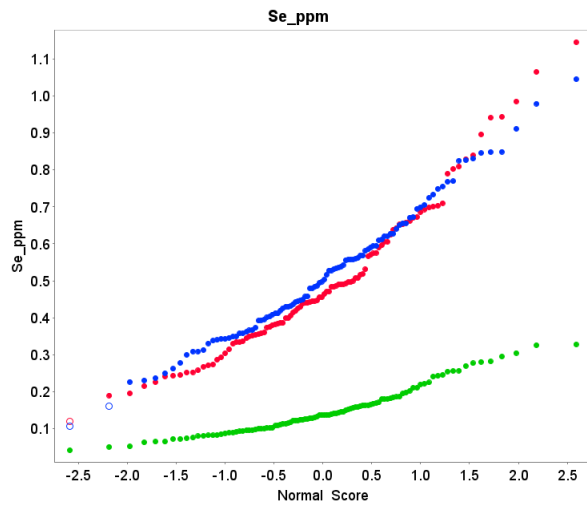
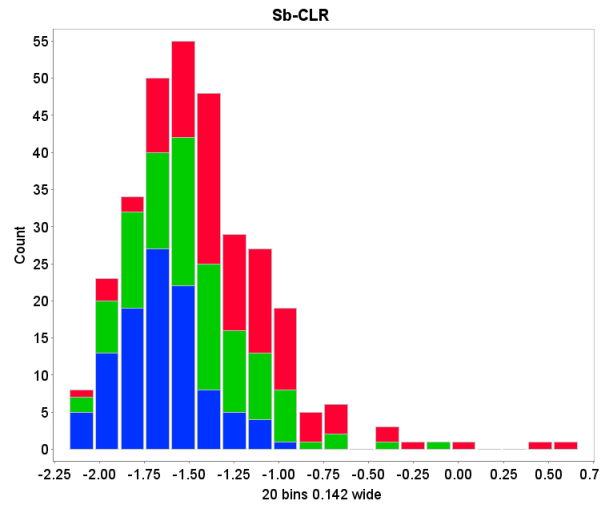
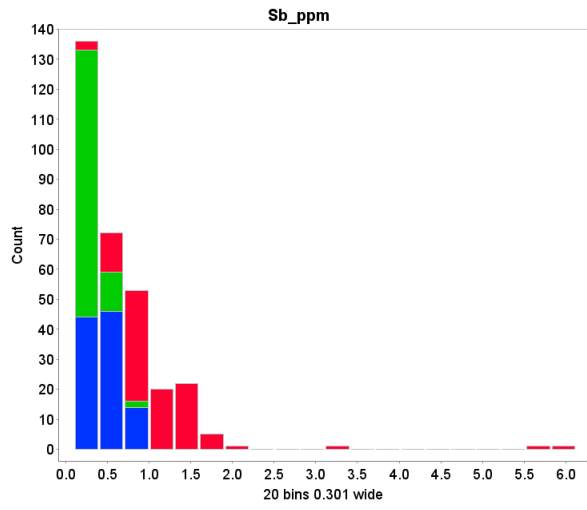


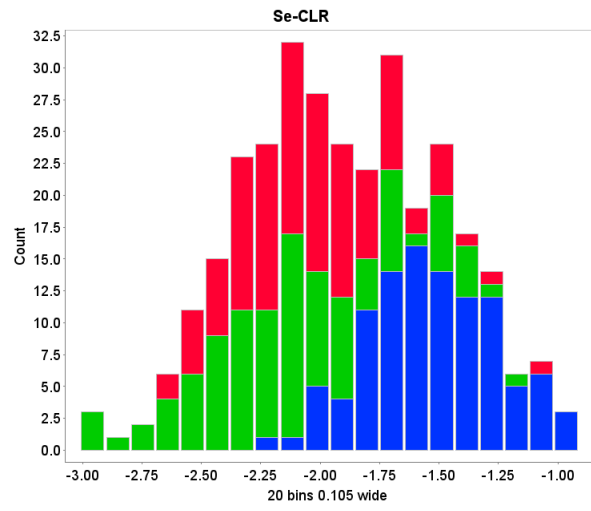
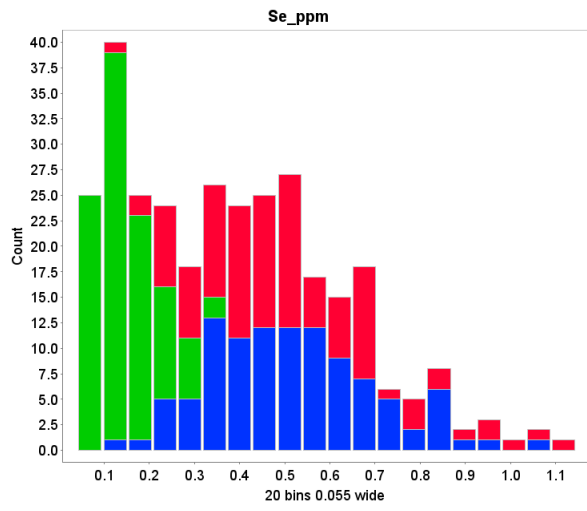
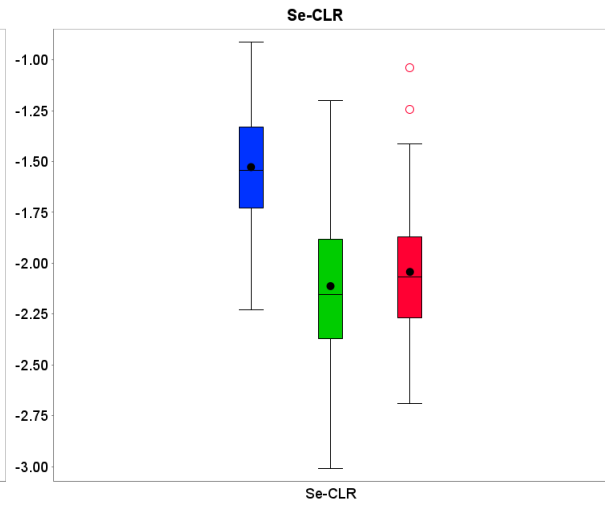
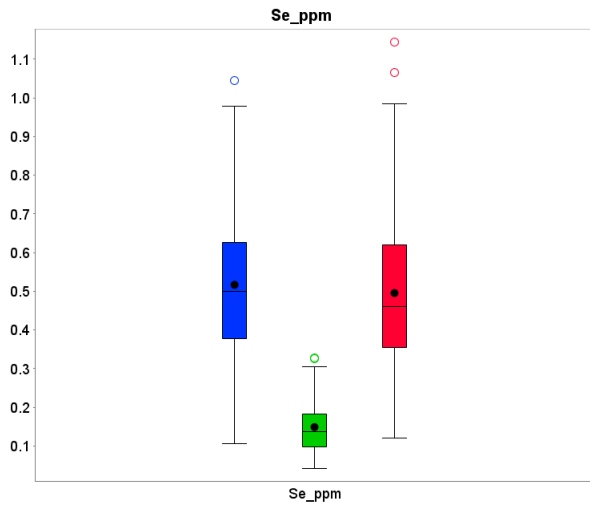


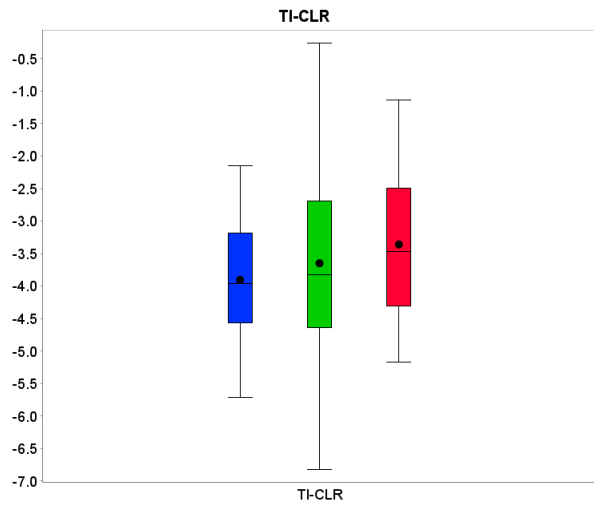
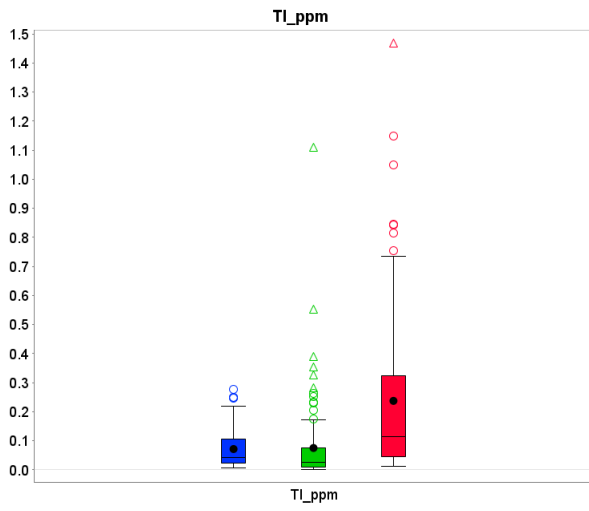
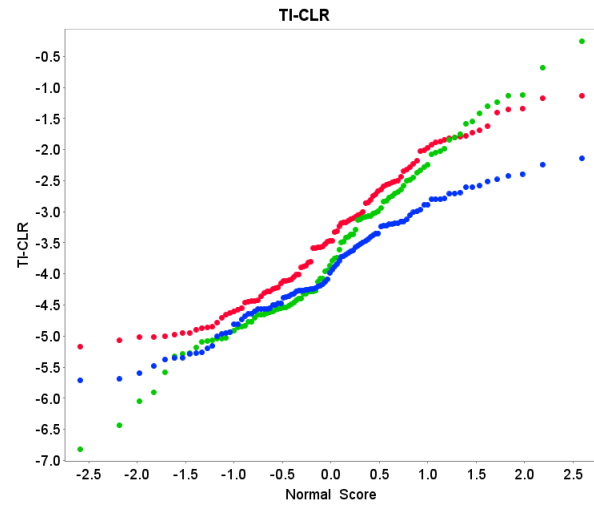
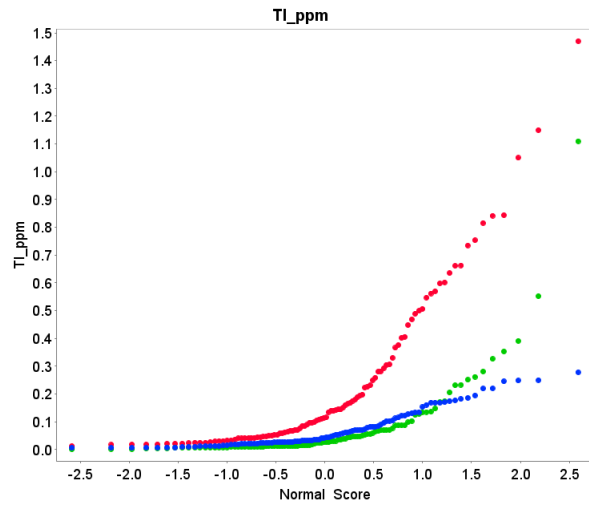


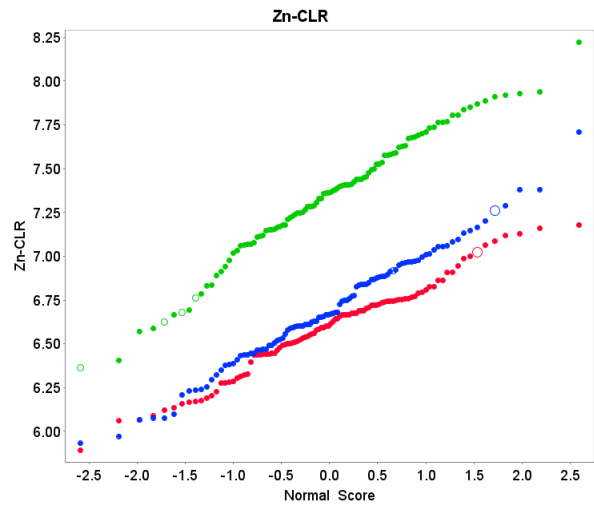
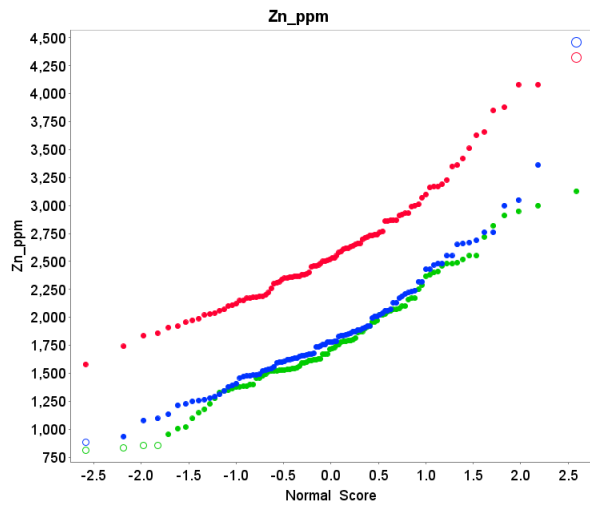
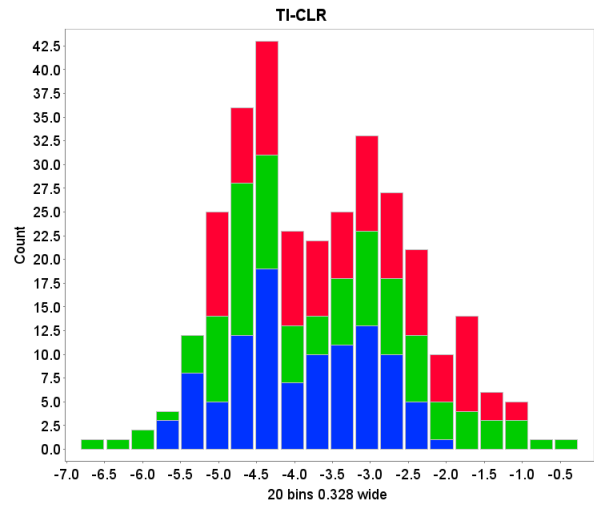
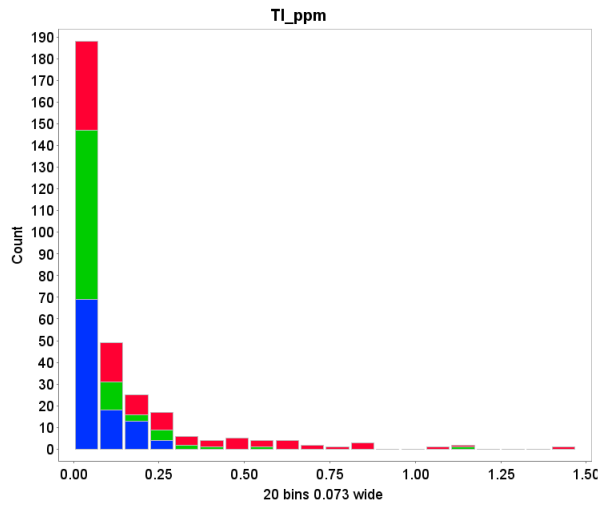


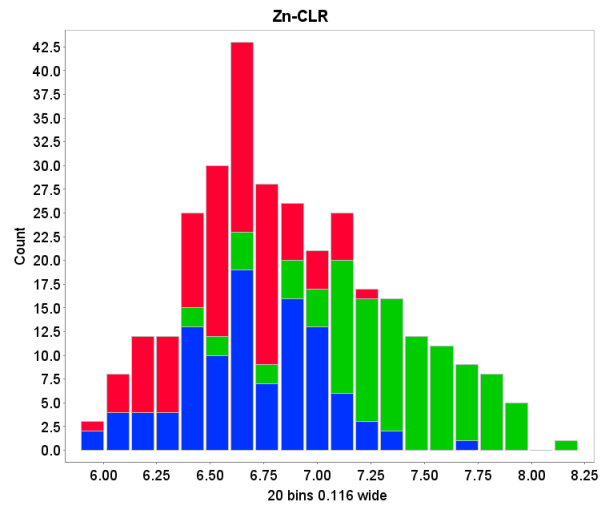
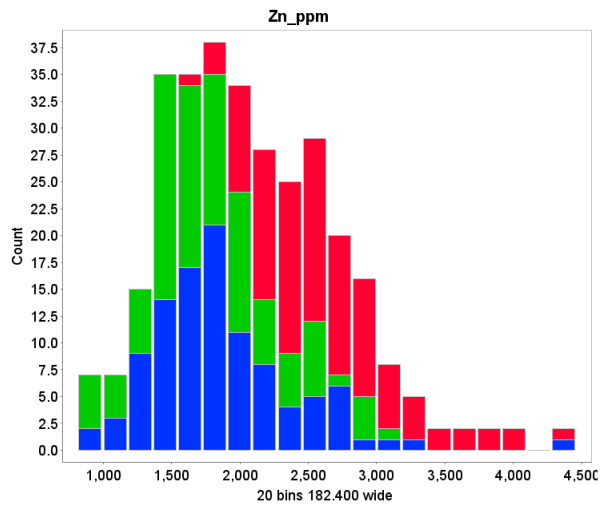
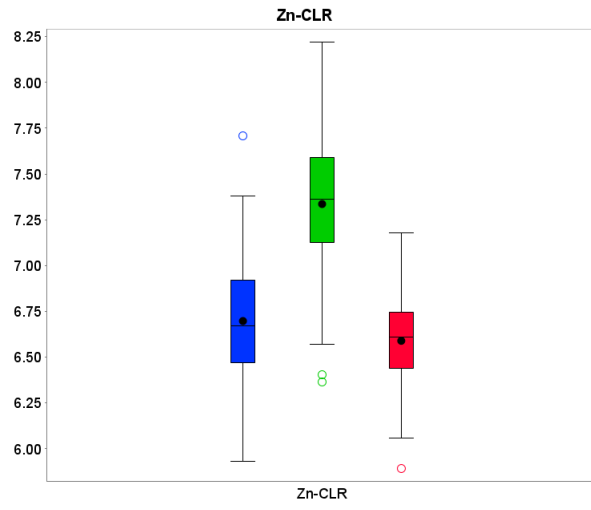
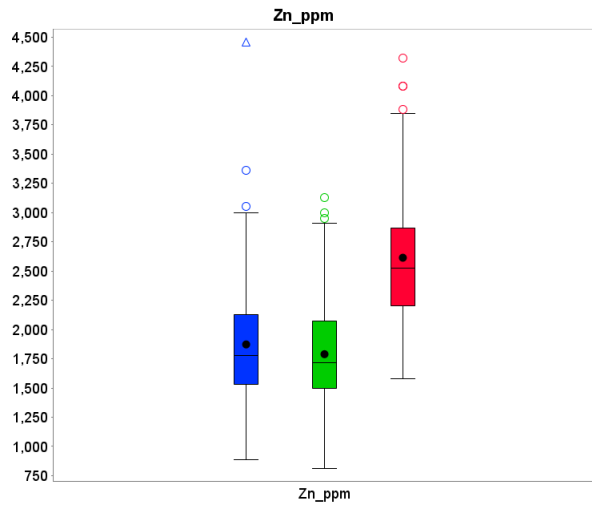






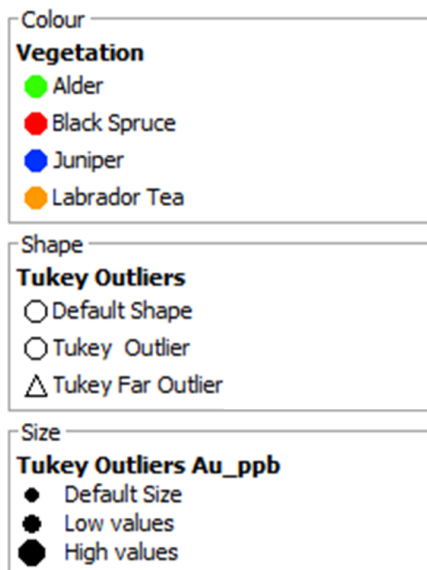


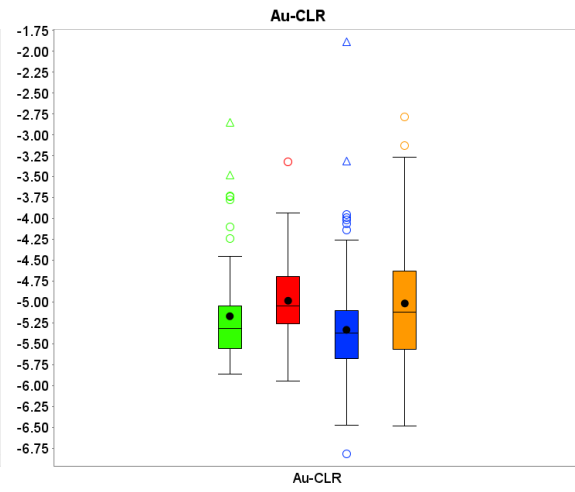
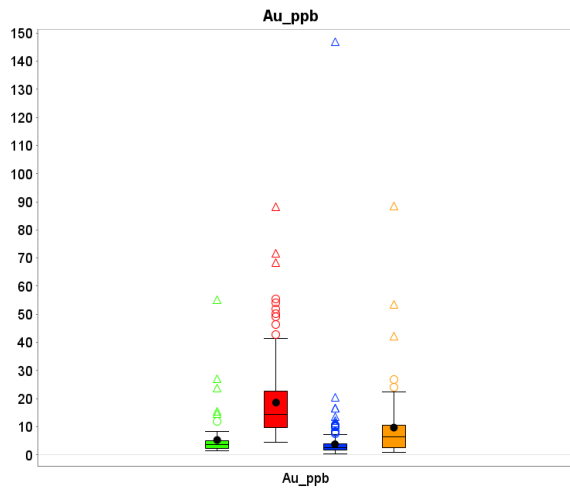
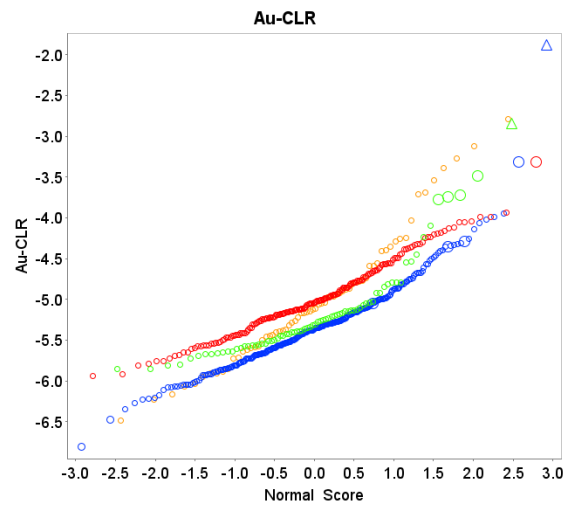
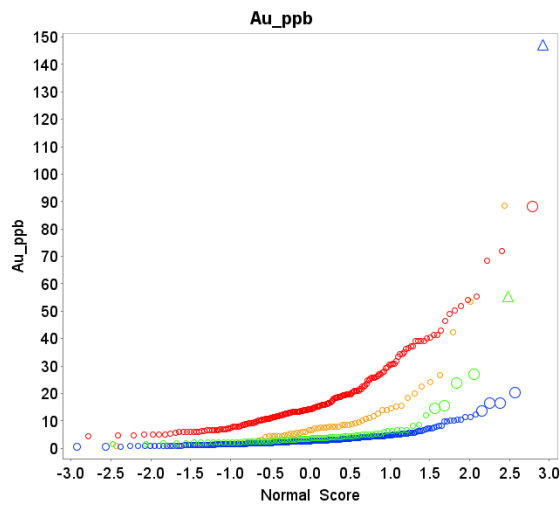


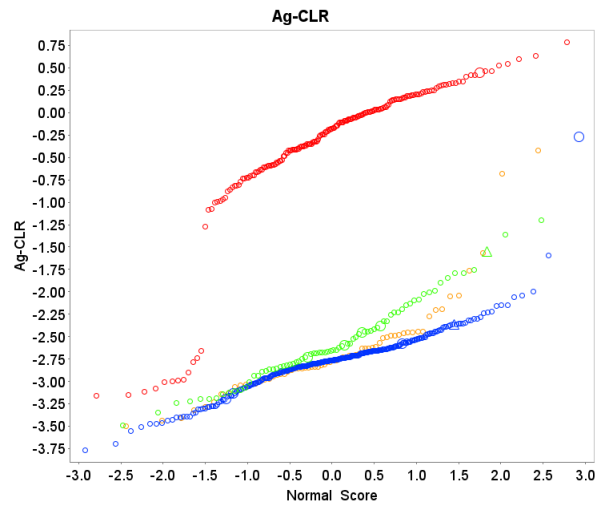
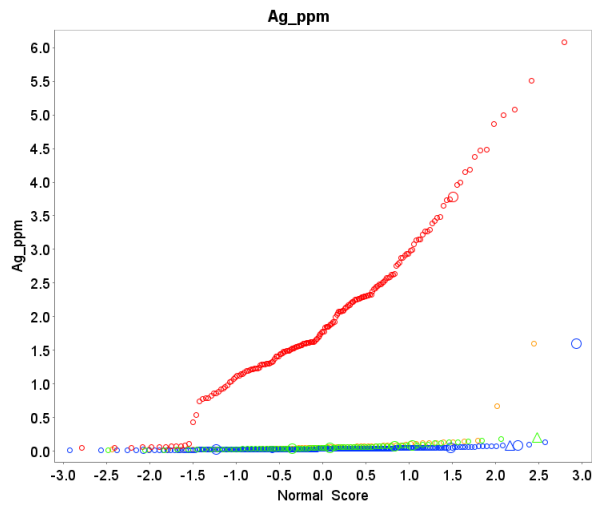
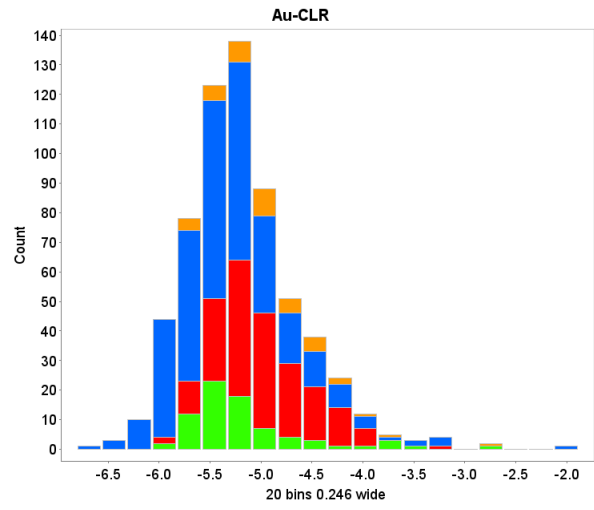
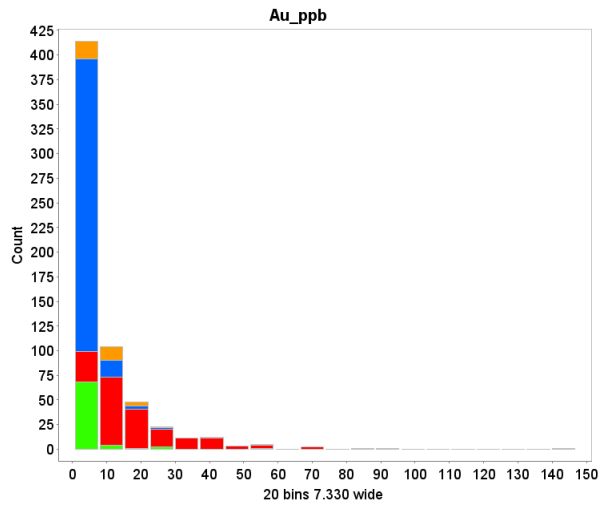


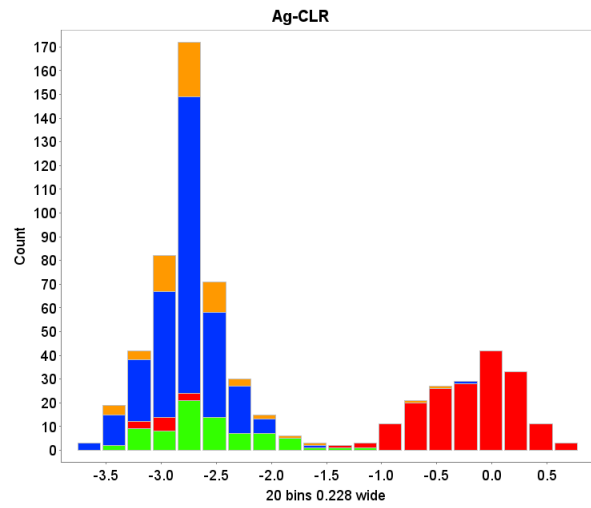
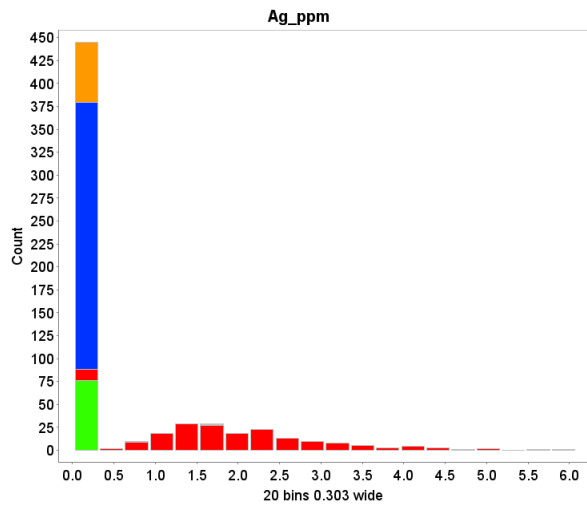
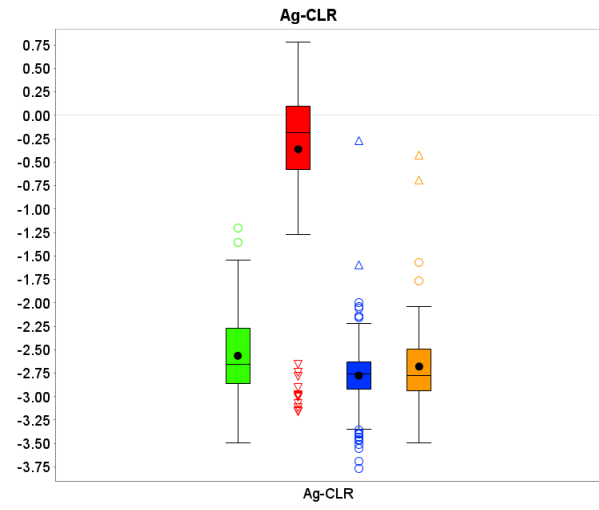
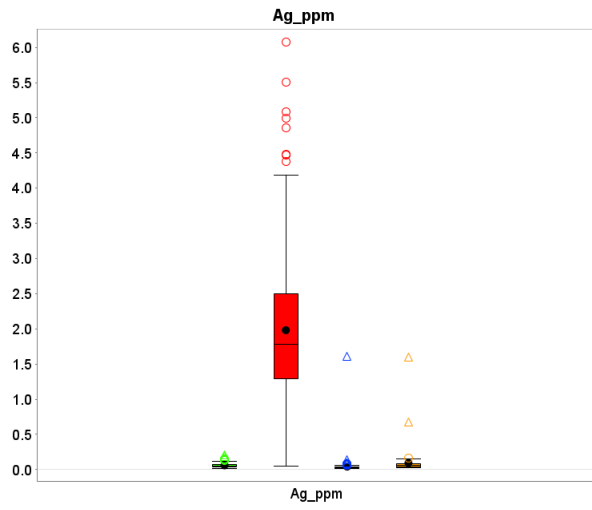
Appendix B

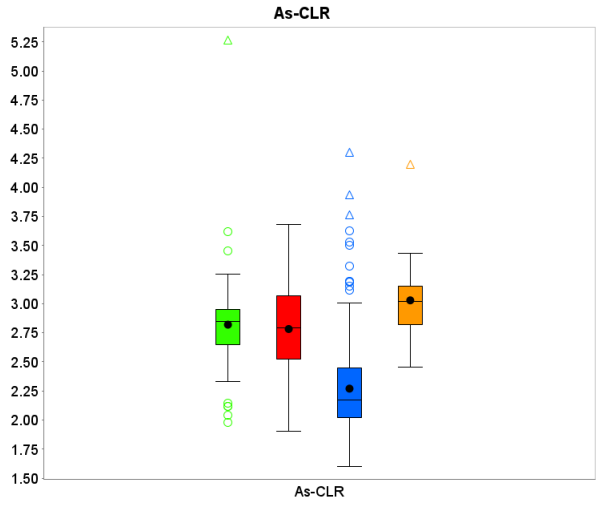
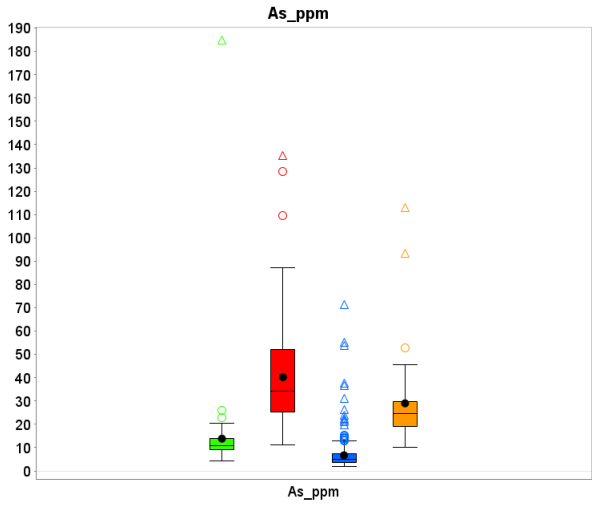
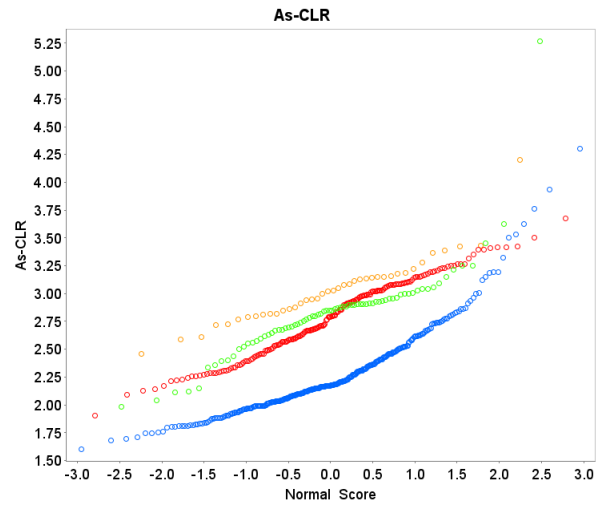
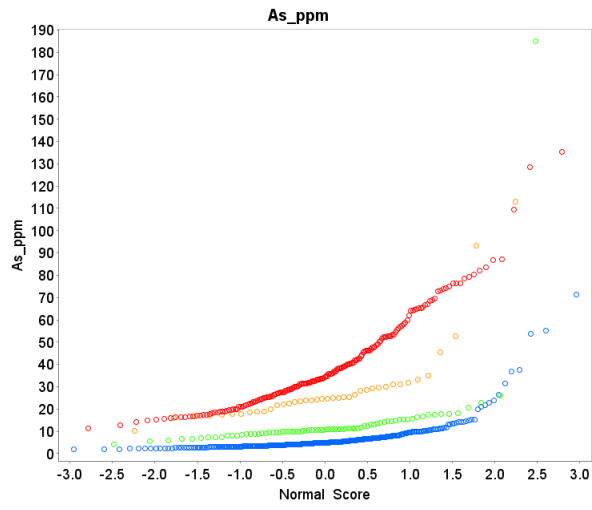
Appendix B compares the raw and transformed data of the Yellowknife City Gold project (YCGP, 2015) using probability plots, scatter plots and histograms. The plots on the right demonstrate the raw data distribution for each element. On the left side, data distribution is normalized using center log-ratio (CLR) transformation. Tukey method was used to show the outliers (circles) and extreme or far outliers (triangles). The figure below shows the legend.

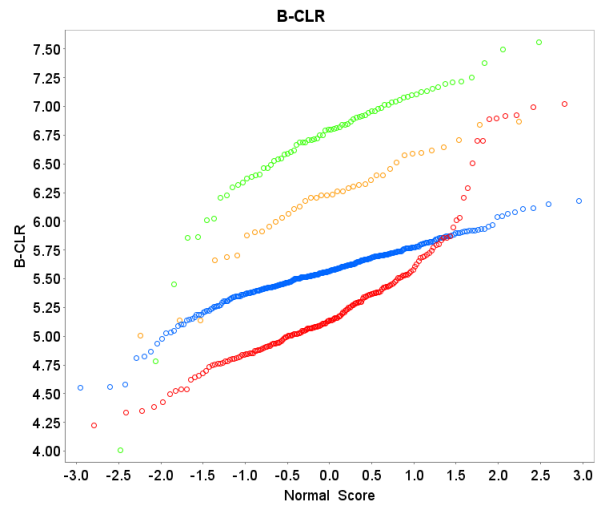
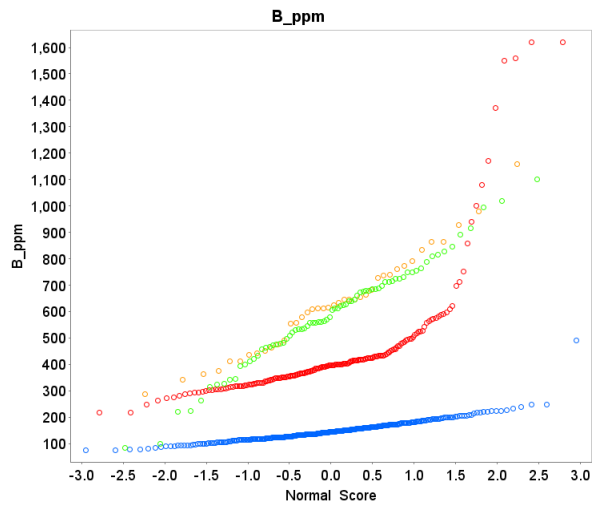
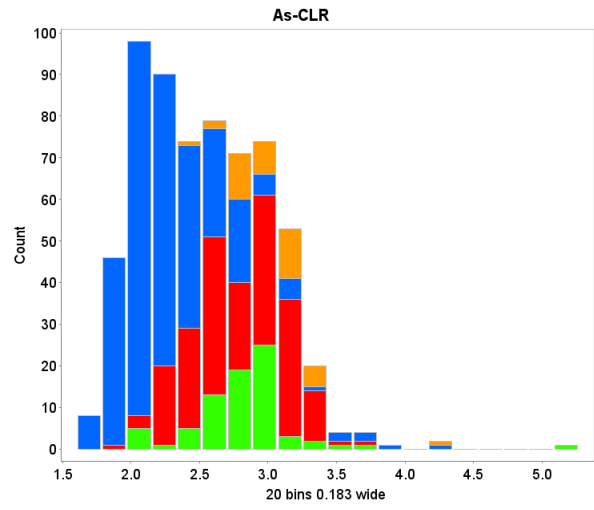
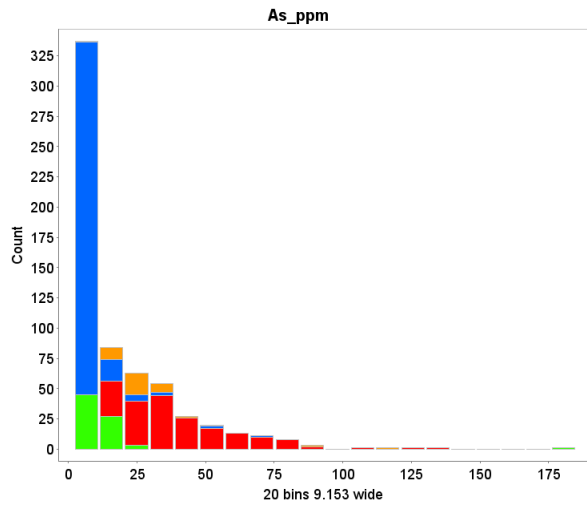


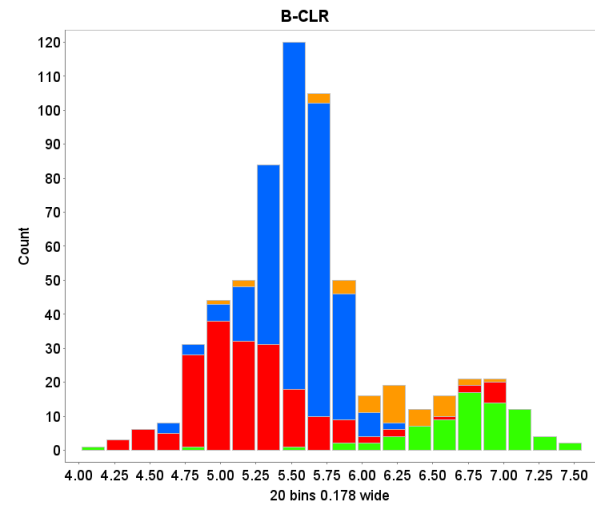
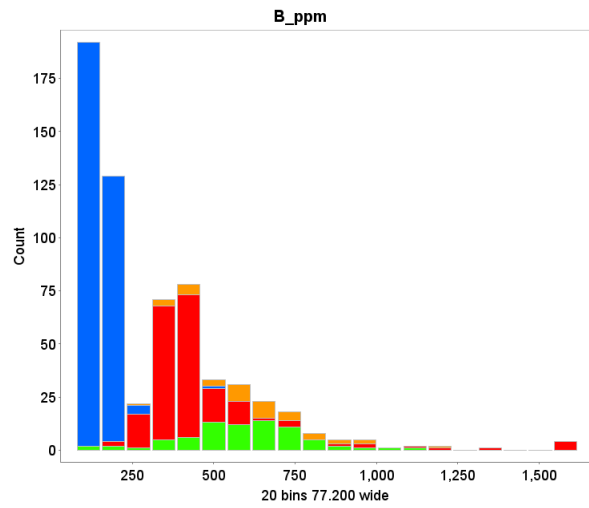
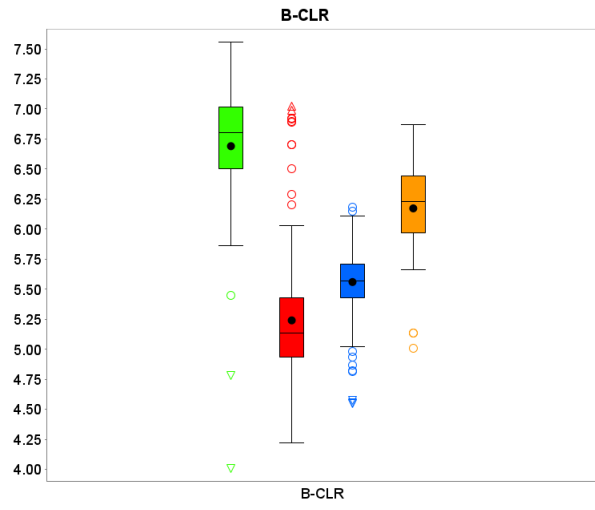
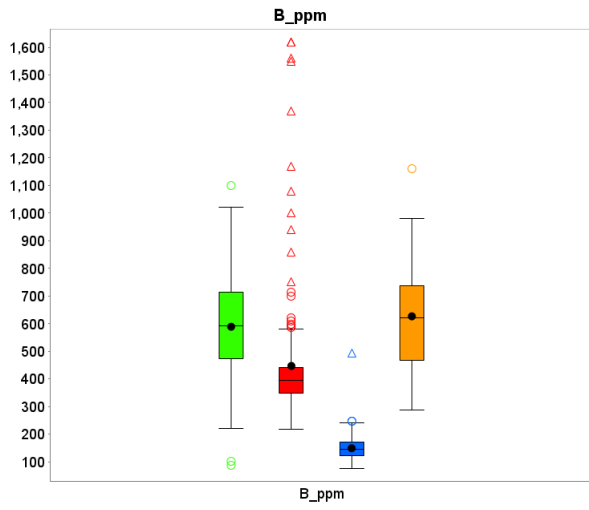


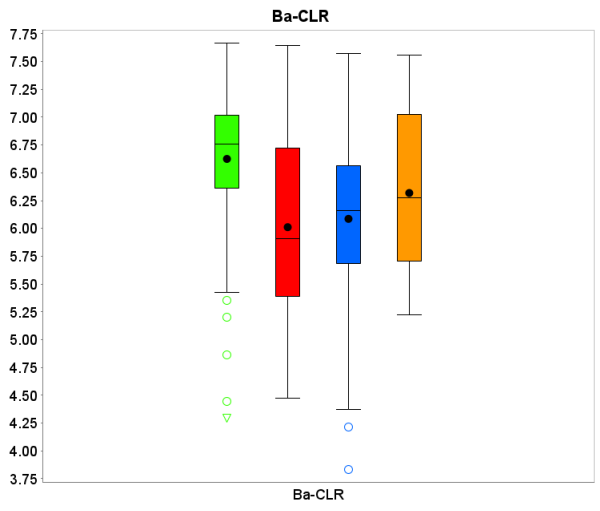
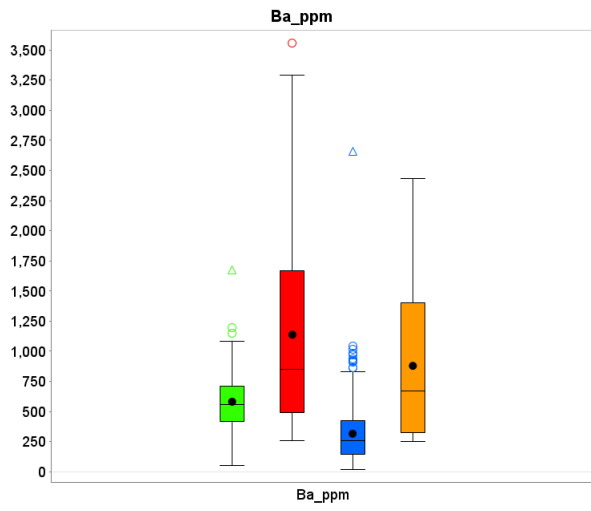
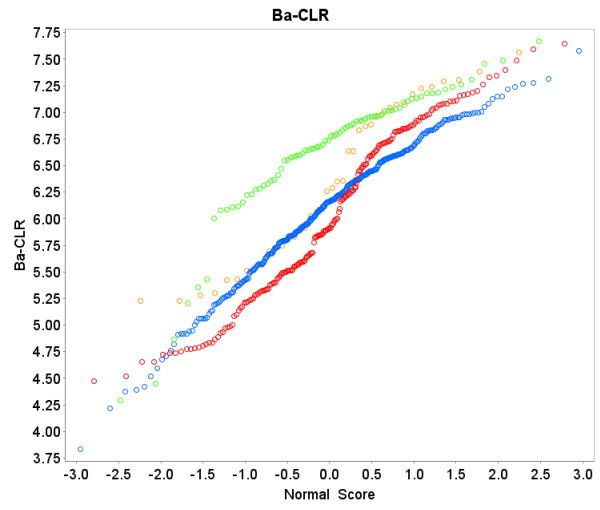
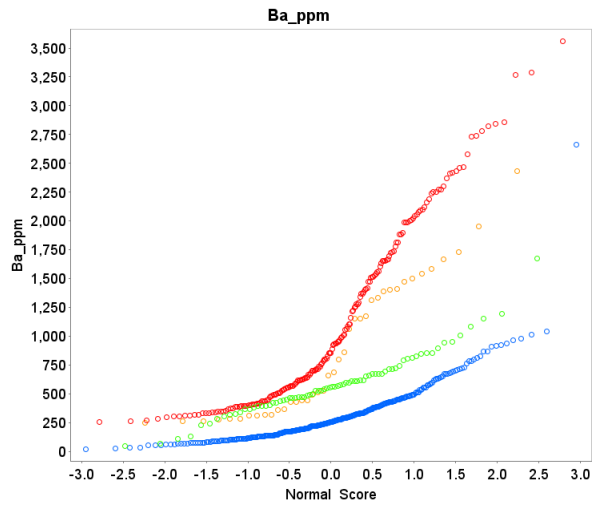


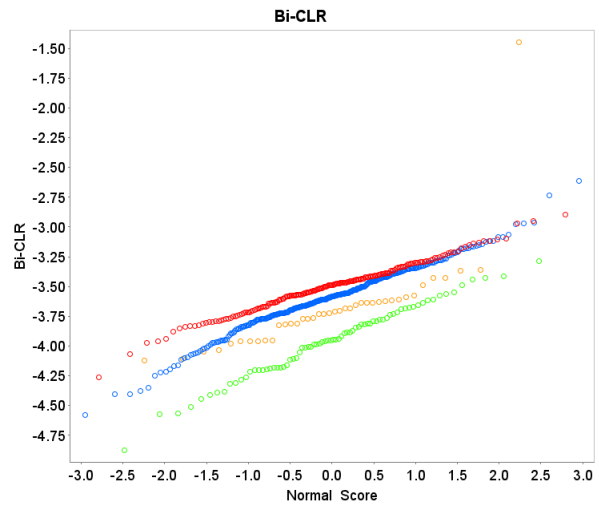
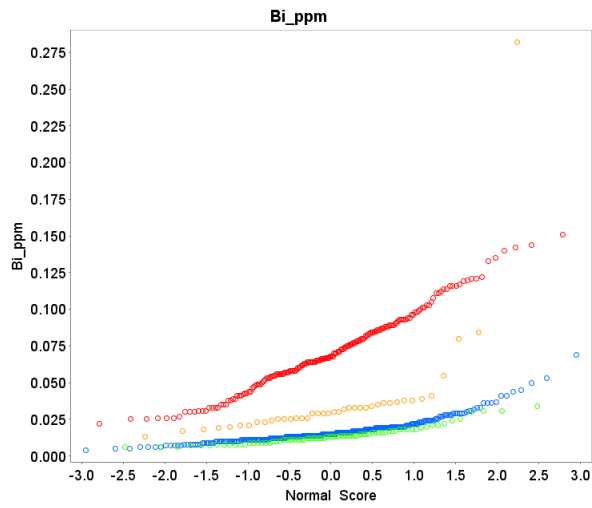
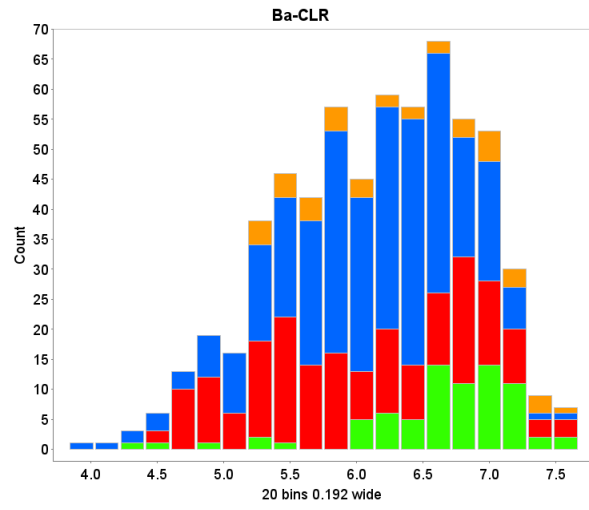
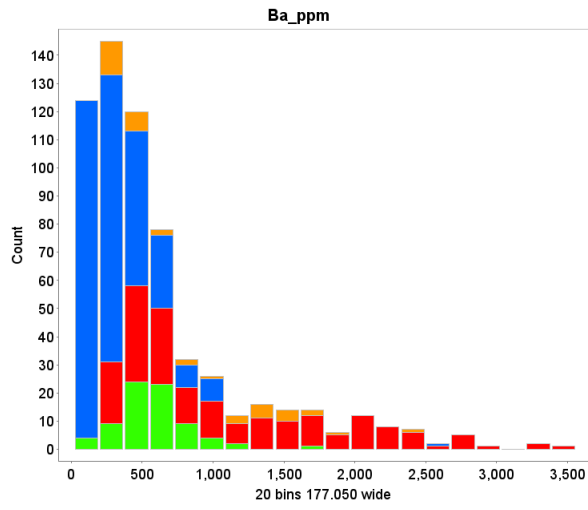


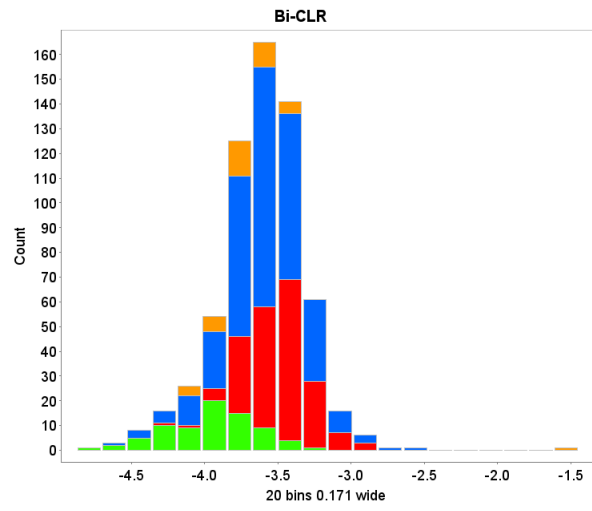
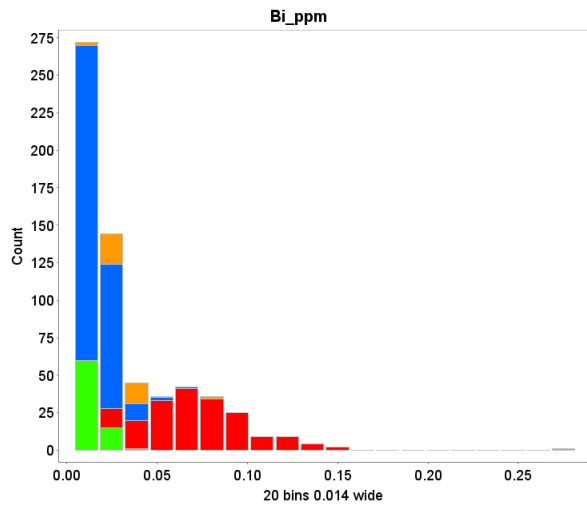
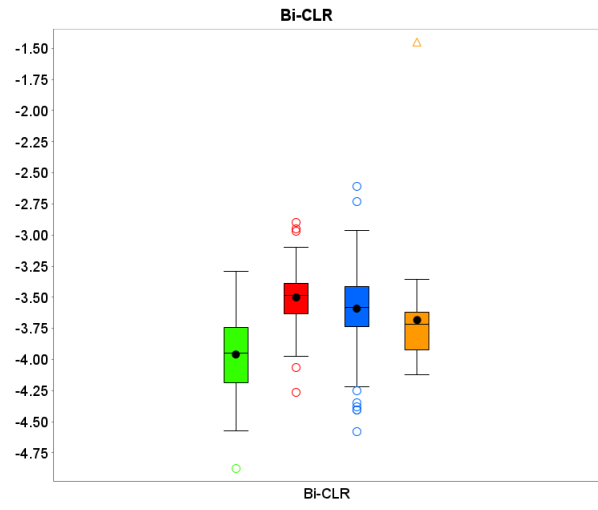
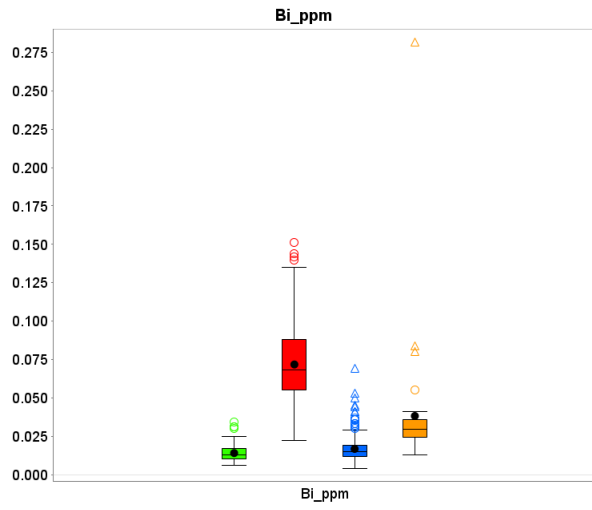


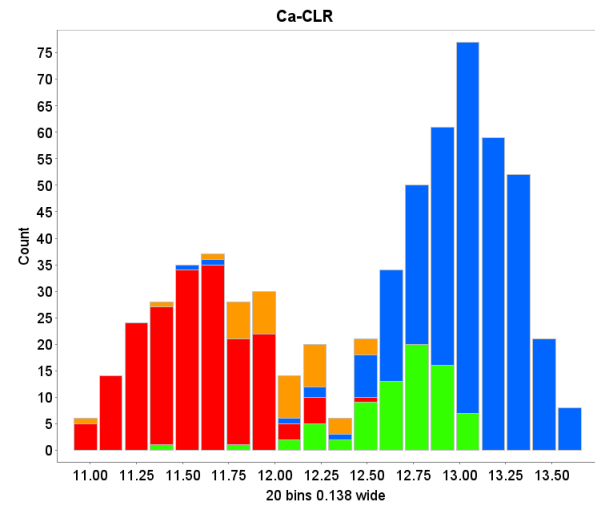
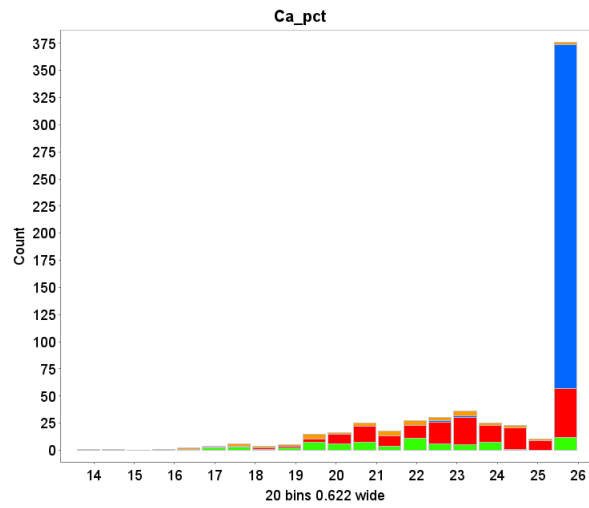
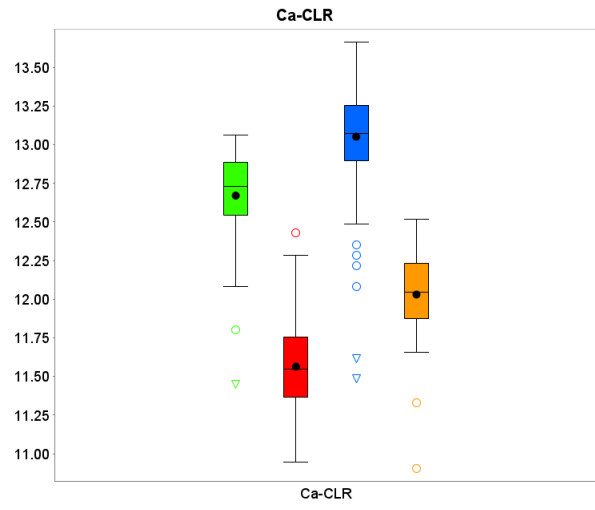
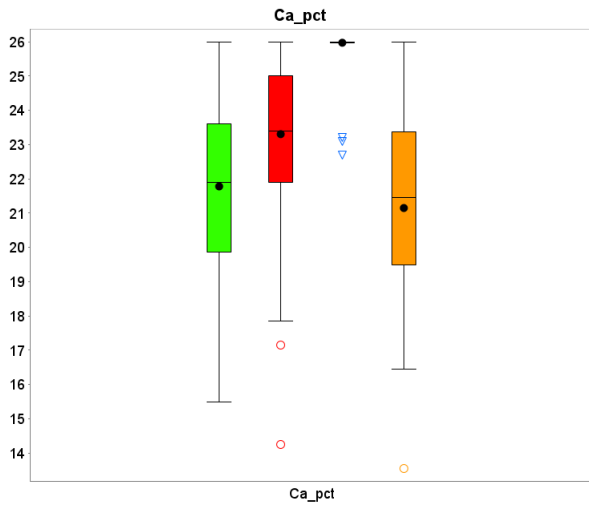


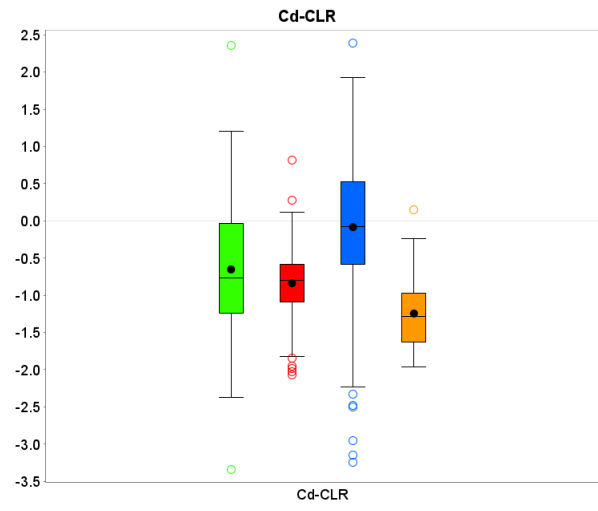
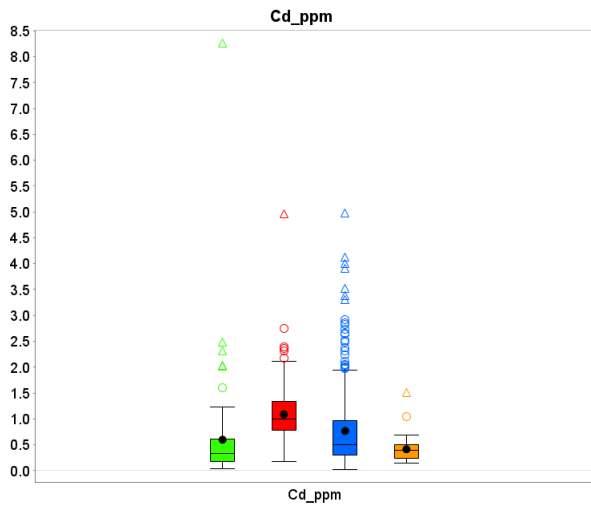
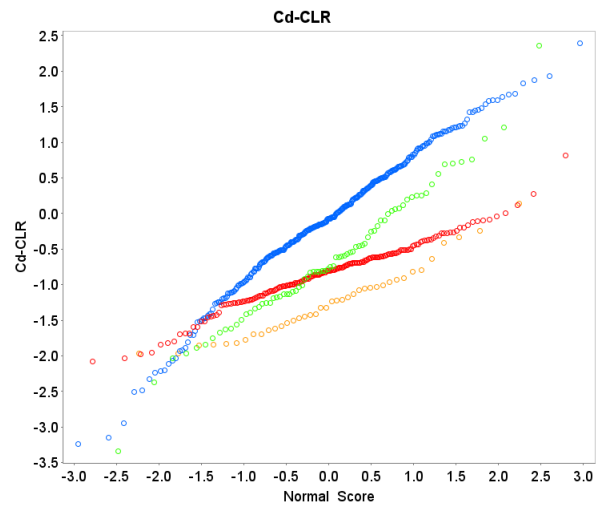
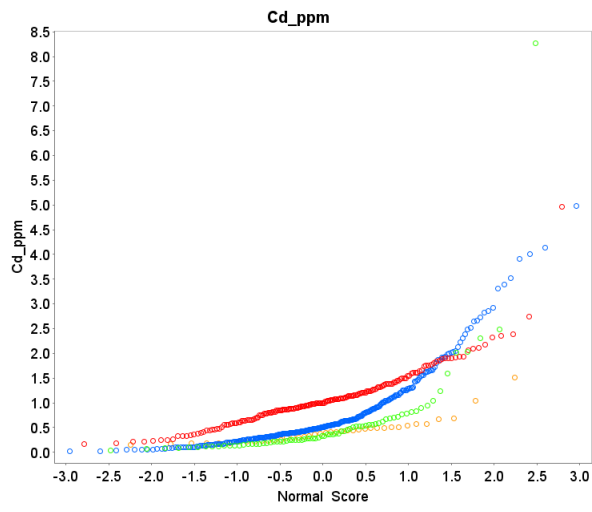


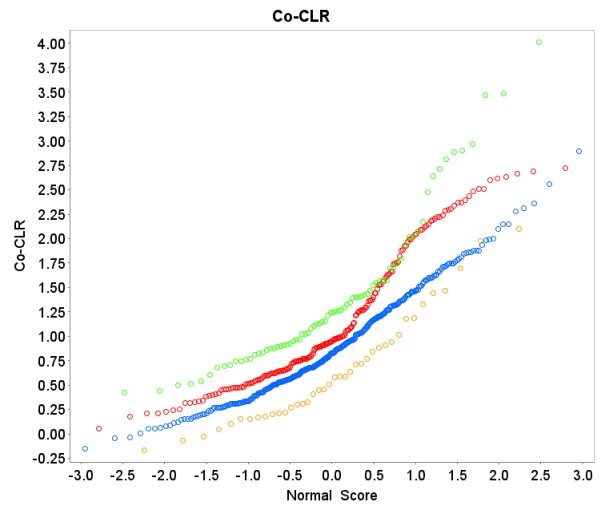
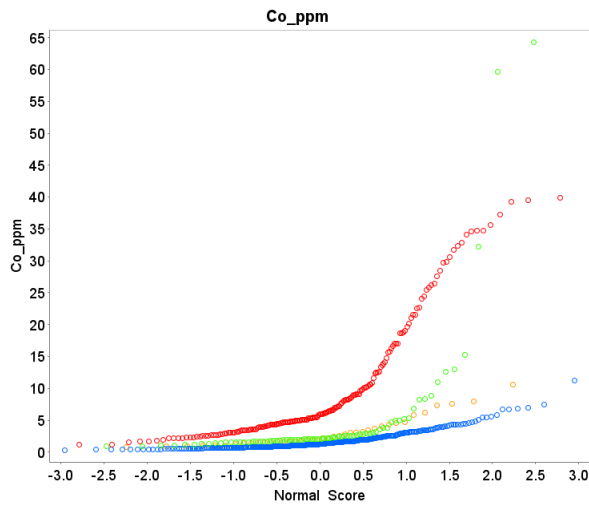
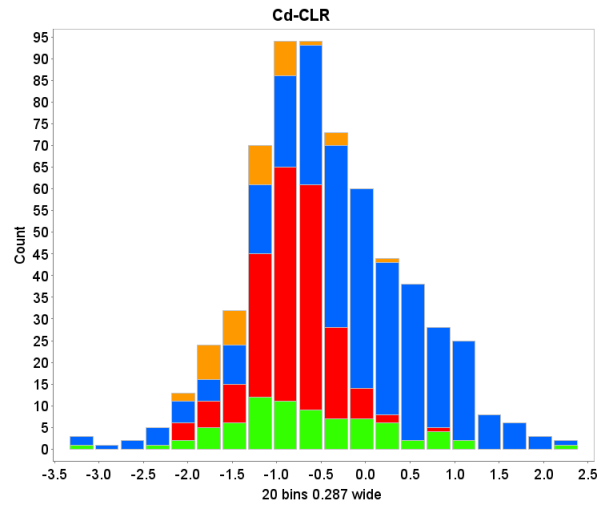
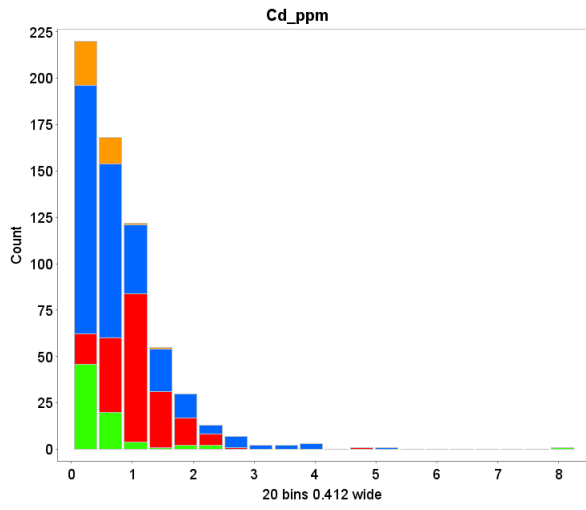


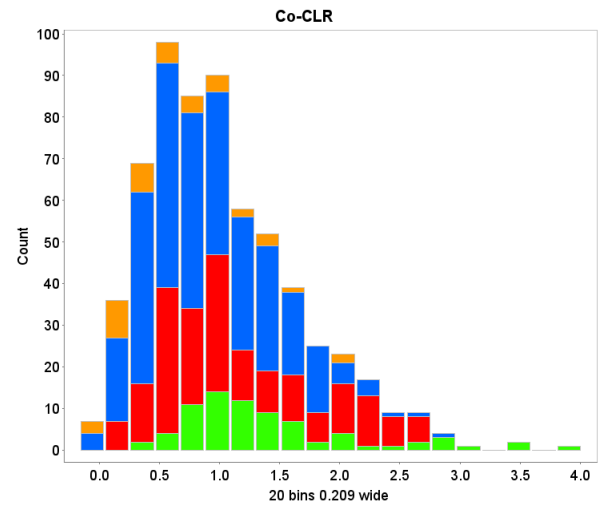
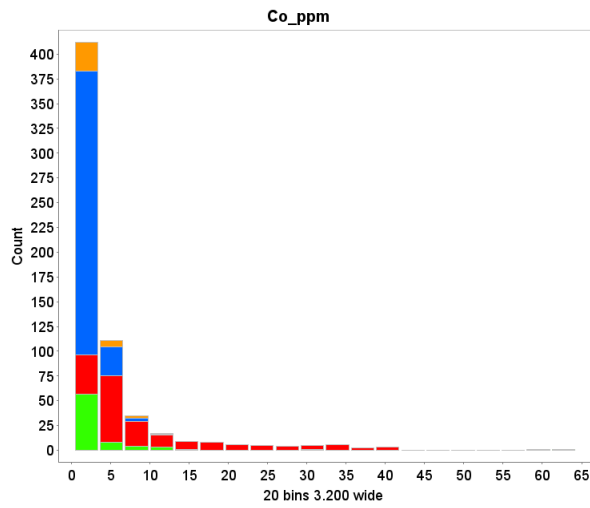
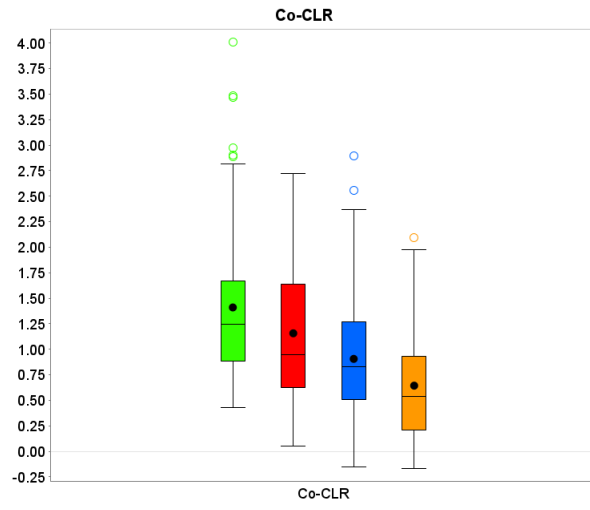
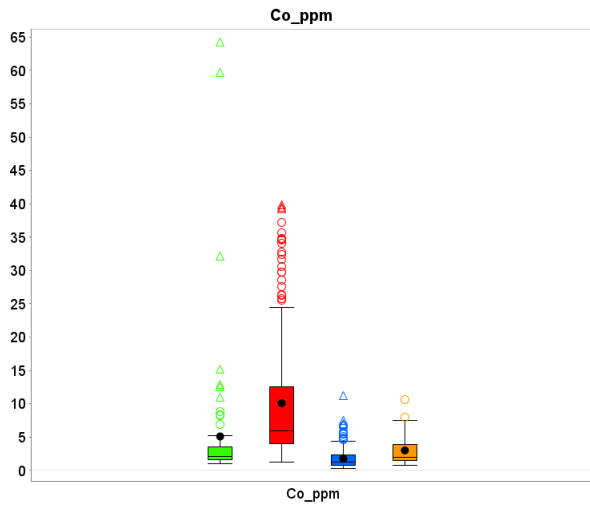


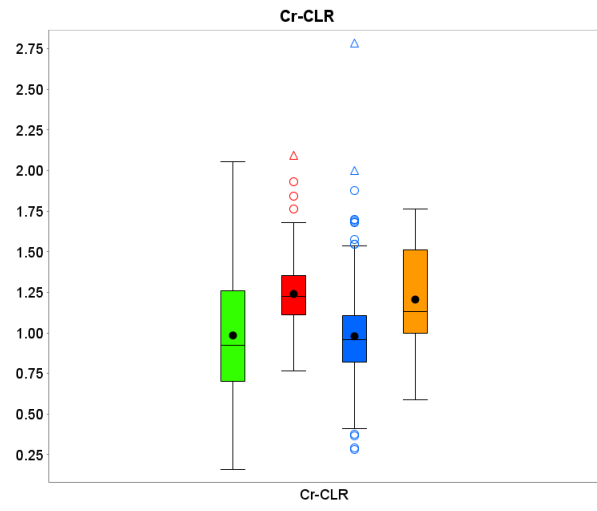
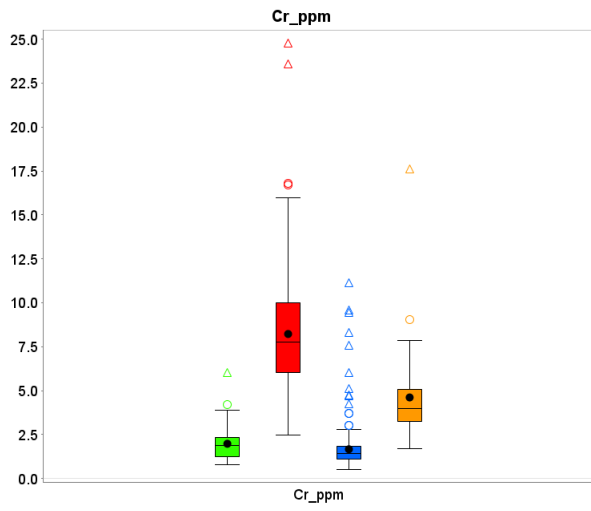
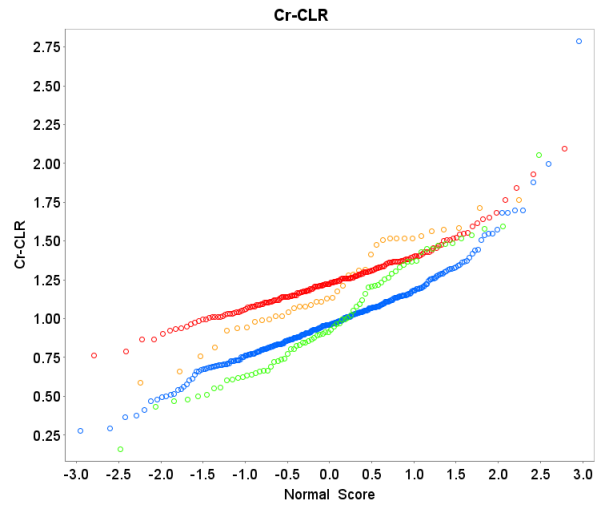
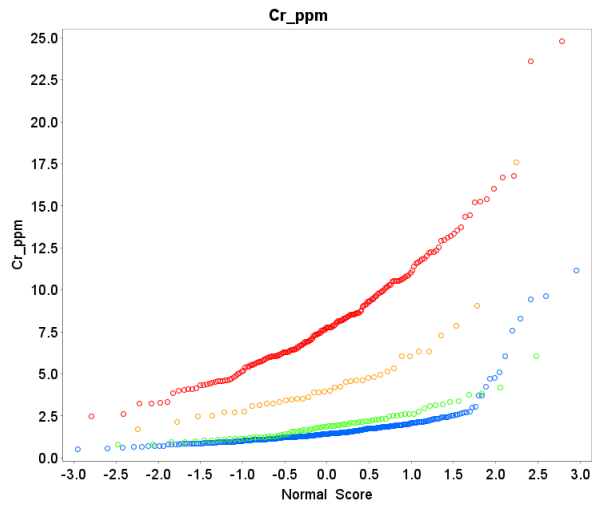


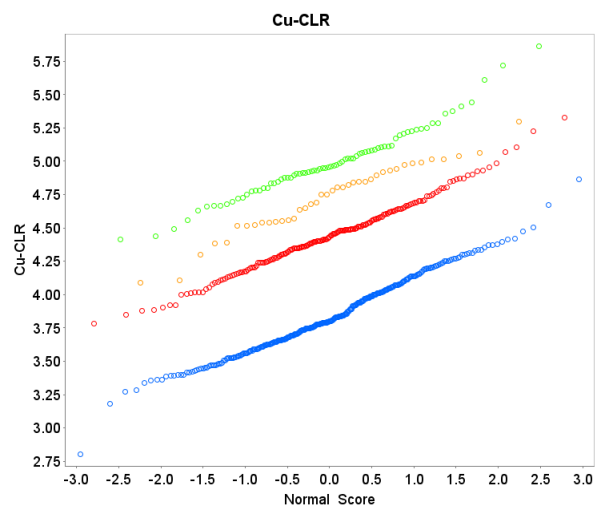
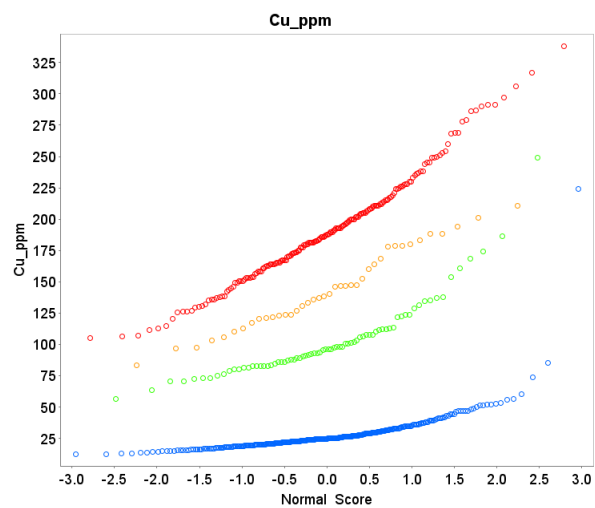
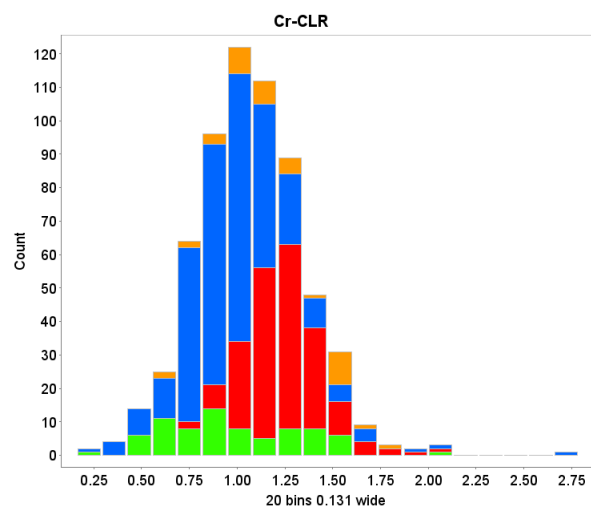
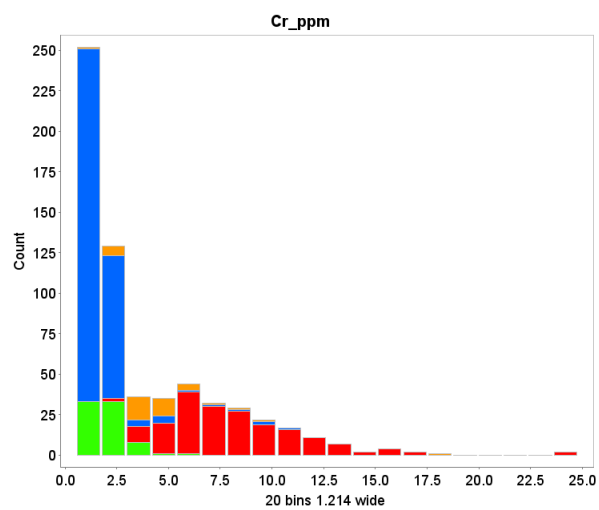


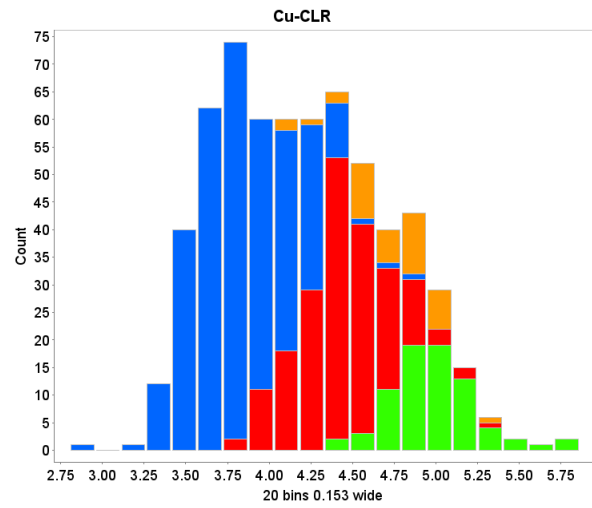
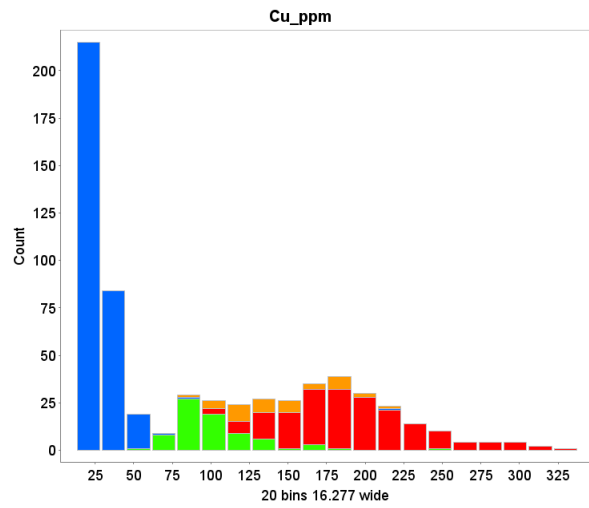
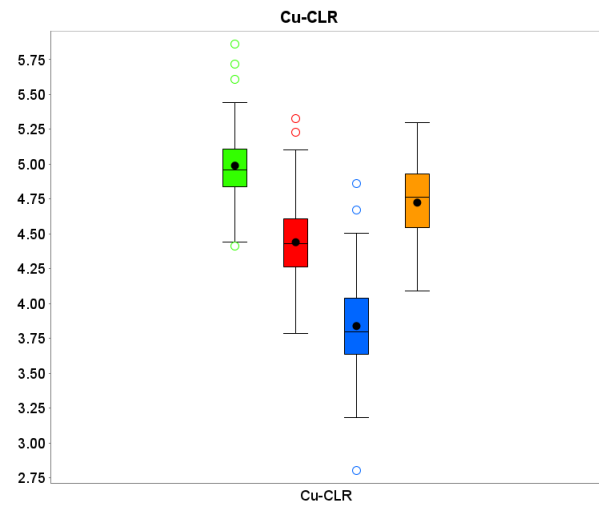
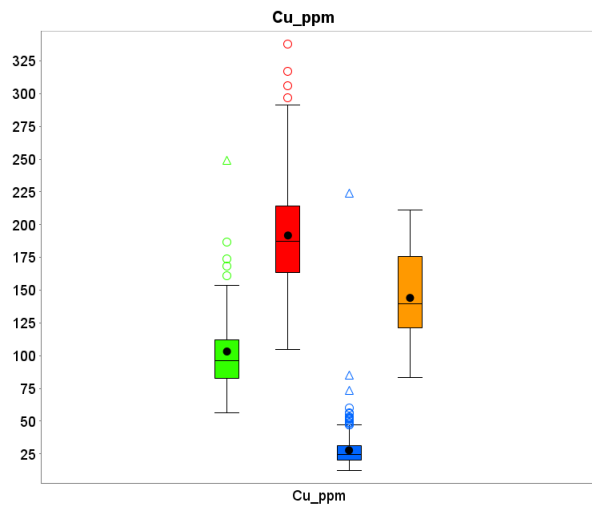


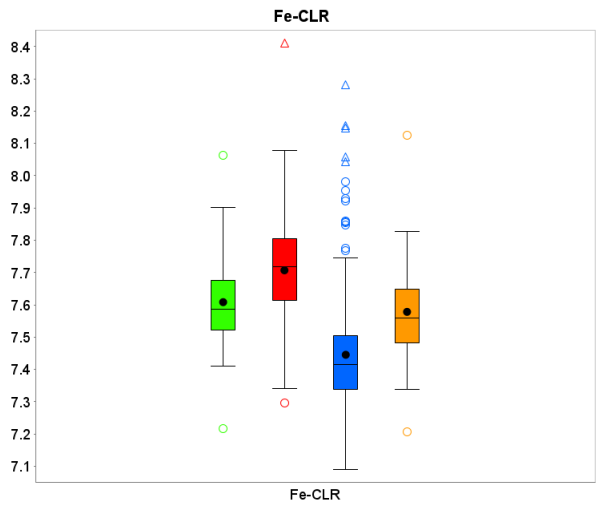
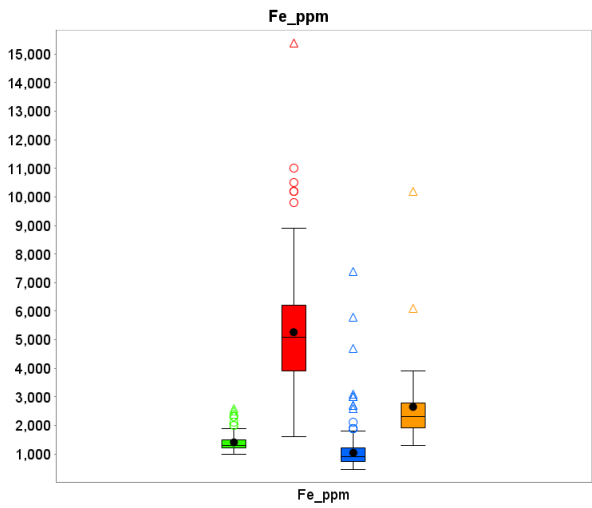
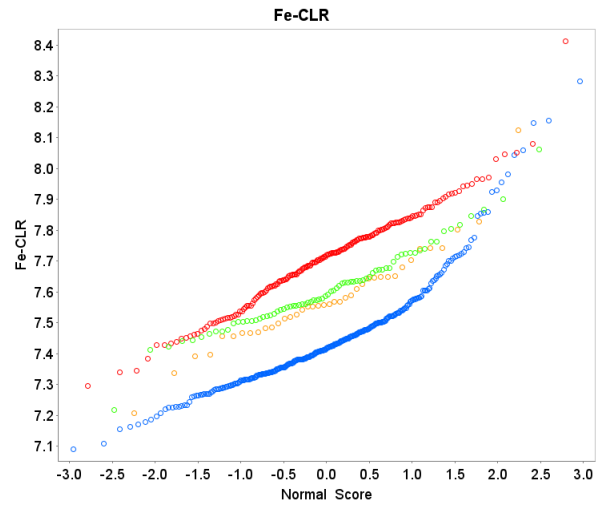
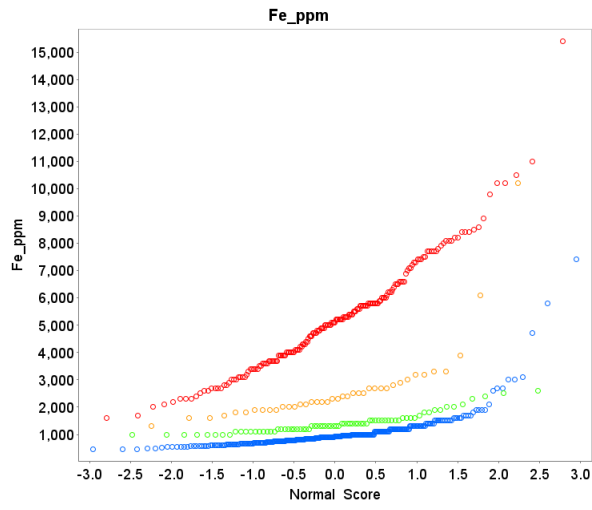


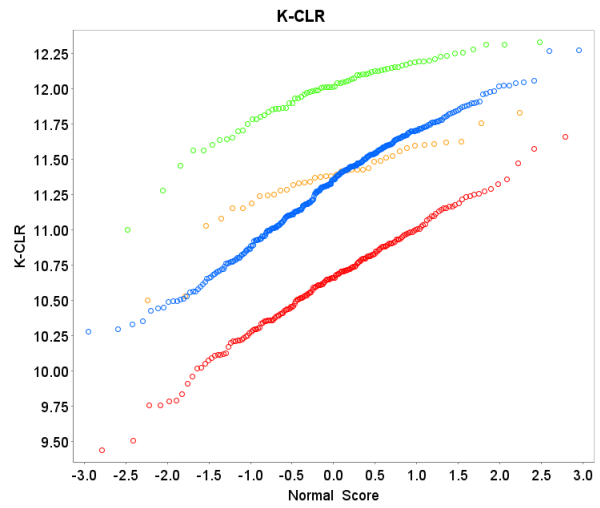
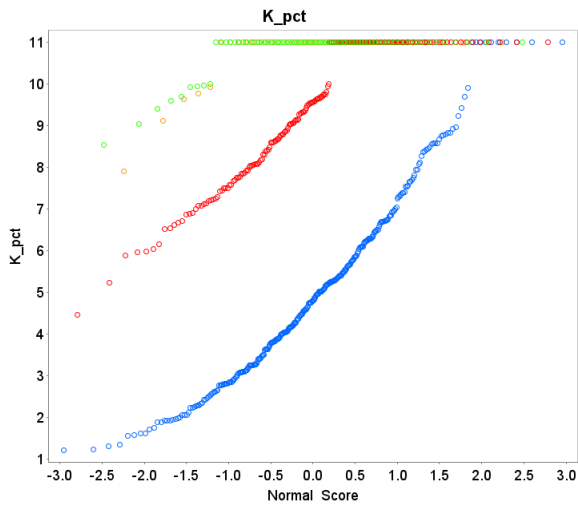
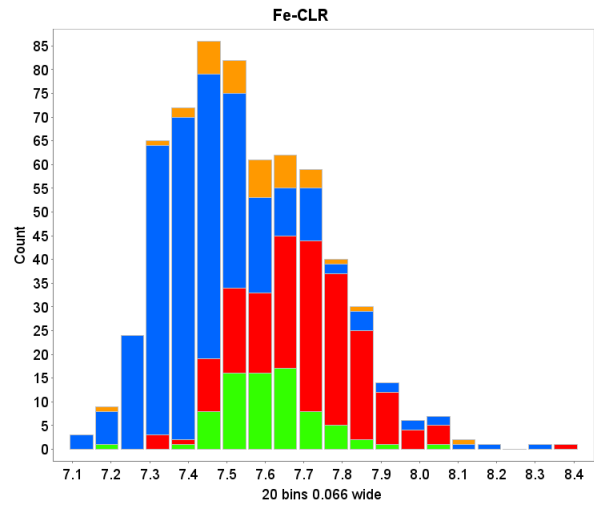
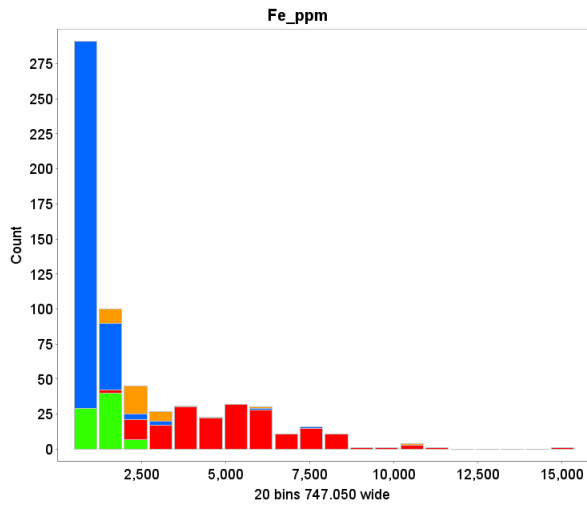


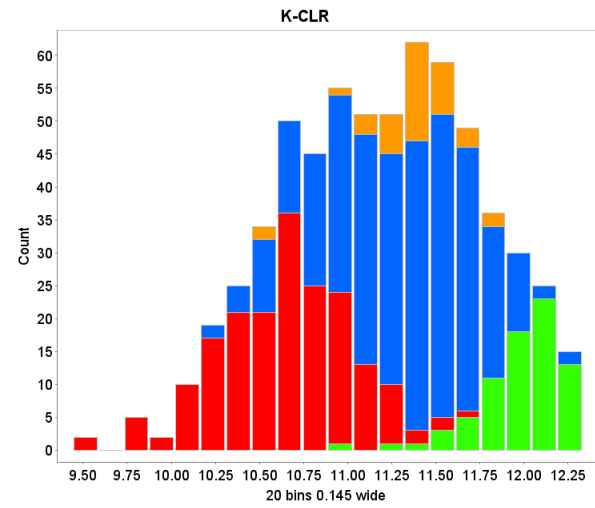
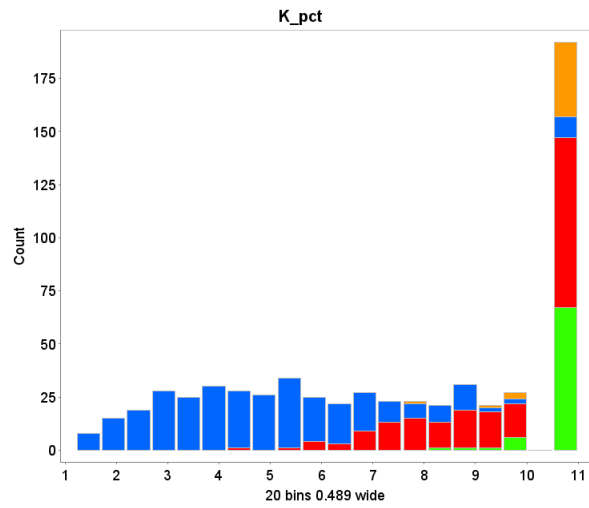
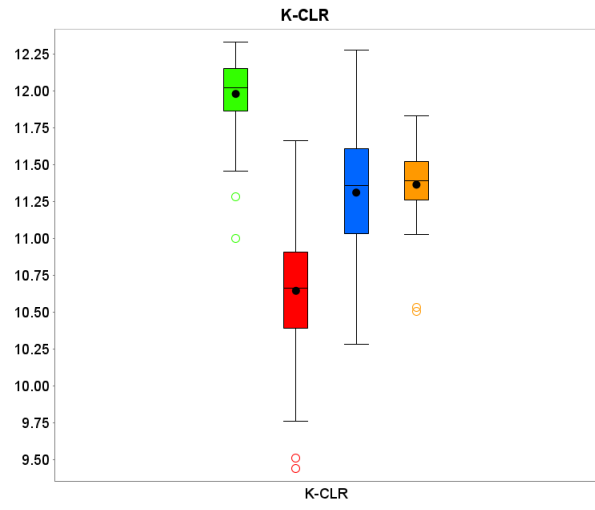
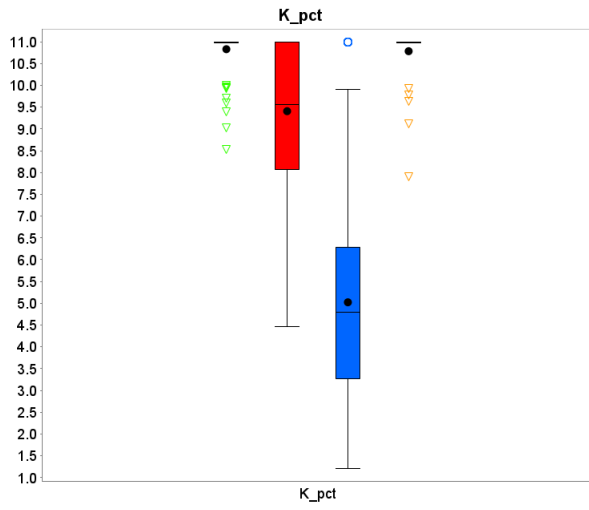


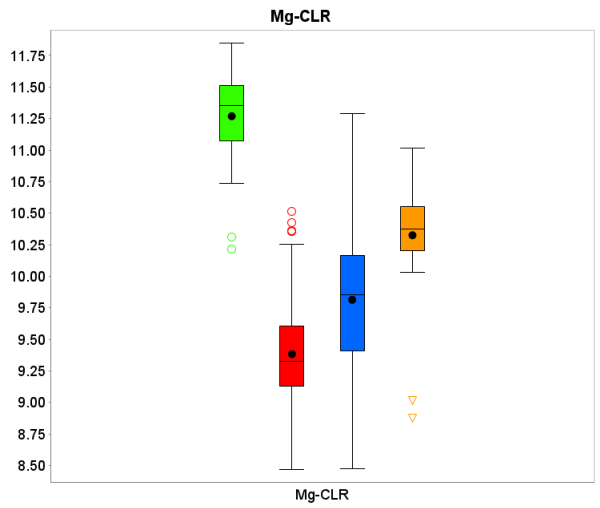
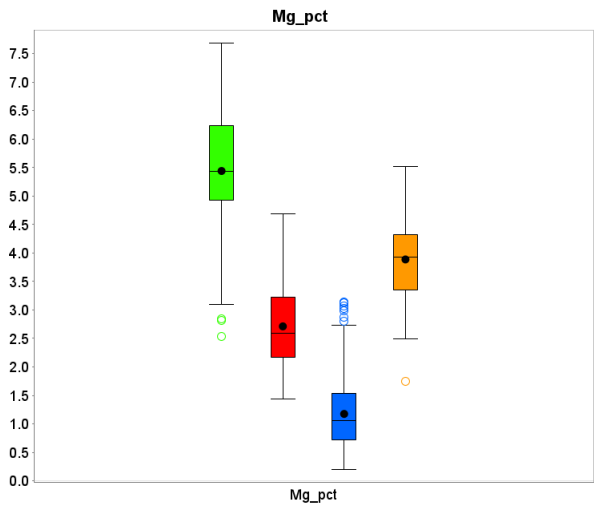
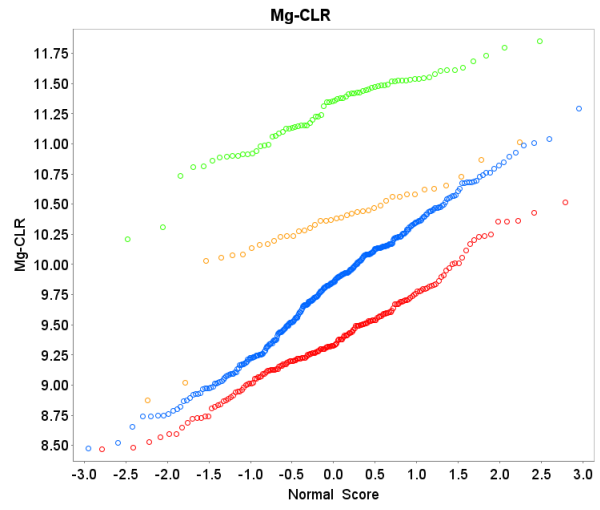
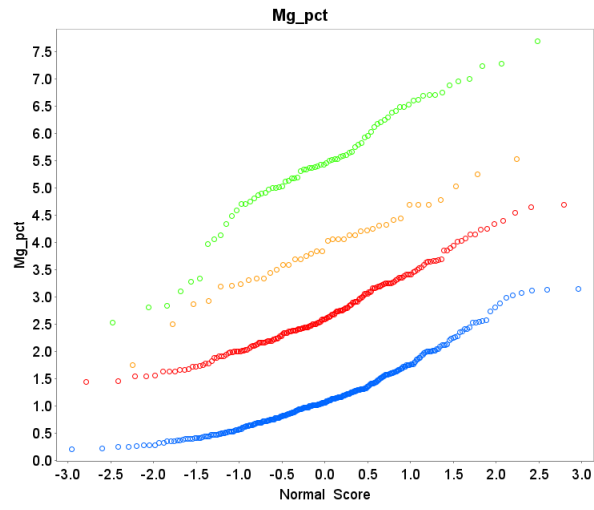


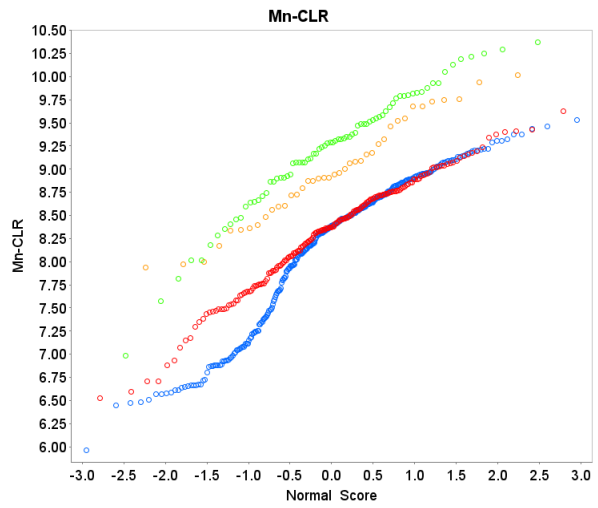
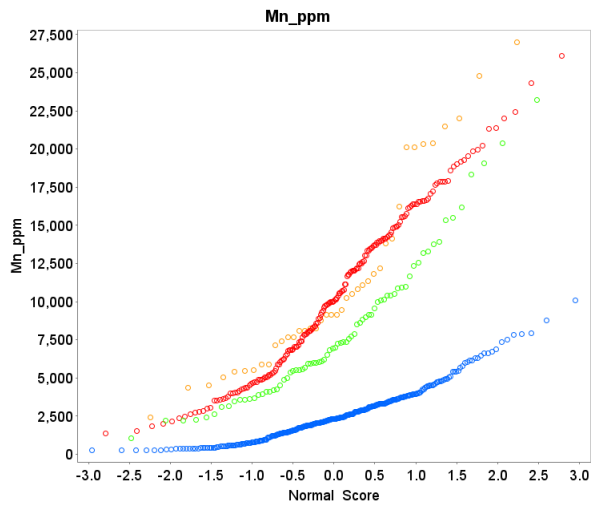
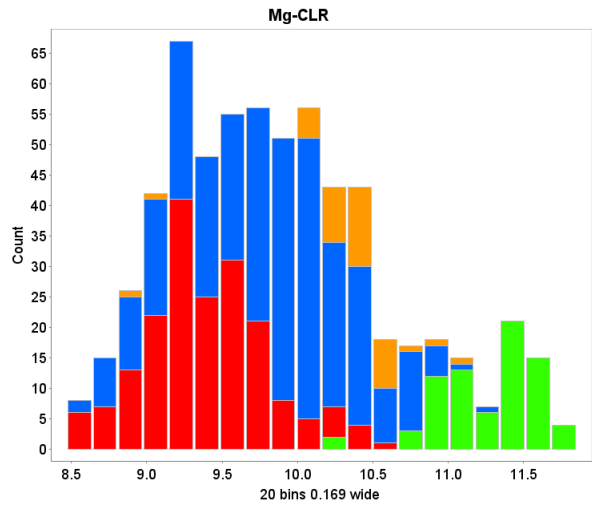
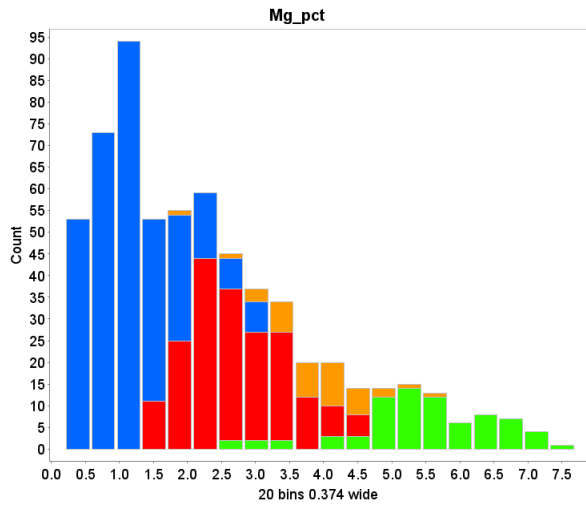


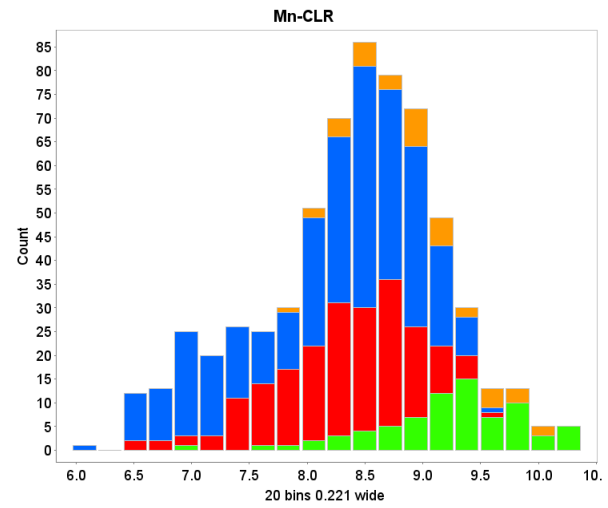
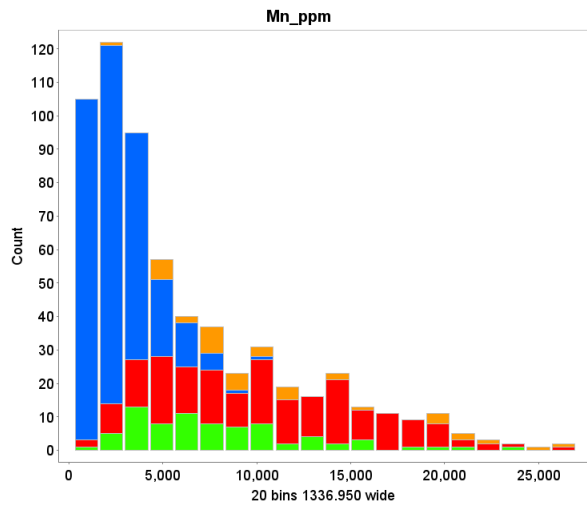
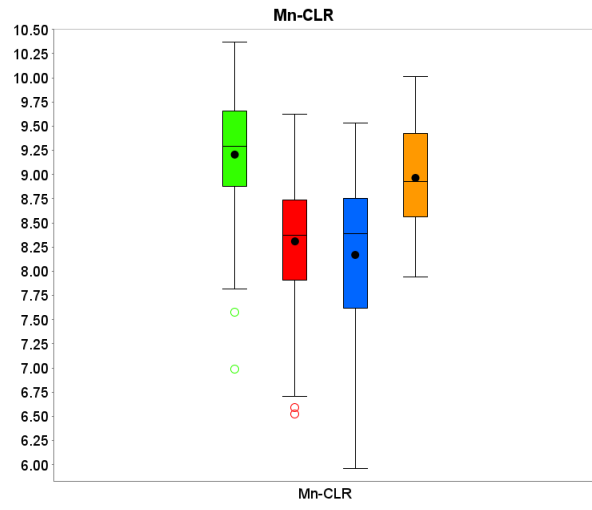
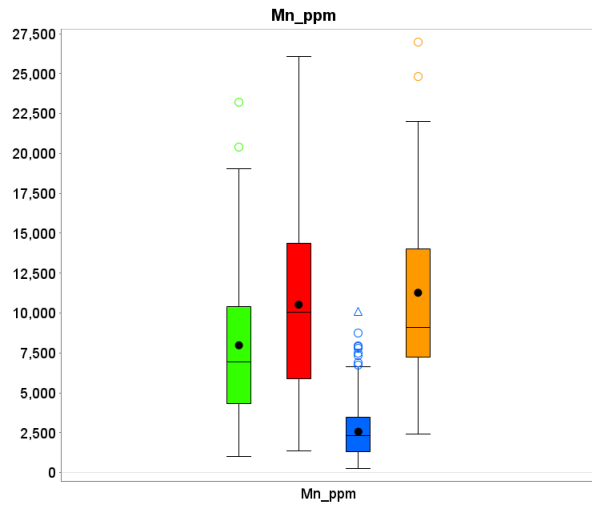


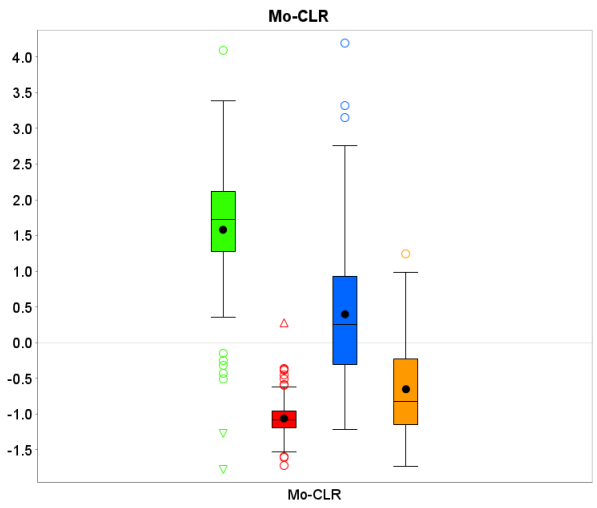
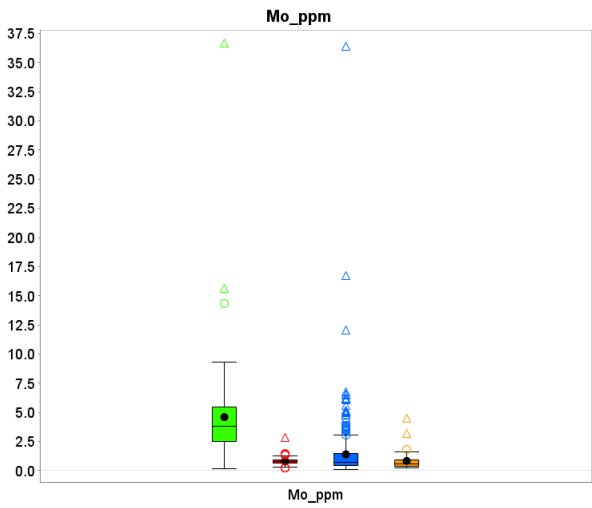
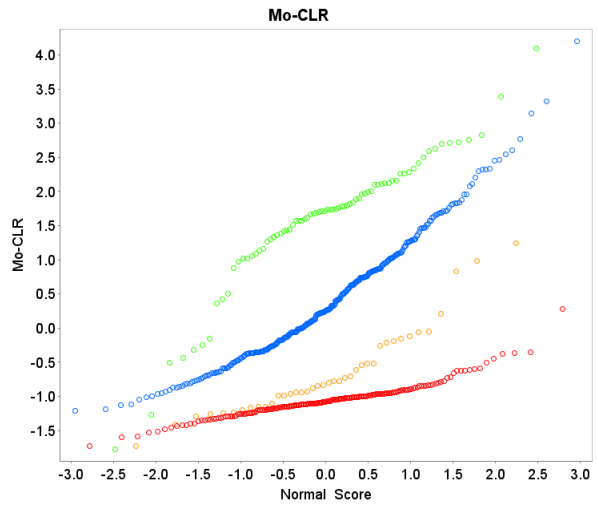
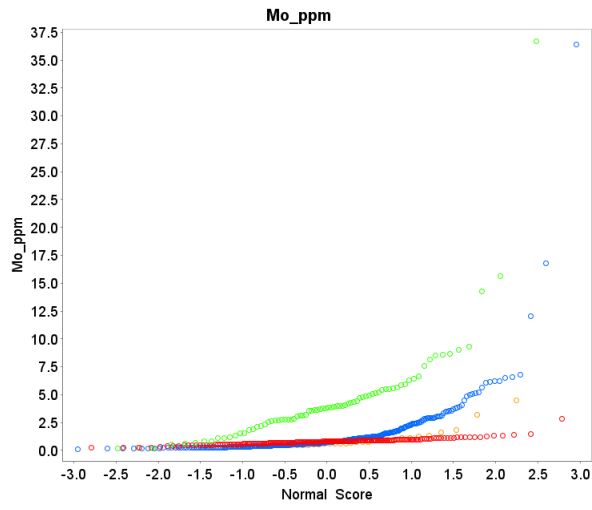


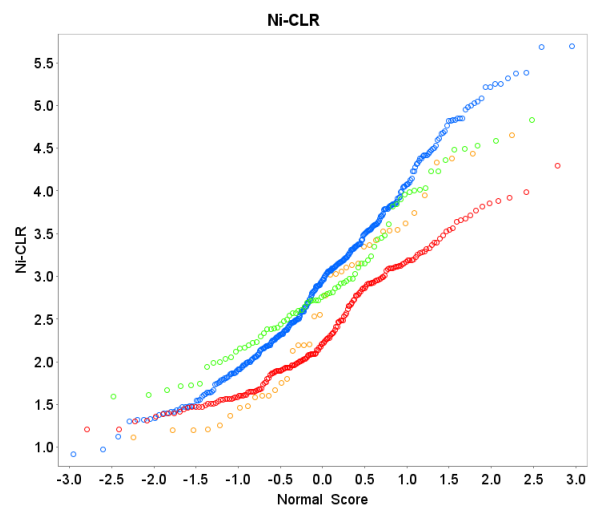
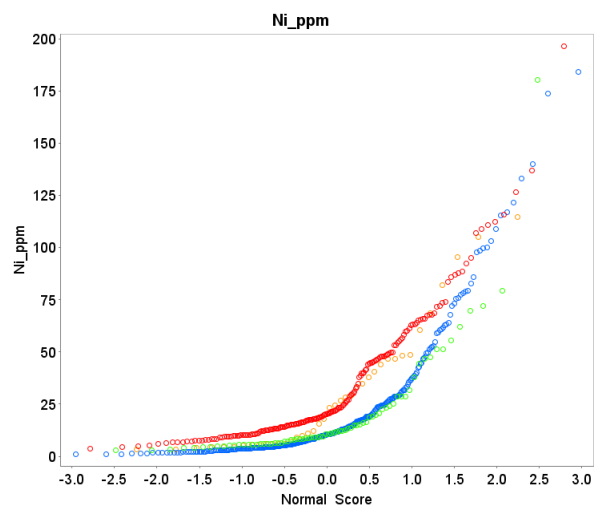
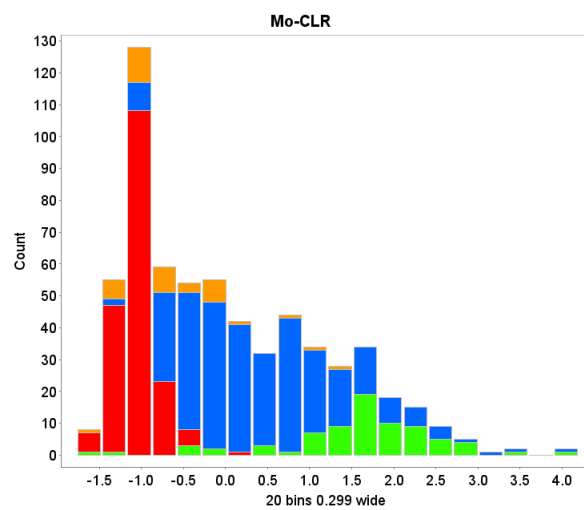
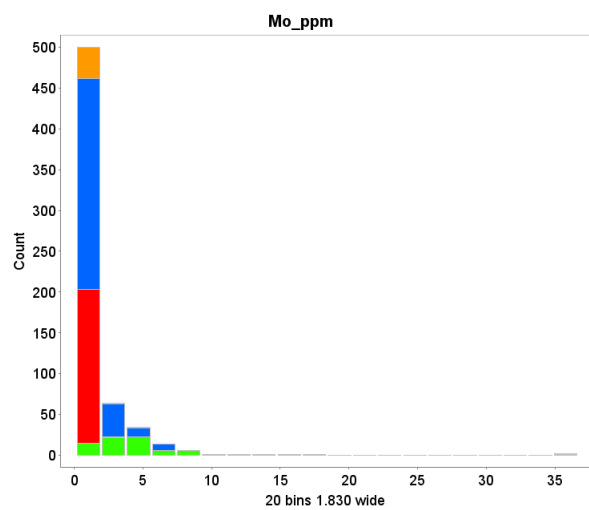


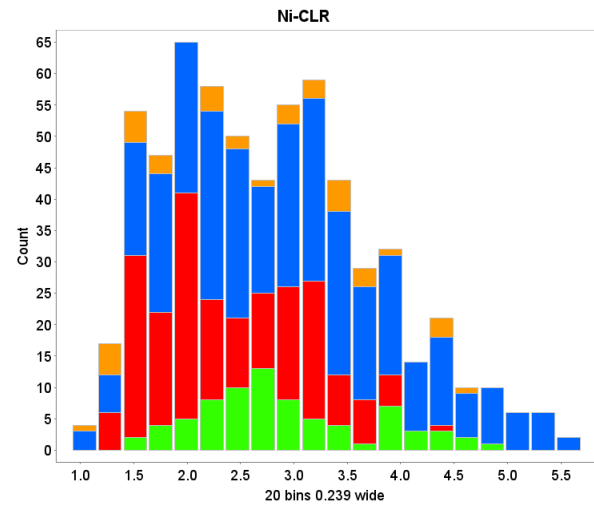
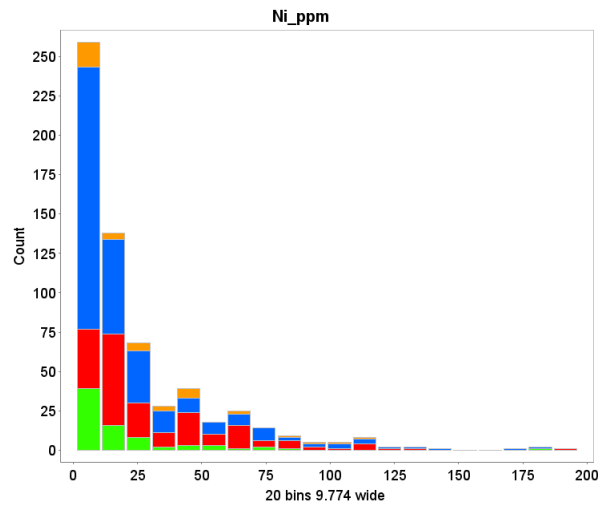
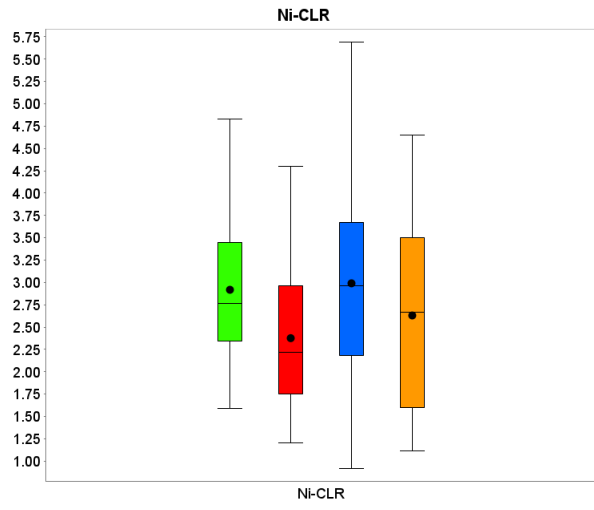
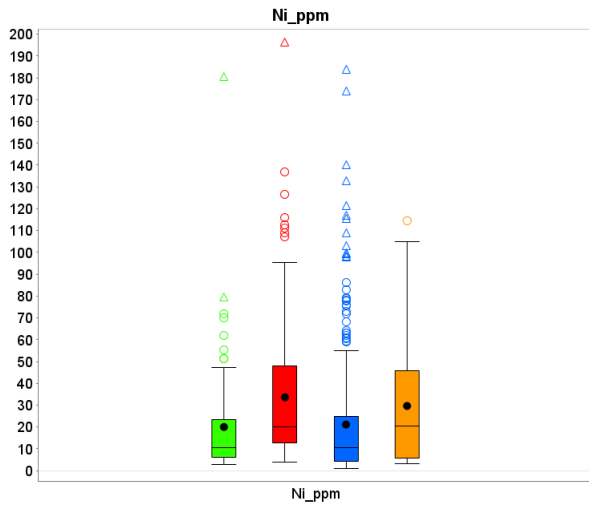


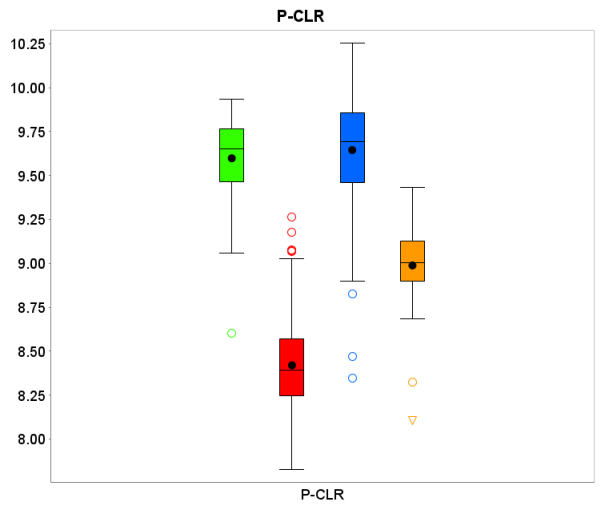
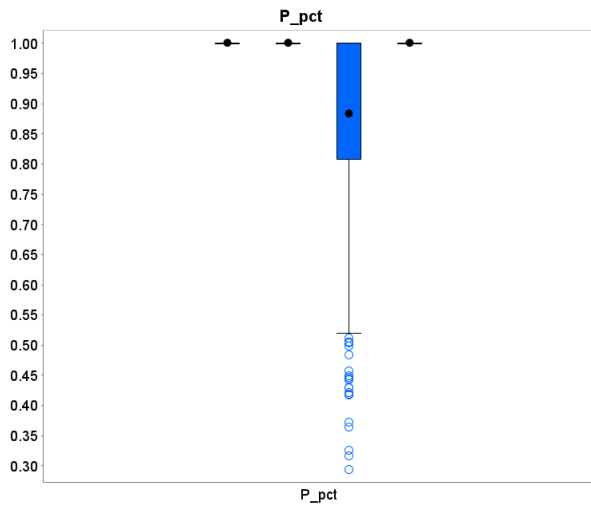
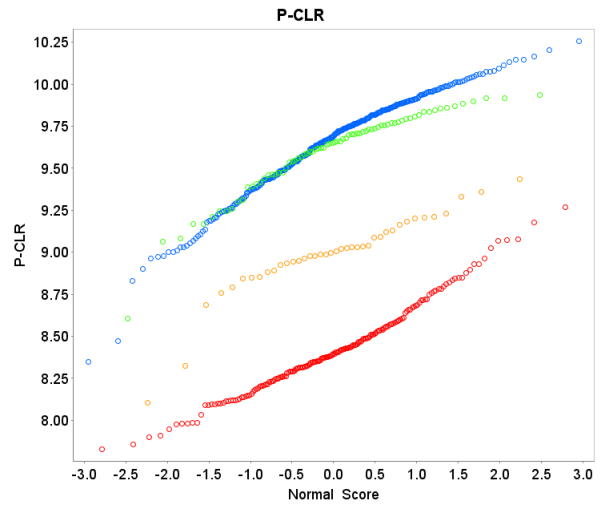
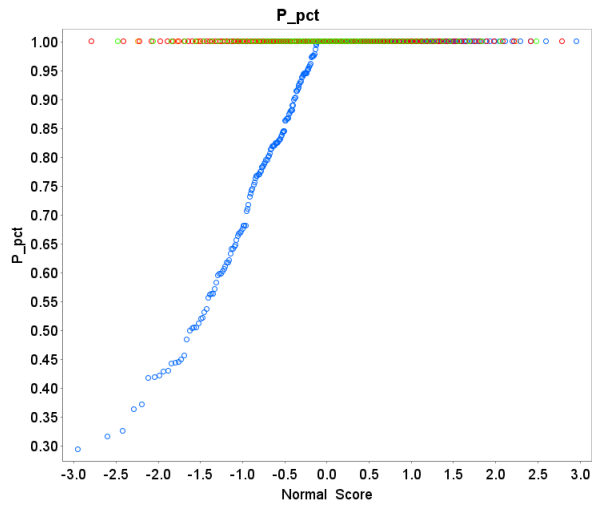


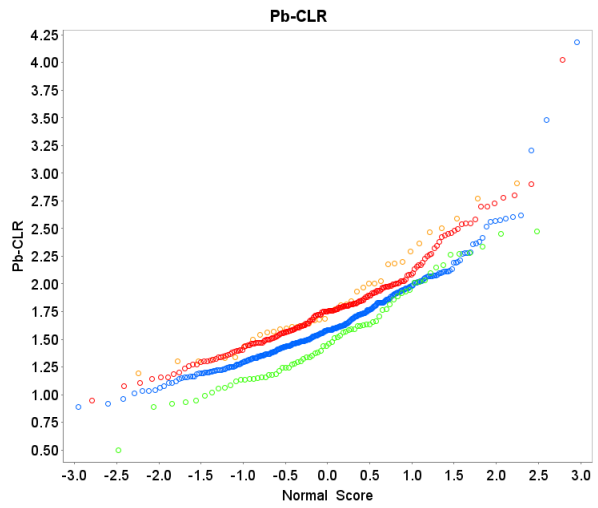
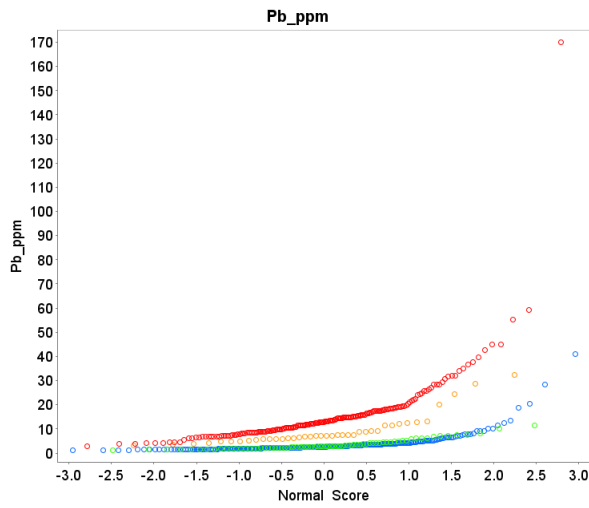
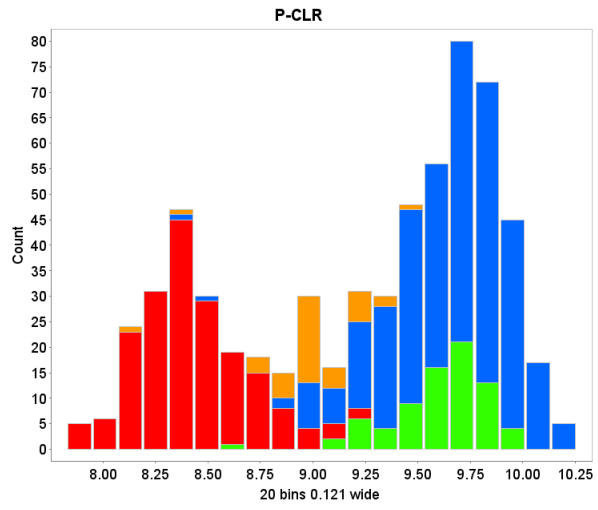
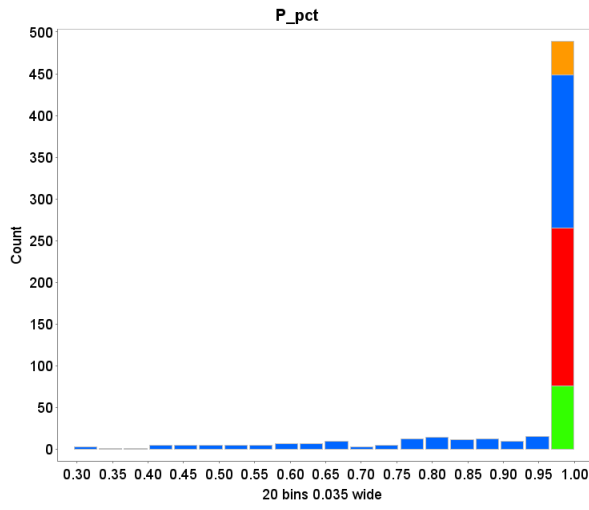


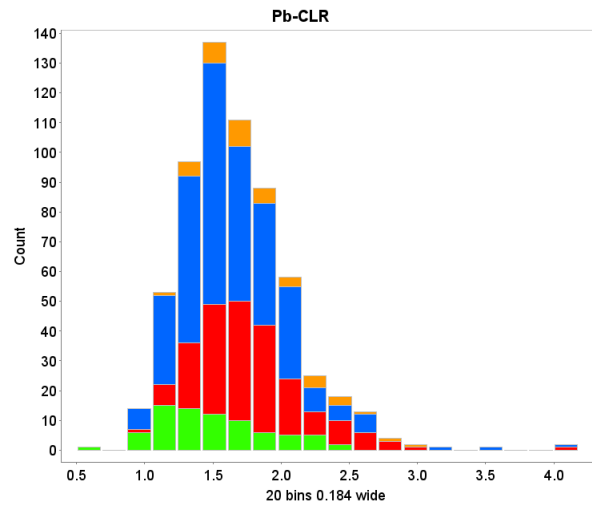
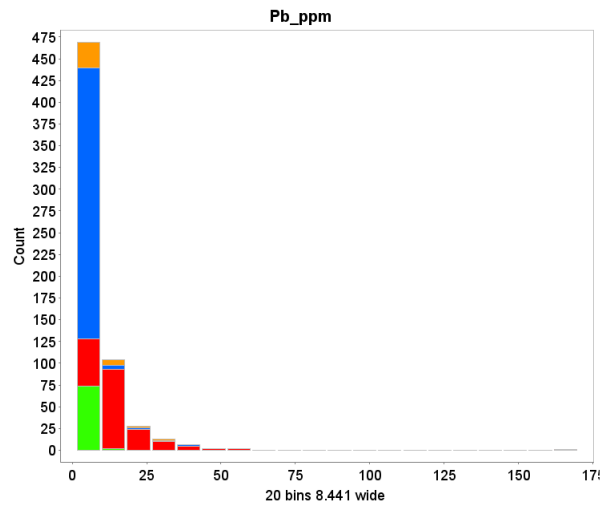
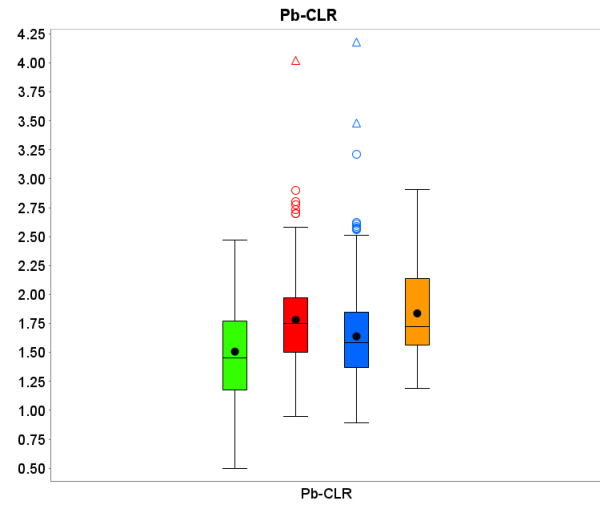
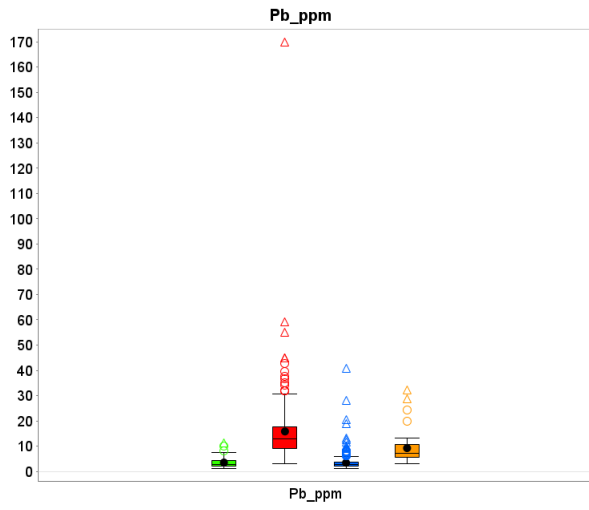


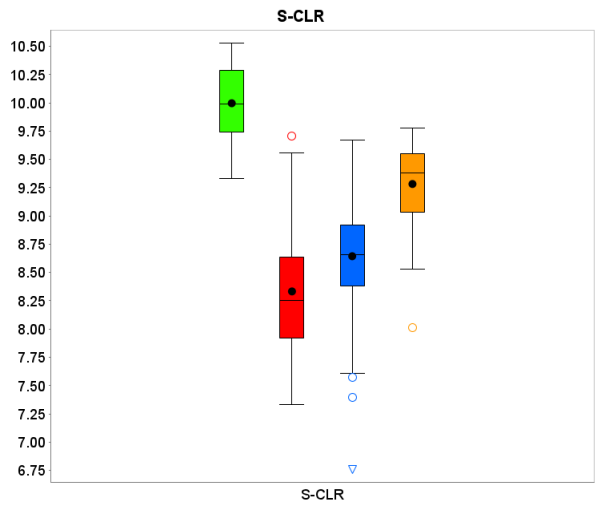
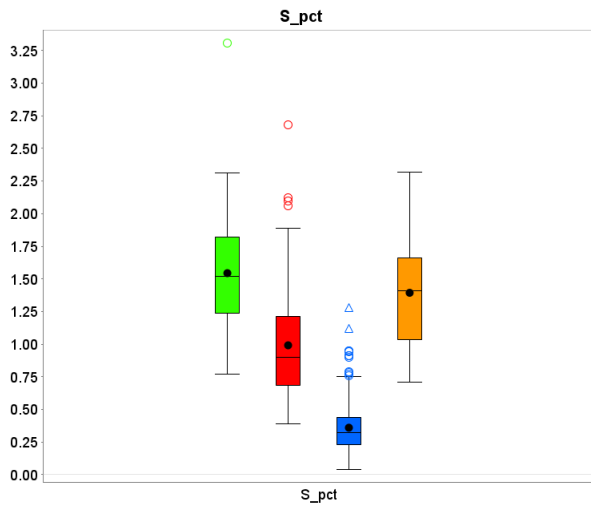
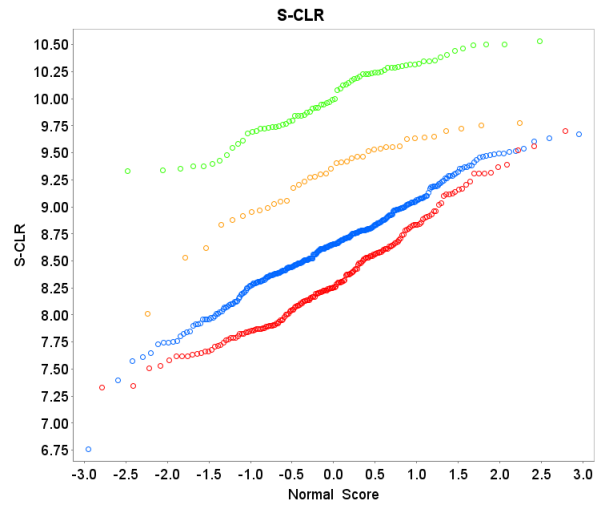
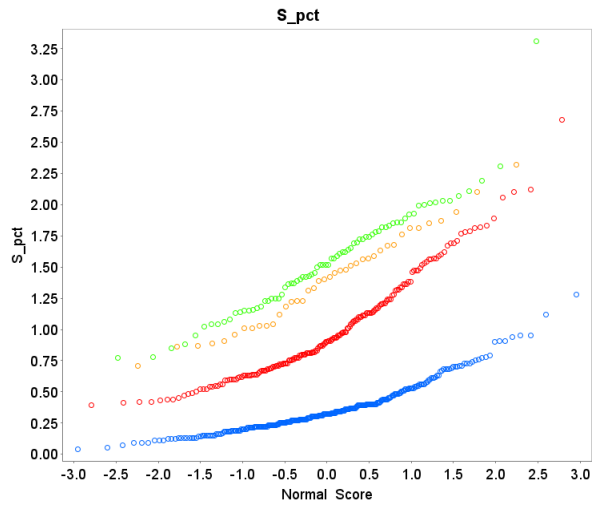


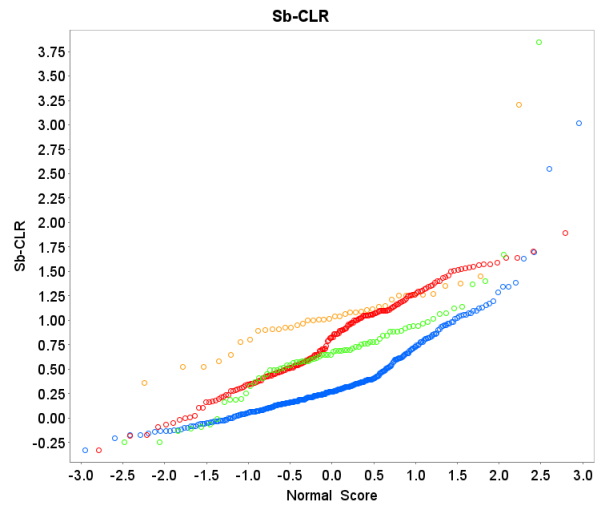
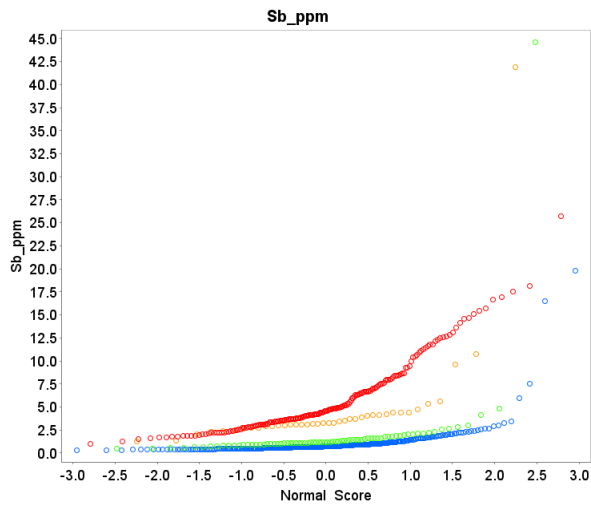
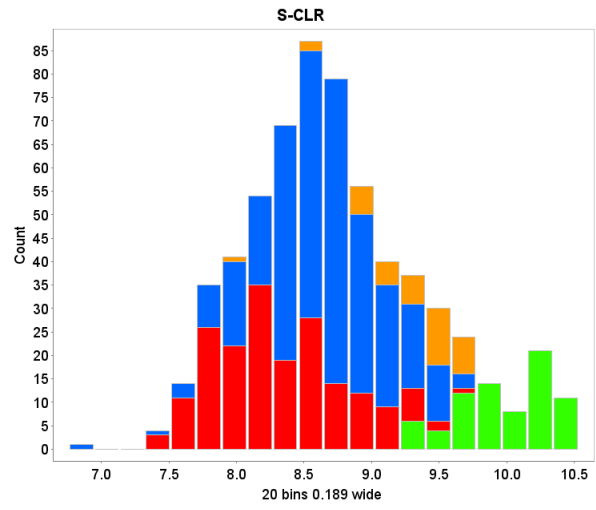
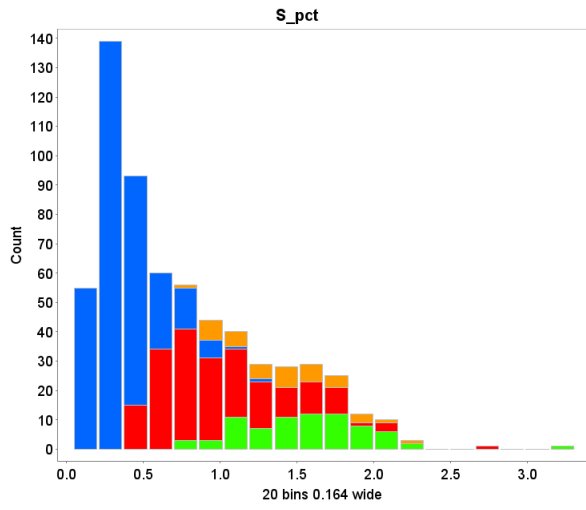


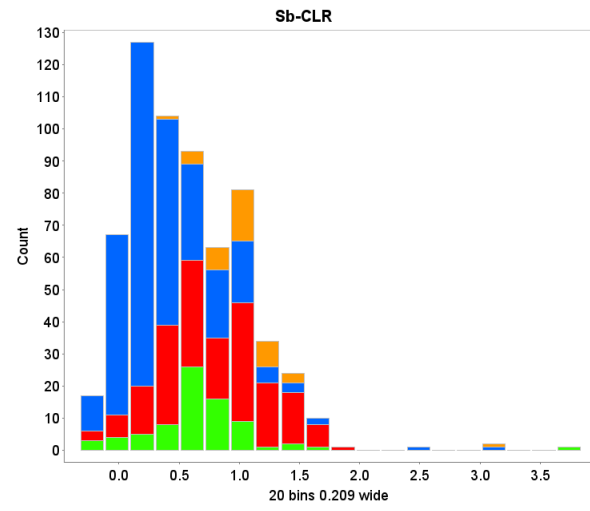
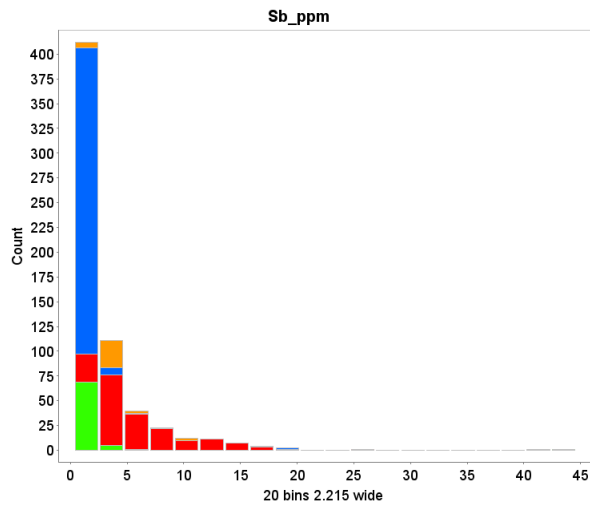
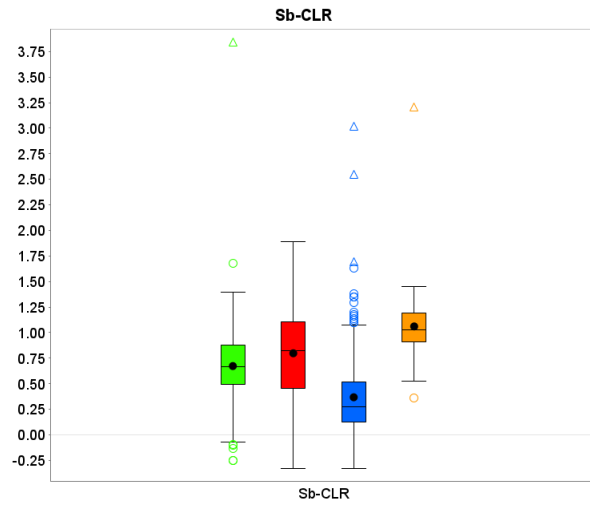
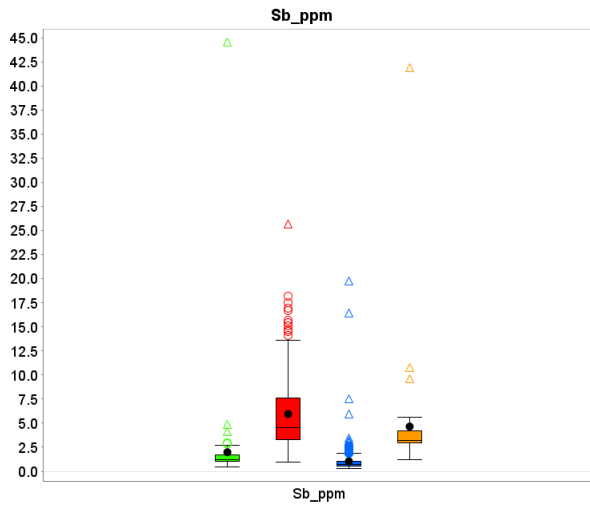


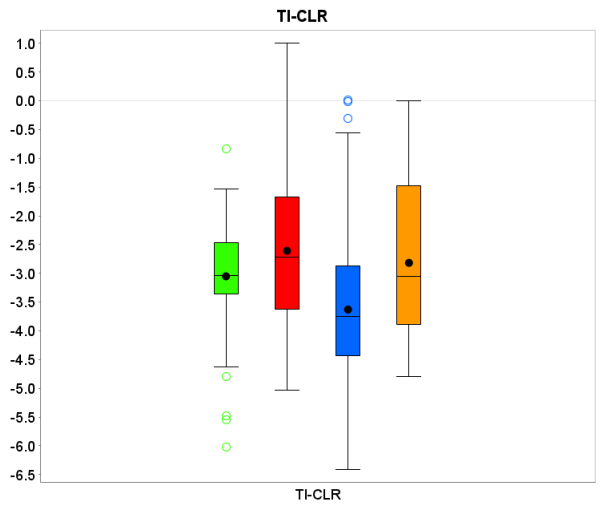
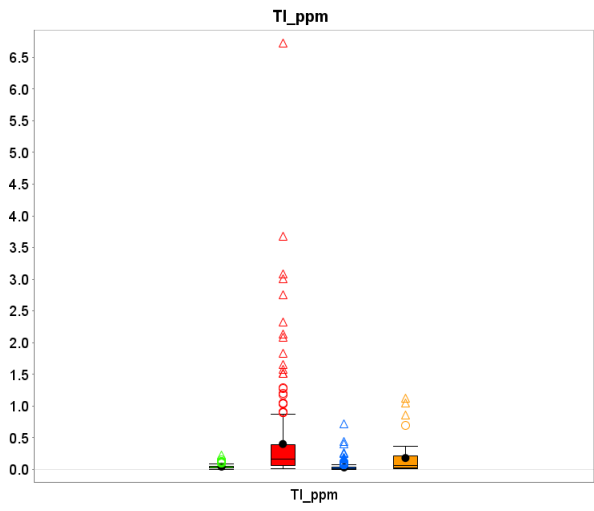
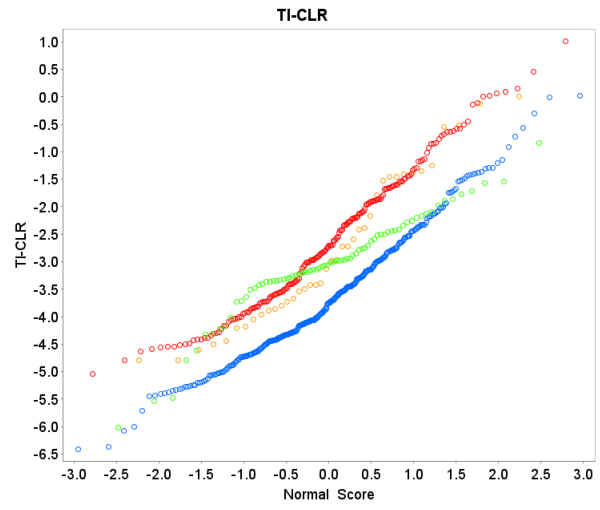
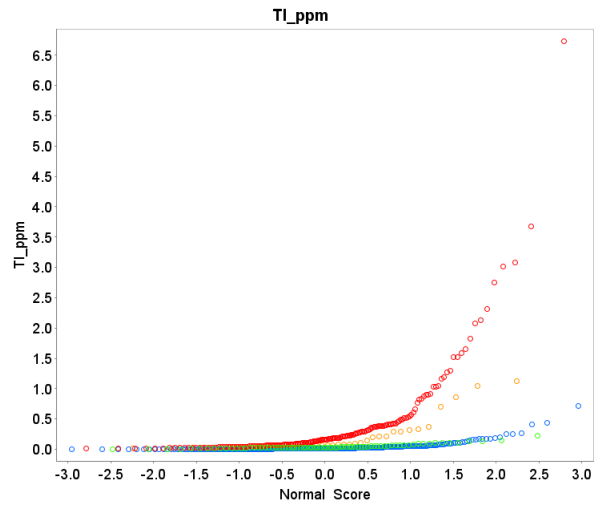


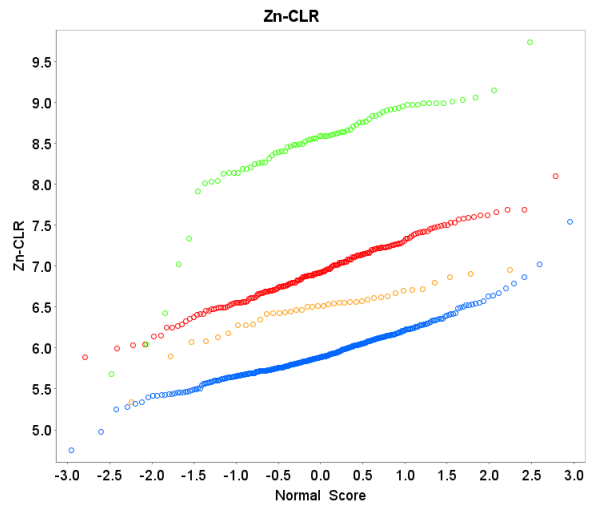
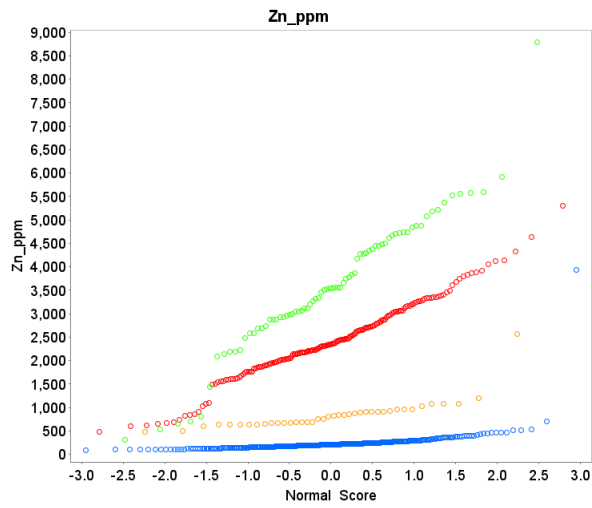
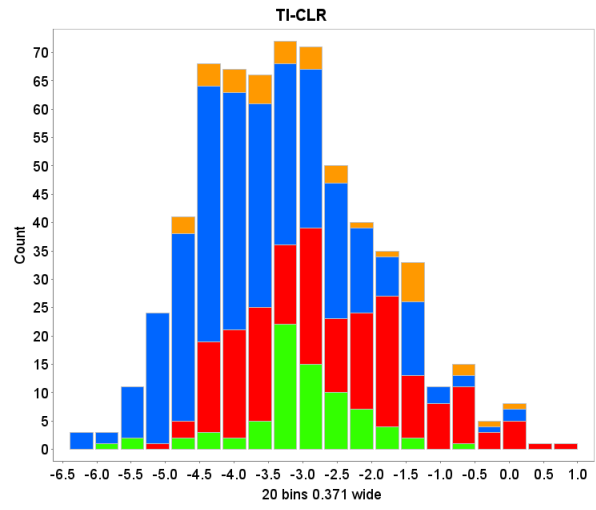
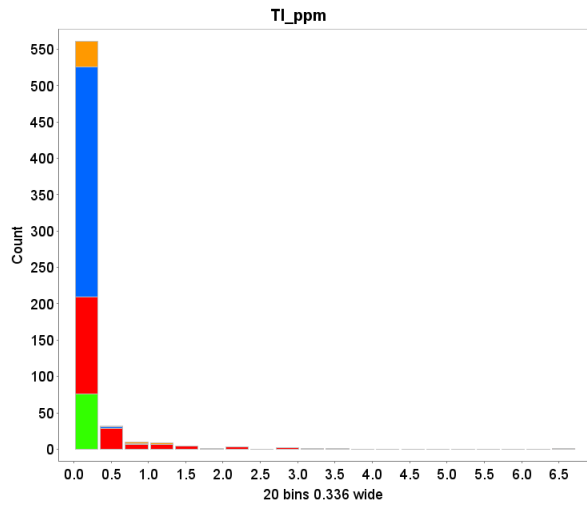


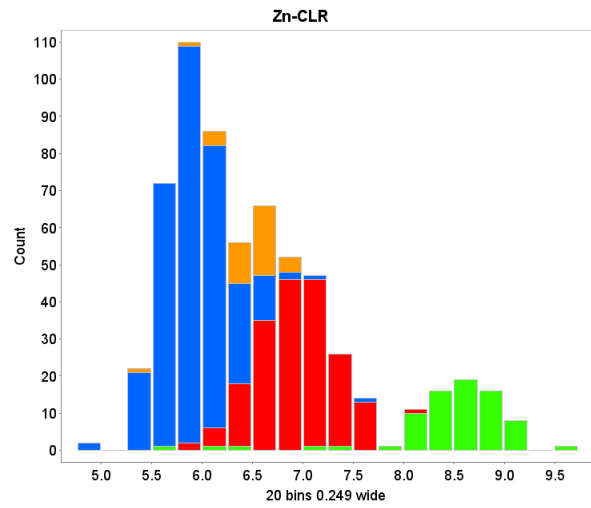
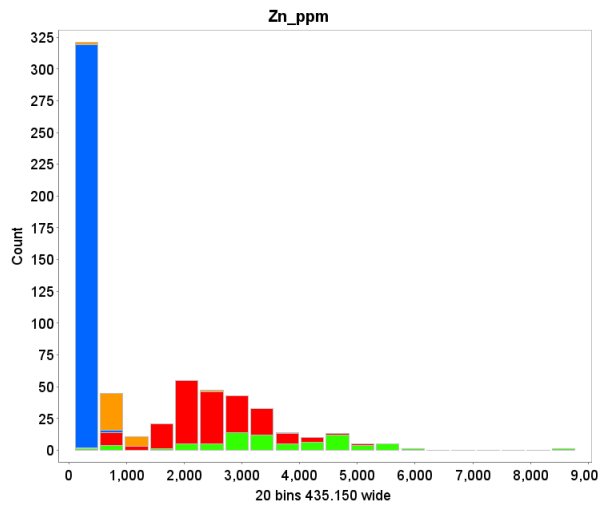
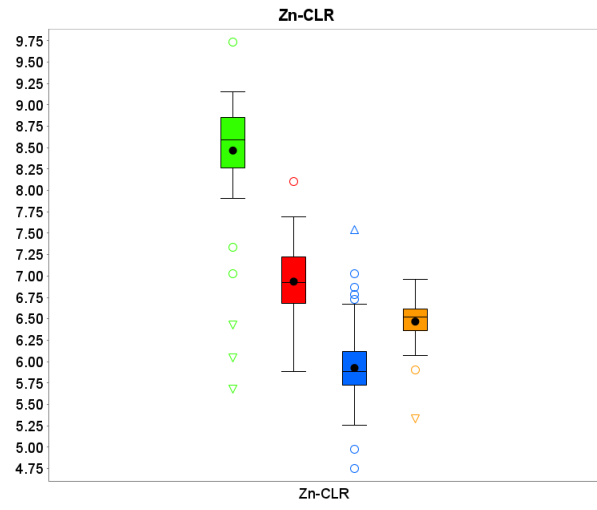
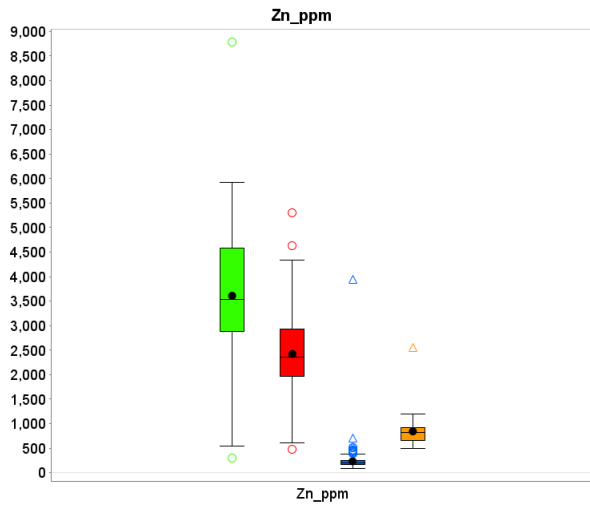






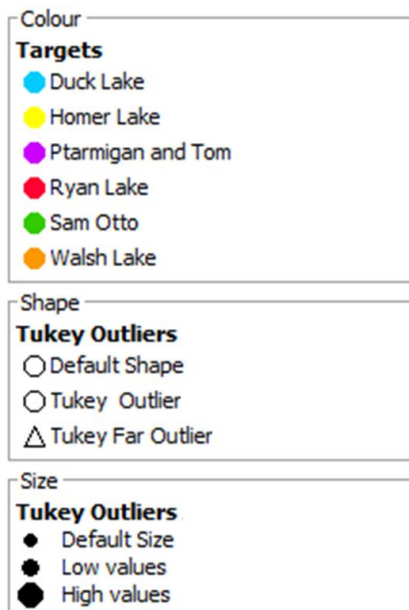


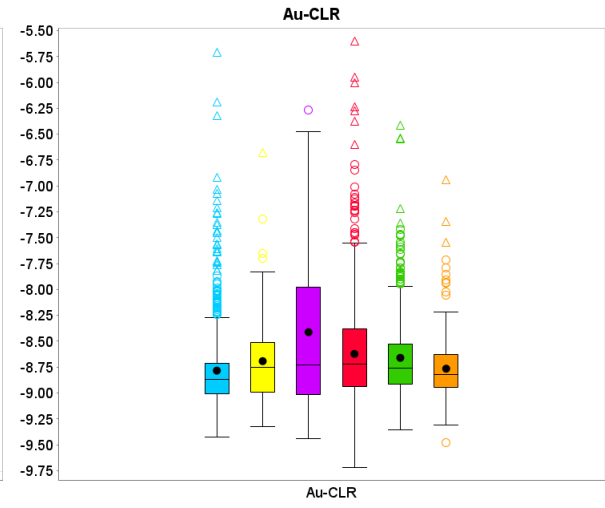
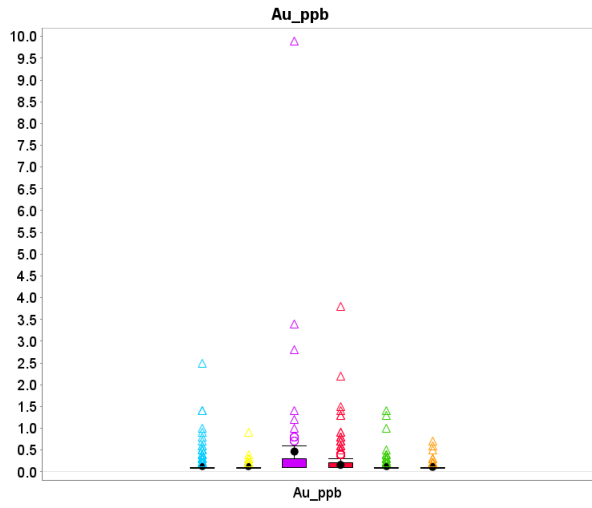
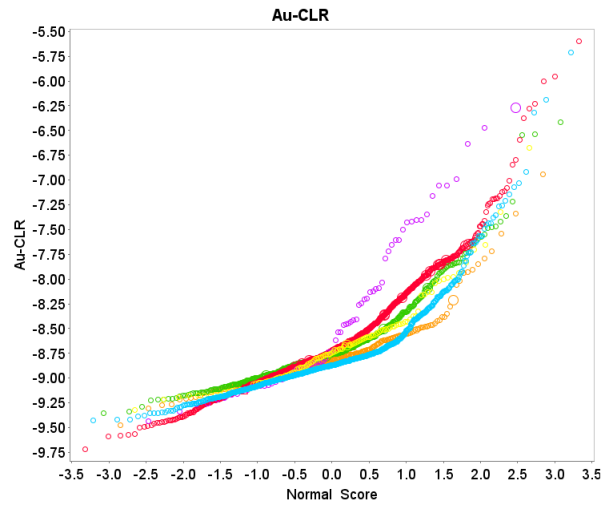
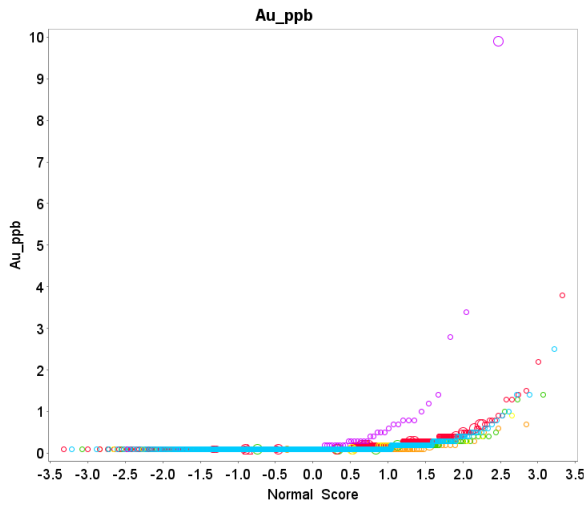


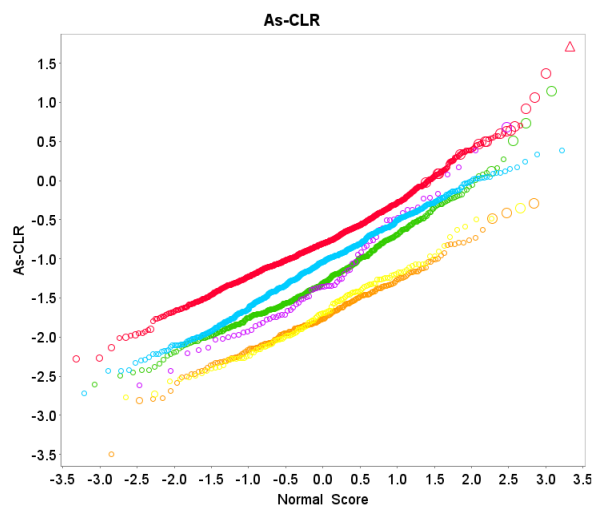
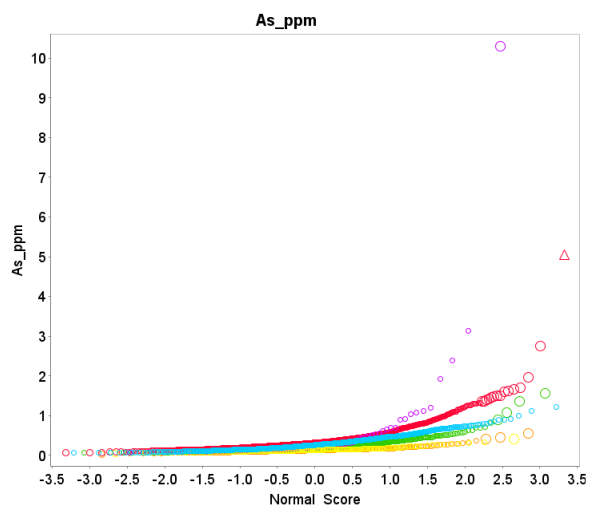
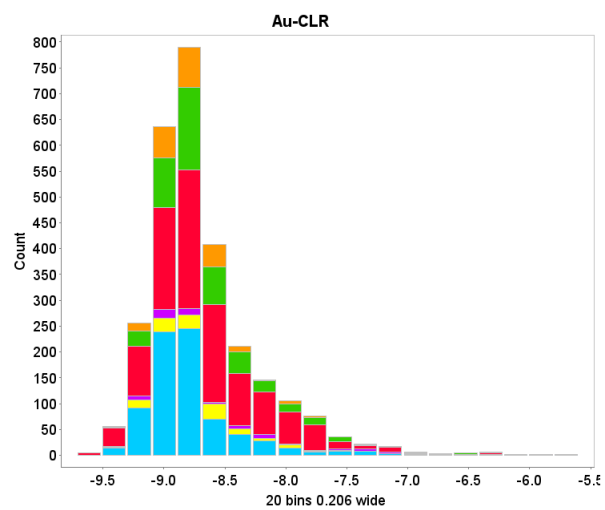
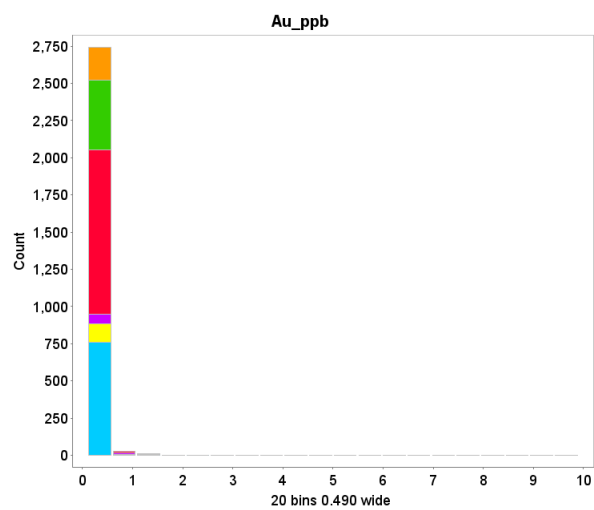


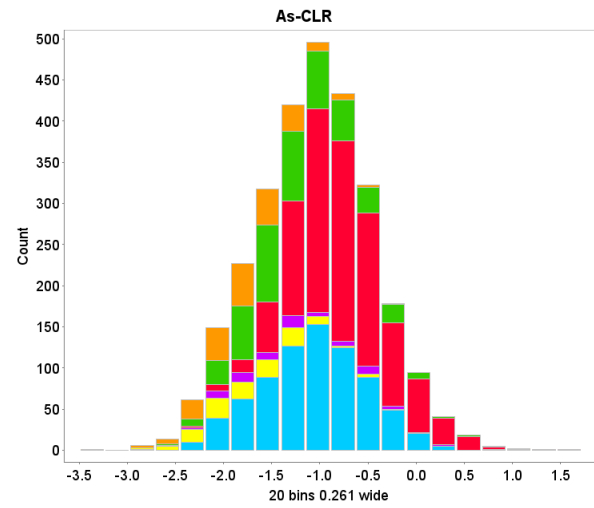
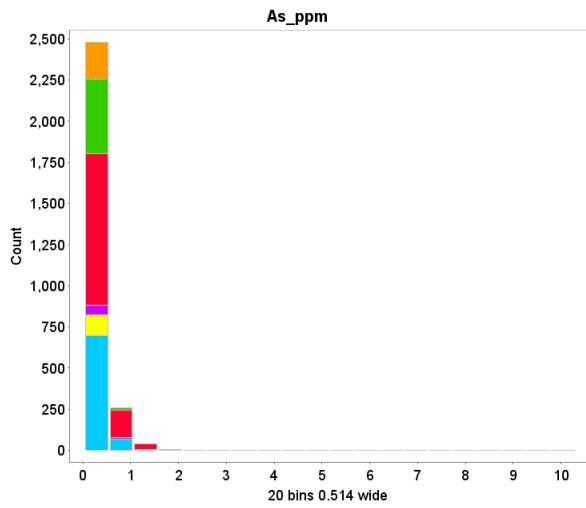
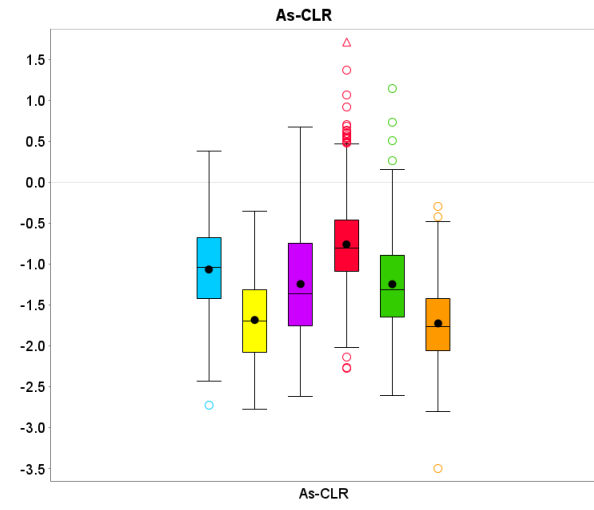
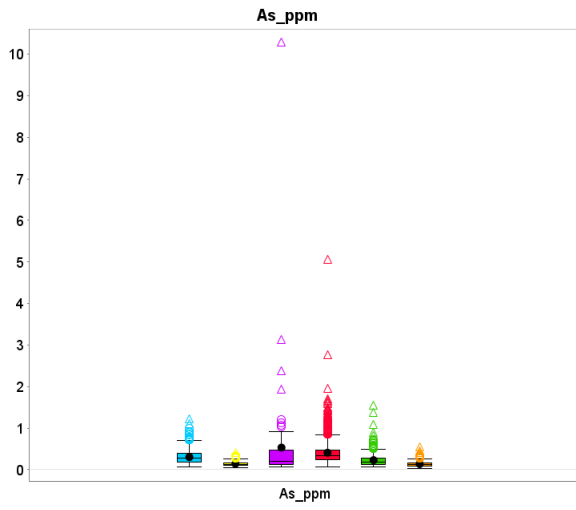
Appendix C

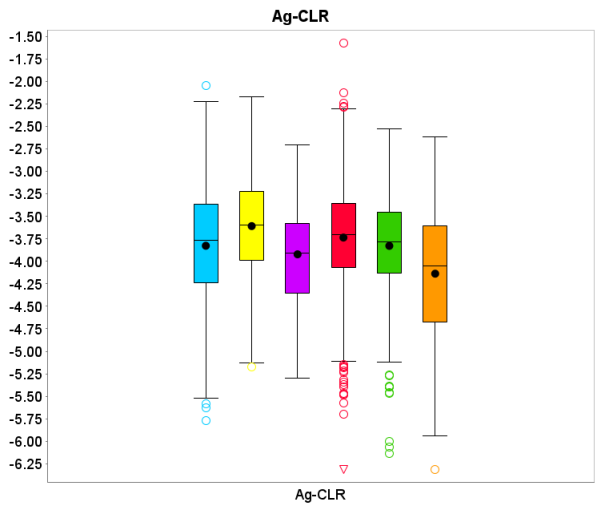
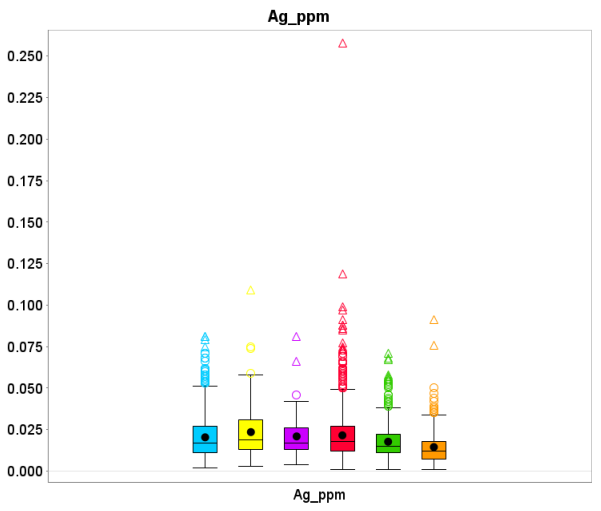
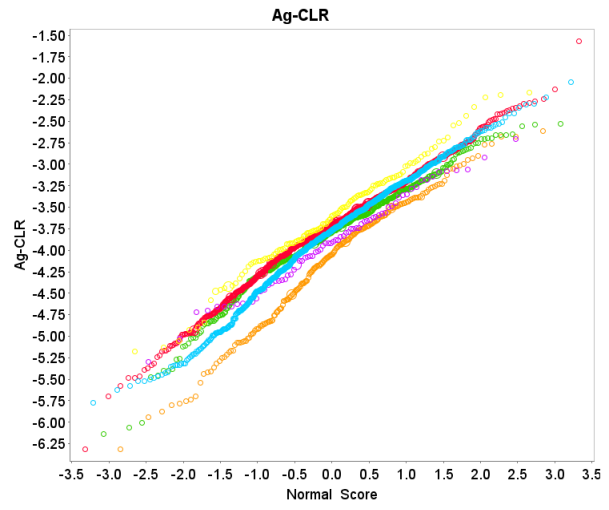
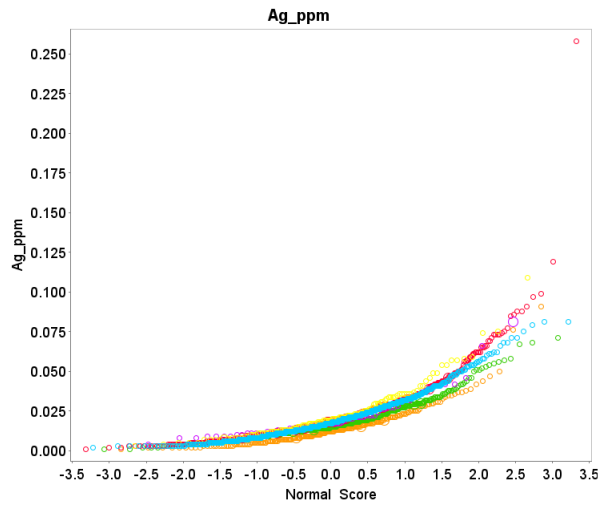
Appendix B compares the raw and transformed data of the Yellowknife City Gold project (YCGP, 2017) using probability plots, scatter plots and histograms. The plots on the right demonstrate the raw data distribution for each element. On the left side, data distribution is normalized using center log-ratio (CLR) transformation. Tukey method was used to show the outliers (circles) and extreme or far outliers (triangles). The figure below shows the legend.

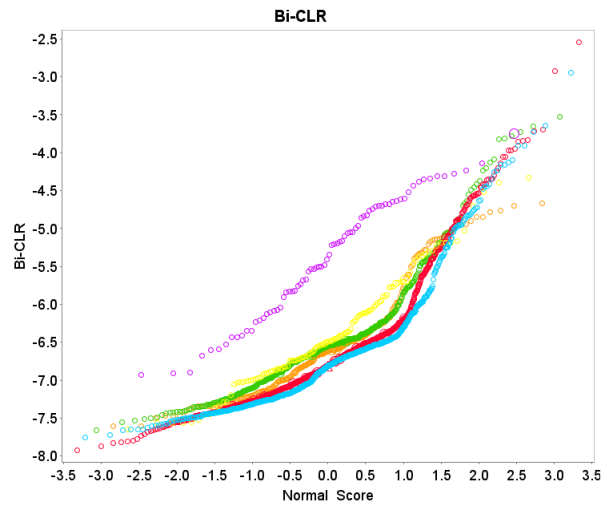
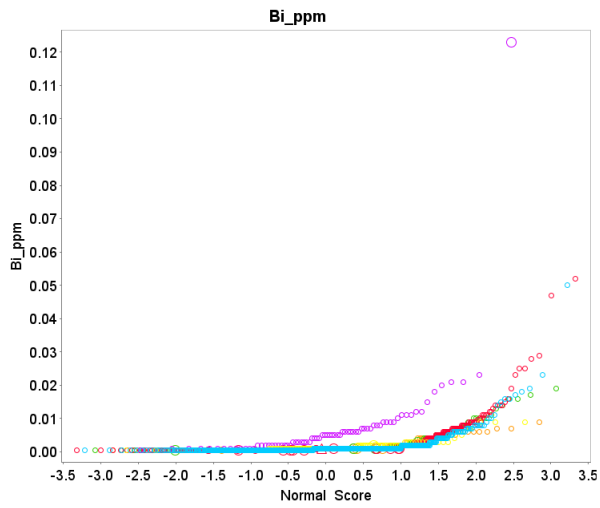
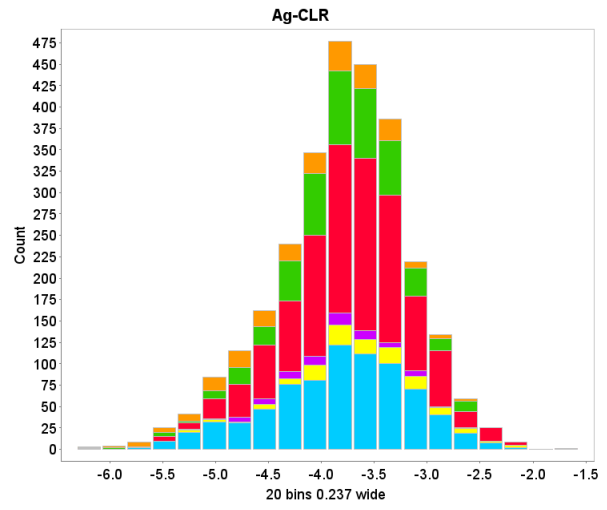
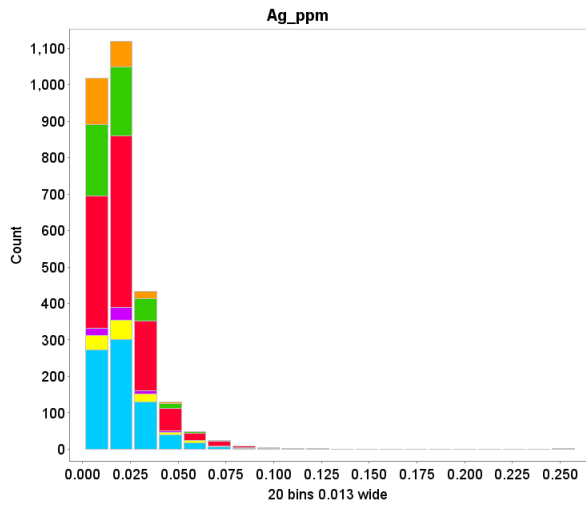


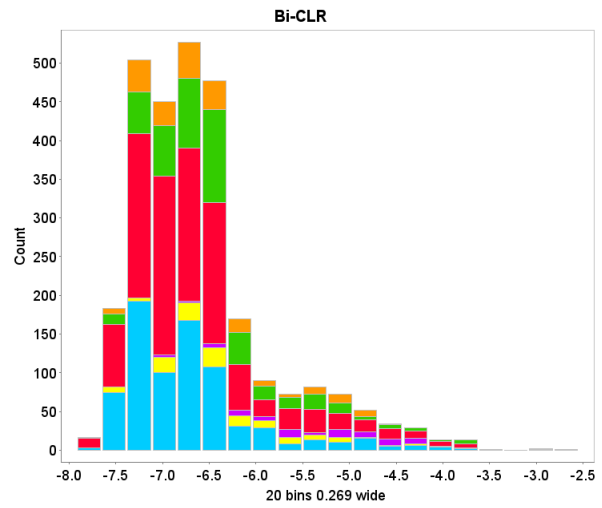
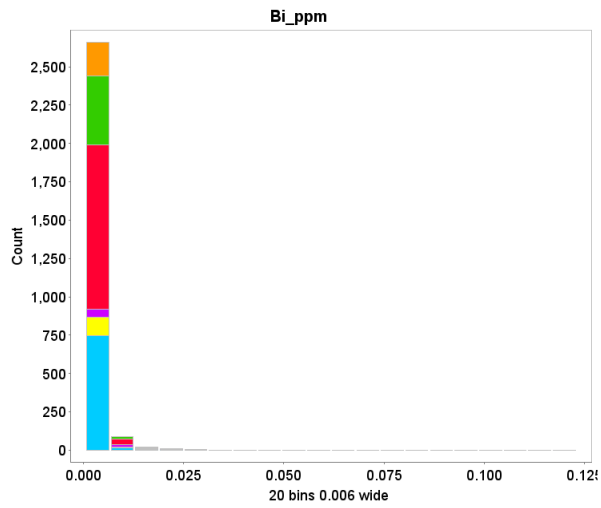
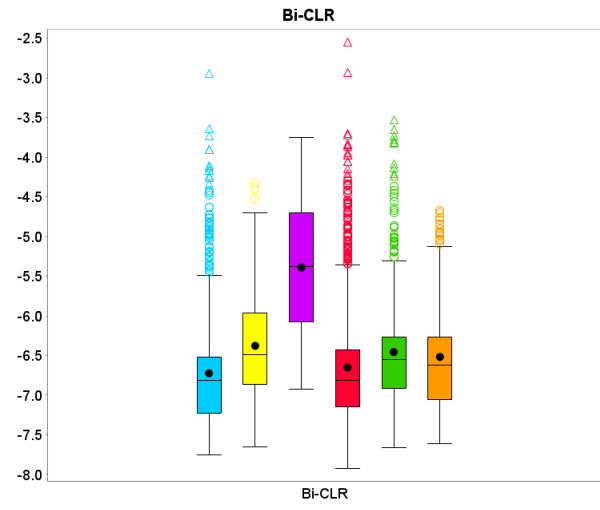
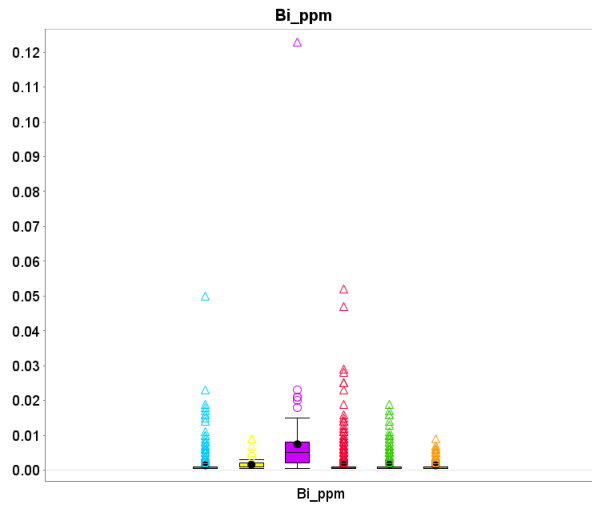


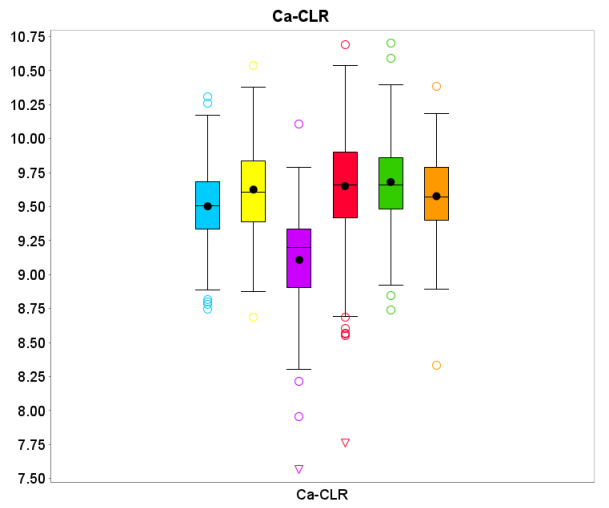
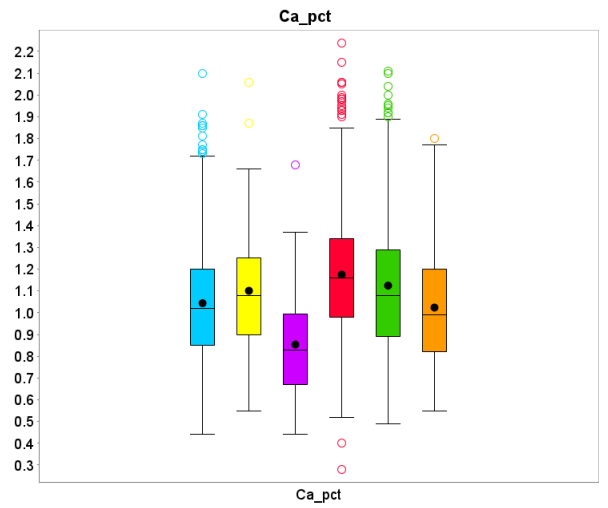
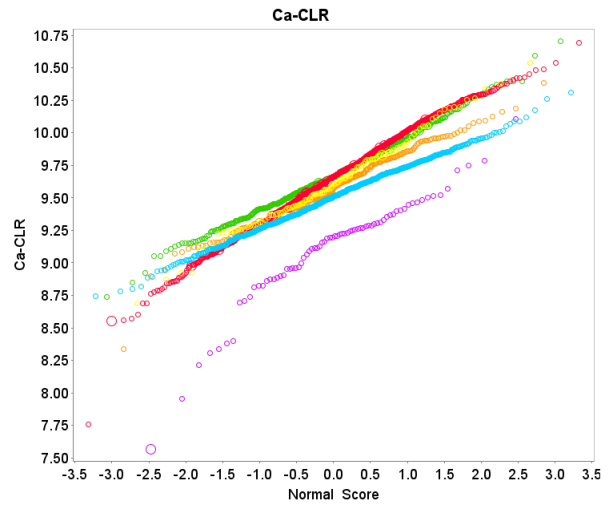
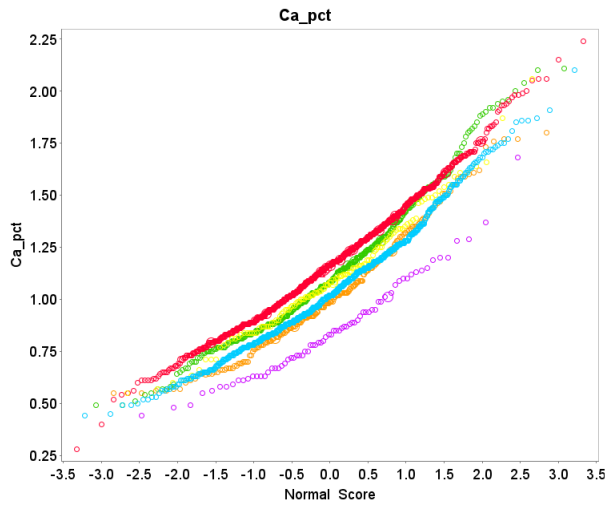


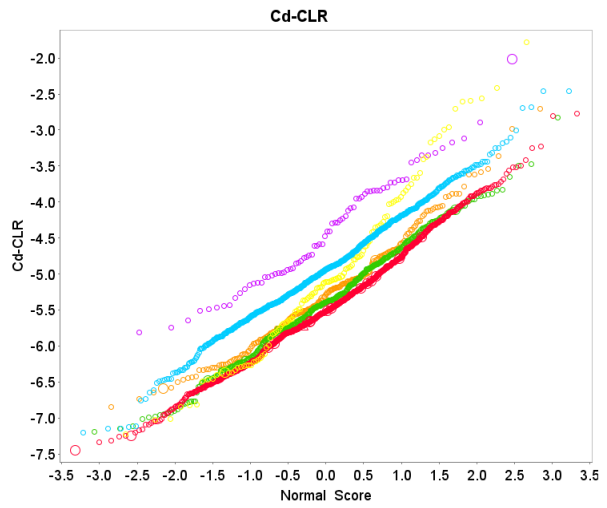
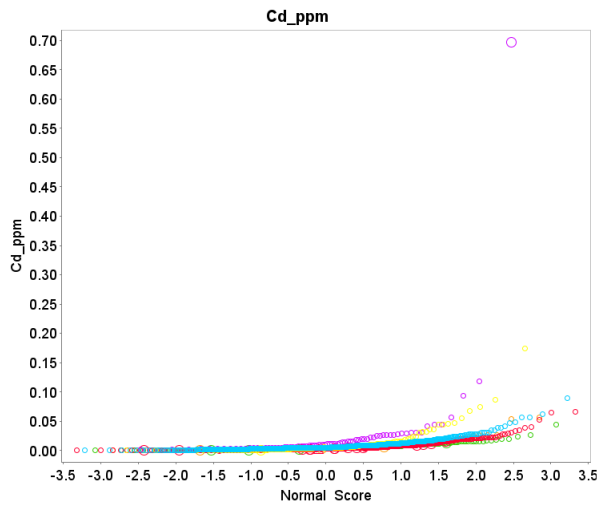
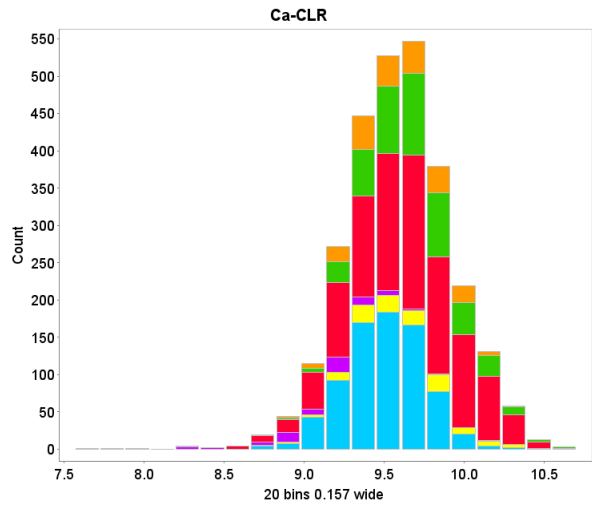
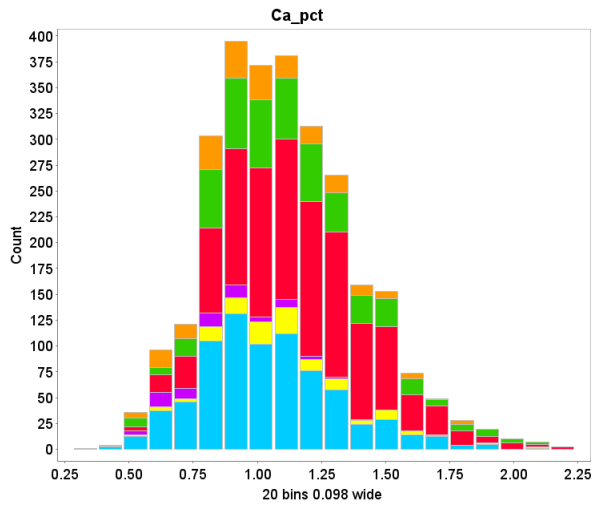


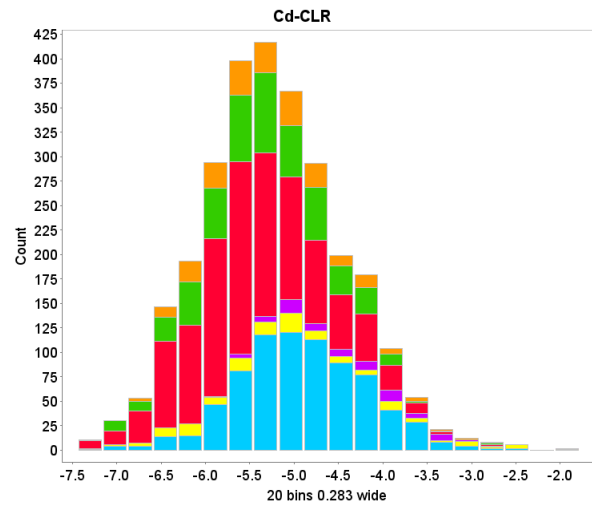
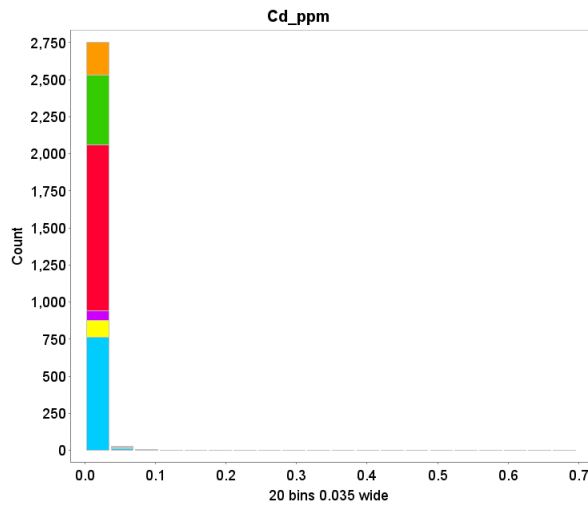
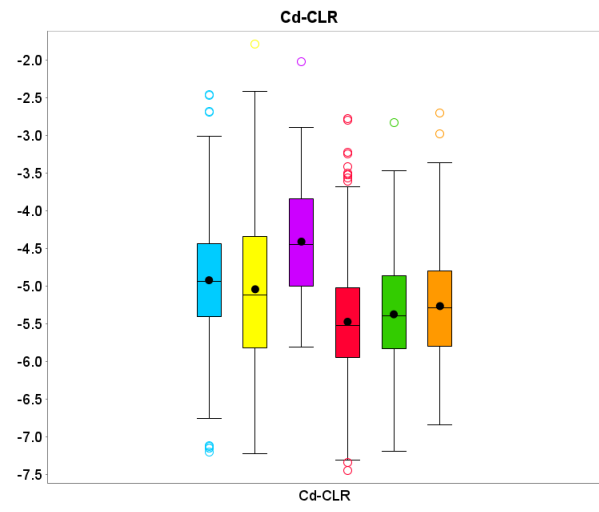
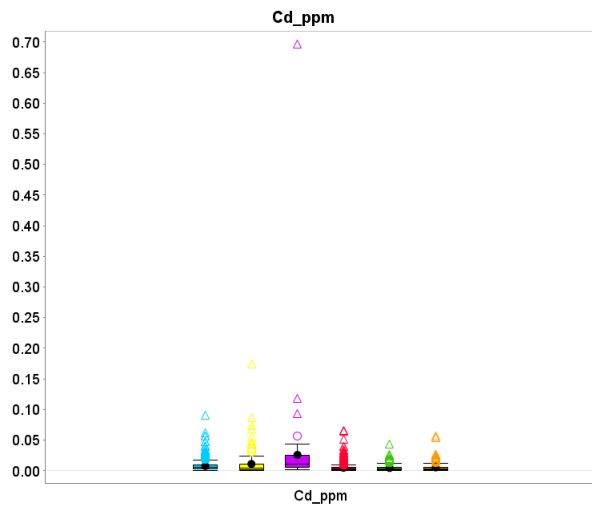


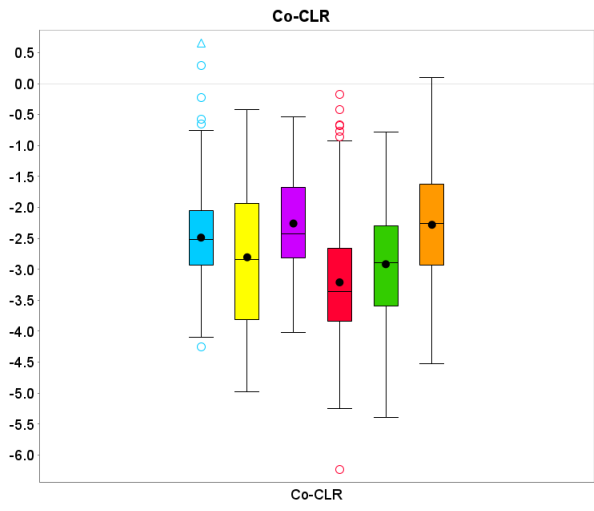
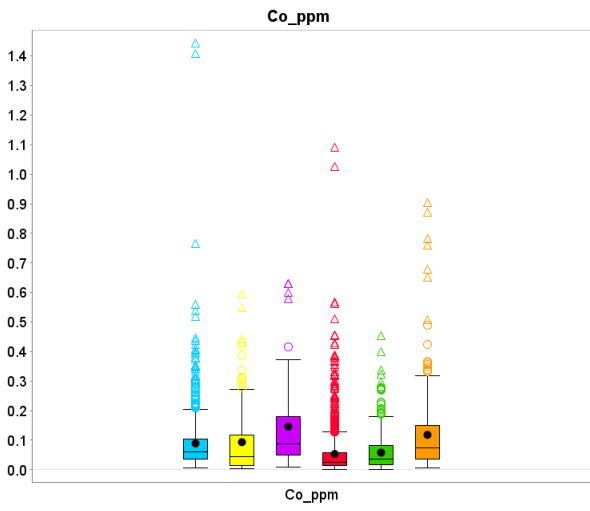
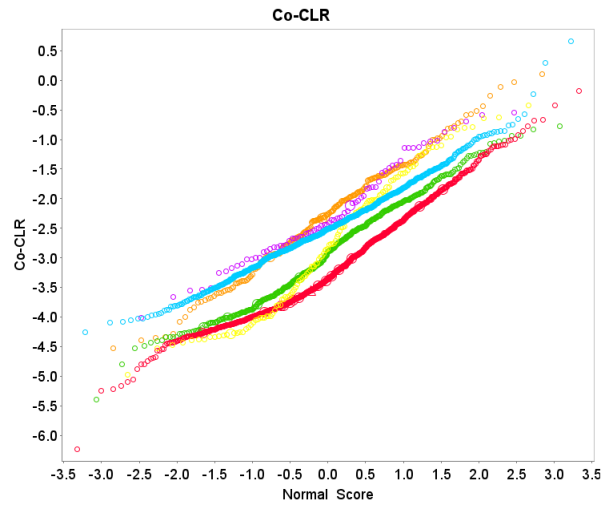
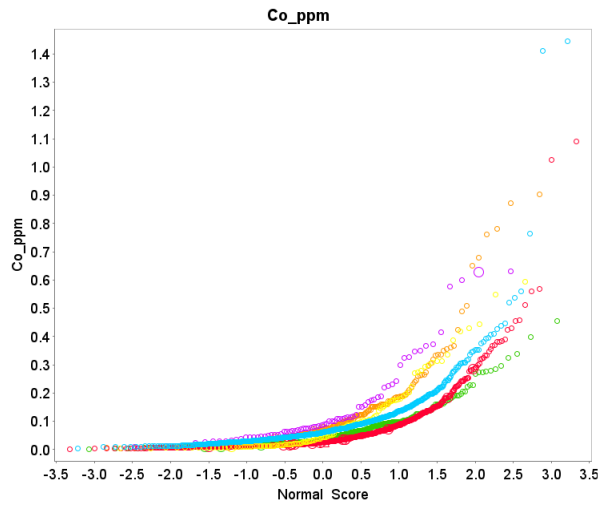


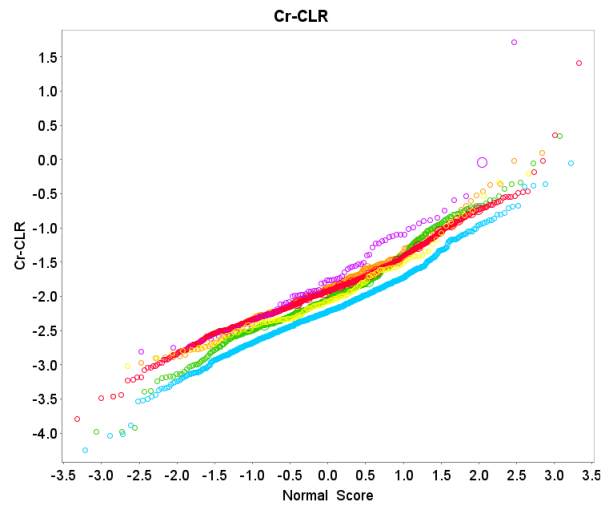
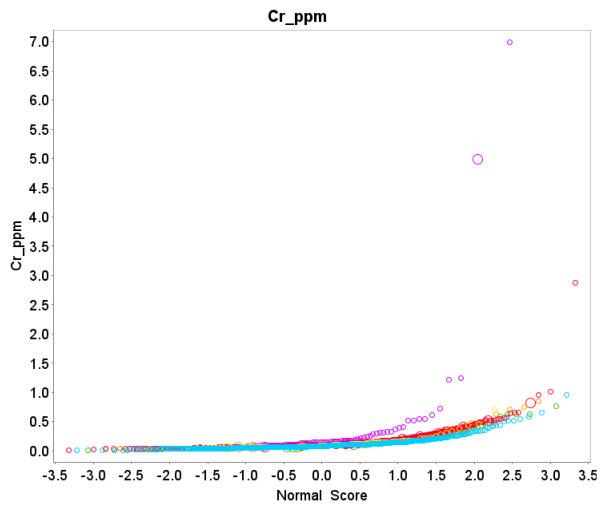
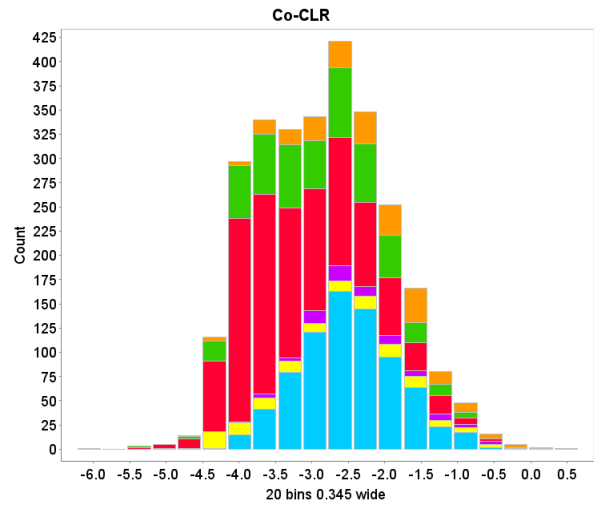
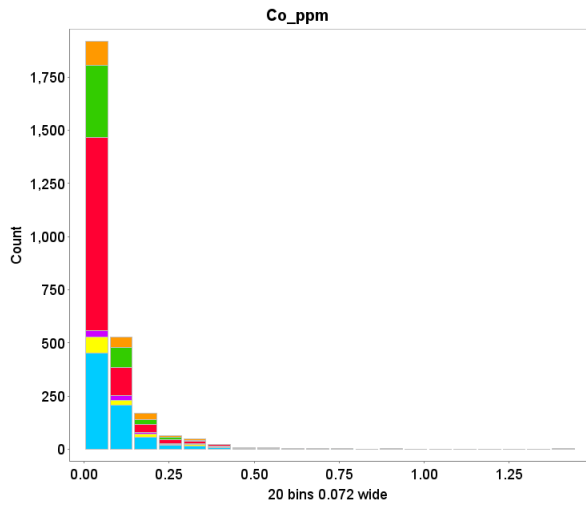


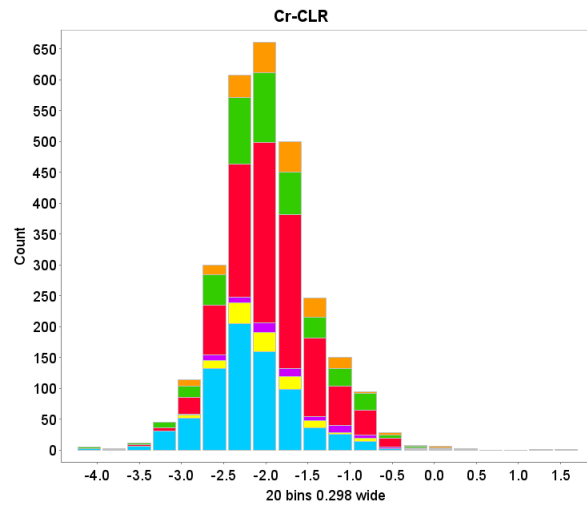
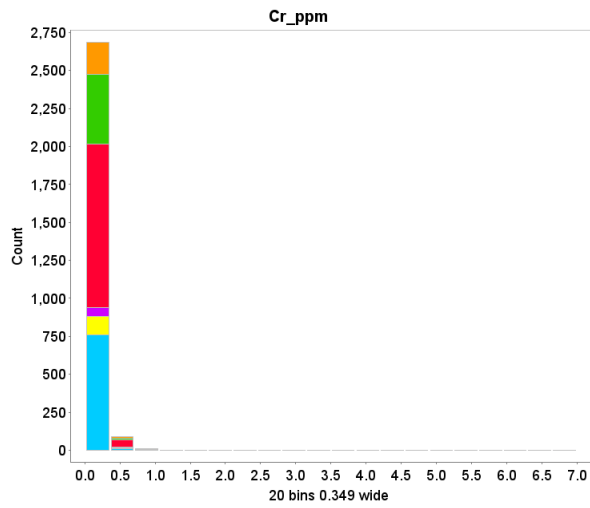
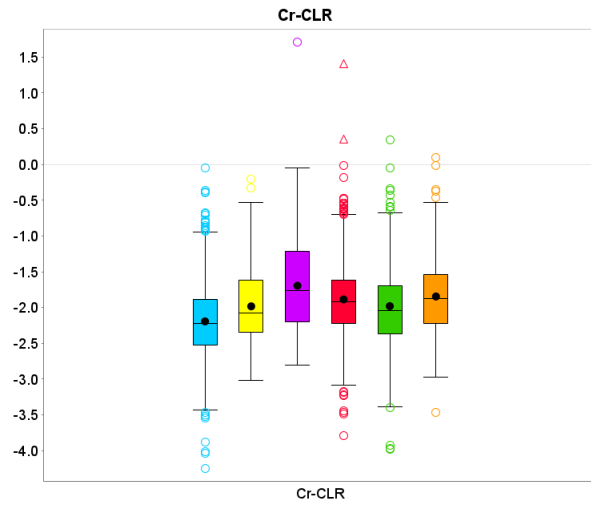
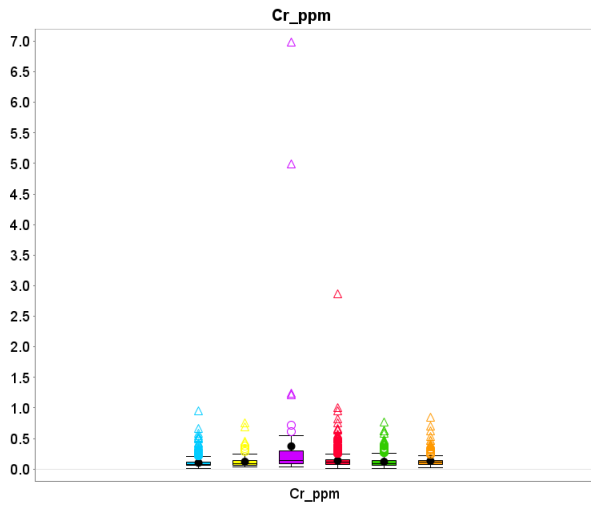


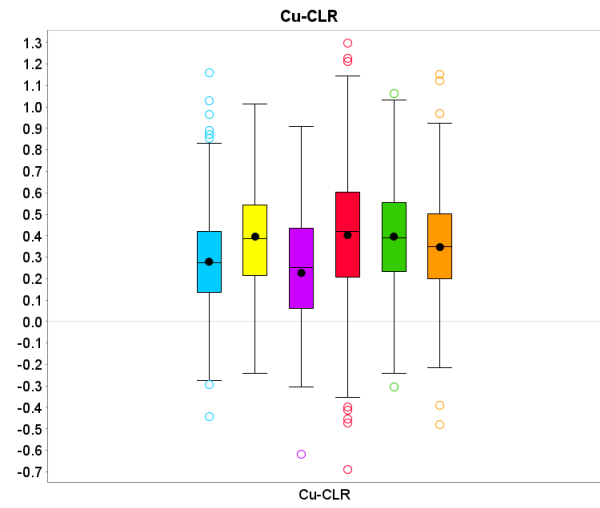
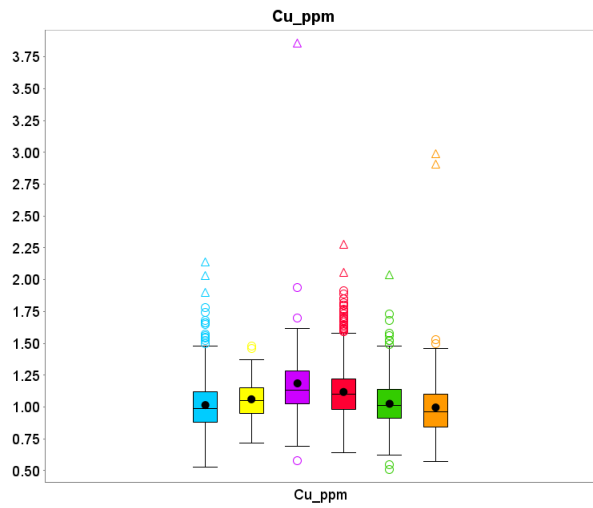
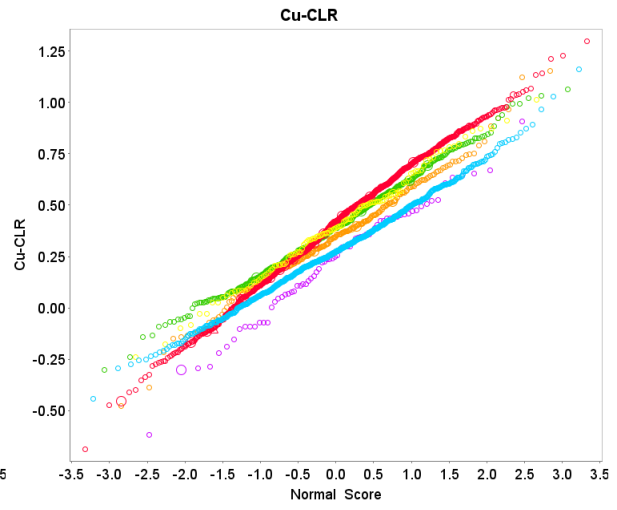
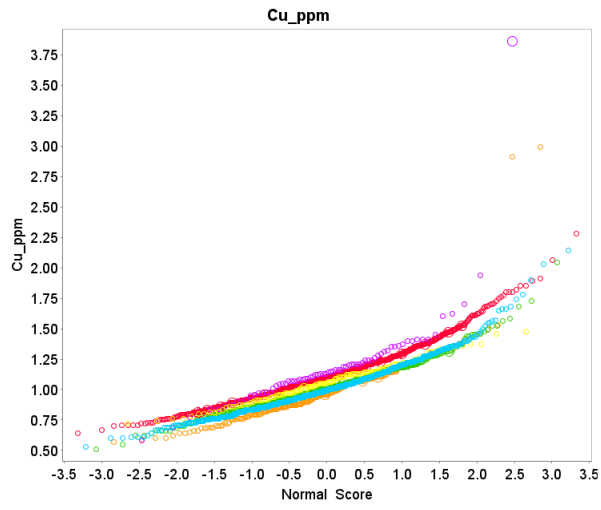


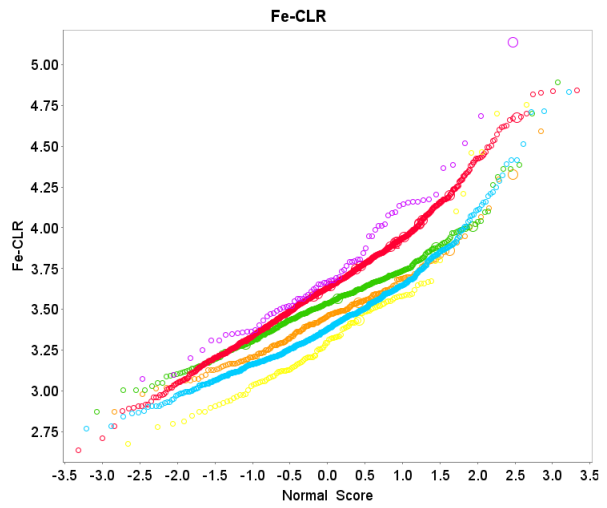
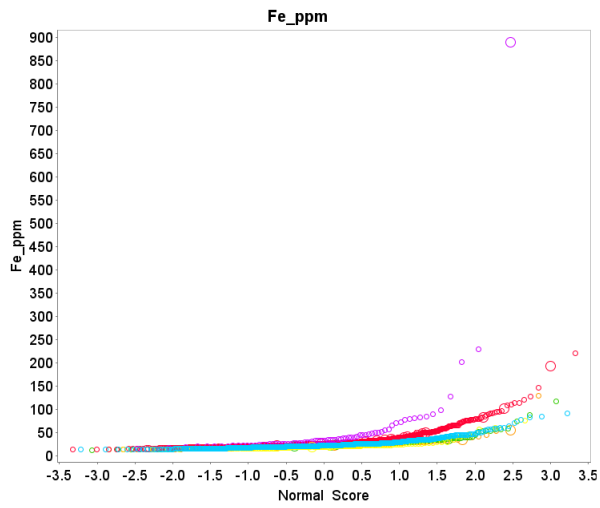
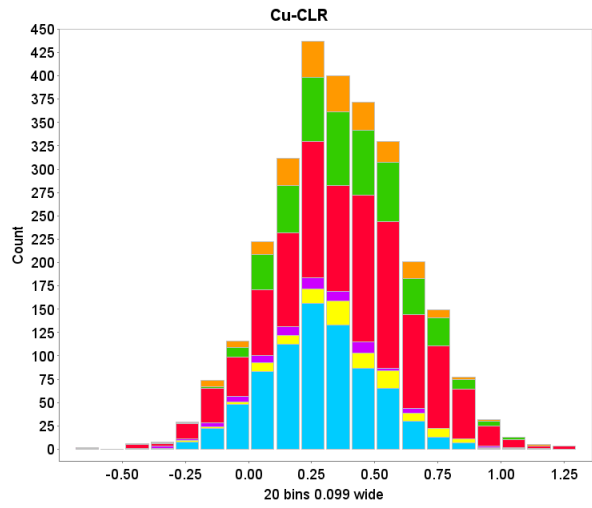
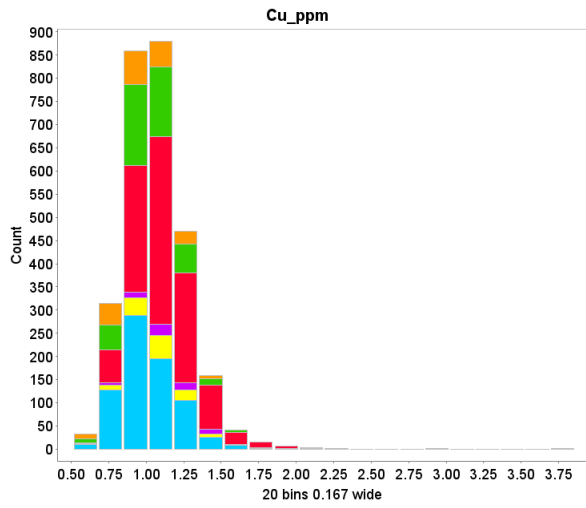


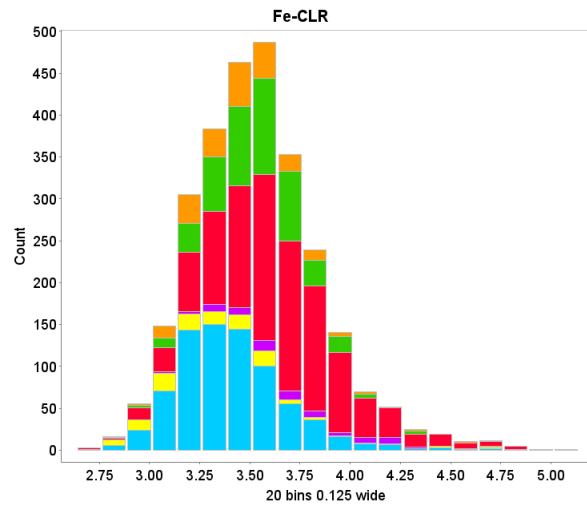
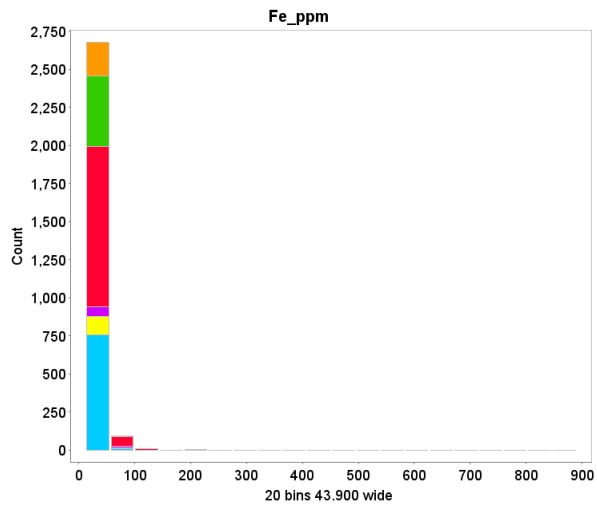
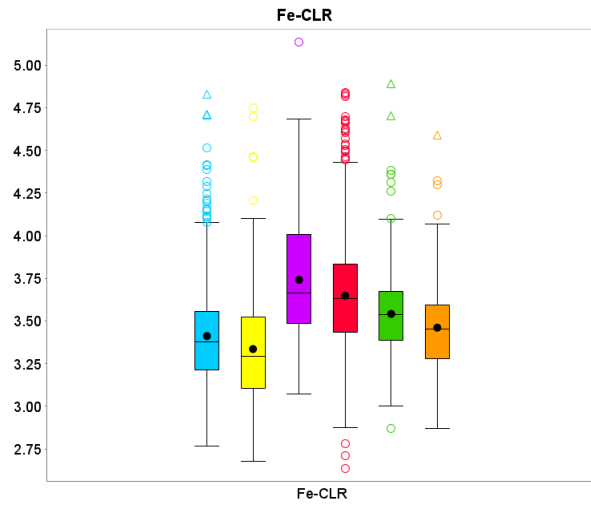
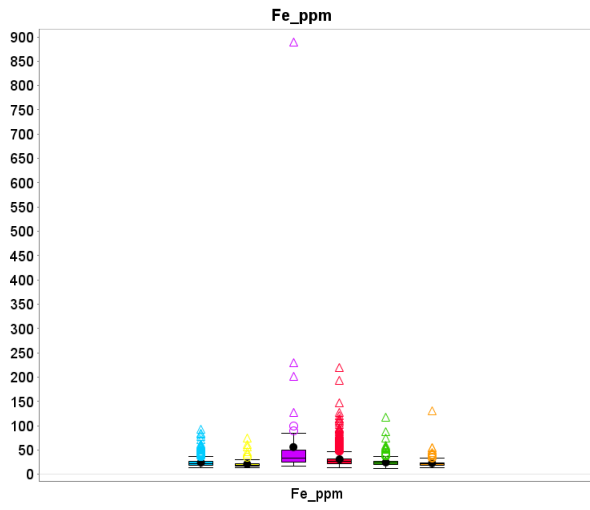


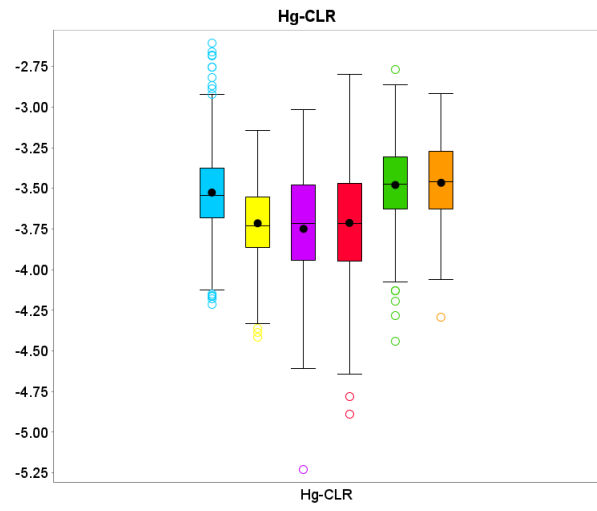
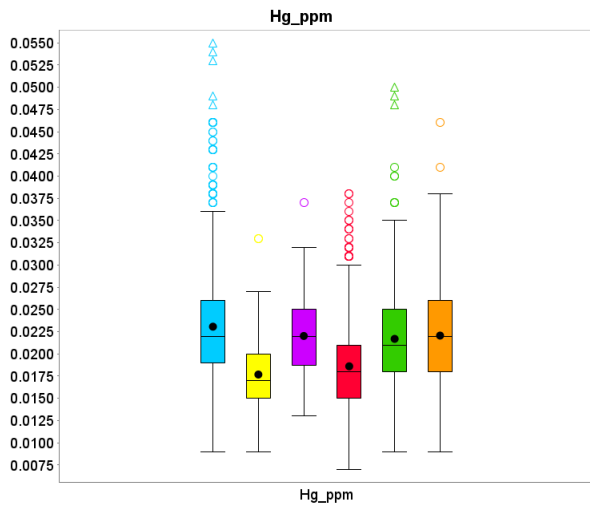
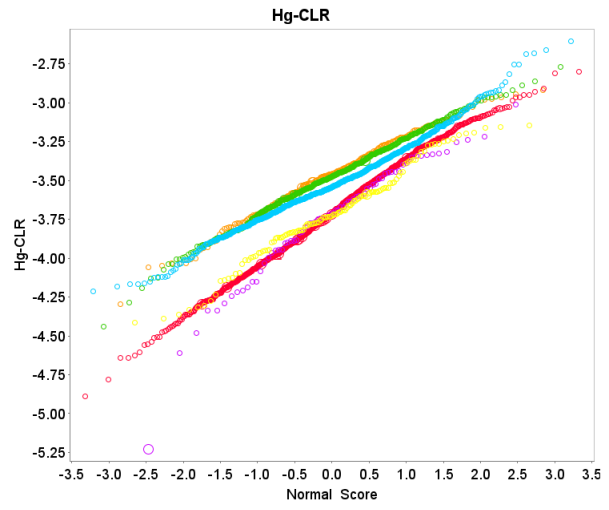
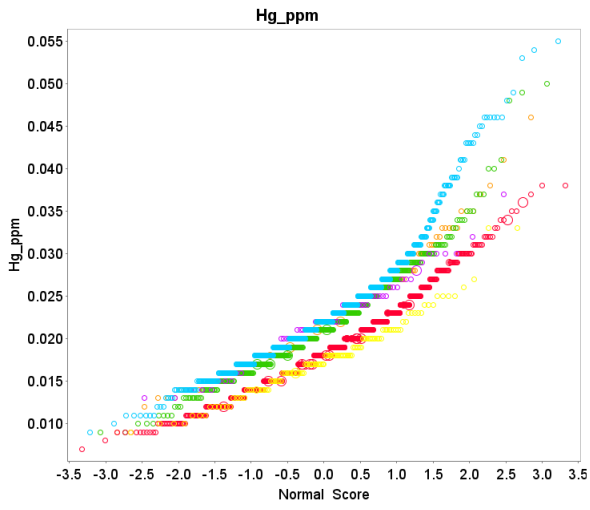


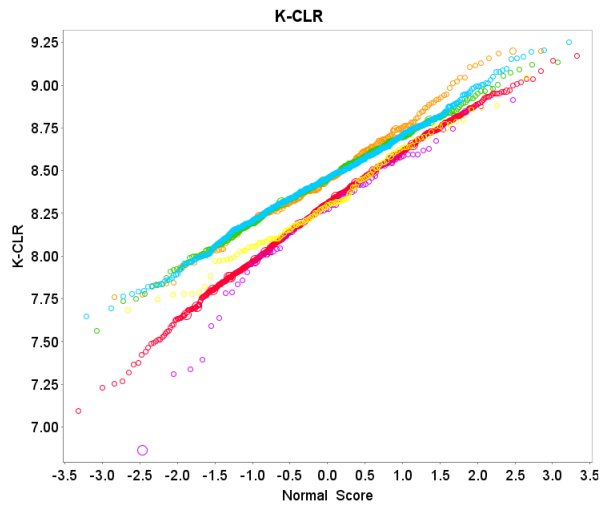
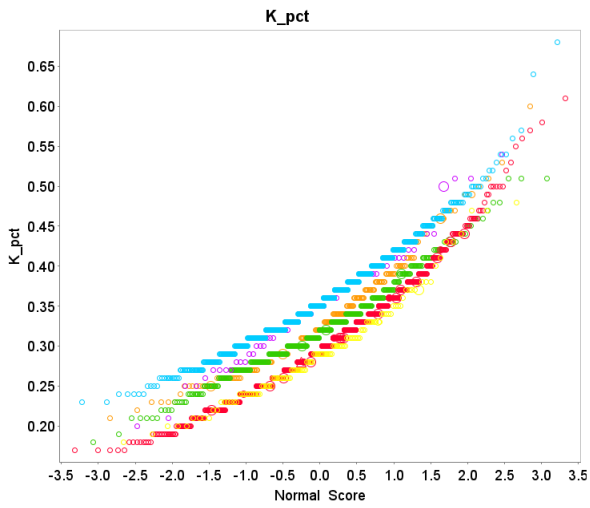
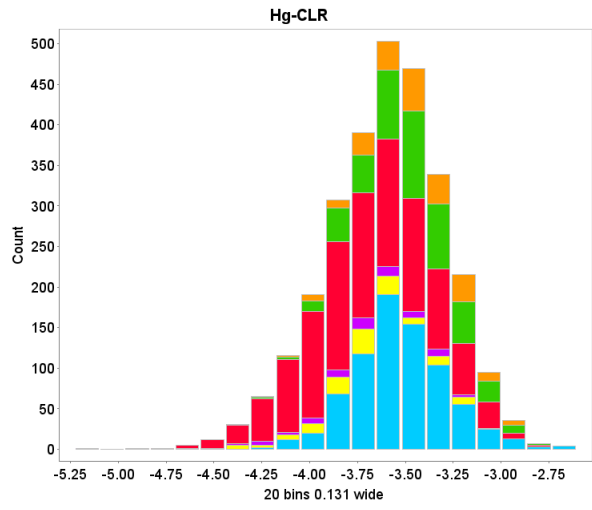
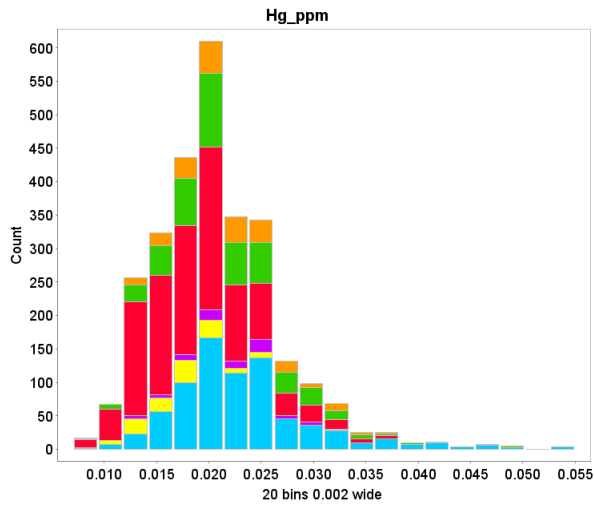


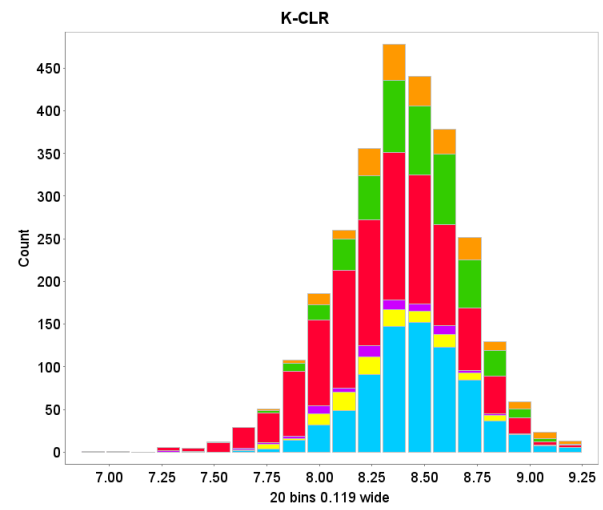
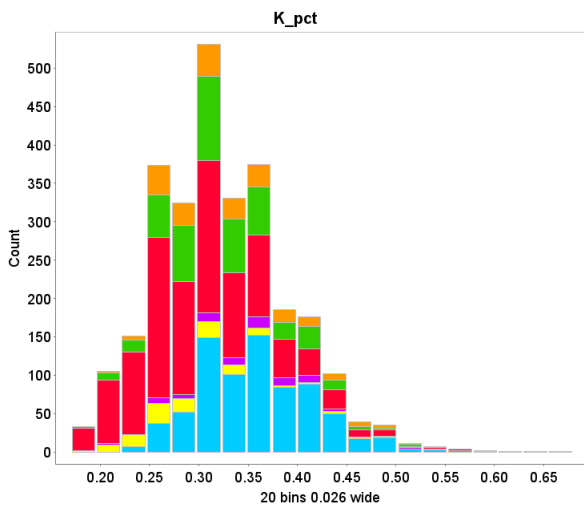
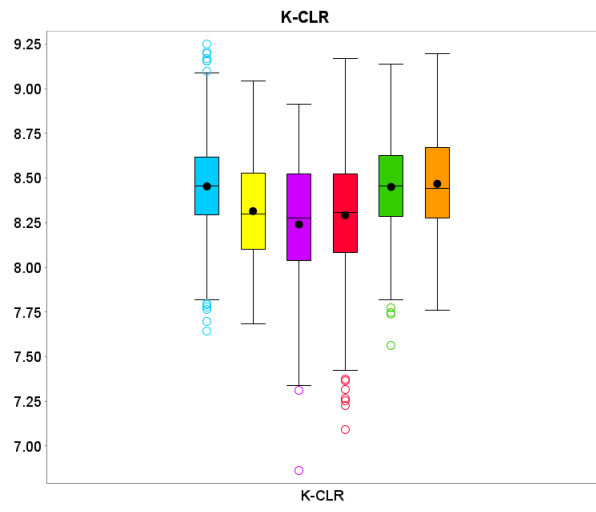
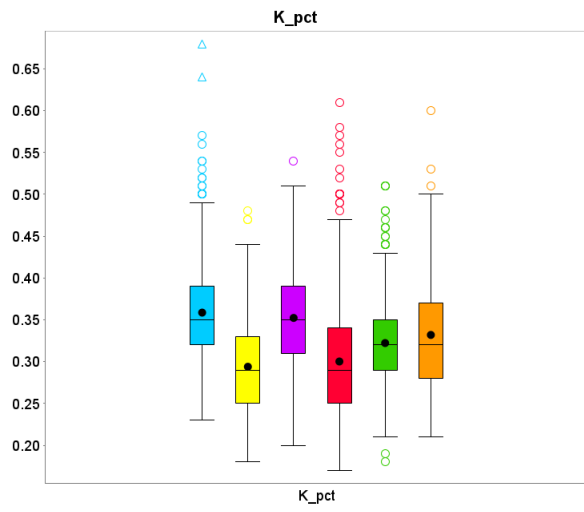


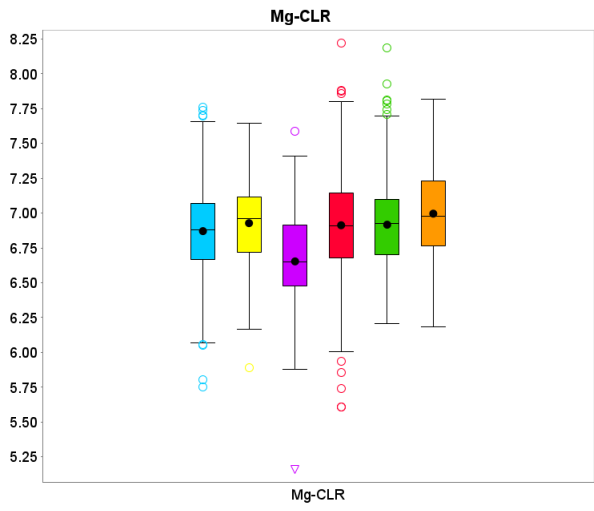
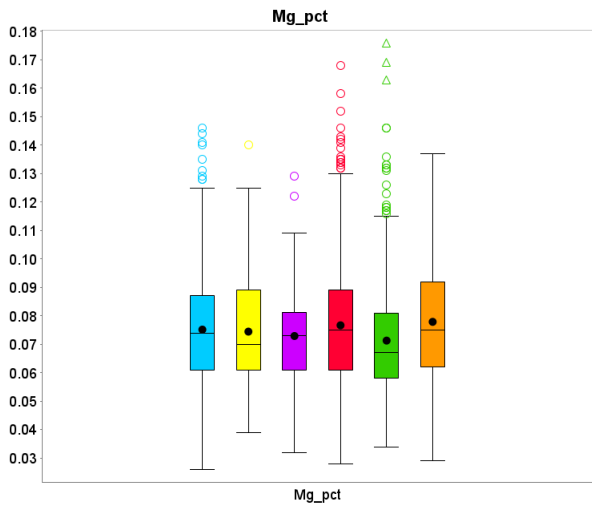
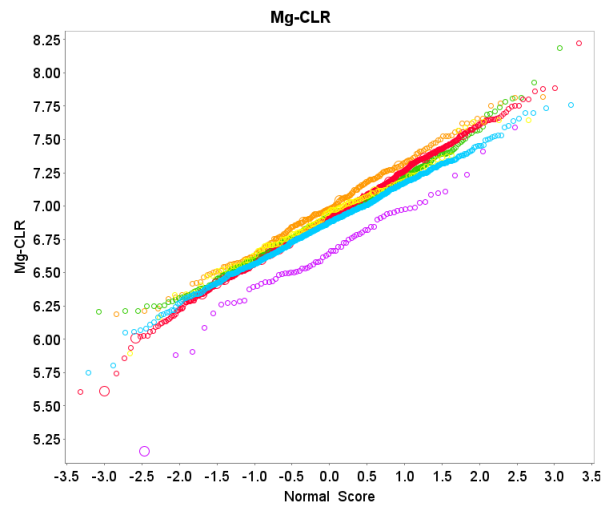
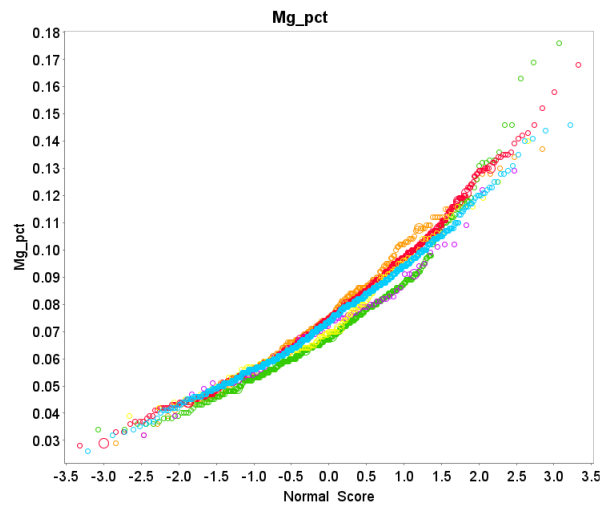


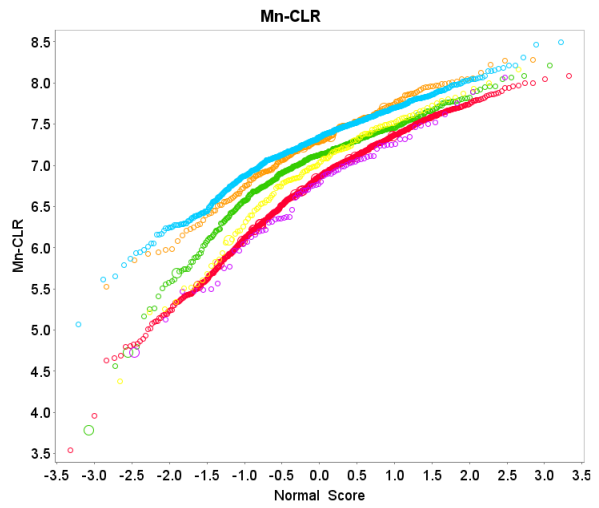
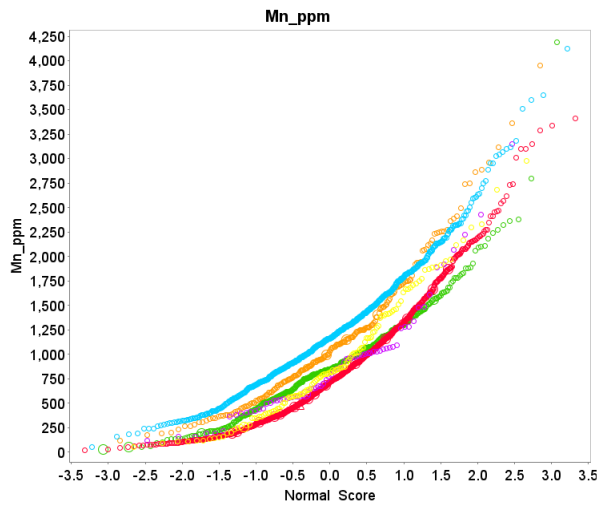
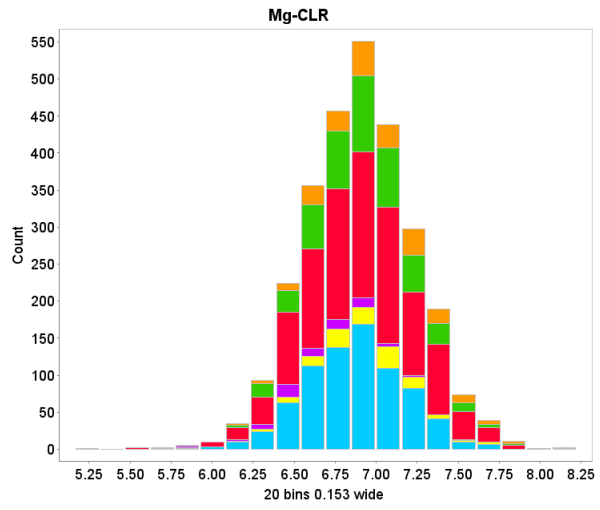
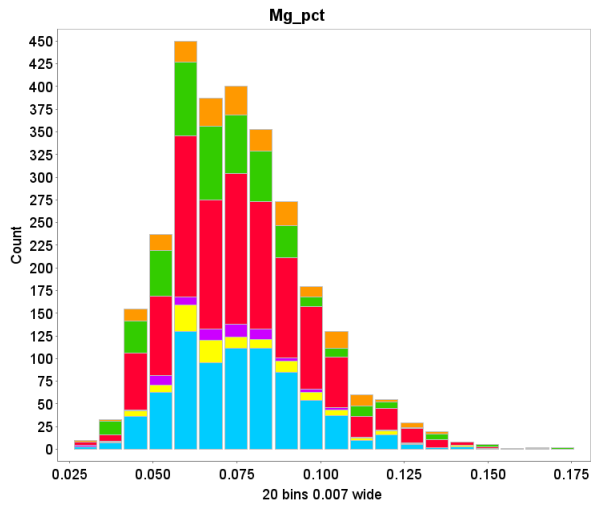


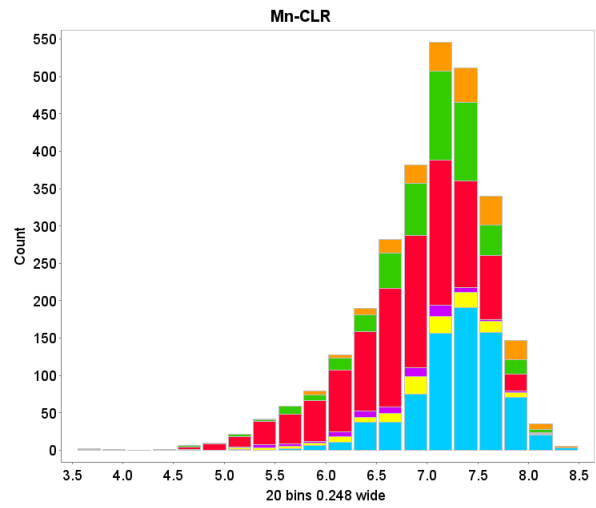
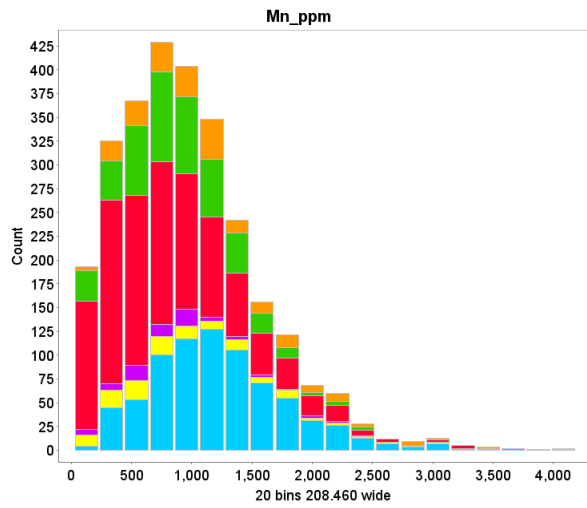
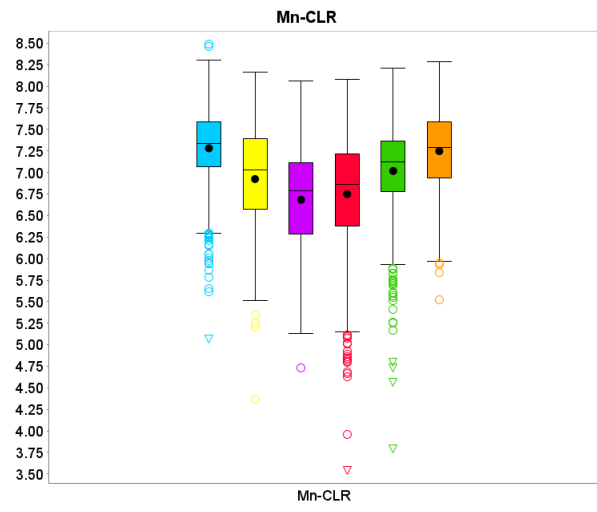
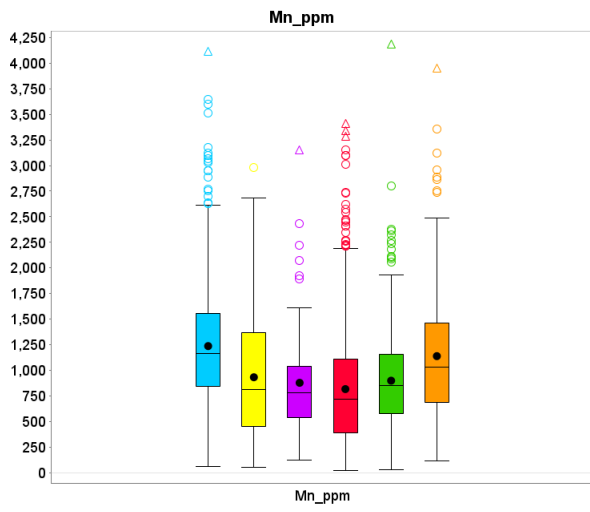


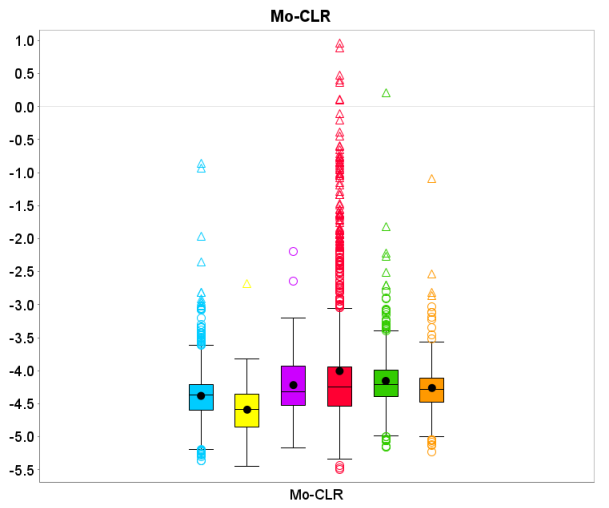
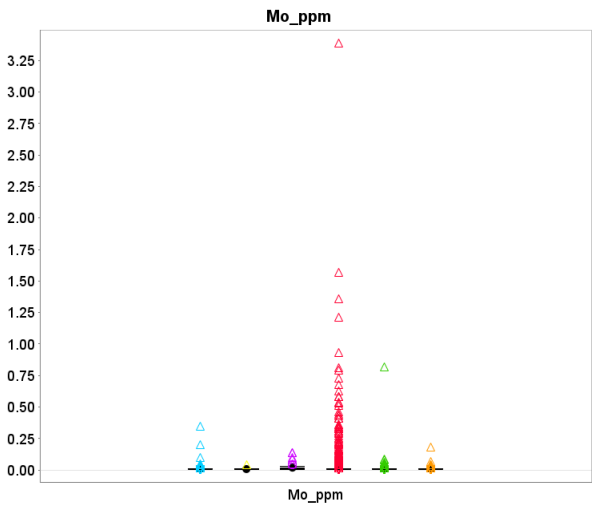
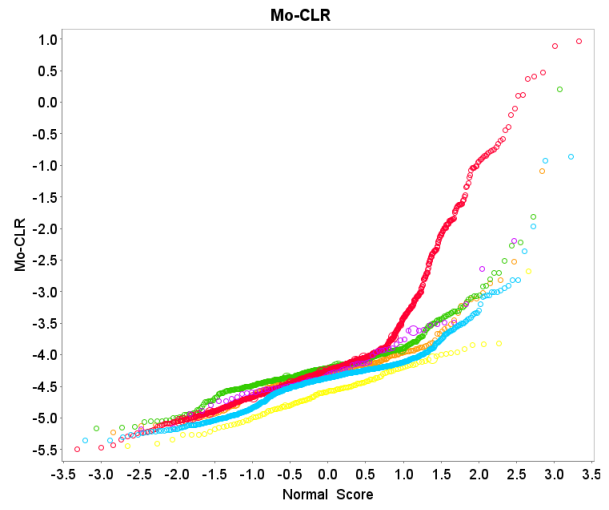
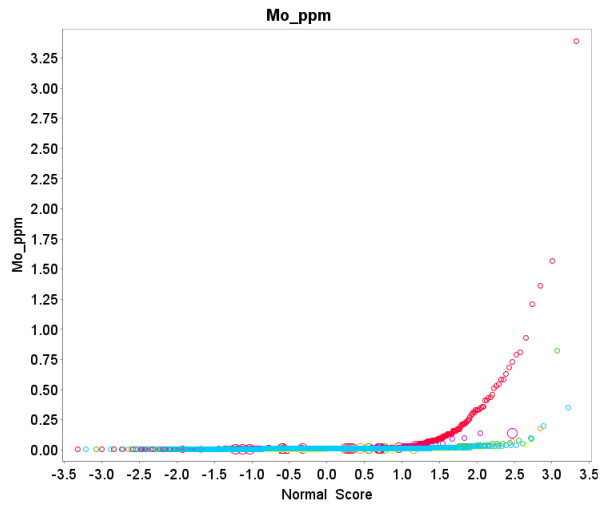


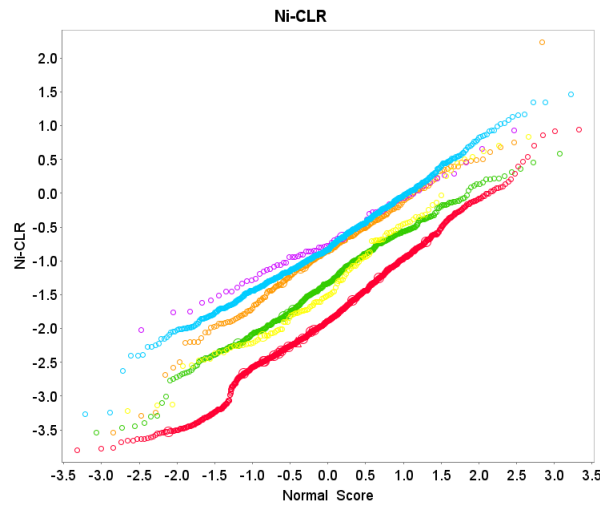
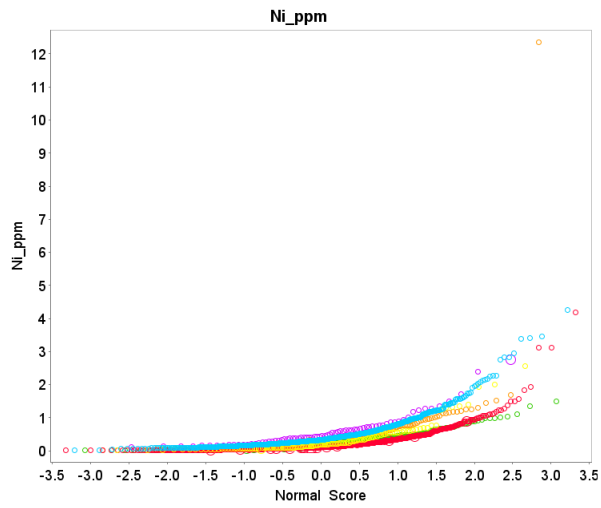
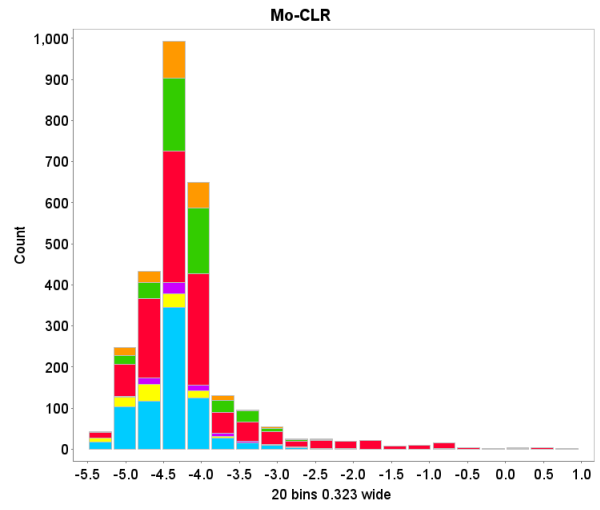
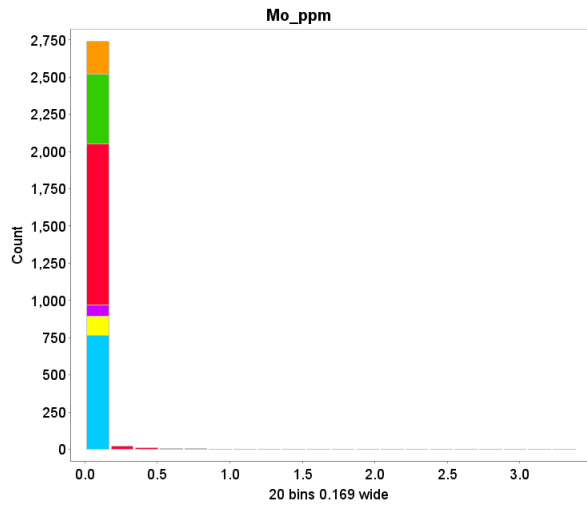


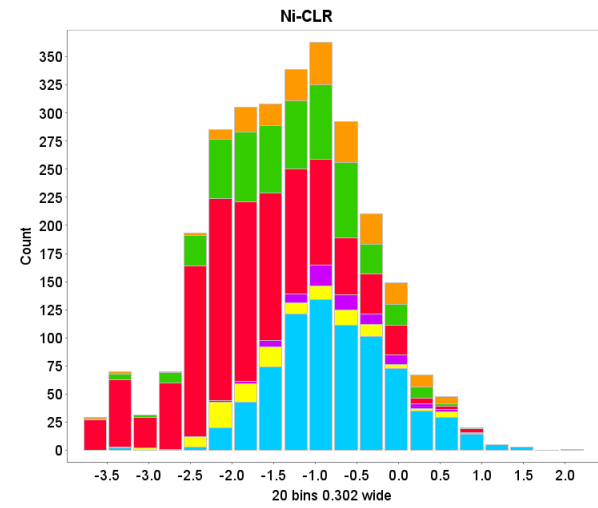
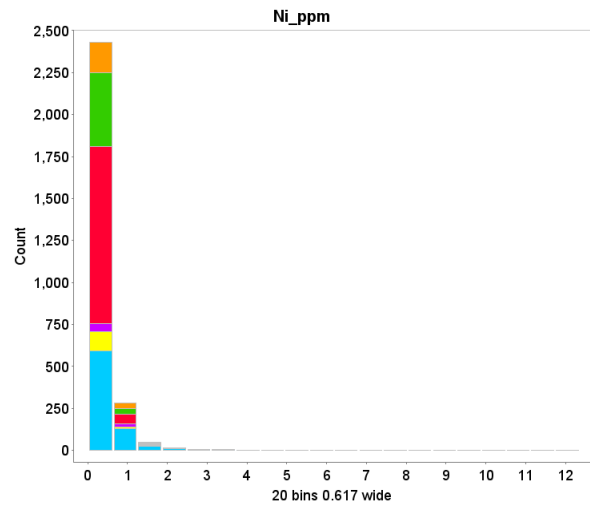
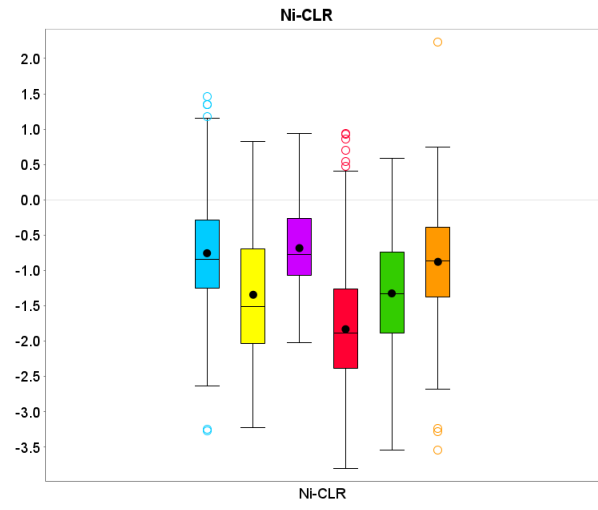
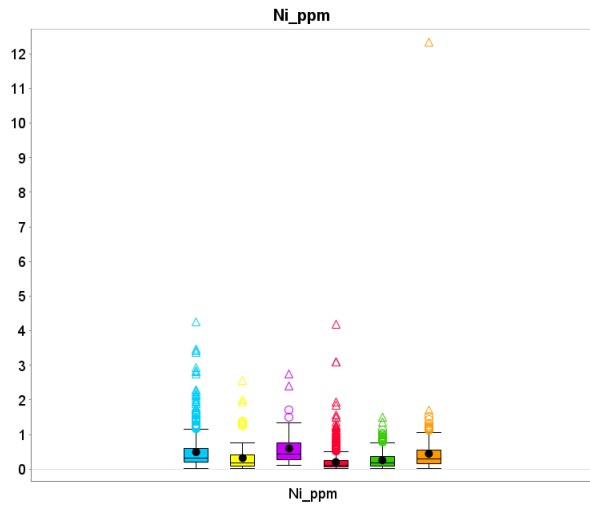


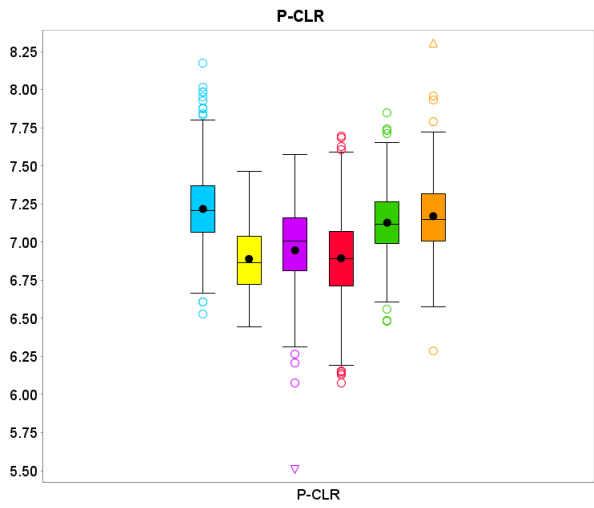
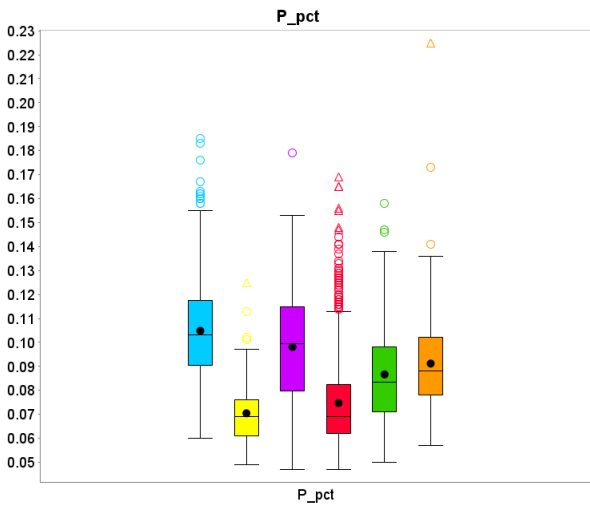
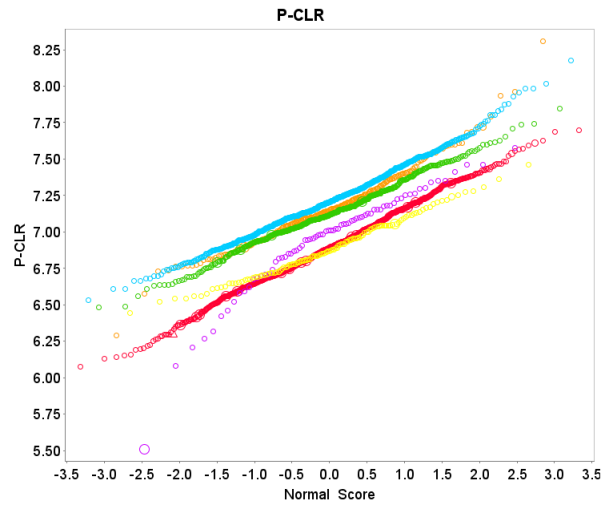
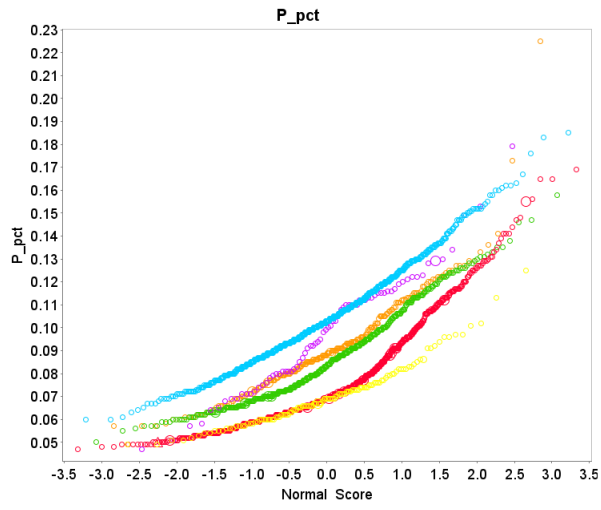


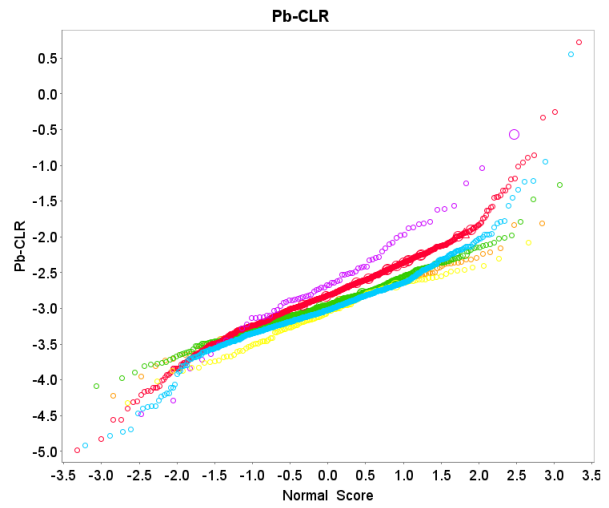
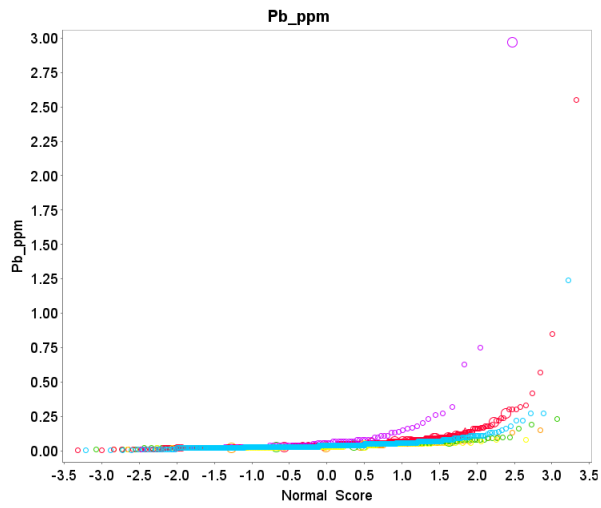
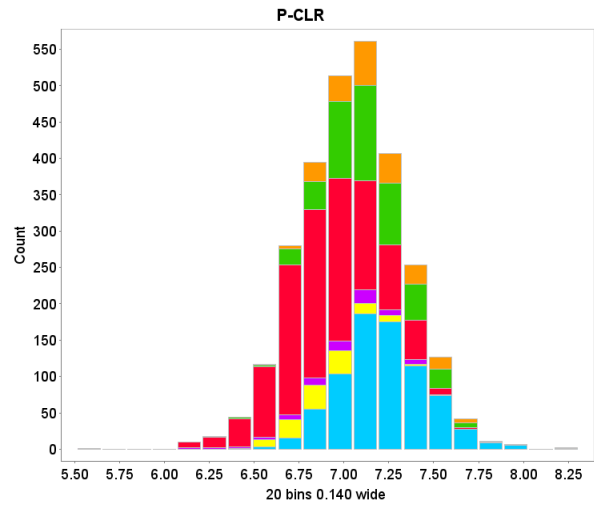
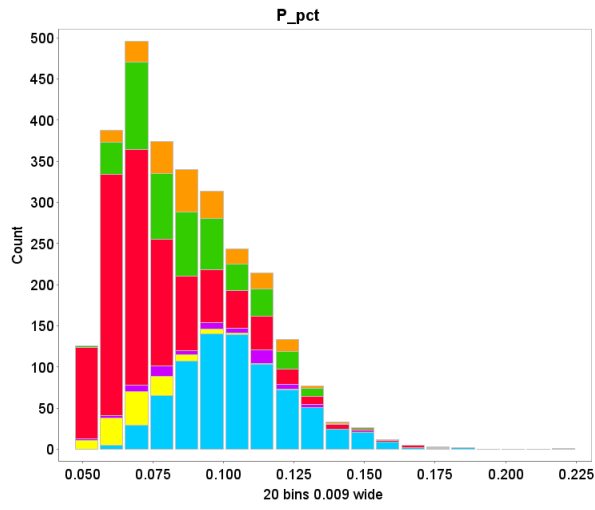


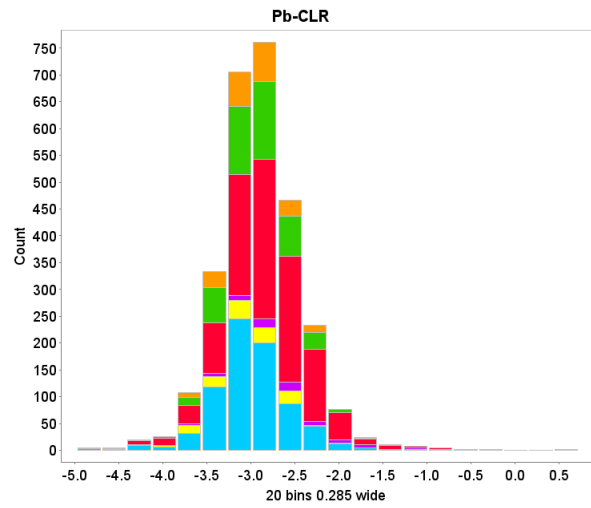
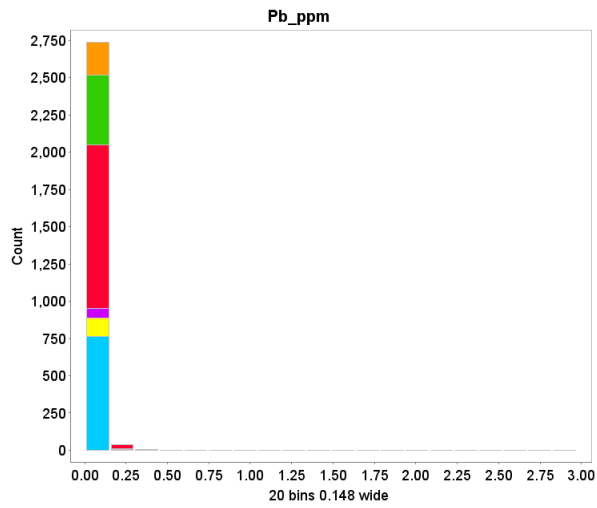
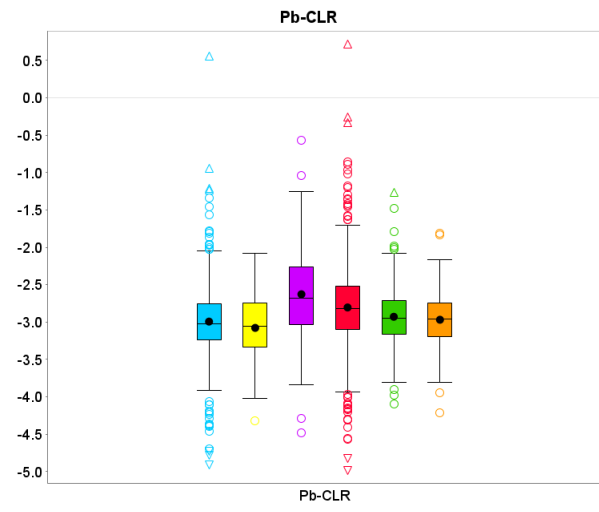
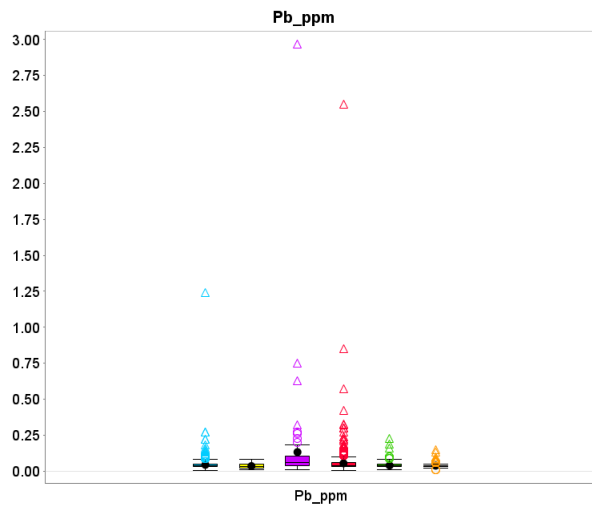


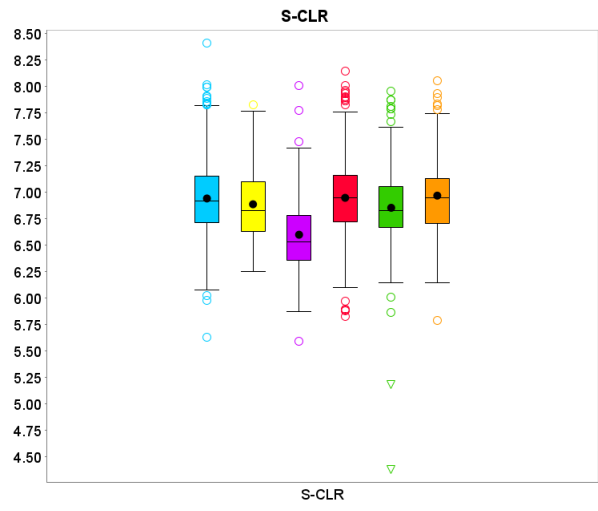
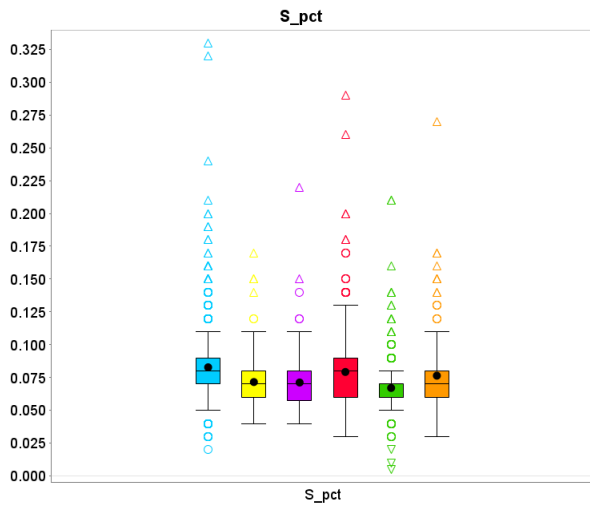
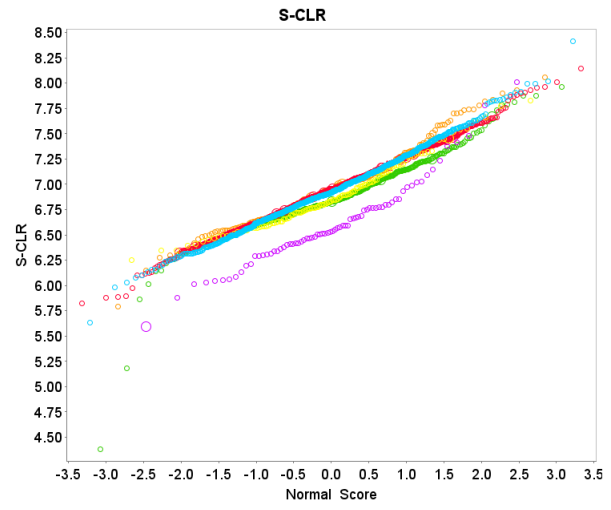
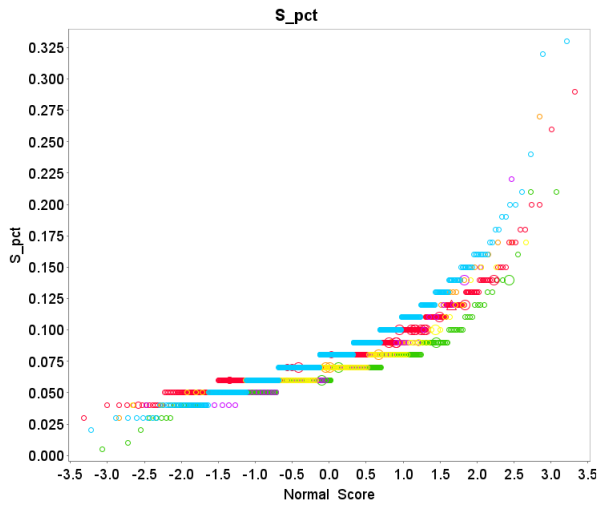


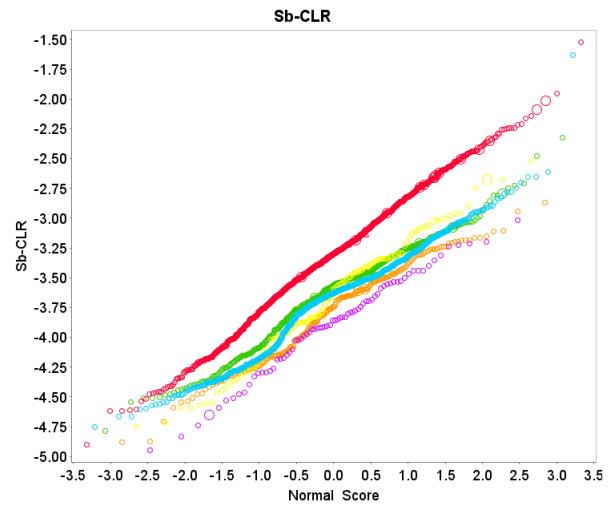
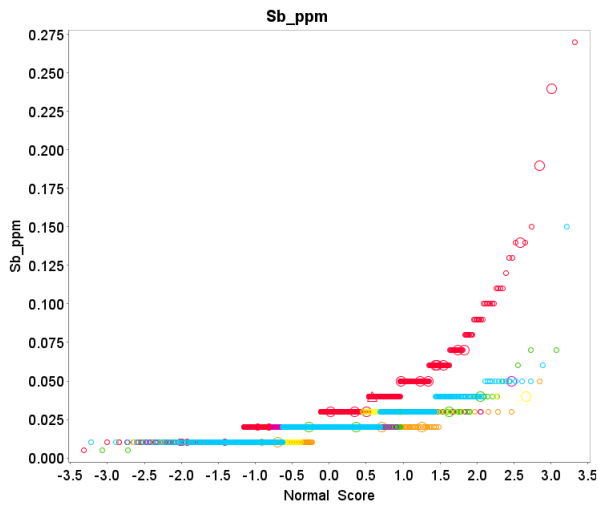
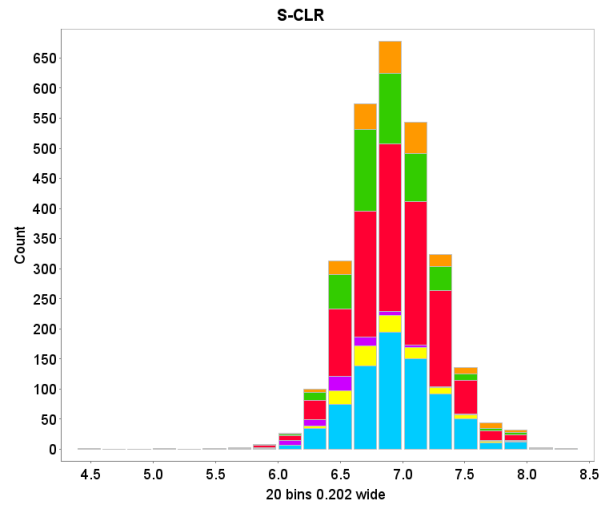
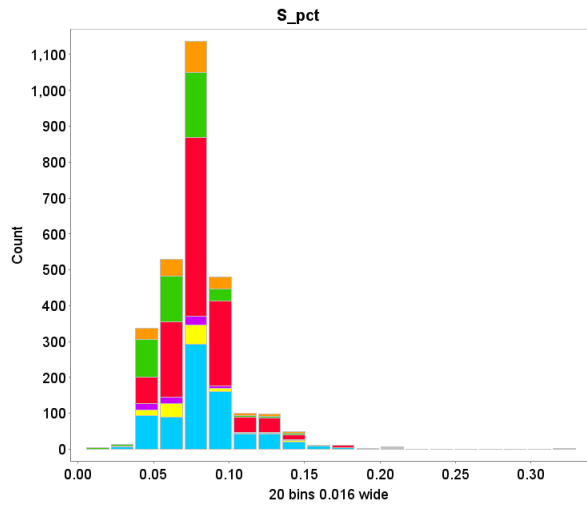


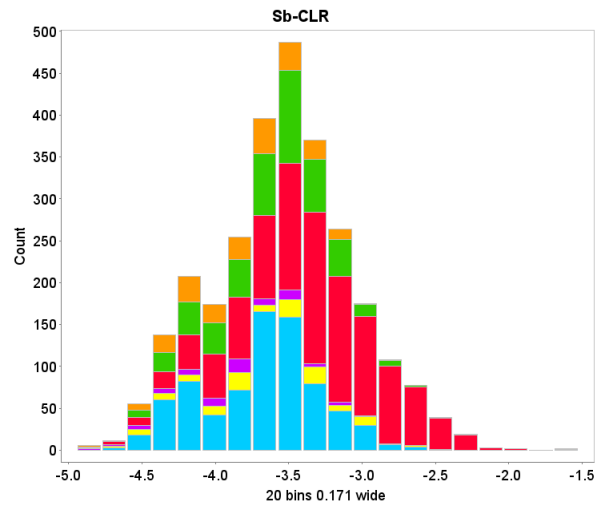
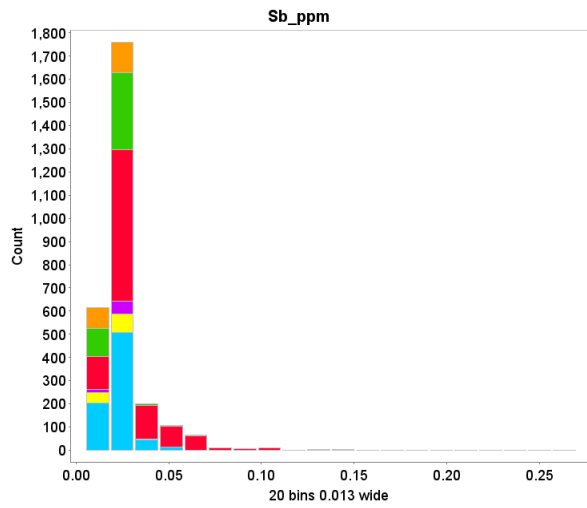
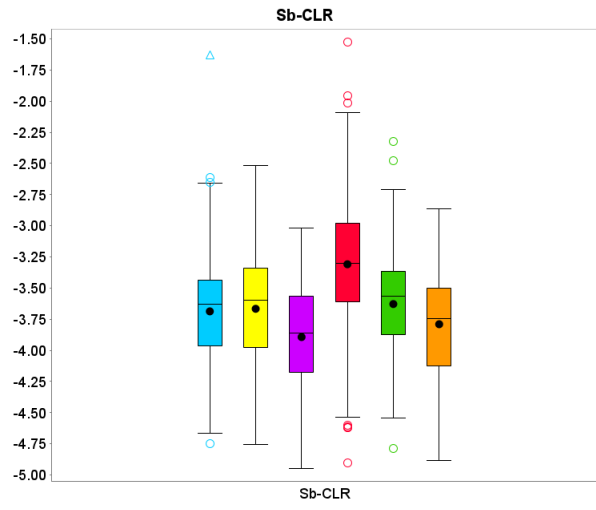
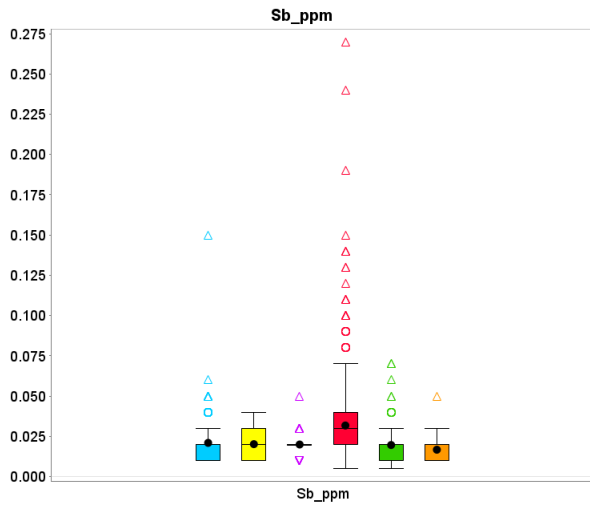


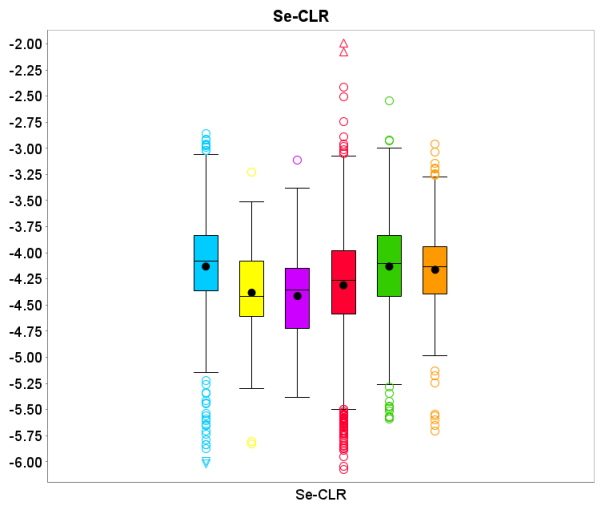
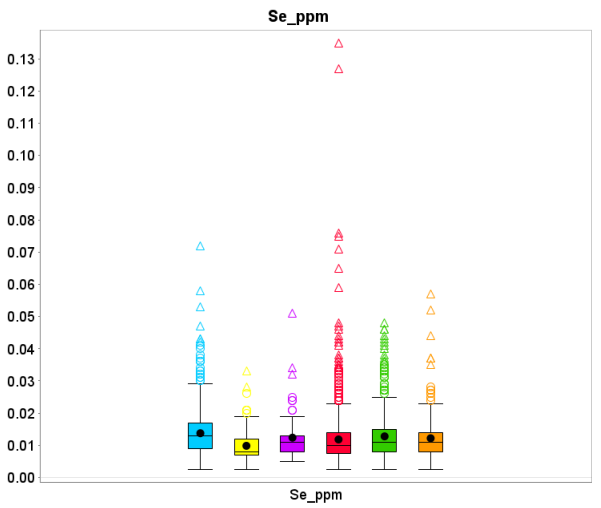
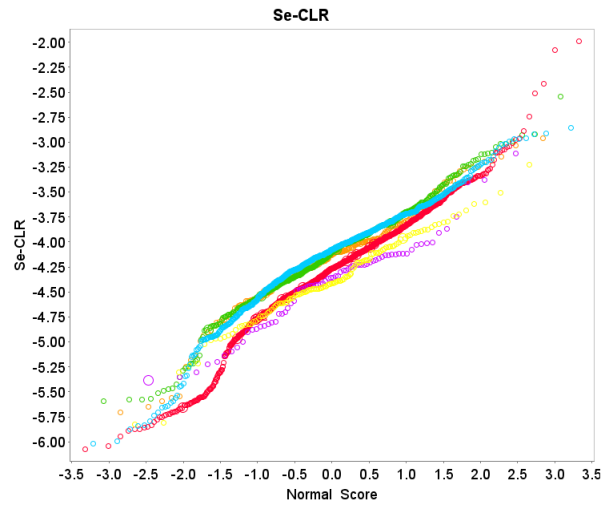
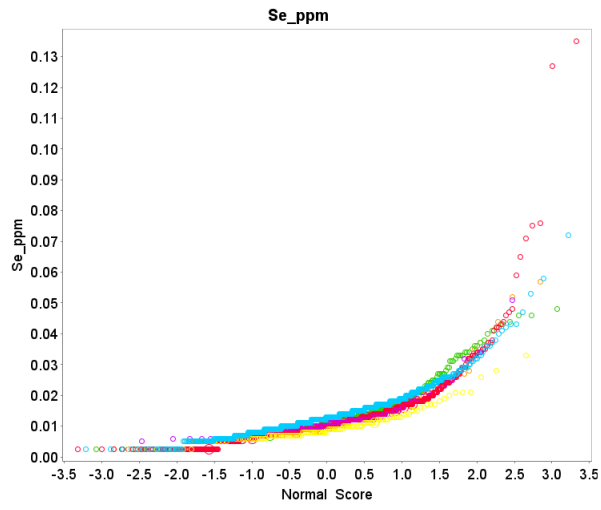


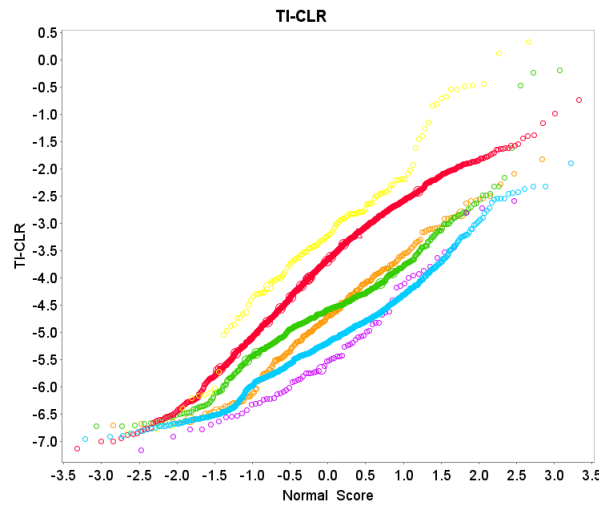
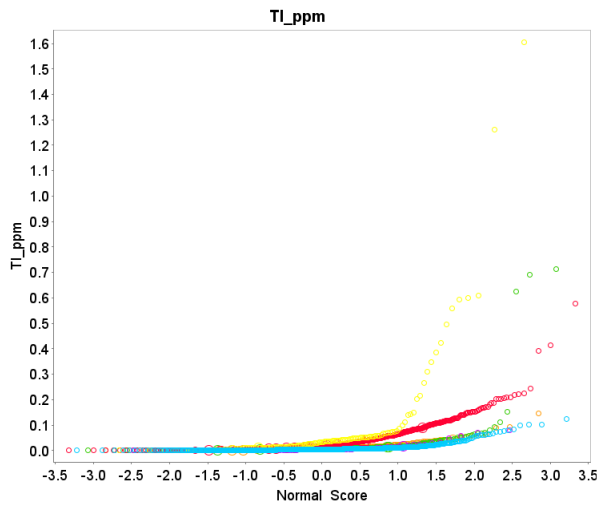
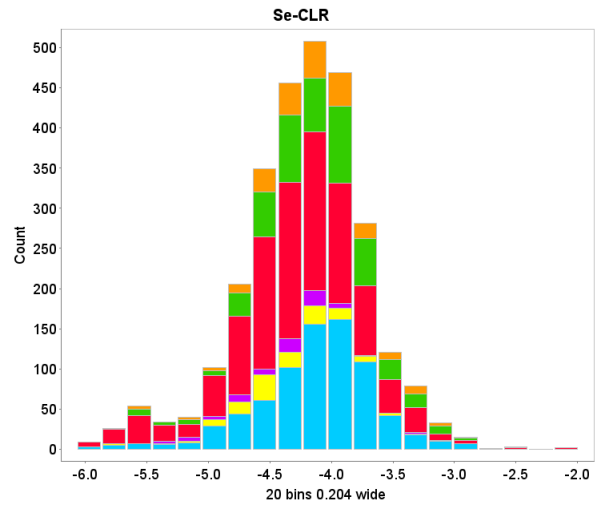
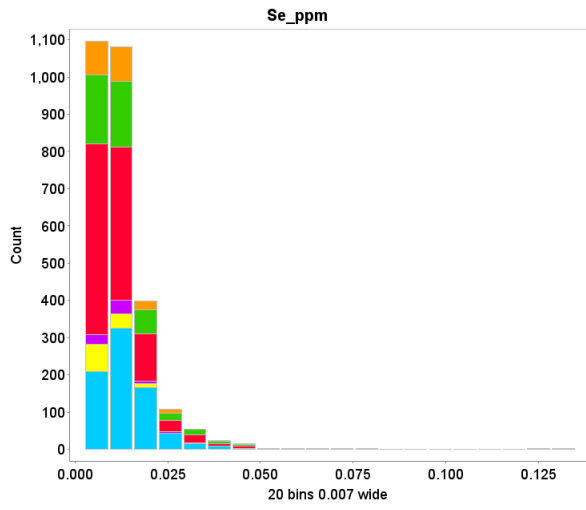


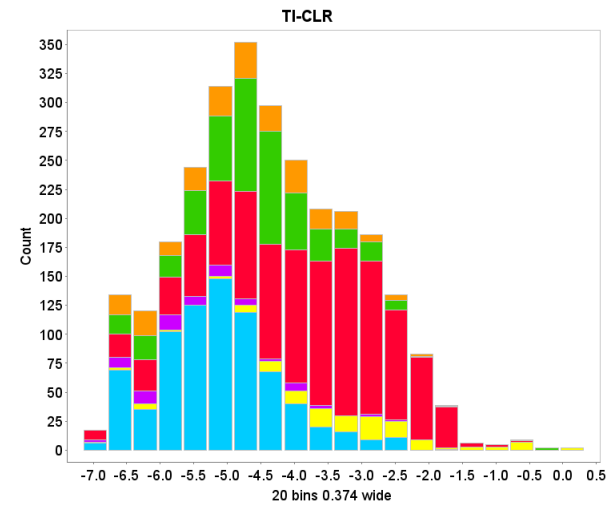
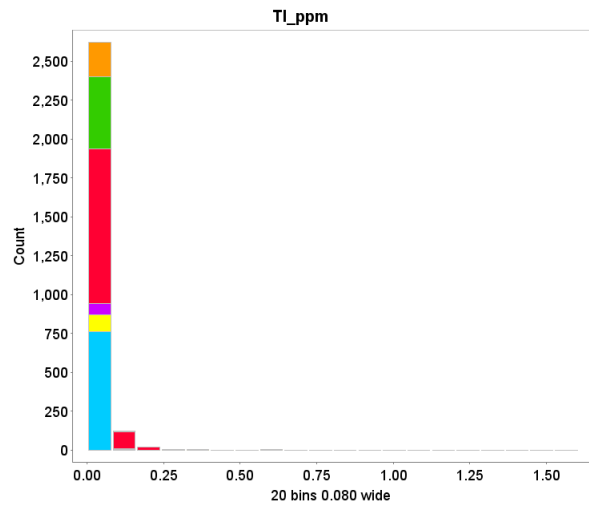
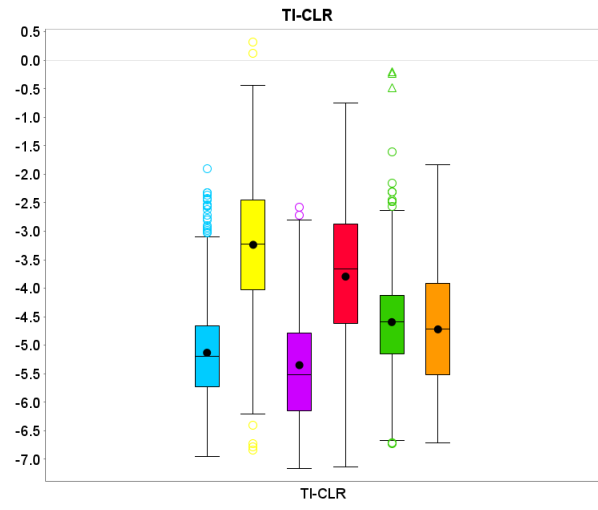
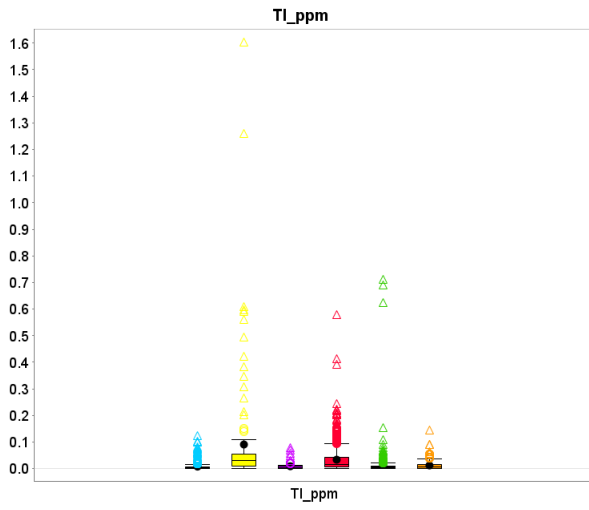


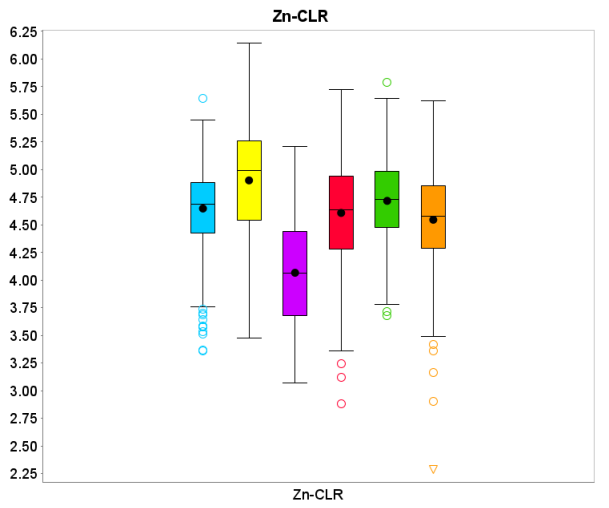
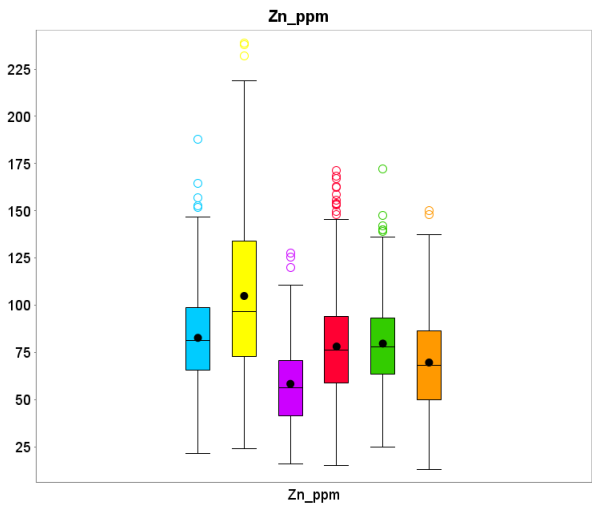
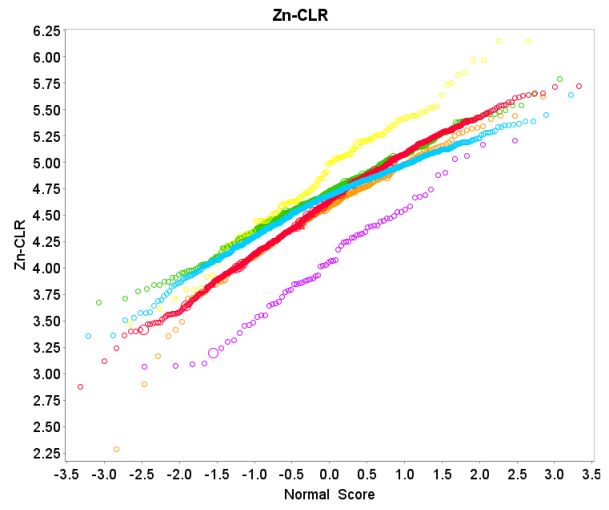
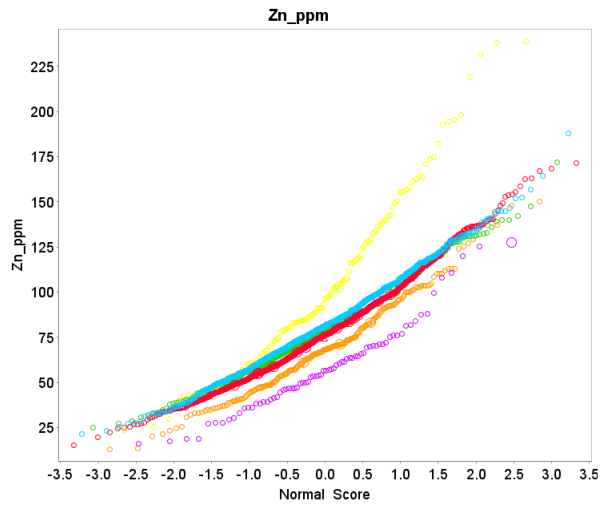


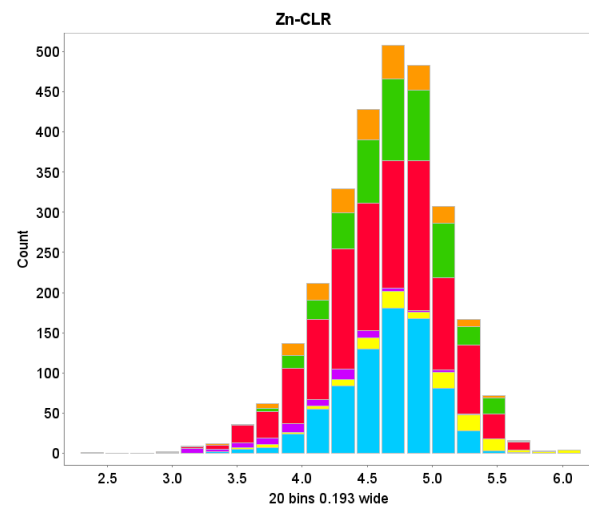
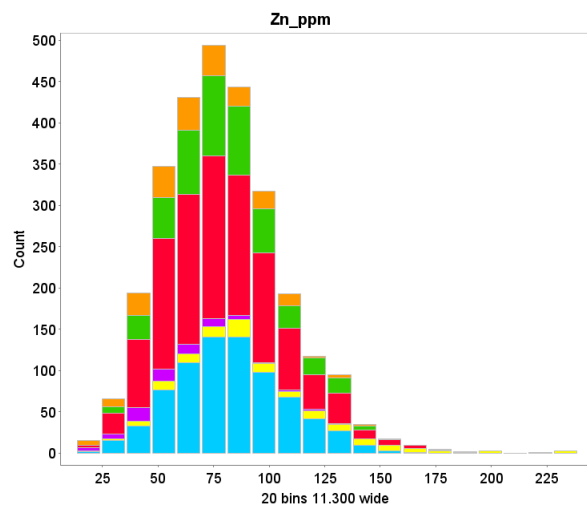












Curriculum Vitae

Name:

Zohreh Ghorbani

Post-secondary Education and Degrees:

- Western University
London, Ontario, Canada
2018-2022 Ph.D. Geology Candidate
- Shiraz University
Shiraz, Fars, Iran
2012-2014 M.Sc. Geochemistry
- Shahid Bahonar University of Kerman
Kerman, Kerman, Iran
2007-2012 BSc. Earth Sciences

Honors and Awards:

- Gordon Suffel Fellowship in Applied Economic Geology, 2022.
- Gordon Suffel Fellowship in Applied Economic Geology, 2021.

- Mitacs Research Training Award (RTA), 2020.
- Arcangelo Rea Family Foundation Graduate Scholarship, 2020.
- Robert W. Hodder International Geoscience Field Experience Award, 2019.
- Canadian light sources (CLS) Graduate Student / Post-Doc Travel Award, 2018.
- IMIDRO Research Award (Iranian Mines and Mining Industries Development and Renovation), 2014.
- Coal Research Bureau of Tabas Research Grant, 2014
- 1st rank in M.Sc. program in Geochemistry at Shiraz University, Iran, 2014.
- 3rd ranking in M.Sc. program in Geology at Shiraz University, Iran, 2014.
- 25th ranking at the graduate-level entrance exam, National educational testing organization, Iran 2012.

Related Work Experience:**Teacher Assistantship**

- Catastrophic Event on Earth History, EARTHSCI 2240F, 2022
- Exploring the Planets, EARTHSCI 2232G (2021)
- Plate Tectonics Theory, Environments and Products, EARTHSCI 2200A, 2020
- The Origin and Geology of the Solar System, EARTHSCI 1086G, 2019- 2020

- Introduction of Geochemistry, EARTHSCI 2230B, 2019
- Catastrophic Event on Earth History, EARTHSCI 2240F, 2018
- Statistical Modelling, Math 306, Sabanci University, 2017
- Graduate Project, ENS 491, Sabanci University, 2016

Research Assistantship

- Yellowknife City Gold Project, Aug 2020 to Aug 2022
- Big Easy Project, Oct 2020 to Jan 2021
- Monument Bay Gold Project, Sept 2018 to Aug 2020

Publications:

- Biogeochemical Prospecting for Gold at the Yellowknife City Gold Project, Northwest Territories, Canada: Part 2- Robust Statistical Analyses, Applied Geochemistry, 2022 (Accepted, under publication process)
- Biogeochemical Prospecting for Gold at the Yellowknife City Gold Project, Northwest Territories, Canada: Part 1- Species Optimization, Applied Geochemistry, 2022: 105423
- Application of the Multivariate Data Analysis to Biogeochemical Exploration at the Monument Bay Gold Project, Manitoba, Canada, Chemical Geology, 2022: 120739

- Biogeochemical Exploration at the Twin Lakes Au Deposit Using Synchrotron Radiation Micro X-ray Fluorescence and X-ray Absorption Near-Edge Structure Spectroscopy, Manitoba, Canada, *Microscopy and Microanalysis*, 26 (2), 2020: 1256-1259
- Arsenic in the rock-soil-plant system and related health risk in a magmatic–metamorphic belt, West of Iran, *Environmental Geochemistry and Health*, 2020, 42(11):3659-3673
- Application of Large-scale Synchrotron X-Ray Fluorescence 2D Mapping of Alteration Styles to Understand Gold Mineralization at the Monument Bay Project, Stull Lake Greenstone Belt, Manitoba, Canada, *Microscopy and Microanalysis*, 26 (2), 2020: 3216-3218
- EPMA Characterization of Gold Associated with Different Sulfide Textures at the Monument Bay Deposit, Manitoba, Canada, *Microscopy and Microanalysis*, 26 (2), 2020: 2182-2184
- Multi-scale SR-XRF Imaging and Characterization of Gold Mineralization at the Monument Bay Deposit, Stull Lake Greenstone Belt, Manitoba, Canada, *Microscopy and Microanalysis*, 26 (2), 2020:1256-1259
- Chemistry, mineralogy and distribution of selected trace elements in the Parvadeh coals, Tabas, Iran, 2016, *Fuel*, vol. 174, pp. 216-224
- Assessment of toxic elements recovery in Parvadeh coal cleaning, Tabas. vol. 24, No. 96, 2015, pp.177-188 (in Persian)

- Mineralogy of coal seam B1, B2, and C1 at Parvadeh Coalfield, Tabas, 28-29, 2013
(In Persian)

Conference and Poster Presentations

- Biogeochemical Prospecting for gold at the Yellowknife City Gold Project, Yellowknife Geoscience Forum, Nov 2022 (Oral Presentation)
- Arsenic Speciation in Lake Sediment and Plant samples at the Yellowknife City Gold Project, Northwest Territories, Canada, determined by toroidal X-ray absorption near edge structure (XANES) spectroscopy, AME Roundup-Association for Mineral Exploration, January 2022 (Poster and Oral Presentation)
- The Path from Raw Data to Robust Data Analysis: The Significance of Data Treatment to Geochemical Interpretation, GAC-MAC LONDON 2021 JOINT ANNUAL MEETING, Nov 2021 (Oral Presentation)
- Application of the Multivariate Data Analysis to Geochemical Exploration at the Monument Bay Gold Project, Manitoba, Canada, Prospectors & Developers Association of Canada (PDAC), March 2021 (Virtual Oral Presentation)
- Statistical Analysis of Biogeochemical data at the Yellowknife City Gold Project, NWT, CA, Recent Developments in Mineral Exploration Research, Western University, March 2021 (Virtual Oral Presentation)
- Application of the Multivariate Statistical Analysis to Biogeochemical Exploration at the Yellowknife City Gold Project, NWT, CA, Northwest Territories and

Nunavut Geoscience Symposium, Virtual, November 2020 (Virtual Oral Presentation)

- Multivariate statistical analysis on major and trace elements in black spruce at the Monument Bay Gold deposit, Manitoba, CA, Prospectors & Developers Association of Canada (PDAC), March 2020 (Poster Presentation)
- Geometallurgy at the Monument Bay Deposit, Stull Lake Greenstone Belt, Manitoba, CA, Prospectors & Developers Association of Canada (PDAC), March 2020 (Poster Presentation)
- Hydrothermal Alteration Footprint of the Monument Bay Gold Deposit, Manitoba, CA, (Final results), Prospectors & Developers Association of Canada (PDAC), March 2020 (Poster Presentation)
- Biogeochemical exploration at the Monument Bay Au-W deposit, Manitoba, CA, AME Roundup- Association for Mineral Exploration, January 2020 (Poster Presentation)
- Biogeochemical exploration using black spruce at the Twin Lakes Gold Deposit, Manitoba, CA, Central Canada Mineral Exploration Convention (CCMEC), November 2019 (Presentation for the Yamana Gold Inc.)
- Gold Mineralization at the Monument Bay Deposit, Stull Lake Greenstone Belt, Manitoba, CA, Prospectors & Developers Association of Canada (PDAC), March 2019 (Poster Presentation)

- Hydrothermal Alteration Footprint of the Monument Bay Gold Deposit, Manitoba, CA, Prospectors & Developers Association of Canada (PDAC), March 2019 (Poster Presentation)
- Evaluation of Pollution Index for Potentially Toxic Elements in Sediments of the Parvadeh Coal Mining Area, Tabas, 2014 (In Persian)
- Distribution of potentially toxic elements in sediments of the Parvardeh coalfield, Tabas, 2013 (Poster Presentation, In Persian).